Production of a safer, osteogenic, tissue engineered bone allograft

A thesis submitted to the University of Manchester for the degree of

Doctor of Philosophy

in the Faculty of Medical and Human Sciences

2014

Christopher Andrew Smith

Institute of Inflammation and Repair

School of Medicine

Contents

I Table of Figures

II List of Tables

III List of Abbreviations

2Θ : 2-Theta

3D: Three-dimensional

αMEM: α-modified Eagles medium

ALP: Alkaline phosphatase

ALPL: Tissue non-specific ALP gene

ASC: Adipose stem cell

BCIP: 5-bromo-4-chloro-3'-indolyphosphate p-toluidine

BCP: 1-bromo-3-chloropropane

BHQ: Black Hole Quencher

BLAP: Bone gamma-carboxylglutamic acid containing protein

BMD: Bone mineral density

BM-MNC: Bone marrow mononuclear cells

BM-MSC: Bone marrow mesenchymal stem cells

BMP: Bone morphogenetic protein

BSA: Bovine serum albumin

BSP: Bone sialoprotein

BTE: Bone tissue engineering

Ca/P: Calcium to phosphate

CBFA: Core-binding factor alpha

CD: Cluster of differentiation

cDNA: Complementary DNA

CFDA-SE: Carboxyfluorescein diacetate succinimidyl ester

DAB: 3',3-diaminobenzidine tetrahydrochloride

DAPI: 4',6-diamidino-2-phenylindole

dH_2O: Distilled water

DMSO: Dimethylsulfoxide

DNA: Deoxyribonucleic acid

ECM: Extra cellular matrix

EDTA: Ethylenediamineteraacetic acid

ELISA: Enzyme-linked immunosorbent assay

FACS: Fluorescence-activated cell sorting

FAM: 6-carboxyfluorescein

FCS: Foetal calf serum

FDA: Federal drug administration

FFCM: Fresh-frozen bone extract conditioned medium

FGF: Fibroblast growth factor

GAPDH: Glycetaldehyde-3- phosphate dehydrogenase

H&E: Haematoxylin and eosin

HBSS: Hanks balanced salt solution

HIV: Human immunodeficiency virus

HKG: Housekeeping gene

HLA: Human leukocyte antigens

HRP: Horseradish peroxidase

IBG: Impaction bone grafting

ICDD: International Centre for Diffraction Data

IFNγ: Interferon-γ

IGF: Insulin-like growth factor

IgG: Immunoglobulin G

IL: Interleukin

IMS: Industrial methylated spirits

kGy: Kilograys

LDH: Lactate dehydrogenase

MCT: Microcentrifuge tubes

MHC: Major histocompatibility complex

mRNA: Messenger RNA

MRPL19: Mitochondrial ribosome protein 19

MSC: Mesenchymal stem cells

MTC: Masson Trichrome

NAT: Nucleic acid testing

NBT: Nitro-blue tetrazolium chloride

NHSBT: National Health Service Blood and Transplant

OC: Osteocalcin gene

OPN: Osteopontin gene

PAA: Peracetic acid

PBS: Phosphate-buffered saline

PCR: Polymerase chain reaction

PDGF: Platelet derived growth factor

p-NP: p-Nitrophenol

p-NPP: p-Nitrophenyle phosphate

PRP: Platelet rich plasma

QRT-PCR: Quantitative real time PCR

RANKL: Receptor activator of nuclear factor kappa-B ligand

RNA: Ribonucleic acid

Runx2: Runt related transcription factor 2

RUNX2: Runx2 gene

SE: Standard error

TAE: Tris-acetate-EDTA

TBS: Tris-buffered saline

TCP: Tissue culture plastic

TE: Tris-EDTA

TGFβ: Transforming growth factor β

TNFα: Tissue necrosis factor-α

VEGF: Vascular endothelial growth factor

WBCM: Washed bone extract conditioned medium

XRD: X-ray diffraction

XRF: X-ray fluorescence

YOA: Years of age

IV Abstract

The use of allograft bone is effective in the treatment of large bone loss following tumour removal or surgery. However, it is not osteogenic due to a lack of viable osteogenic cells and the remaining marrow material is potentially harmful to the recipient. Sterilisation techniques, such as gamma irradiation, are routinely used to improve the safety of these grafts; however this fails to remove the immunogenic material and may diminish the bones innate properties. Thus, wash techniques are being developed to remove the deleterious marrow, whilst retaining the native properties of the bone so that through tissue engineering, pre-osteogenic cells may be added to aid osseointegration. To this end, this study utilised a novel wash process (developed by the National Health Service Blood and Transplant Tissue services (NHSBT)) on whole human femoral heads, to assess the resulting material's suitability as a biological scaffold for bone tissue engineering (BTE). Following the wash process, marrow removal efficiency was analysed by biochemical testing and histological assessment, and biocompatibility of fresh-frozen and washed human bone was assessed using extract cytotoxicity assays with BM-MSCs. The results showed a marrow removal efficiency of 99.5%, leaving a material with only 16.7 ng DNA/100mg of dry material, and which histologically displayed minimal cellular content demonstrating that this was an efficient wash process producing an acellular biological scaffold material (<50ng DNA/100mg bone). Extract cytotoxicity testing indicated the material was biocompatible. Uniaxial compression to failure was performed on $1cm^3$ cubes using bone samples from mirrored location of bilaterally halved femoral heads, with one half washed, whilst the other was fresh-frozen. A random orientated "clinical" model was also utilised, with samples processed as fresh-frozen, washed and irradiated for comparative assessment. There was no significant change in the mechanical strength of the washed material compared to fresh-frozen samples or between sterilisation types, suggesting the washed bone was mechanically comparable to existing bone allograft stock. BM-MSCs from both young (≤50 years) and old donors (≥70 years) were seeded on washed bone cubes from young and old donors, and cultured in standard or osteogenic media. Samples were analysed at 0, 14 and 28 day timepoints for cell viability, osteogenic gene expression, alkaline phosphatase activity and histological analysis. Results indicated significant fold increases in cell metabolism at day 14 and 28, in both medium types compared to day 0 ($p \leq 0.001$). QRT-PCR data showed increased expression of osteogenic markers RUNX2 ($p \leq 0.001$), osteopontin ($p \leq 0.001$) and osteocalcin ($p \leq 0.001$) in both standard and osteogenic media with significantly higher RUNX2 and osteocalcin in osteogenic medium samples at day 28. Expression of osteogenic genes was significantly higher in young donor cells seeded on the washed bone compared to old donor cells, as was expression in BM-MSCs cultured on old donor bone compared to young bone. This implies that the washed bone was able to induce osteogenic differentiation in BM-MSCs, that young donor cells were better able to differentiate than old, and that old donor bone was better able to induce osteogenic activity. Additionally, patient-matched BM-MSCs and ASCs, and BM-MSCs and BM-MNCs were seeded onto washed bone cubes and cultured for 28 days in standard or osteogenic media, with gene expression and metabolic activity assessed. The washed bone was able to induce osteogenic differentiation of ASCs. Moreover, BM-MNCs when cultured on washed bone also expressed osteogenic genes, indicative of osteogenic differentiation. These results indicate the efficacy of a novel wash process in producing a biological acellular scaffold suitable for bone tissue engineering. Interestingly, data also suggests that the age of the cell donor and bone donor may effect osteogenic differentiation of seeded cells which has significant implications clinically.

V Declaration

No portion of the work referred to in the thesis has been submitted in support of an application for another degree or qualification of this or any other university or other institute of learning.

VI Copyright statement

i. The author of this thesis (including any appendices and/or schedules to this thesis) owns certain copyright or related rights in it (the "Copyright") and s/he has given The University of Manchester certain rights to use such Copyright, including for administrative purposes.

ii. Copies of this thesis, either in full or in extracts and whether in hard or electronic copy, may be made only in accordance with the Copyright, Designs and Patents Act 1988 (as amended) and regulations issued under it or, where appropriate, in accordance with licensing agreements which the University has from time to time. This page must form part of any such copies made.

iii. The ownership of certain Copyright, patents, designs, trademarks and other intellectual property (the "Intellectual Property") and any reproductions of copyright works in the thesis, for example graphs and tables ("Reproductions"), which may be described in this thesis, may not be owned by the author and may be owned by third parties. Such Intellectual Property and Reproductions cannot and must not be made available for use without the prior written permission of the owner(s) of the relevant Intellectual Property and/or Reproductions.

iv. Further information on the conditions under which disclosure, publication and commercialisation of this thesis, the Copyright and any Intellectual Property and/or Reproductions described in it may take place is available in the University IP Policy (see http://documents.manchester.ac.uk/DocuInfo.aspx?DocID=487), in any relevant Thesis restriction declarations deposited in the University Library, The University Library's regulations (see http://www.manchester.ac.uk/library/aboutus/regulations) and in The University's policy on Presentation of Theses.

VII Acknowledgments

Firstly, I would like to thank all of my supervisors; Prof Judith Hoyland, Dr Stephen Richardson, Mr Tim Board and Dr Paul Rooney, for giving me the opportunity to undertake this study, and providing me with their support during it, which has helped me achieve so much. In particular I would like to thank Judith and Steve for their knowledge, help, guidance and understanding during the study, without which I would not have enjoyed the PhD as much as I did, especially during the difficult times. I would also like to thank them for the time they spent answering my questions, conversing about science and academia, and for helping me develop myself as an academic scientist.

Thank you to Tim Board for his clinical insight and for inviting me to view him perform hip replacement surgery so I could see first-hand the clinical need for my work. And thank you to Paul Rooney for his expertise and guidance in the practicalities of producing bone grafts, and for making sure I felt part of the group at Speke.

I would also like to thank the staff; Pauline Baird, Andy Fotheringham, Daman Adlam and Sonal Patel at the University of Manchester, and Mark Eagle and Penny Hogg at the NHSBT site in Speke for all their hard work, for welcoming me into your labs, finding me samples, and giving me the help I needed to learn and undertake new protocols and techniques. Thank you also to the other students in the post-grad room, both past and present, including; Louise, Nicola, Russell, Kim, Fran, Ricardo, Shanaz, Jude and the newbies for keeping me sane, sharing tips and tricks and having a good natter when needed. I wish you all the best of luck.

Finally, a big thank you to my family; mum, dad, granddad, auntie Chris, uncle Dave and Molly, who have supported me without fail during my studies, have listened to my ramblings whenever I achieved success, and my moaning and complaints when I hadn’t, particularly during infection season! I would especially like to thank the long suffering Carly for all her hard work, especially listening to me, her constant words of encouragement and pep talks, and who by now must know more about bone and tissue engineering than most people care to.

I have greatly enjoyed my time with the group, but look forward to returning to being a normal, employed, non-student and continuing my career.

Chapter 1

General introduction

This study will aim to assess the use of a novel wash process for whole human femoral heads in order to produce an allograft scaffold for bone tissue engineering, which may improve clinical outcome over currently available allografts. Initially, the impact of the wash process on the biocompatibility and mechanical stability of the allograft bone will be assessed. Subsequently, innate biological properties of the resultant bone scaffold will be assessed, focussing on its ability to induce osteogenic differentiation of human bone marrow mesenchymal stem cells (BM-MSC). Finally, alternative osteogenic cell sources will be assessed on the washed bone scaffold with a view to developing a clinically viable bone tissue engineering strategy. As such, the introduction will cover aspects of bone tissue development, remodelling and healing, as well as bone sterilisation and wash techniques used for the production of structures in tissue engineering.

1.1 Bone biology

1.1.1 Formation of bone in developmental stages

Bone is a complex, functionally rigid organ, composed of organic connective tissue, highly specialised cells and inorganic mineral crystals. This rigid, strong, but lightweight mineralised composite structure is essential for mechanical stability and mineral metabolic homeostasis and contains the bone marrow essential for blood production (Bilezikian *et al.,* 2008). During an individual's life, bone formation can be segmented into three levels: development and the formation and modelling of new bone; maintenance and the remodelling of existing structures to hone use; and decline, whereby more bone is resorbed than is deposited, although this is usually as result of age-related diseases such as osteoporosis (Bilezikian *et al.,* 2008).

The bones of the human skeleton are formed either by intramembranous or endochondral ossification. These two distinct methods rely on different specialised cell types within the mesenchyme, which are produced during foetal development (Rosen *et al.*, 2009). During condensation of the mesenchyme, cells are directed to differentiate into either cartilage producing chondrogenic cells or bone matrix producing osteoblasts. In areas of bone formed by intramembranous ossification, such as the skull and jaw, the expression of runt-related transcription factor 2 (Runx2) and subsequent osteogenic differentiation of mesenchymal stem cells (MSC) into osteoblasts is required, whilst the formation of the majority of the skeleton by endochondral ossification relies upon the chondrogenic differentiation (Figure 1.1) (Rosen *et al.,* 2009).

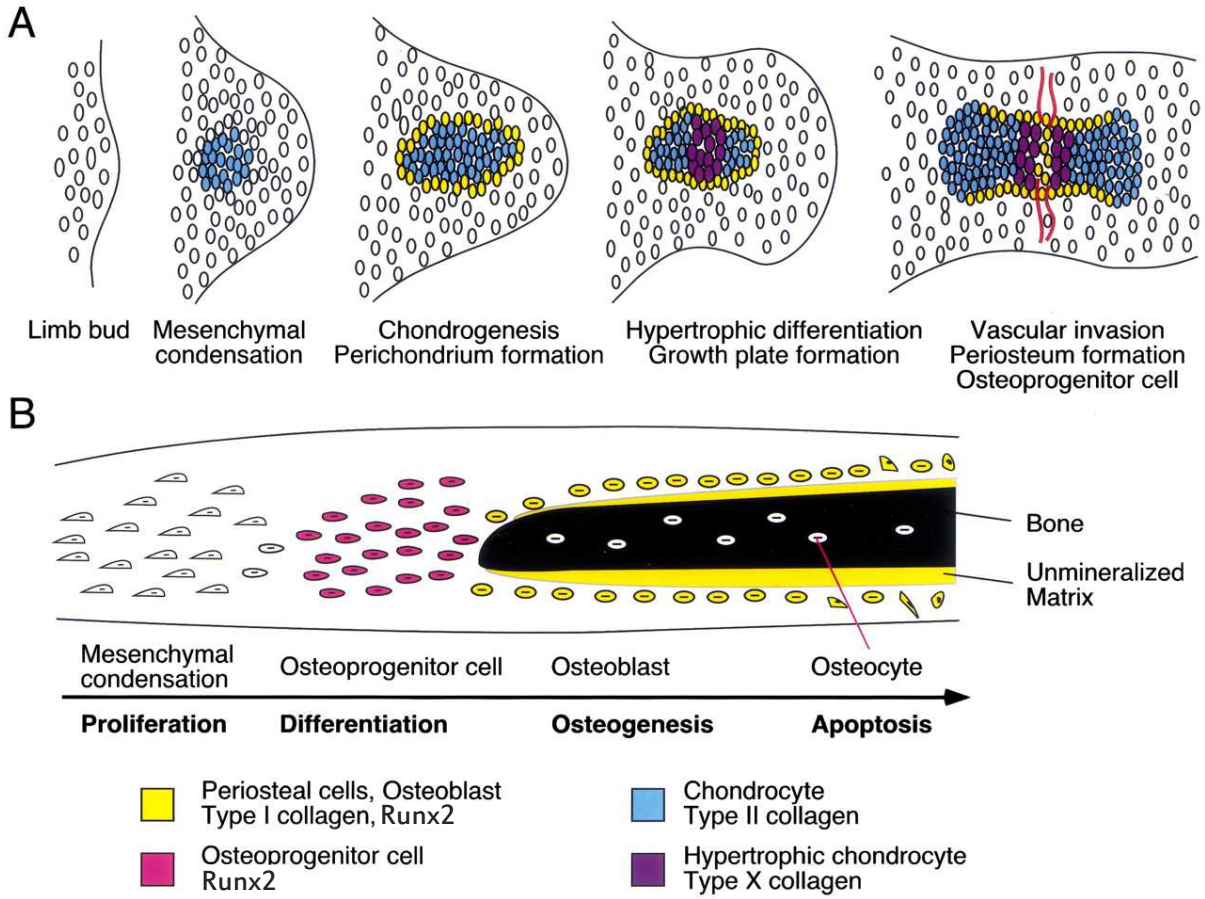

Figure 1.1: Bone development processes of endochondral ossification and intramembranous ossification. In endochondral bone formation (A) the condensation of the mesenchyme initiates the differentiation of mesenchyme cells into chondrocytes, which express type II collagen to create a cartilage matrix. Chondrocytes in the centre of the cellular mass become hypertrophic, changing their protein expression to type X collagen. Continued growth of the region causes the formation of a surrounding perichondrium, which is accompanied by the invasion of blood vessels and additional stem cell, which differentiate into bone producing osteoprogenitors and osteoblast and form a centre of ossification. Alternatively, in intramembranous ossification (B), the condensation of neighbouring mesenchyme causes the differentiation of mesenchymal cells into osteoporgenitors. These cells express the osteogenic transcription factor Runx2, and further mature into osteoblasts, producing new type I collagen rich bone matrix which is subsequently mineralised. This process happens in a progressive, layered form. Original image adapted from Ornitz and Marie, (2002).

The two separate differentiation pathways are regulated initially by the hedgehog/Wnt signalling pathways (Hill *et al.,* 2005; Day *et al.,* 2005). Interaction of the Wnt signalling proteins, termed cytokines, with cell surface receptors of the Frizzled family (FRZ), prevents the breakdown of cytoplasmic β-catenin by sequestering the β-catenin phosphorylating protein, axin (Figure 1.2). In the osteoblast requiring intramembranous model of bone production, high levels of β-catenin in the cell are maintained through preservation of Wnt signalling (Hu *et al.,* 2005), which in turn induces the expression of the essential osteogenic promoter transcription factor Runx2 (aka core binding factor alpha 1 (CBFA1) (Ducy *et al.,* 1997; Otto *et al.,* 1997). This transcription factor is the primary promoter of osteogenic differentiation, and after heterodimerising with core-binding factor β (Cbfβ), and itself binding to the promoter region, and inducing the transcription of the transcription factor osterix (Nakashima *et al.,* 2002; Nishio *et al.,* 2006). The two transcription factors further promote the differentiation of cells along the osteogenic lineage, activating the transcription of several osteogenic proteins including collagen I, osteopontin and osteocalcin (Ortuno *et al.,* 2013; Komori, 2005; Komori *et al.,* 1997). The increase in β-catenin and subsequent osteogenic differentiation via Runx2 decreases the production of the chondrogenic transcription factor Sox9 and by doing so prevents the formation of chondrocytes and endochondral ossification bone formation.

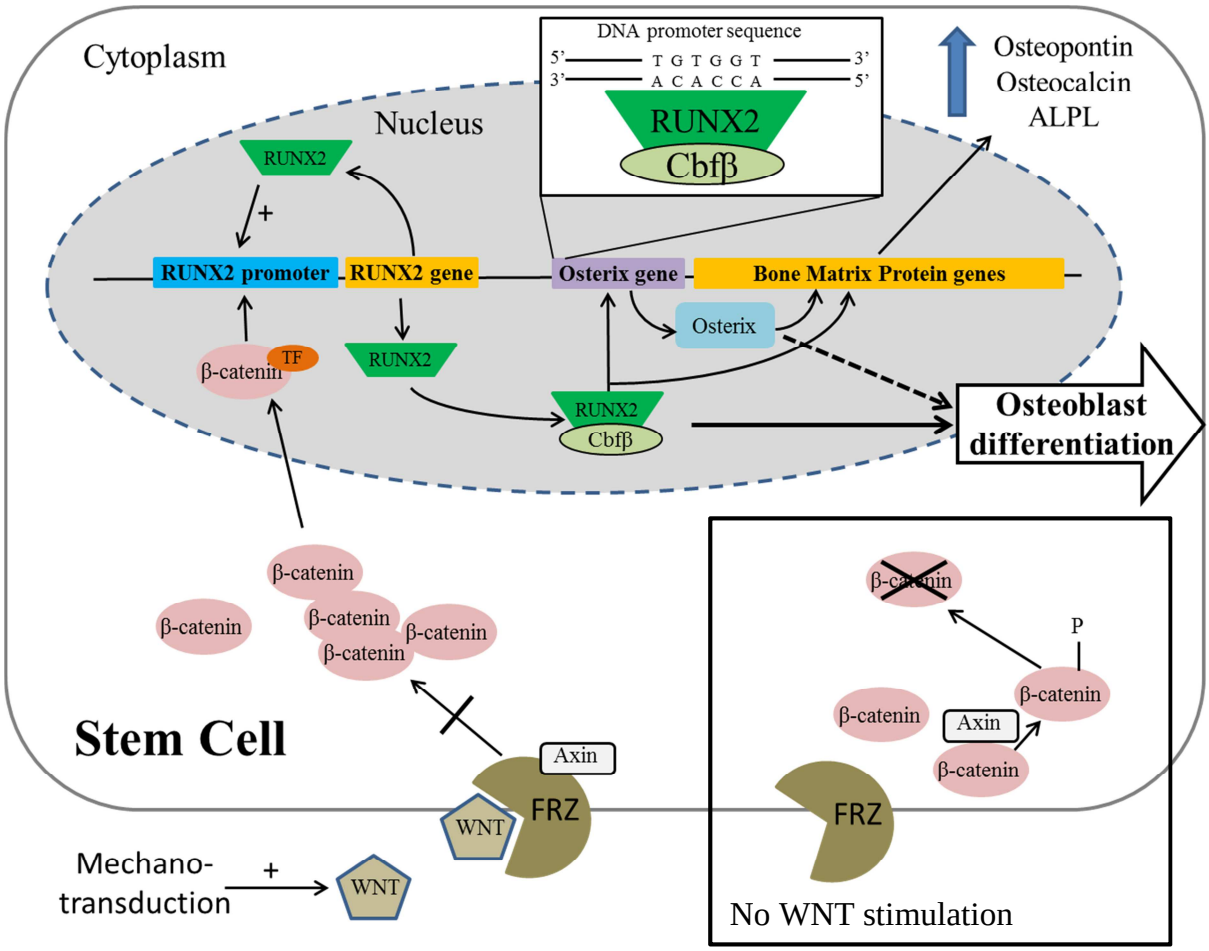

Figure 1.2: Stimulation and role of the primary osteogenic promoter RUNX2 in the osteogenic differentiation of stem cells. Stimulation by mechno-transduction leads to an increase in the expression and release of WNT, which once bound a receptor of the frizzled (FRZ) family, promotes the formation of a complex with axin. This complex bound axin is unable to phosphorylate β-catenin, preventing its breakdown and enabling it to transverse to the nucleus, where it binds the promoter region of the RUNX2 gene. RUNX2 heterodimerises with Cbfβ and subsequently binds the 5'-TGTGGT-3' promoter region present in the genes for osterix and the major bone matrix proteins (e.g. osteocalcin and alkaline phosphatase (ALPL)), as well as the RUNX2 promoter region; causing a positive feedback loop. Together RUNX2 and osterix further promote the transcription of the bone matrix proteins, driving the osteogenic differentiation of the cell.

The alternate bone producing pathway of endochondral ossification is required for the production of long bones in the foetus, whereby condensation of the mesenchyme begins the differentiation of MSCs in chondrocytes through Sox9 signalling (Akiyama *et al.*, 2002; Akiyama *et al.*, 2004); thereby beginning the production of a cartilaginous matrix, which becomes mineralised through hypertrophy and subsequent osteoblast inclusion. The skeleton is formed by a combination of the two processes; however, after initial formation, the majority of bone turnover more resembles intramembranous ossification (Brighton and Hunt, 1991), whilst healing is dependent on both of these processes combined.

1.1.2 Formation and maintenance of skeletal bone

Bone matrix itself is a composite material of proteins and rigid minerals, allowing for a lightweight but strong, flexible and adaptive system capable of withstanding large mechanical stresses whilst maintaining a certain degree of elasticity and remodelling capabilities. The modelling and remodelling of the bone further enables a certain degree of flexibility in its structure, either thickening or removing bone to facilitate its functional need.

This modelling to suit need occurs as a result of the activity of bone resorbing osteoclasts and bone synthesising osteoblasts. Osteoclasts originate from haemopoietic stem cells in a similar pathway to macrophages, and excrete demineralising acids and matrix proteases to actively remove mineralised bone matrix from the surface of bone, in osteoclastic pits (Boyle *et al.*, 2003). Osteoblasts, as mentioned previously, originate from MSCs (Figure 1.3), with the main function of producing mineralised connective tissue in response to resorption or healing factors. These two cell types work in response to growth factor cues from other cell types, as well as interactions between the two to produce new bone (Matsuo and Irie, 2008; Takahashi *et al.*, 1988).

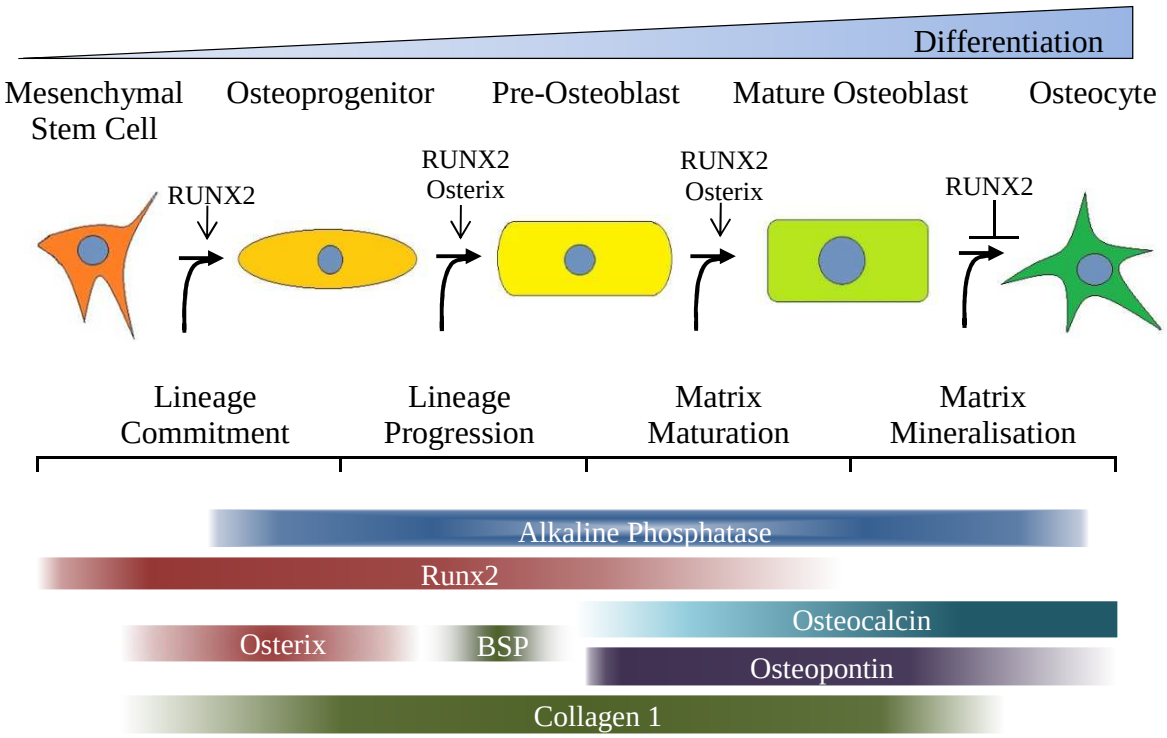

Figure 1.3: Lineage commitment of mesenchymal stem cells to the osteogenic lineage. Diagram displays the differentiation of MSCs to osteocytes, the common stages of development and essential transcription factors as well as the relative expression times and levels (colour saturation) of transcription factors (red), structural proteins (green), maturation markers (turquoise and purple) and mineralisation enzymes (blue).

The biological connective tissue is comprised primarily of type I collagen fibrils, together with a multitude of different non-collagenous connective proteins including osteocalcin, osteopontin, fibronectin, laminin, hyaluronic acid and bone sialoprotein (BSP) (Urist *et al.*, 1983; Nilsson *et al.*, 1998; Roach, 1994). The constituents of this extra-cellular matrix (ECM) can dictate the biochemical nature of the bone produced; influencing the attachment, behaviour and differentiation of osteogenic cells and osteoclasts, and ultimately determining bone production and remodelling (Hidalgo-Bastida and Cartmell, 2010). This is caused by different ECM molecules having unique adhesive and activity-regulating qualities (Frith *et*

al., 2010; Thibault *et al.,* 2007). Two such proteins, osteopontin and osteocalcin, are the most abundant non-collagenous proteins present in the ECM and are both thought to be involved in mineralisation and later resorption.

In bone, osteopontin is expressed by pre-osteoblasts and osteoblasts and to some extent resorbing osteoclasts and osteocytes (Merry *et al.,* 1993; Sodek *et al.,* 2000), in response to activation of its promoter sequence by Runx2 (Nakashima *et al.,* 2002; Ducy *et al.,* 1997). Although its function is not completely understood, osteopontin is commonly located at the mineralisation front and plays a large role in the regulation of mineral crystallinity (the type of crystals present) of the bone and remodelling (Holm *et al.,* 2014; Qiu *et al.,* 2004; Hunter *et al.,* 1996; Roach, 1994), whilst allowing binding of osteoclasts to promote remodelling (Reinholt *et al.,* 1990; Rodriguez *et al.,* 2014). Unlike osteopontin, osteocalcin (aka bone gla-protein (BGLAP)) is only produced by mature osteoblasts, and it is therefore considered a specific marker of osteoblast activity and bone production (Brown *et al.,* 1984). Primarily located in fully mineralised tissue, osteocalcin is also believed to be involved in the regulation of matrix mineral state through its interactions with the collagen matrix (Chen *et al.,* 2014; Roach, 1994). Although its function is not fully understood, the vitamin K dependent protein (Hauschka *et al.,* 1989) is able to bind hydroxyapatite through calcium binding (Hoang *et al.,* 2003), and when released from bone by resorption may be involved in endocrine regulation of insulin secretion (Lee *et al.,* 2007). Additionally, osteocalcin deficient mice only display increases in their bone density with little resorption, demonstrating that osteocalcin may also be a promoter of osteoclast chemotaxis, binding and activity (Neve *et al.,* 2013; Chenu *et al.,* 1994; Hoang *et al.,* 2003), and important for later bone remodelling (Ducy *et al.,* 1996; Roach, 1994). Together, osteopontin and osteocalcin may serve to not only bind bone cells, but also interconnect the protein lattice and improve the toughness of the ECM (Poundarik *et al.,* 2012).

Additional non-collagenous ECM proteins, such as laminin or fibronectin, dictate cell activity through specific interactions with cell surface integrins (Brighton and Hunt, 1991) and downstream signalling (Gordon *et al.,* 2009), leading to changes in cell viability and *de novo* bone formation (Au *et al.,* 2007; Jaiswal *et al.,* 2000). This tailoring of activity is essential for bone upkeep, altering lineage specificity of cells to maintain the bone (Santiago *et al.,* 2009; Frith *et al.,* 2010), which is essential in later remodelling of bone matrix (Klees *et al.,* 2007). Additionally, growth factors such as bone morphogenetic proteins (BMP) 2, 4 and 7 are encapsulated in the proteinaceous matrix (Pietrzak *et al.,* 2006). These BMPs belong to the transforming growth factor β (TGFβ) superfamily and, whilst they have no immediate structural function, they are essential controlling factors in the event of bone remodelling and the production of new bone (Chaudhary *et al.,* 2004; Urist, 1965).

This organic ECM is collectively known as osteoid, and is "glued" together with hydroxyapatite, a form of calcium mineral, which is deposited by osteoblasts whilst they produce the new organic matrix (Nefussi *et al.,* 1985; Anderson, 2003). The hydroxyapatite is then enzymatically changed by a tissue non-specific isozyme of the enzyme alkaline phosphatase (ALP) (Henthorn and Whyte, 1992; Hessle *et al.,* 2002; Orimo, 2010), a membrane bound variant present in multiple tissue types including liver, bone and kidney, but which is highly expressed in mineralising osteoblasts. Though this protein is anchored to the cell membrane, it is released by the osteoblast as part of matrix forming vesicles, which act as nucleation sites for matrix mineralisation and are essential to the formation of mineralised tissue (Morris *et al.,* 1992). Whilst the full mechanism by which this enzyme functions is not well understood, the enzyme works to increase the local concentration of phosphate ions, thereby promoting the binding of these ions to the protein/ hydroxyapatite mesh to produce the dense and strong mineralised tissue (Hessle *et al.,* 2002; Whyte *et al.,* 1994).

During the deposition of osteoid, osteoblasts may become encapsulated by their own matrix in structures known as lacunae, where they further differentiate into osteocytes. The presence of osteocytes denotes a later stage bone formation, as these cells do not proliferate and often live for extremely long periods of time. These entrapped cells communicate through a network of processes which travel through canaliculi, so that the cells may translate information and regulate bone production primarily in response to mechanical stress and damage to the rest of the structure, leading to remodelling and repair (Bonewald, 2011).

1.1.3 Remodelling of bone to suit need

In foetal development and healing, the initial, rapidly produced bone is termed "woven bone", and is characterised by the presence of unorganised collagen fibres. Whilst the composition of this mineralised ECM is identical to mature bone, its scaffold-like structure is different in organisation, osteocyte phenotype and mineral crystallinity (Shapiro, 2008), and is not as mechanically strong as lamellar bone (Buckwalter *et al.*, 1996a; Buckwalter *et al.*, 1996b). Therefore, in response to mechanical force transduction (Uthgenannt *et al.*, 2007), or fracture healing signals, entrapped osteocytes and pre-osteogenic cells signal to permit remodelling of the woven bone (Haudenschild *et al.*, 2009; Robling *et al.*, 2008; Kelly and Jacobs, 2010). This process of remodelling involves the alteration of the bones' structure, and the reorganisation of woven bone into lamellar, and in doing so establishes its mechanical strength.

Throughout remodelling, osteocytes express regulatory proteins which promote cell specialisation (Bonewald, 2011) and determine the activity of osteoblasts and osteoclasts, triggering tissue regeneration. Osteoclast activity and the resorption of bone causes the release of the growth factors and proteins locked in the bone ECM. The matrix and growth

factors present in an environment induce changes in osteogenic protein expression, ALP activity and subsequent mineralisation of the ECM thereby dictating the differentiation, maturation and activation of osteoprogenitor cells and as such the type of bone produced (Huang *et al.,* 2007; Foschi *et al.,* 2012; Supronowicz *et al.,* 2011; Smith *et al.,* 2011). These growth factors continue to activate cells in an intrinsic fashion, leading to further remodelling, thereby causing a positive osteogenic cycle (Table 1.1).

Through remodelling, a mature composite mineral matrix termed osseous tissue is formed, which accounts for the mechanical stability seen in bone. However, the osseous tissue is not one complete solid block of material; instead voids are intentionally produced and refined by the bone cells to create different structures, which ultimately help distribute the load placed upon the bone, whilst reducing weight and creating a unique niche environment in which bone marrow is contained. These structures are known as load bearing cortical and load distributing trabecular bone.

Table 1.1: Soluble and matrix factors involved in the promotion and activation of bone remodelling					
Factor	**Type**	**Released by**	**Affects**	**Function**	**References**
FGFα (Fibroblast growth factor)	Cytokine	Bone resorption Osteoprogenitor Osteoblasts	MSCs Osteoprogenitors Osteoblasts	Promotes migration and proliferation of osteoporgenitors Promotes osteogenic activity	Stoilov *et al.*, 1995 Eswarakumar *et al.*, 2002 Smith *et al.*, 2011 Chaudhary *et al.*, 2004 Nam *et al.*, 2011
TGFβ	Cytokine	Bone resorption Pre-osteoblasts Osteoblasts	MSCs Osteoblasts	Increases osteogenic gene expression including osteopotegerin	Smith *et al.*, 2011 Tang *et al.*, 2009 Takai *et al.*, 1998 Wildemann *et al.*, 2007 Chen *et al.*, 2012a
BMP2 (TGFβ superfamily)	Cytokine	Bone resorption Osteoblasts	MSCs Osteoblasts	Induces osteoblastic differentiation in MSCs and promotes osteoblast activity	Chen *et al.*, 2012a Fan *et al.*, 2014
BMP7 (OP1) (TGFβ superfamily)	Cytokine	Bone resorption Osteoblasts	MSCs Osteoblasts	Induces osteoblastic differentiation in MSCs and promotes osteoblast activity Clinical use improves graft integration	Smith *et al.*, 2011 Di Bella *et al.*, 2010a Chaudhary *et al.*, 2004 Sampath *et al.*, 1992 Chen *et al.*, 2012a Salkeld *et al.*, 2001
IGF I (insulin-like growth factor)	Cytokine	Bone resorption Osteocytes	MSCs Osteoblasts	Induces osteoblastic differentiation in MSCs and promotes osteoblast activity	Xian *et al.*, 2012 Sheng *et al.*, 2014 Huang *et al.*, 2007 Kalajzic *et al.*, 2005 Smith *et al.*, 2011
Sphingosine 1-phosphate	Cytokine	Osteoclasts	Osteoblasts	Increases RANKL expression	Ryu *et al.*, 2006
RANKL (TNF member)	Cytokine	Osteoblasts	Osteoclasts	Promotes osteoclastogenesis Increase in osteoclast activity	Udagawa *et al.*, 1999 Lee *et al.*, 2014
Osteoprotegerin	Soluble receptor	Osteoblasts Osteocytes	Binds RANKL	Binds RANKL thereby preventing differentiation and activation of osteoclasts	Kong *et al.*, 1999 Thirunavukkarasu *et al.*, 2000
Osteopontin	Bone ECM protein	Osteoblasts during osteoid deposition	Osteoclasts	Promotes binding of osteoclasts for bone resorption	Rodriguez *et al.*, 2014 Reinholt *et al.*, 1990
Osteocalcin	Bone ECM protein	Osteoblasts during osteoid deposition Bone resorption	Osteoclasts	Chemo-attractant to osteoclast cells, promoting adhesion and bone resorption	Neve *et al.*, 2013 Chenu *et al.*, 1994 Ingram *et al.*, 1994 Ducy *et al.*, 1996

1.2 Structure and function of bone

1.2.1 Mechanical function of bones

Fundamentally, bones are rigid structures which are used to support the soft tissue of the human body, allowing the binding of muscles for movement, and meeting at joints, which enables this movement. In particular, it is this mechanical function that means long bones withstand a large amount of compressive force, both in constant support of weight and in the increase in load during movement. To achieve this, long bones are cylindrical in form, and comprise of dense bone material which allows them to efficiently direct force through their structure, as well as intricate mesh like configurations, which work to evenly distribute it.

1.2.1.1 Cortical bone

The cortical bone typically forms the dense, minimally porous outer shell of intact bones and bony structures. It is surrounded by the periosteum, a connective sheath, important in bone maintenance and healing, able to produce bone in thin sections, and which supplies the bone with nutrients whilst enabling soft tissue such as muscles to anchor to the bones surface via tendons (Kojimoto *et al.,* 1988). The cortical bone is comprised of osteons, cylindrical structures produced by osteoblasts. These building blocks of bone are produced by cells surrounding blood vessels and nerves in Haversian canals, and consist of concentric layers of mineralised bone ECM termed lamellae, which are produced in a contracting manner to tightly encircle the original blood vessel (Rho *et al.,* 1998). These osteons are routinely redeveloped, with new osteons produced to surround new channels, which have been formed through the “cutting cone” action of osteoclasts (Currey, 2002; Buckwalter *et al.,* 1996b).

This type of bone material is required for direct load bearing structures, and typically the direction of the osteon depicts the direction of load the system is built to withstand. These osteon structures are relatively narrow in diameter (0.1-0.4mm), but can be several millimetres in length. These osteons, or haversian systems, are surrounded by a cement sheath, which is produced so as to bind the new structure into the original bone and reduce the risk of cracks forming in the osteon structures (Currey, 2012) (Figure 1.4).

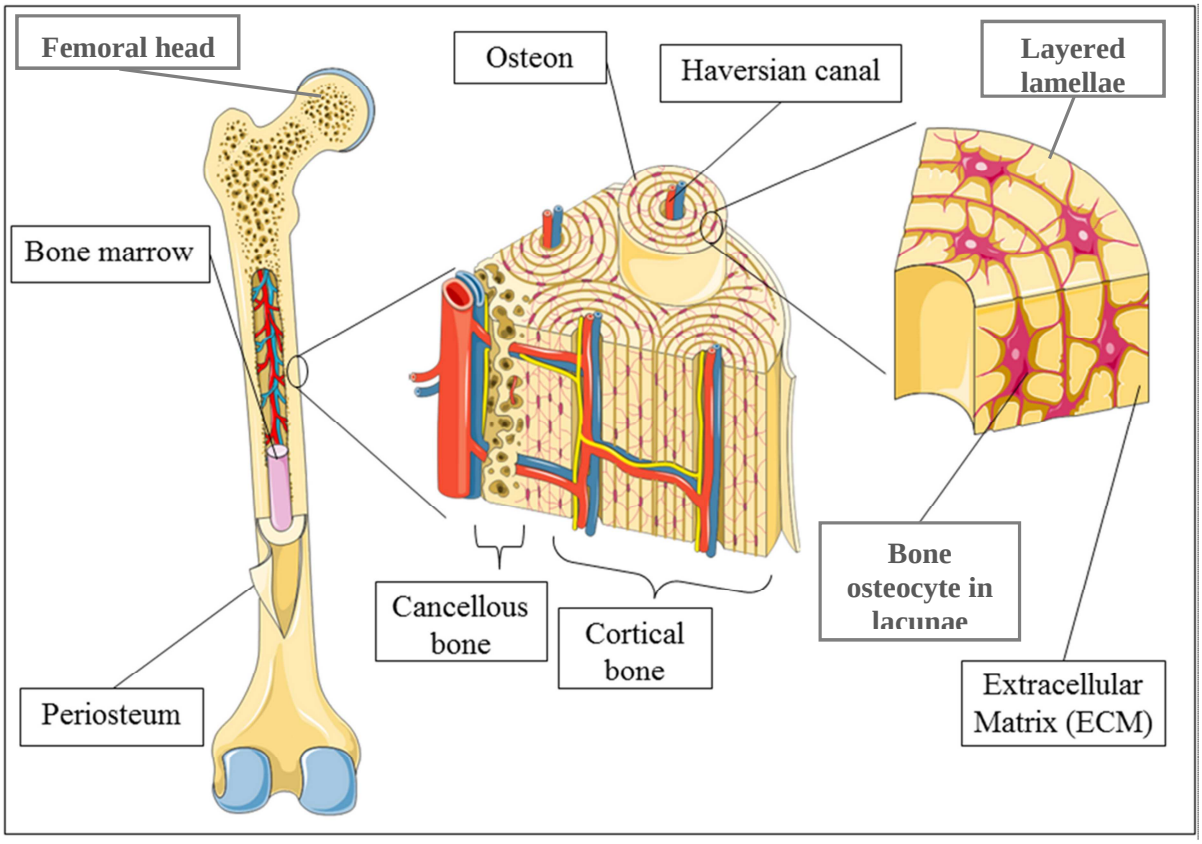

Figure 1.4: Schematic diagram depicting the basic structures of bone and cellular structures. Long bones are comprised of cortical and cancellous bone, which themselves are formed by layers of ECM termed lamellae. Osteons are fashioned using this lamellar construction and represent the building block of cortical bone. Mature osteocytes can be located in lacunae structures formed as the cells encapsulate themselves in the ECM they produce, and are connected by microscopic tubes called canaliculi. Image adapted from original by Bao *et al.*, (2012).

Where long bones join each other or the body, such as the hip, large joints allow movement whilst also supporting a normal load. The hip joint (the meeting of the femur and the pelvis) is the largest joint in the body and is able to regularly withstanding forces as high as 260% of the individuals body weight, particularly in activities such as running and jumping (Bergmann *et al.,* 2001).

In order to achieve this, a large contact area is required at the joint to allow smooth un-impinged movement, and distribution of load due to constant changes in load site. As such, the femur (the long bone involved in the hip joint) ends in a bulbous structure, known as the femoral head. The femoral head acts to enable the smooth movement of the leg, by distributing the site and directionally changing force of the moving joint into a consistent uniaxial force running down the shaft of the femur. To do so, the femoral head is internally comprised of a sponge like trabecular bone structure, rather than one solid mass of bone material, and acts to distribute the forces through compression and tension (Figure 1.5). This trabecular bone is able to collectively support a large amount of weight, while reducing the need for excess bone material, therefore reducing the total mass of the bone. Trabecular bone is therefore relatively abundant in areas where shock and sudden stresses are common, such as the end of long bones where the large joints meet, thereby absorbing and dampening the initial stress of joint impact (Hayes *et al.,* 1978).

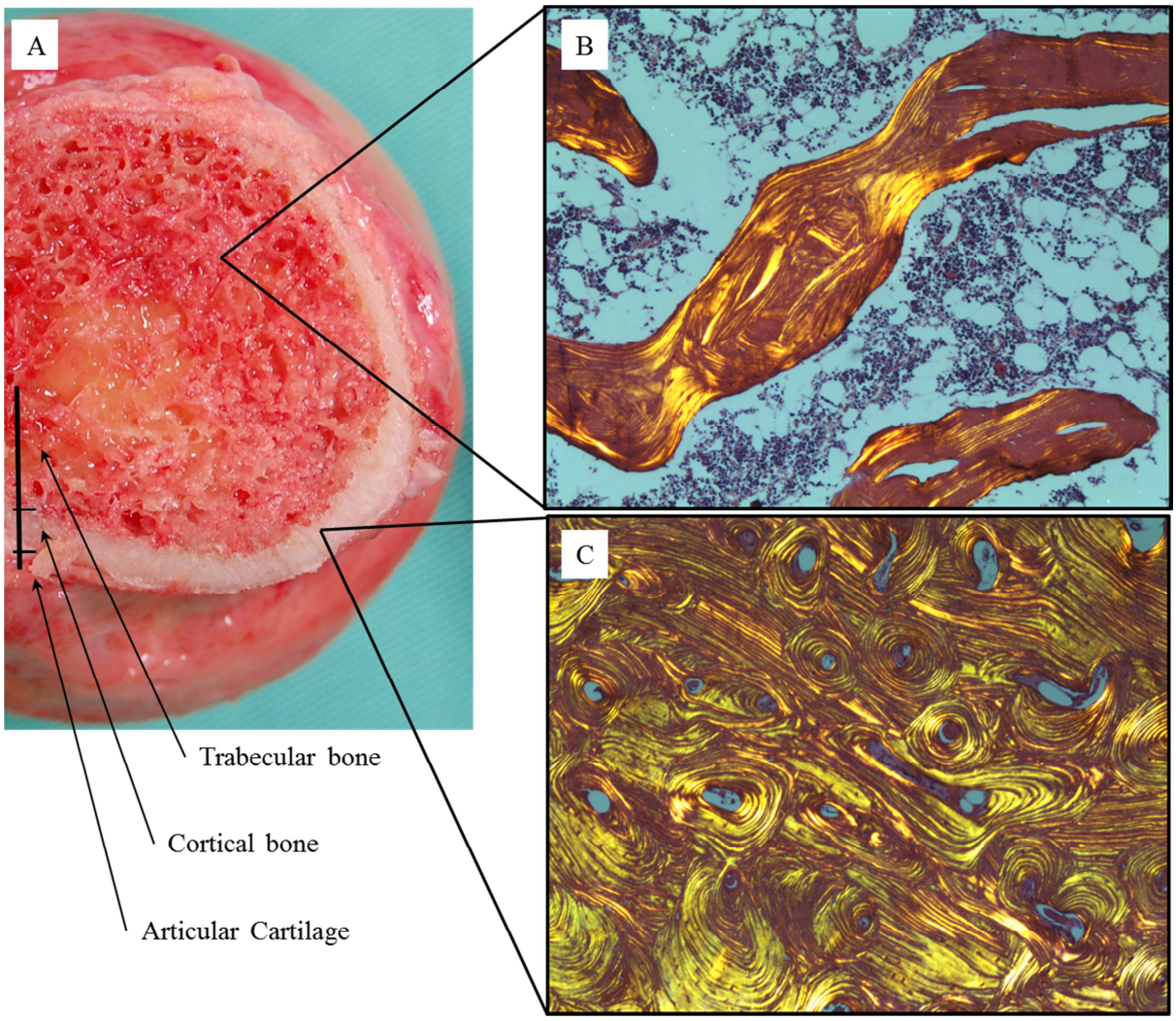

Figure 1.5: Diagram depicting the internal structure of the femoral head (A). The sponge like structure of the trabecular bone (B) within the femoral head is comprised of lamellar ECM layers, which incorporate the cell rich bone marrow. This trabecular mass is encapsulated by the cortical bone shell (C) of the femoral head, a dense form of bone comprised of osteons, which is itself covered by articular cartilage. Femoral head Image adapted from original in by Steven Fruitsmaak. (http://commons.wikimedia.org/wiki/File:Caput_femoris_cortex_medulla.jpg# mediaviewer/File:Caput_femoris_cortex_medulla.jpg). Histology images captured at x75 magnification.

1.2.1.2 Trabecular bone

This trabecular system, also known as cancellous bone, is a sponge-like mesh structure, highly porous, and encapsulated by a cortical shell and coated by the endosteum, a lining membrane of osteoblasts and pre-osteoblasts. The endosteum membrane produces new trabecular bone, by the deposition of new osteoid tissue on the trabecular struts, similar in lamellar construction to osteons. The trabecular bone, whilst not as mechanically strong as cortical, is able to support mechanical load, and works to distribute the load evenly through an interconnected lattice of trabeculae (Martin, 1991; Martin, 1984). Importantly, this mechanical distribution of force is also important in directing the osteogenic activity of cells, with the architecture (Tayton *et al.,* 2012), and rigidity (Haudenschild *et al.,* 2009) of the material promoting the osteogenic cell activity if required. As such, the trabeculae are produced in structures along the direction of compression and tension in accordance with Wolff's law (Frost, 1994), enabling the trabeculae to adapt to changing mechanical stress, preventing breakage by shear force, of which bone is relatively weak at resisting.

Whilst cortical bone contains only minimal vasculature, the cancellous structure is surrounded by blood vessels and many different cells, creating a unique niche containing the bone marrow. This marrow component is comprised of a mesh-like ECM containing multiple cell types, including haematopoietic stem cells, adipose cells, endothelial cells and erythrocytes as well as MSCs (Bianco, 2011; Augello *et al.,* 2010). Within this tissue, new blood cells are formed, growth factors are synthesised, and the large surface area in contact with bone allows for mineral ion deposition and homeostasis. This unique niche environment enables interaction between the bone matrix, marrow and bone producing cells, through either juxtacrine or paracrine pathways, and is important for osteoblast and osteoclast differentiation and bone homeostasis (Ern *et al.,* 2010; Hammoudi *et al.,* 2012).

1.2.2 Bone ageing

As the individual ages in advanced maturity, the process of decline in bone is most apparent with changes to composition and structure. The balance between the numbers and activity of osteoblasts and osteoclasts changes, with the apoptosis of osteoblasts, and a decrease in activity of remaining bone producing cells (Zhou *et al.,* 2008). The diminished osteoblast activity leads to structural changes in trabeculae (Green *et al.,* 2011; Chen *et al.,* 2008; Viguet-Carrin *et al.,* 2010; Turunen *et al.,* 2013), and increases the risk of fracture due to insufficient upkeep of the bone (Wang *et al.,* 2002). This process is most noticeable in patients with diseases in bone metabolism such as osteoporosis, in which a severe loss of bone producing cells leads to a significant decrease in bone mass and structure, particularly in the trabecular system. This can result in a very weak and fragile bone structure, which increases its susceptibility to fatigue (Li *et al.,* 2012b; Hildebrand *et al.,* 1999).

1.3 Bone healing and surgical intervention

1.3.1 The process of fracture healing in bones

Although bone is structurally rigid, it is also one of the few organs which are able to regenerate, even after sections of bone are physically separated from each other. This is in part due to the composite nature of the bone, along with the encapsulated growth factors and the response of osteoblastic, pre-osteoblastic cells and importantly multipotent stem cells, to growth factors released after a fracture. During the healing process, the action of endochondral and intramembranous ossification are utilised by the body to immobilise the fragments of bone in a healing callus and bring the pieces together. After the initial facture, this process is divided into three major phases; the inflammation of the area and initial formation of a haematoma; new endochondral bone formation; and the resorbtion of collagenous callus and it's remodelling into bone (Figure 1.6). Additionally, the process of remodelling is then used extensively in response to a healing environment, where the initial laying down of fast produced mineralised matrix is reorganised into working bone.

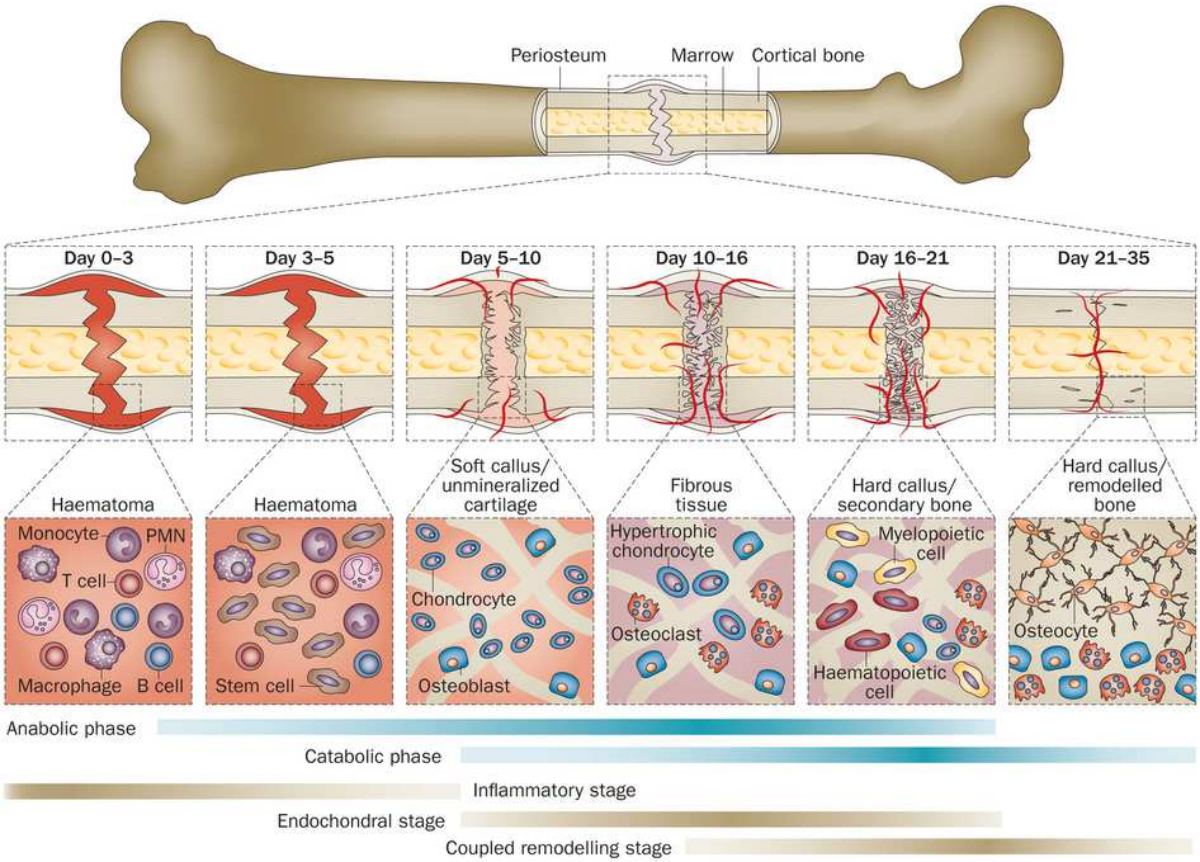

Figure 1.6: The major processes of new tissue synthesis (anabolic) and tissue remodelling processes (catabolic) during bone fracture healing. The initial formation of the haematoma is followed by the metabolic processes of bone healing through the phases of; inflammation, endochondral bone formation and coupled bone remodelling. These phases have been split into biological stages, which display the cell types present and their expected time frame (as assessed from mouse model). (Original image by Einhorn and Gerstenfeld (2015)).

1.3.1.1 The formation of a haematoma and the initiation of the inflammatory phase

As a result of fracture occurrence and damage to the normal bone, blood vessels in the Haversian canals, medullary cavity and surrounding tissue are ruptured. The damage to the local vasculature network releases blood, marrow and blood clotting factors into the fracture cleft, subsequently causing coagulation and the formation of a haematoma. This begins the process of inflammation of the fracture site and the surrounding periosteum, initiating an anabolic process to produce new tissue in an attempt to mechanically stabilise the area.

Vasospasms and vasoconstriction reduces the blood flow into the area, thereby decreasing the influx of nutrients and oxygen, and results in hypoxic conditions. The hypoxic conditions cause the release of growth factors such as PDGF (platelet derived growth factor), IGF (insulin–like growth factor), VEGF (vascular endothelial growth factor) and FGF-2 (fibroblast growth factor) by osteocytes contained in and around the damaged area as they die. These growth factors, together with the promotional effect of the hypoxic conditions, act as chemoattractants, encouraging the activation, migration and proliferation of osteogenic cells such as MSCs, pre-osteoblasts and osteoblasts (Seppa *et al.,* 1982; Stoilov *et al.,* 1995), as well as pro-inflammatory macrophages, into the healing cleft (Kark *et al.,* 2006).

The migrated cells infiltrate the fibroblast rich haematoma, orchestrating angiogenesis and osteogenic differentiation. Specifically, the inflammatory process is continued by the recruited macrophages, which increase their expression of pro-inflammatory cytokines and growth factors, such as interleukin-1 (IL) and IL-6, in turn promoting the release of VEGF (Street et al., 2002), and further promoting the migration of MSC and osteoblasts into the inflamed area (Fiedler et al., 2005; Mayr-Wohlfart et al., 2002). This influx of different cell

types and new blood vessel infiltration, transforms the haematoma into granulation tissue; a mix of loosely bound cells and perforating blood vessels.

The growth factor rich environment and inflammation, initiates an increase in the proliferation and osteogenic differentiation of MSCs and osteoprogenitor cells (Eswarakumar *et al*., 2002), present under areas of the periosteum distally (furthest away) to the fracture site. These differentiating cells release BMPs 2, 4, and 7, and other osteogenic growth factors, promoting the process of intramembranous ossification and the formation of hard tissue, surrounding the soft granulation tissue, in response to motion of the fracture site (Phillips, 2005).

1.3.1.2 Endochondral bone formation

In the periosteum and granulation tissue proximal (closest to) the fracture ends, a soft callus begins to form as undifferentiated MSCs begin to proliferate and differentiate into chondrogenic cells. A return to normoxic conditions in this soft callus results in the alteration in the growth factor PDGFβ's concentration, and a change in the ECM protein secretions of the fibroblasts in the healing cleft, promoting the release of fibrin (Seppa *et al.,* 1982). The secretion of fibrin, together with the production of collagen type II by the chondrocytes, results in the soft granulation tissue quickly developing into a collagenous callus, which further stabilises the fracture site.

Osteoblast migration to the boundary between the hard outer, and soft inner callus progresses osteogenesis through the release of signalling factors, which initiate differentiation of MSCs and pre-osteoblastic cells into osteoblasts (Smith *et al.,* 2011; Huang *et al.,* 2007). As these osteoblasts mature they cease to proliferate, and instead increase production of bone ECM

proteins such as osteocalcin and osteopontin, which are deposited by the osteoblasts as they from the tissue at the boundary.

Chondrogenic cells in the centre of the soft callus continue to proliferate and deposit new collagen type II and other cartilaginous proteins, however at the boundary with the hard callus, calcification of the cartilaginous matrix causes a phenotypic change in the chondrocytes present. These chondrocytes undergo hypertrophy, and start to produce less collagen type II, instead expressing the osteogenic transcription factor Runx2 and releasing matrix forming vesicles through a budding action. As the matrix forming vesicles, containing ALP and calcium, ossify the remaining soft cartilaginous callus, the hyperthrophic chondrocytes undergo apoptosis leaving cavities within the newly formed tissue into which osteoblasts, osteoclasts and other bone marrow cell types penetrate. The colonising osteoblasts further release bone ECM proteins and mineralise the newly formed bone material, transforming the callus into a bony state, while the osteoclast resorb the endochondral cartilaginous tissue.

1.3.1.3 Combined remodelling of the bony callus

As the callus becomes mineralised, the anabolic processes of the cells subside to lower levels, and a phase of predominantly catabolic actions begins, with only specific bone producing processes continuing. During this phase the unrequired cartilaginous matrix proteins are resorbed by chondroclasts, and in their place osteoblasts deposit and mineralise new bone ECM proteins, to produce woven bone. The unordered, structurally inferior, bulky trabecular three-dimensional (3D) lattice structure of the woven bone, initially deposited by the osteoblasts, is symptomatic of the rapid production of new bone, and is adapted by the process of remodelling; the combined action of the resorbing osteoclast and depositing

osteoblast, to produce ordered mature bone. This combined remodelling continues well after the end of the fracture healing phases, removing the unnecessary callus over time, and returning the structural integrity of the bone.

This healing process slowly returns the fracture site back to lamellar bone material which, as described previously, is adapted to suit its mechanical load requirement. Although this process is suitable for small areas of bone loss, the body is unable to heal large areas of lost bone stock. As such, surgical techniques are used to help restock areas of large bone loss, with transplanted bone material known as bone graft. Importantly, the bone graft helps bridge the healing cleft, and is tied into the existing bone through the process of osseointegration, in a very similar process to fracture healing (Boden *et al.,* 1976; Burchardt and Enneking 1978), with host-derived inflammation and initial healing aided by the presence of the bone filler.

1.3.2 Bone grafts in surgery

Surgical intervention and bone grafts are crucial in the treatment of damaged bone which has been lost through infection, disease, removal of tumour, physical trauma, and increasingly also during revision surgery such as the hip due to an ever ageing population and the failure of primary implants (De Long *et al.,* 2007). Transplantation of bone graft material in these circumstances is extremely beneficial to the patient, improving the ability of these areas to heal and remain functional (McNamara, 2010). These grafts are either autograft (from the host themselves), biological allograft (from a donor) or synthetic grafts, with each material having its individual advantages and disadvantages relating to their osteogenic and bone healing properties. However, common to the majority of graft materials used is the promotion of intramembranous ossification as a method of bone healing, as this has been shown to be superior in bone healing to endochondral ossification/healing (Wong and Rabie, 1999).

In excess of 620,000 primary hip, and 676,000 primary knee joint replacements were conducted in the UK between 2003 and 2013 (National Joint Registry, 2014) with a 14.2% rise in the total number of joint replacements undertaken in the UK between 2012 to 2013 (180,433 to 205,686). Additionally, in the US, over 800,000 primary hip and knee surgeries were conducted in 2005; however, based on historical procedure rates and population projections, it is estimated that by 2030 the number of total hip arthroplasties will have increased by 174%, from 208,600 to 577,000 procedures, and the number of knee arthroplasty procedures will increase by 673%, from 450,000 to 3.48 million (Iorio *et al.,* 2008) (Kurtz *et al.,* 2007). This constant rise in need places increasing strain on available bone stocks, as well as the performance of bone grafts themselves.

The first truly modern form of allograft bone grafting dates back to 1668 when the surgeon Job van Meekeren successfully repaired a soldier's skull by using xenograft bone material from that of a canine skull (Donati *et al.,* 2007). Today, bone graft is routinely used in numerous surgical applications (Damien and Parsons, 1991) including primary and revision hip surgeries (Patil *et al.,* 2012), maxillofacial and orthodontic surgery (Catone *et al.,* 1992), spinal fusion (Boden, 2002), total knee arthroplasty (Dorr *et al.,* 2006; Samuelson, 1988), void filling (due to exclusion of tumours or disease) (Mankin *et al.,* 1996; Donati *et al.,* 2000), and the agglutination of non-unions (Borrelli *et al.,* 2003; Megas, 2005). However, as with the first bone graft, the successful osseointegration of the bone is critical to its use in surgery. Most surgical procedures utilise the technique of impaction bone grafting (IBG) to reconstruct bone from a morcellised bone "adhesive", delivering successful outcomes (Board *et al.,* 2006b). IBG's small particle size allows it to be manipulated into small crevices and pockets, such as in revision hip surgery, where morcellised bone is compacted into the osteonecrotic recesses left by the removal of the failed primary femoral stem. Surgeons fill this recess to reconstitute the lost cancellous bone, thereby enabling cement interdigitation

and anchorage of the replacement prosthetic femoral head. An example of this role can be seen in the reconstruction of the acetabulum, whereby a “shelf graft” is produced by using bone allograft in conjunction with screws, in order to stabilise the cup prosthesis and strengthen weakened structures, thereby returning some mechanical function (Figure 1.7) (Deirmengian *et al.,* 2011; Patil *et al.,* 2012). These surgical uses demonstrate a requirement that the graft display healing capabilities as well as biomechanical stability, and though IBG is used for ease, larger particles exhibit a greater osteogenic effect (Miron *et al.,* 2011). Indeed in surgical use of grafting for implant fixation, larger bone fragments as big as 10mm have displayed superior results over small particles (Bolder *et al.,* 2003; Ullmark, 2000).

The outcome of surgery is largely dependent on successful osseointegration and fusion of the bone via the process of osteogenesis and typically surgeons look for new bone formation, and signs of osseointegration, within two weeks to two months after surgery. Therefore, grafts are required which are osteogenic, osteoconductive, can undergo resorption, contain osteoinductive cues and which are mechanically stable enough to reduce movement and allow appropriate fixation (Giannoudis *et al.,* 2007; Hutmacher, 2000). The osteoconductivity of the material relates to its ability to act as a scaffold, supporting new host-derived bone formation, and is fundamental to all grafting materials, whilst the osteoinductive capacity corresponds to the ability of the bone to stimulate osteoprogenitor cells, driving their differentiation down an osteogenic lineage, thereby directing protein synthesis and deposition for *de novo* bone formation (definitions by Albrektsson and Johansson (2001)).

Grafts deficient in these qualities lack effective osseointegration and are likely to fail. Indeed, the failure rate of allograft bone has been reported to be as high as 72% (Jeffery *et al.,* 2003), with bone unable to heal adequately due to osteonecrosis, disease or excessive fracture movement. These complications often result in non-unions (Einhorn, 1998), the loosening and failure of implants (Jeffery *et al.,* 2003; Kwong *et al.,* 1993) and insufficient

osteogenesis, and are common in already osteonecrotic tissue, such as in the management of bone lost through tumours (Mankin *et al.,* 1996; Donati *et al.,* 2000). The failure in bone healing and osseointegration in either primary or revision surgery cases requires further revision procedures, and the addition of new bone graft material, in an attempt to improve the osteogenic conditions of the site (Berner *et al.,* 2012; Ateschrang *et al.,* 2009). However, these surgical procedures are technically more complex, increasing the risk of further failure and associated patient morbidity as well as increasing cost (Pekkarinen *et al.,* 2000).

Figure 1.7: Pre-operative radiograph images of severe acetabular bone loss, and implant failure. Images display the failed acetabular cup including broken screws, with large bone loss causing loosening and migration into the pelvis (A), and the two year follow up of reconstruction of the acetabulum shelf using a structural bone allograft and reconstruction ring (B) which displays an increase in opacity of tissue surrounding implant, indicative of *de novo* bone formation, remodelling and incorporation. Images adapted from Patil *et al*. (2012).

1.3.3 Types of graft material available

The use of bone grafts has flourished to the point that there are now multiple biological and synthetic materials available. Any graft material utilised must possess properties which fulfil a biochemical and mechanical function and ultimately determine the level of integration into the host. The graft must also remain nontoxic and biocompatible allowing cell colonisation, improving osseointegration and hence bone repair.

1.3.3.1 Synthetic grafts

The use of synthetic grafts is not as prevalent as the use of biological tissue. Their limited osteoconductive and osteoinductive abilities are a hindrance, and combined with a reduced or absent rate of resorption, greatly affect healing (Zimmermann and Moghaddam, 2011). It is for this reason that biological materials are still more potent than synthetic grafts. Nonetheless, with their constructive potential having been demonstrated, synthetics are steadily becoming more prevalent in surgical procedures (Bostrom and Seigerman, 2005). Common synthetic materials include hydrogels (Burdick and Anseth, 2002; Schantz *et al.*, 2003; Castillo Diaz *et al.*, 2014), ceramics (Ohgushi, 2014), polymers (Ko and Cho, 2013) and hydroxyapatite constructs (Wolfe *et al.*, 1999; Qian *et al.*, 2013). Synthetic grafts are commonly fabricated to structurally resemble biological grafts (Binulal *et al.*, 2010), with the use of composites to enhance osseointegration and *de novo* bone formation (Polini *et al.*, 2011; Bassi *et al.*, 2012), and modifications to the materials surface to replicate natural bio-activity (Whiteside *et al.*, 2010).

1.3.3.2 Biological grafts

Biological grafts are separated into two main groups; autograft and allograft. Autografts are deemed the "gold standard" of bone grafts and currently represent the preferred form of graft available. They are derived from the host, avoiding the risk of immune response, and increasing the likelihood of osseointegration. This material is highly osteogenic and contains the osteoconductive scaffold; the osteoinductive matrix and incorporated growth factors; and importantly, osteogenic MSCs. These innate factors all contribute to promoting osseointegration.

Whilst autografts may be the gold standard, the use of this material has disadvantages. The most common location of graft retrieval is the patient's iliac crest, situated at the top of the pelvic bone. The removal of bone from this site is a complicated and dangerous procedure that can lead to a high percentage of patients experiencing moderate to severe discomfort (15% and 21.9% respectively) (Hill *et al.*, 1999) and site morbidity (Ebraheim *et al.*, 2001; Russell and Block, 2000). Additionally, this type of bone autograft has a limited availability due to being living bone removed from the patient's iliac crest, with large areas of bone removal leading to pelvic instability, increased risk of fracturing, possible bowel herniation and nerve damage (Russell and Block, 2000). Graft material from older patients also exhibits decreased osteogenic capabilities, containing fewer pre-osteogenic and osteogenic cells (Hernigou *et al.*, 2005).

Conversely, allografts are a more plentiful alternative to autograft and are harvested from organ donors, both living and deceased. However, allografts impose problems as well; namely the need for tissue typing to reduce the risk of an immune response and the possibility of disease transfer hinders their use, and thus requires processing techniques to remove potentially damaging material. These allografts have no osteogenic potential as they contain

no osteogenic cells; however they are still osteoconductive and osteoinductive and capable of osseointegration (Miller and Block, 2011), and in certain clinical situations have displayed results comparable to autograft (Lansford *et al.*, 2013).

1.3.4 Sterilisation of grafts to improve safety and osteogenic potential

Due to their superior regenerative abilities compared to synthetic grafts, biological allografts are widely accepted to be the most effective form of grafting material (Zimmermann and Moghaddam, 2011). However, although unsterilised fresh-frozen bone allograft is commonly used in the UK, it can be detrimental to patient health, containing bacterial and viral loads, such as human immunodeficiency virus (HIV) and Hepatitis C (Varettas and Taylor, 2011), as well as eliciting an immune response (Chalmers, 1959). The immune response in particular may prevent the graft from adequately integrating into the host (Sun *et al.*, 1998), as well as potentially causing further necrosis of the surrounding tissue, thereby leading to additional bone loss (Burwell, 1985). Therefore, due to this risk, donated biological allograft material undergoes strict testing, with stringent donor selection, donor blood serology and sample bacteriology and virology testing undertaken to minimise risk. However, although these tests are undertaken, the potential risks to the patient has led to some authorities advising that biological allograft should be sterilised (American Association of Tissue Banks, 2006) and that grafts should be processed as much as possible to remove any potential negative effects on the patient (2004/23/EC, 2004).

In-depth research has been conducted into the most effective method of sterilisation (Delloye *et al.*, 2007; Bostrom and Seigerman, 2005). This has led to the development of multiple methods, including gamma irradiation, chloroform/ethanol delipidation, hydrogen peroxide and supercritical CO_2, with advantages and disadvantages associated with each (Table 1.2).

However, by sterilising the material, the chemical, physical and biomechanical properties of the bone can be negatively affected, further hindering graft incorporation into the host. The most detrimental impact being the effect on biomechanical nature and biocompatibility of the bone, as its primary function is as a stable structural platform which cells can survive upon.

Table 1.2: Table demonstrating the strength of biological properties, from high (+++++) to low (+), of differently treated biological allografts in relation to the gold standard autograft.

Processing type	Biocompatible	Osteoconductive	Osteoinductive	Mechanical stability	Osteogenic	Major problems	References
Autograft	+++++	+++++	+++++	++++	+++++	Limited volume Surgical complications to patient	Miller and Block, 2011
Fresh-frozen allograft	++	+++++	++++	++++	N/A	Infection and immune response	Miller and Block, 2011
Gamma irradiation	++	++++	++	+++	N/A	Mechanical alterations Free radical degeneration Immune response	Mitchell *et al.*, 2004 Yamamoto *et al.*, 2012 Costain and Crawford, 2009
Acids (e.g PAA)	+++	++++	+++	+++	N/A	Impedes cell proliferation Matrix protein degeneration	Bormann *et al.*, 2010
Hydrogen peroxide	+++	+++	++	+++	N/A	Matrix incorporated protein denaturation	DePaula *et al.*, 2005 Beebe *et al.*, 2009
Ethylene dioxide	++	++	++	+++	N/A	Use of dangerous chemicals Reduced osteoinductive ability	Munting *et al.*, 1988 Aspenberg *et al.*, 1990
Chloroform/ Ethanol	+++	+++	++	++	N/A	Reduction of mechanical stability and degeneration of ECM	Cornu *et al.*, 2000
Supercritical CO_2	++	++++	++++	++++	N/A	Fails to adequately destroy bacterial spores Expensive apparatus	Mitton *et al.*, 2005 Spilimbergo and Bertucco 2003

1.3.4.1 Gamma sterilisation

The most common form of sterilisation, gamma irradiation, involves irradiating bone material with 25 kilograys (kGy), in order to achieve the level required to deactivate HIV and other infectious organisms (Hamer *et al.,* 1999). This process of sterilisation relies on the denaturation of biological tissue through both direct ionisation (Dziedzic-Goclawska *et al.,* 2005) or by free radicals, which are produced during the process (Akkus *et al.,* 2005). However, the processes that sterilise the material may also detrimentally affect the biological matrix and may alter the biomechanical stability, and latent osteoconductive and osteoinductive properties (Nguyen *et al.,* 2007).

Whilst irradiation to 25kGy is required for safe sterilisation, levels as low as 17kGy can cause significant changes to the strength and flexibility of the bone allograft (Currey *et al.,* 1997; Cornu *et al.,* 2000). Any decrease in matrix stability could be explained by the free radical denaturation of collagen cross-linking (Hamer *et al.,* 1996; Hamer *et al.,* 1999) allowing unhindered fracture propagation which dramatically decreases the mechanical properties of the structure (Mitchell *et al.,* 2004). Importantly, the failure in mechanical properties impacts heavily on the clinical use of the bone graft and may lead to large subsidence of the implant (Hassaballa *et al.,* 2009), a greater propensity to develop large detrimental fractures (Dux *et al.,* 2010) and a diminished resistance to fatigue crack propagation (Mitchell *et al.,* 2004), and as such requiring further surgical intervention.

Although the mechanical stability of grafts is important, the effect on biocompatibility and osteoinductive ability is also an issue with gamma irradiated material. *In vitro*, grafts which had been gamma irradiated displayed decreased cellular adhesion to the graft compared to fresh-frozen (Fawzi-Grancher *et al.,* 2009), potentially affecting the osteoclastic resorption of the material, thus affecting remodelling (Kluger *et al.,* 2003). In addition, the process of

ionisation and the action of free radicals can change lipids and proteins within the structure; producing cytotoxic agents such as peroxidised lipids (a result of irradiation) which cause cell death (Moreau *et al.,* 2000), as well as denaturing or depleting the osteoinductive matrix incorporated proteins trapped in ECM (Dziedzic-Goclawska *et al.,* 2005; Ijiri *et al.,* 1994). In addition, gamma sterilisation fails to remove the potentially immunogenic marrow material which, as previously described, may subsequently harm the integration of the bone graft.

The retention of the potentially harmful marrow material by this common sterilisation process has led to the development of a number of wash processes which may be used in conjunction with gamma irradiation, or more commonly as separate sterilisation techniques. The majority of novel cleaning methods include compound chemical and mechanical centrifuge steps designed to remove separate fractions at different stages, starting with cellular structures and ending with DNA (deoxyribonucleic acid), viral particles and soluble proteins. These methods often include a multitude of chemicals, which have the potential to alter bone chemistry and mechanical properties, and include detergents, rinses and powerful oxidising agents (Beebe *et al.,* 2009).

1.3.4.2 Wash techniques for sterilisation of bone allograft

Composite wash sterilisation methods constitute the majority of novel cleaning methods, utilising mechanical centrifugation to physically remove soft tissue marrow, and chemical washes to sterilise the matrix, denaturing DNA, viral particles and soluble proteins, even demonstrating decellularisation of the material (Ma *et al.,* 2013; Hashimoto *et al.,* 2011; Dutra and French, 2010). These methods often include a multitude of chemical detergents, rinses and powerful oxidising agents (Beebe *et al.,* 2009); however even simple washes have demonstrated an improvement in biocompatibility (Board *et al.,* 2009).

Composite techniques have been demonstrated to reduce the infectious viral particles titre by as much as $4\log^{10}$ and kill harmful bacteria such as *S. aureus, P. aeruginosa* and *B. subtilis* (Pruss *et al.,* 2003). This occurs as soft tissue is removed; allowing chemical washes to destroy biological molecules. The complete removal of marrow not only removes the potentially harmful particles, but may also improve the biomechanical property of the material, by preventing pressure build during compression which might otherwise damage trabecular structures (Halgrin *et al.,* 2012).

However, the osteoinductive qualities of the bone may be hampered by the sterilisation process, either by a single step, or a combination of multiple steps. The use of chemicals, such as acids and strong oxidisers for sterilisation purposes, has been demonstrated to reduce the latent osteoconductive and osteoinductive abilities, as well as the biocompatibility of the bone (Bormann *et al.,* 2010; DePaula *et al.,* 2005; Kluger *et al.,* 2003). However, the results of several studies utilising these chemicals in the wash methods have not recorded any alteration in the biocompatibility, osteoinductive capacity or mechanical properties of bone (Haimi *et al.,* 2009; Pruss *et al.,* 2003; Mroz *et al.,* 2006; Dufrane *et al.,* 2001) and would therefore suggest that chemical sterilisation is no more damaging than gamma irradiation (Mikhael *et al.,* 2008; Schwiedrzik *et al.,* 2011). Additionally, the majority of washes have only been tested on relatively small sized particles and as such wash process suitable for processing/sterilising large structures are still unavailable.

Nonetheless, the qualities of a grafting material can greatly affect the outcome of surgery and it is therefore important to improve the qualities exhibited by bone graft materials by removing the negative health issues of rejection and disease seen in biological allografts. Composite sterilisation techniques have the potential to completely remove the harmful marrow material, and display comparable or superior osteogenic and biomechanical qualities in comparison with gamma irradiation. As such, the utilisation of an appropriate wash

process can produce safe, biocompatible and osteoinductive bone material which is suitable for tissue engineering, and the addition of an osteogenic cell source to improve the osteogenic capacity of all grafts, diminishing potential of graft failure and the need for additional revision surgery.

1.4 Tissue engineering allografts to improve clinical outcome

1.4.1 Addition of MSCs

In bone tissue engineering (BTE), allografts act as a stable 3D scaffold to be populated by recipient osteogenic cells upon insertion into the body. The allograft itself offers no osteogenic advantage to the patient, such as is seen in autologous tissue transplant, due to the removal of the viable osteogenic and pre-osteogenic cells, such as MSCs. Tissue engineering, specifically BTE, offers the opportunity to improve the osteogenic capability of acellular allografts by combining them with growth factors and MSCs to produce enriched or "vitalised" grafts. Specifically, the addition of MSCs to an appropriate matrix environment generates improved unions (Xie *et al.,* 2007; Tiedeman *et al.,* 1991; Rougraff and Kling, 2002), with increased bone density and site vascularisation and biomechanical features *in vivo,* all essential in the process of graft osseointegration (Runyan *et al.,* 2010; Di Bella *et al.,* 2010b).

MSCs were first reported by Friedenstein *et al.* (1966) as fibroblast like cells in bone marrow, which retained their ability to proliferate and differentiate (Friedenstein *et al.,* 1987; Luria *et al.,* 1987), and can be recovered from the various areas of the body such as bone marrow, adipose tissue and dental pulp (Zuk *et al.,* 2002; Hattori *et al.,* 2004; Yamada *et al.,* 2011; Matsumoto *et al.,* 2008). These multipotent cells are characterised by their adherence to tissue culture plastic (TCP), the presence of cluster of differentiation (CD) cell surface antigens CD44, CD73, CD90 and CD105 and absence of others (e.g. CD34 and CD45), as

well as their ability to differentiate along three different lineages; adipogenesis, chondrogenesis and importantly osteogenesis (Dominici *et al.,* 2006).

Typically MSCs are isolated from a bone marrow, which also contains other bone marrow mononuclear cell (BM-MNC) types, such as pericytes, endothelial cells and osteoblasts. Whilst, this BM-MNC fraction may also be used clinically, advanced culture methods are commonly used to isolate and expand the small percentage of MSCs naturally found in the bone marrow to sufficient numbers for use in BTE. The use of these cells alone has been shown to improve the healing of non-unions (Hernigou *et al.,* 2005); however they are generally used to best effect in combination with graft material and can be further combined with growth factors, such as BMP2 and BMP7 (Salkeld *et al.,* 2001; Di Bella *et al.,* 2010b), to produce BTE allografts, which may improve the clinical outcome of graft incorporation (Figure 1.8).

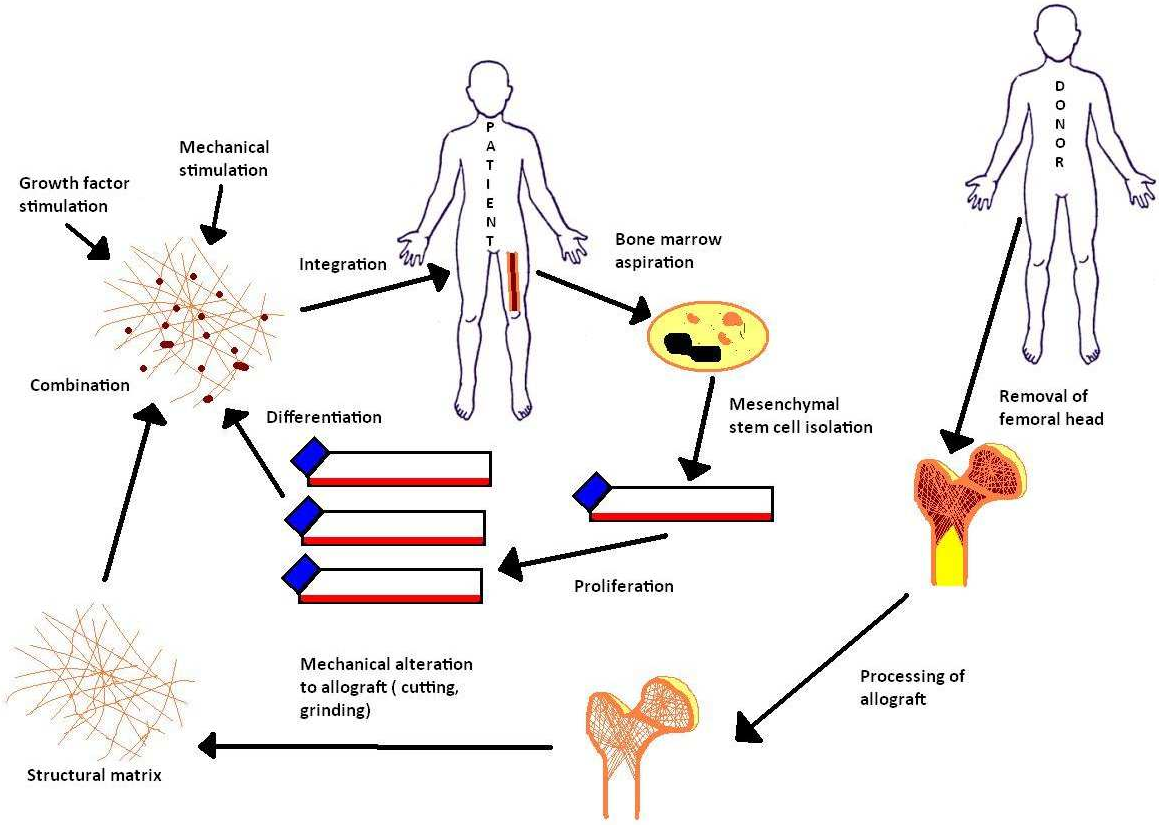

Figure 1.8: Diagram displaying the process of tissue engineering from biological allograft. Biological matrix from donor is washed and sterilised, with all biological material removed. The subsequent structural matrix is combined with cultured osteogenic cells, procured from the patient themselves, and growth factors to aid in osseointegration. This tissue engineered allograft can then be used for a surgical procedure.

1.4.2 Clinical application of MSC tissue engineered bone grafts

In clinical application, tissue engineered bone constructs have displayed potential in a varied number of fields including restoration of limb function (Quarto *et al.*, 2001), enabling return of physiological bone function and stimulating/supporting processes enabling new tooth eruption and migration (Hibi *et al.*, 2006; Pradel *et al.*, 2008).

Tissue engineered reconstruction of non-unions (Ateschrang *et al.,* 2009), large long bone defects (Quarto *et al.,* 2001; Krečič Stres *et al.,* 2007), maxillofacial surgery in augmentation of the sinus (Voss *et al.,* 2010; Shayesteh *et al.,* 2008), reconstruction of the alveolar cleft (Hibi *et al.,* 2006; Pradel *et al.,* 2008) and void in-filling after cyst removal (Pradel *et al.,* 2006; Mesimaki *et al.,* 2009), have led to mixed results in the production of mature, integrated bone.

The clinical use of synthetics grafts has enabled the construction of premade bespoke grafts which may be used to reconstruct difficult voids in load bearing positions (Quarto *et al.,* 2001). While the osteoconductive and inductive predictability of the material is assured, the general bone forming potential of the matrix is lower than that of a biological graft, at best supporting low levels of *de novo* bone formation (41.3%) and good osseointegration (93%) (Shayesteh *et al.,* 2008). The low levels of synthetic *de novo* bone formation highlight the need for biological scaffolds which are able to consistently display good osteoinductive, osteoconductive and biomechanical properties. As such, the ability to produce large biologically derived structures for bespoke grafts would be of benefit.

The relatively high *de novo* bone formation of biological grafts in clinical applications (79.1%) (Hibi *et al.,* 2006) advocates the use of materials such as platelet-rich gels, and xenograft material Osteovit® (Pradel *et al.,* 2006; Pradel *et al.,* 2008; Zambonin and Grano, 1995). Tissue engineered biological allografts have also displayed comparable, if not superior results to autograft in terms of bone density and overall bone strength (Pradel *et al.,* 2006).

However, whilst some applications have recorded excellent stability of the graft and return of structural integrity (Quarto *et al.,* 2001; Mesimaki *et al.,* 2009), a decreased rate of integration and the loss of implants have been attained by others (Voss *et al.,* 2010). This difference may be explained by the initial stability of the matrix used for the tissue

engineering, with a lower stability mesh displaying low levels of implant stability (Mesimaki *et al.,* 2009).

1.4.3 Issues associated with tissue engineered allografts

Augmented tissue engineered allograft bone material still displays decreased integration and bone growth, in comparison to autograft, and highlights the need for tissue engineered allografts with improved osteoconductive and inductive features, which will support the osteogenic addition of MSCs. This is highlighted by the low reliability and reproducibility between studies; however low patient numbers and multiple material variants also fail to demonstrate a clear hierarchy of preferred cell or matrix types (Mesimaki *et al.,* 2009). This is complicated further by the introduction of expensive culture expansion and materials (Krečič Stres *et al.,* 2007). Unfortunately, as well as being expensive, time spent in culture expansion affects cell differentiation ability, and may account for the low level of reproducibility (Yang *et al.,* 2014; Wagner *et al.,* 2008; Baxter *et al.,* 2004). Importantly, for clinical use of the patients own autologous stem cells, the age of the donor may also have a negative effect on the osteogenic differentiation and activity of cells, with increasing age resulting in fewer BM-MSC (Hernigou *et al.,* 2005) and reduced osteogenic capacity (Wagner *et al.,* 2009; Mueller and Glowacki, 2001). Additionally, lower numbers of BM-MSCs means that longer culture expansion times are required, which may result in a further decrease in osteogenic function (Niemeyer *et al.,* 2010; Cornejo *et al.,* 2012).

Colonisation of a material by culture with the osteogenic cells relies heavily on its ability to influence cell adherence, differentiation and ultimately osteogenic activity. In particular, the use of washed structures for BTE enables the use of the bone's naturally incorporated growth factors, its osteoconductive surface and mechanical stability. However as with cell age, as

described previously, the age of the donor may affect the osteogenic activity of a bone graft. As such this too may account for some of the variability seen in the clinical use of natural BTE scaffolds.

1.5 Aims of the study

Bone grafts are crucial in the treatment of damaged bone which has been lost through disease, injury or surgery. Grafts are either biological, autograft (from the patient themselves), allograft (from a donor) or synthetic. Whilst autografts are considered the gold standard, they are limited and often detrimental to the health and wellbeing of the patient. The development of increasingly safer and more sophisticated allografts has seen them becoming more common; utilising the biological structural capabilities of the donor bone, they appear to be the most effective alternative. However, their use does incur problems with tissue typing required to reduce the risk of an immune response and the possibility of disease transfer to the recipient. The sterilisation of allografts is able to remove this inherent risk to a patient's health; however this can alter the biological and mechanical properties of the graft, thus causing a diminished osteoconductive, inductive and osteogenic response from the recipient. Significantly, tissue engineering has the potential to revitalise these diminished characteristics. This process involves utilising the qualities of the biological matrix with the addition of MSCs or progenitor cells and growth factors, creating a viable alternative to the use of autografts; however this process also requires biocompatible and osteoinductive materials.

The need for sterilisation techniques, which do not reduce the biochemical and mechanical functions of the allograft as severely, has resulted in a novel wash process being developed in collaboration with the National Health Service Blood and Transplant tissue services (NHSBT) (Rooney *et al.,* 2006). This novel wash process involves a combination of warm water washes, chemical washes and centrifugation, together with sterilisation steps to clean whole femoral heads, thereby producing large amounts of bone material in a relatively fast manner. This method, based on preliminary data, reports the fast and effective removal of

99% of harmful components (Board *et al.*, 2006a). However for this to be of use clinically, a comprehensive analysis of biocompatibility, biomechanical stability and an assessment of the materials osteoinductive capacity are required.

1.5.1 Aims

The overall aim of this research is to test the ability of a novel wash process to produce a biological material/scaffold for use in BTE. In order to achieve this, the washed material must be assessed for remaining marrow contamination, its biocompatibility, biomechanical stability and its ability to support an osteogenic cell type and its osteogenic activity.

The thesis is therefore divided into the following main objectives:

Chapter 2: Assessment of the biological and biocompatibility properties of the washed bone. This will be achieved by washing living-donor bone using the novel wash process. The soluble biological marrow components contained in the waste solutions will be assessed as they are removed from the structure. The biocompatibility will be tested in both proximity and extract cytotoxicity assays.

Chapter 3: Investigation of the biomechanical properties of the washed bone in parameters of yield and failure. The washed bone will be directly compared to unwashed bone by the use of a halved femoral head mirrored sample compression model, using uniaxial load on a Lloyd system LRX plus compression rig. In addition, to ascertain whether the wash process is more or less damaging than US standard sterilisation method gamma irradiation, a more clinically relatable random axial model will be utilised to examine alterations in material strength in young and old samples for both unwashed and washed and gamma irradiated forms of both.

Chapter 4: Assessment of the potential of the washed bone to allow adherence of culture expanded BM-MSCs and support their osteogenic differentiation and activity. In addition, the effect of cell donor age and bone donor age will be examined to determine if either factor has an influence on osteogenic activity. To achieve this, BM-MSCs taken from young and old cell donors will be seeded onto bone cubes from young and old bone donors, with their relative osteogenic gene expression and ALP activity assessed.

Chapter 5: Preliminary assessment of the use of alternate sources of osteogenic cells, namely adipose derived MSCs and concentrated BM-MNC from bone marrow. As such, BM-MNCs, and MSCs from both bone marrow and adipose tissue will be seeded onto washed bone, and the seeding efficiency, viability and gene expression analysis of osteogenic genes will be assessed.

Chapter 2

Assessing the effects of a novel wash process on the biochemical and biocompatibility properties of the bone

2.1 Introduction

Fresh-frozen human allograft bone is currently the most effective alternative to the gold standard autograft, sharing many of its osteogenic characteristics. These characteristics are presently lacking in synthetic materials which has meant that clinically, biological allografts are the primary choice of allograft bone material (Zimmermann and Moghaddam, 2011). In the UK, fresh-frozen grafts are, to date, still acceptable and the most common form of bone graft material; however they require stringent quality controls including strict donor selection, serology, microbiological and viral nucleic acid testing (NAT) in order to minimise the risk of immune response and disease transfer to the patient. Despite these controls, investigations into the infectious potential of the fresh-frozen grafts have suggested an infection risk as high as 22% (Varettas and Taylor, 2011).

This continued potential for harmful disease transmission has meant that some health authorities advise that allograft material is sterilised by gamma irradiation before clinical use (American Association of Tissue Banks, 2006). Gamma irradiation involves subjecting the target material to a dose of 25kGy in order to achieve the level of radiation required to denature biological tissue and particles such as HIV and other infectious organisms (Hamer *et al.,* 1999). This denaturation occurs through an attack on biological materials either by the direct effect of gamma irradiation (Dziedzic-Goclawska *et al.,* 2005) or by free radicals, produced by the radiolytic excitation of trapped water molecules (Akkus *et al.,* 2005). However, there are many disadvantages to the use of this sterilisation method. In particular, production of cytotoxic peroxidised lipids may cause osteogenic cell death (Moreau *et al.,* 2000), diminishing the ability of host progenitor or osteogenic cells to adhere (Fawzi-Grancher *et al.,* 2009), and thereby weakening osteogenic potential of the bone. Finally, gamma irradiation fails to remove the dead cell matter and marrow which contains antigenic

cell types (Czitrom *et al.,* 1985) and thus it can still elicit an immune response (Bos *et al.,* 1983). It is for these reasons that fresh-frozen material is still favoured (Costain and Crawford, 2009).

An immune response, and possible immune rejection, by the host has the potential to delay or even prevent an osteoinductive phase and the grafts incorporation into the host bone (Sun *et al.,* 1998). The host immune response is initiated primarily through interaction of human leukocyte antigens (HLA) present on the surface of all cells. Also known as major histocompatibility complexes (MHC), there are 2 main classes (I and II), which together instruct the body as to whether a tissue is “self” or “non-self”. Within bone marrow, MHC class I antigens are present on all cells including osteoblasts, osteoclasts, bone marrow cells and adipocytes, with class II only expressed by bone marrow cells (Feng *et al.,* 2012). Alongside cell presented antigens, the fresh-frozen bone marrow also contains necrotic bodies, which further stimulate the immune system. Initially these antigens activate dendritic cells causing the release of pro-inflammatory cytokines such as tissue necrosis factor-α (TNFα), interferon-γ (IFNγ) and several chemo-attractive interleukins, which further attract innate immune system cells such as macrophages. MHC class I antigens further interact with CD8+ cytotoxic T-cells, resulting in the release of cytotoxic agents and cytokines, which continues cell activation and migration. MHC class II antigens react exclusively with CD4+ T-helper cells, and initiate an antibody mediated attack of the foreign tissue. These processes are designed to rid the area of foreign bodies; however they often lead to the destruction of surrounding tissue (Burwell, 1985).

The response by the host is thought to be both cell and antibody mediated, similar to any organ rejection, and even extends to severe inflammation (Burwell, 1985) and the destruction of the vasculature network leading to areas of necrosis, further slowing down osseointegration. Guidelines by the European directive (2004/23/EC, 2004) for the use of

tissue and cells from donors, implies that allografts should be processed to remove as much risk as possible to the patients' health. As such, it is therefore only prudent that the marrow material should be removed from allograft bone to improve biocompatibility, and subsequently the overall clinical outcome of the graft.

Alternative sterilisation or wash methods have been described for human bone material, either in addition to, or as a replacement for gamma irradiation and are being used clinically in varying amounts (Bostrom and Seigerman, 2005). These methods utilise mechanical centrifuge and chemical washes to sterilise the matrix, denaturing DNA and soluble proteins to remove the soft tissue, leaving behind a scaffold devoid of cellular material, whilst retaining biocompatibility and its latent osteoinductive and osteoconductive abilities (Hassaballa *et al.*, 2009). Though simple washes have demonstrated a beneficial influence on biocompatibility (Board *et al.*, 2009), wash methods often include a multitude of chemical detergents, rinses and powerful oxidising agents to ensure removal of bacterial and viral material as well as dead, native cells (Beebe *et al.*, 2009). Unfortunately, the use of strong chemicals and processes may also affect the biocompatibility of the structure (DePaula *et al.*, 2005; Kluger *et al.*, 2003), although wash methods including peracetic acid (PAA) (Haimi *et al.*, 2009; Pruss *et al.*, 2003) and alcohols (Mroz *et al.*, 2006) demonstrate little to no effect on the biocompatibility of the material. This study utilised a novel bone allograft wash process developed by the NHSBT blood and tissue services, to remove marrow from whole femoral heads. This wash process is a modification of that published by Yates *et al*. (2005) to include the chemical sterilants PAA and hydrogen peroxide alongside multiple wash centrifuge steps and warm water baths.

2.1.1 Aims

The potential for complete removal of immunogenic cellular components has led to marrow removal techniques becoming more prevalent in the production of biological materials required as scaffolds in tissue engineering applications (Ma *et al.*, 2013; Hashimoto *et al.*, 2011; Dutra and French, 2010). Although these wash processes may remove the dead marrow material, and in doing so improve the access of the structure for cell seeding, it should not weaken the beneficial properties of the graft.

This study was therefore designed to assess the efficacy of a novel wash process developed by the NHSBT, and ascertain the effect its use may have on the biocompatibility of the bone. As such, the initial aims of this study were to i) assess the efficacy of removal of the dead marrow material from the bone during the wash process, and ii) examine the biocompatibility of the wash bone graft compared to unwashed fresh-frozen controls.

2.2 Materials and methods

2.2.1 Utilisation of a novel wash process on whole femoral heads

2.2.1.1 Femoral head acquisition and cohort details for wash efficiency

Fresh-frozen femoral heads were obtained, with ethical approval, through the NHSBT Tissue Services, from consenting live donors undergoing hip replacement surgery. For the assessment of wash efficiency, a total of 13 femoral heads were used from individuals aged below 50 years of age (YOA) (young) (N=5, aged 38–46 years, mean 42 years) and above 70 YOA (old) (N=8, aged 71–82 years, mean 77 years); for full details see Table 2.1. Following removal from the donor, femoral head samples were stored at -80°C until required.

Table 2.1: Femoral head sample details for biochemical testing of wash protocol efficiency

Sample ID.	Sex	Age (years)	Experiment used
≤50 YOA			
457 356	Male	38	Wash Efficiency
457 282	Male	41	Wash Efficiency
458 034	Female	42	Wash Efficiency
457 354	Male	43	Wash Efficiency
447 995	Male	46	Wash Efficiency
≥70 YOA			
151 300	Female	71	Extended Wash
447 799	Male	71	Extended Wash
156 251	Male	77	Wash Efficiency
449 505	Female	77	Wash Efficiency
457 447	Male	78	Wash Efficiency
452 911	Male	79	Extended Wash
455 486	Male	79	Wash Efficiency
459 330	Male	82	Wash Efficiency

2.2.1.2 Femoral head wash process

Whole fresh-frozen femoral heads were removed from -80°C storage and defrosted overnight at 5°C. All external soft tissue was removed using a scalpel and forceps, before the femoral neck was detached using an oscillating De Soutter saw (NS3A De Soutter; Aston Clinton, Buckinghamshire, UK) opening up the femoral head to the wash process. The femoral neck was included in the wash process as a separate piece to maximise available material.

The femoral heads were first submerged in 300ml distilled water (dH_2O), pre-heated to 60°C, and sonicated in an ultrasonic water bath (F5300b; Decon, Hove, UK) for 15 minutes at 60°C. A temperature of 60°C was chosen to ensure the liquidation of the lipid component of the bone marrow, whilst simultaneously acting to pasteurise it. The femoral heads were transferred to 300ml fresh dH_2O preheated to 60°C and agitated on an orbital shaker (IOC400; Weiss-Gallenkamp, Loughborough, UK) at 200rpm, 60°C, for five minutes, then transferred into 300ml of dH_2O and agitated at 200rpm for 30 minutes at 60°C. The femoral heads underwent a centrifuge-wash combination three times, in which they were first placed on bespoke perforated platforms within the sample pots (Figure 2.1) and centrifuged at 1850*xg* for 15 minutes at ambient temperature in a floor standing centrifuge (Sorvall, using rotor RC3BP; Thermo Scientific, Hemel Hempstead, UK), then submerged in 300ml dH_2O preheated to 60°C, and agitated in an orbital shaker at 200rpm, 60°C for 10 minutes. After three centrifuge-wash steps the femoral heads were sonicated for 10 minutes at 60°C in 300ml pre-warmed (60°C) sterilant solution containing 3% hydrogen peroxide (v/v), (H3410; Sigma-Aldrich, Gillingham, UK) and 0.02% PAA (v/v) (77240; Sigma-Aldrich, Gillingham, UK), in dH_2O (Patent pending). Samples were transferred to 300ml of 70% (v/v) ethanol and sonicated for 10 minutes at 21°C. Finally, femoral heads underwent two washes in 300ml dH_2O, and agitated at 200rpm for 10 minutes at 60°C, before being centrifuged at 1850*xg* for

15 mins at ambient temperature to remove any remaining liquids (Table 2.2) (Smith *et al.*, 2014a).

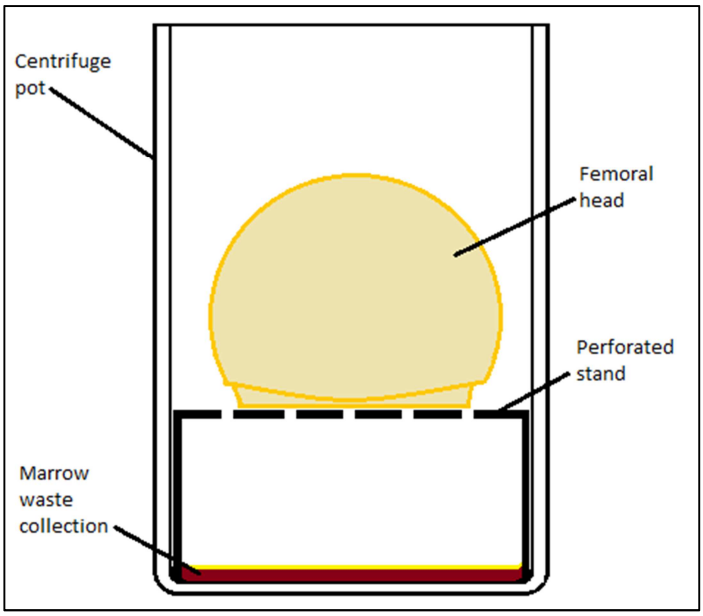

Figure 2.1: Bespoke centrifuge pot for the separation of femoral head from marrow material during centrifugation. Femoral heads were placed on a perforated platform inside of a centrifuge pot, thereby elevating them from the marrow waste removed during centrifugation.

Table 2.2: Wash procedure protocol for use on whole femoral heads

Step No.	Description	Solution	Temp (°C)	Time (Mins)
1	Sonication	dH_2O	60	15
2	Rinse	dH_2O	60	5
3	Wash 1	dH_2O	60	30
4	Centrifuge 1	NA	21	15
5	Wash 2	dH_2O	60	10
6	Centrifuge 2	NA	21	15
7	Wash 3	dH_2O	60	10
8	Centrifuge 3	NA	21	15
9	Wash 4	dH_2O	60	10
10	Chemical sterilants	3 % H_2O_2, 0.02 % PAA	60	10
11	Ethanol	70 % Ethanol	21	10
12	Wash 5	dH_2O	60	10
13	Wash 6	dH_2O	60	10
14	Centrifuge 4	NA	21	15

2.2.2 Assessment of wash efficiency through evaluation of residual material in washed femoral heads

The efficiency of the wash process in removing the soluble marrow components from the whole femoral heads was assessed in order to ascertain effectiveness and quality assurance.

This was achieved by comparing the sum of the detectable soluble factors present in the spent wash solutions to a sample taken from a final residual step. This step was designed to remove any remaining soluble marrow components after the wash process, as a quality assurance assay. As such, an additional wash step was conducted. For this additional wash step, an intact half of a femoral head was required. Therefore, washed femoral heads were laterally bisected along the coronal plane to produce two equal halves. One half was used while the other was stored for further use. The femoral head half from each donor was weighed and submerged in dH_2O, pre-heated to 60°C, equal to 5x (ml) its weight (g). These were agitated at 200rpm for one hour at 60°C. This residual wash solution sample was assessed alongside samples taken from during the waste wash solutions.

2.2.2.1 Assessment of soluble marrow components in waste solutions

To assess the removal of marrow contaminants from the whole femoral head, samples of wash solutions were collected after each step of the protocol (N=14). Biochemical assays were used to test for the contaminants; DNA (PicoGreen), soluble protein (Bradfords) and haemoglobin (Drabkins). These techniques were used to assess the presence of these factors in the used wash solutions discarded during the sterilisation process, thereby assessing their removal from the bone.

2.2.2.1.1 DNA assay

The DNA content of waste solution samples were assessed by PicoGreen assay, performed according to the manufacturer's protocol (P7589; Life Technologies, Paisley, UK).

Distilled water was used to dilute 20x Tris-EDTA (ethylenediaminetetraacetic acid) (TE) buffer stock (supplied with kit) to 1x TE for use in the assay. Pico-green reagent was diluted 200-fold using 1x TE buffer to its working concentration. Serial dilution of supplied DNA standard stock (100mg/ml) was used to produce a high DNA concentration eight point standard curve with values 1000, 500, 250, 125, 62.5, 31.25, 15.625 and 7.81ng/ml (concentrations correct after PicoGreen reagent addition).

Samples were diluted as needed in 1x TE buffer before 50µl of each was plated in triplicate in a 96-well fluorescence plate (B1196-51A; Thermo Scientific, Hemel Hempstead, UK) along with standards and blank (TE buffer), and mixed in a ratio 1:1 with 50µl of PicoGreen reagent. The plates were incubated for five minutes at 21°C in the dark, and read at 485/528nm (FLx800; BioTek, Bedfordshire, UK). The equation of the trend-line for the standard curve was used to convert raw data into actual DNA values.

2.2.2.1.2 Protein assay

The soluble protein content of waste solution samples was assessed by Bradford assay (B6916; Sigma-Aldrich, Gillingham, UK), run according to the manufacturer's protocol.

A BSA (bovine serum albumin) stock solution (2000mg/ml) was made by dissolving 2000mg of BSA (A9418; Sigma-Aldrich, Gillingham, UK) in 1ml of dH_2O, and serial dilution used to create an eight point high concentration standard curve with values 1000, 500, 250, 125, 62.5, 31.25, 15.625 and 7.81mg/ml (concentration correct after addition of Bradford reagent).

Samples were diluted as required using dH_2O. A 50µl aliquot of each sample was loaded in triplicate into a clear 96-well incubation plates (3860-096 (Iwaki); Thermo Scientific, Hemel Hempstead, UK) before 50µl of Bradford reagent was added to all wells. Plates were then incubated for five minutes at 21°C before being read at 595nm (ELx808; BioTek, Bedfordshire, UK). A standard curve was produced and the equation of its trend-line used to convert raw data into mg/ml protein values.

2.2.2.1.3 Haemoglobin assay

Drabkins solution (D594; Sigma-Aldrich, Gillingham, UK) was used to analyse the Haemoglobin present on the waste solutions, as this method reduces variable background readings, which could otherwise have produced spurious results. Drabkins reagent was produced by adding one vial (5ml) to 1L dH_2O and 30% (v/v) Brij 35 solution (B4184; Sigma-Aldrich, Gillingham, UK) added according to manufacturer's protocol. This reagent solution was filtered using a 0.45µm filter (2053-025; Thermo Scientific, Hemel Hempstead, UK) before use to remove insoluble particles. A Cyanmethemoglobin stock solution was created by dissolving 180mg of human haemoglobin (H7379; Sigma-Aldrich, Gillingham, UK) per 1ml of Drabkins solution. The Cyanmethemoglobin solution was diluted 250-fold by adding 40µl to 10ml of the Drabkins solution. This in turn was used to produce the standards of 717, 478 and 239µg/ml. Waste solution samples were filtered using 0.45µm filters to remove impurities, particularly bone fragments and fat globules which could greatly affect the assay, and diluted using dH_2O as required. Finally, 100µl of samples and standards were plated in 96-well clear incubation plates and mixed with 100µl of Drabkins solution. The plate was incubated for five minutes at 21°C and read at 540nm (ELx808; BioTek, Bedfordshire, UK). Similar to DNA and protein, the equation for the standard curve trend-line was used to convert raw data into actual values of µg/ml.

2.2.3 Re-assessment of wash efficacy after elimination of geode material from femoral head.

The dissection of the femoral head halves exposed sub-chondral cysts (geodes) and osteophytes in the femoral heads which, due to their enclosed structure, were not affected by the wash protocol (Figure 2.2). The femoral heads used in this study were clinically rejected samples from living patients; in deceased donor samples these types of structures are considered rare. Therefore comparative studies on both halves of bisected, washed femoral heads (N=3, see Table 2.1 for full details) were used to determine if this geode material significantly altered the residual contamination. One half was kept “intact” whilst geode material was removed from the other with a De Soutter saw, to excise usable trabecular material. Figure 2.3 displays the femoral head halves before and after this procedure.

An extended residual wash protocol was undertaken to assess the efficiency of the wash process and the remaining level of contamination in only the wash trabecular material. In addition to the residual wash protocol (described in section 2.2.2), the femoral head halves were centrifuged at 1850*xg* for 15 minutes at 21°C. The combination of residual wash and centrifuge was repeated three times with a final wash in dH_2O. Samples taken from the waste solutions were tested for DNA, protein and haemoglobin contamination (as described in section 2.2.2.1). Together these additional waste solutions signified a more detailed assessment of residual contamination.

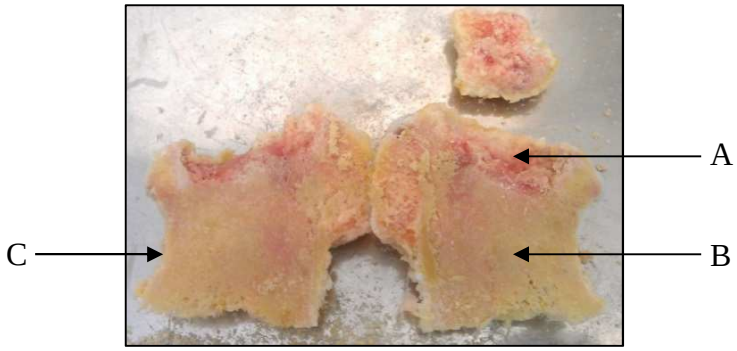

Figure 2.2: Photograph displaying unwashed geode in washed femoral head. Presence of the geode (A) in the femoral head, leads to thickening of the surrounding trabecular material (B). This trabecular material, together with the cortical shell (C) traps the marrow, meaning the head is insufficiently washed.

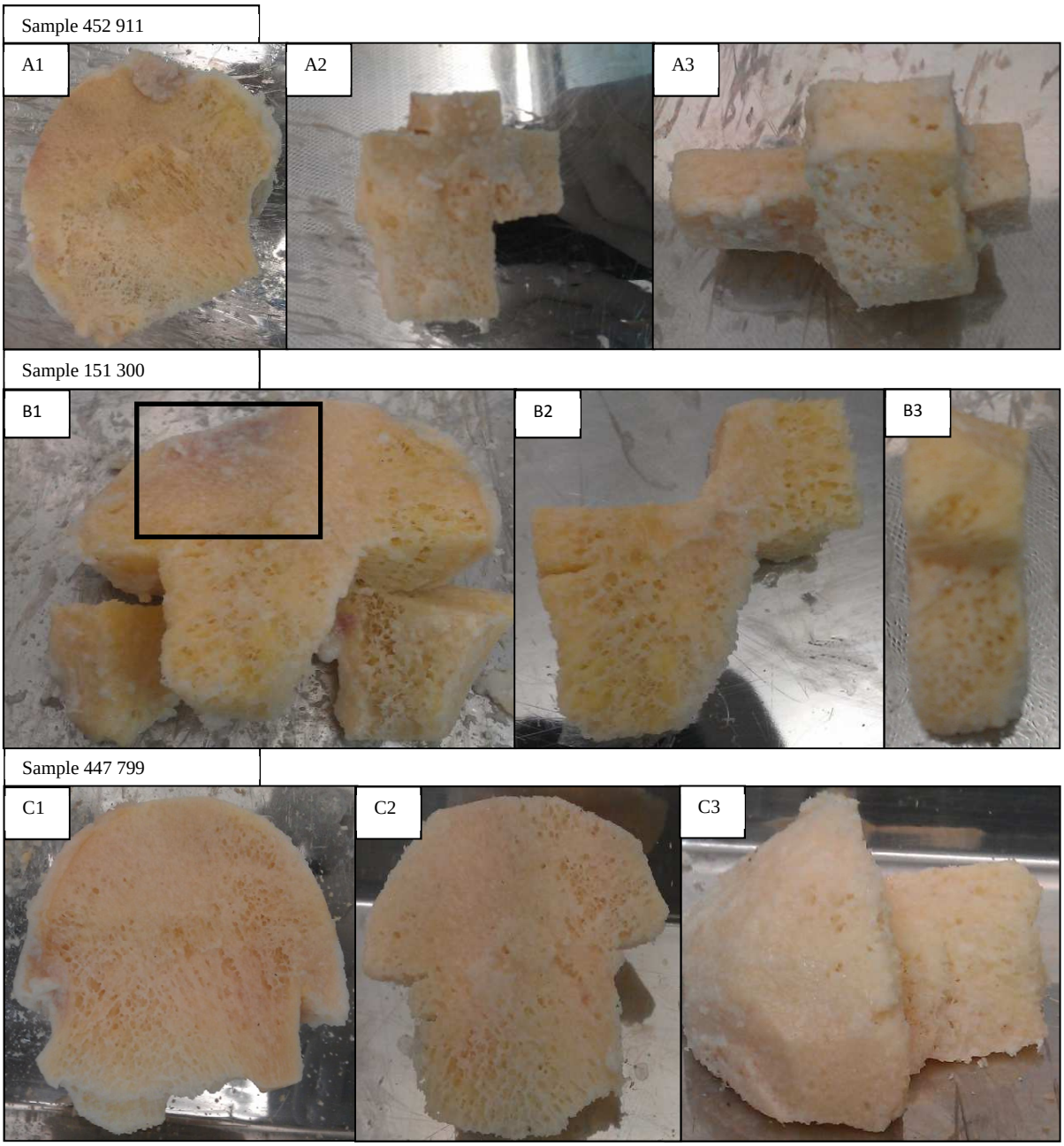

Figure 2.3: Dissection process of washed femoral heads, demonstrating the removal of the cortical shell and sub-chondral cysts to excise trabecular material. Images display the uncut femoral head halves of three different donors (A1, B1 and C1) and the subsequent trabecular material excised after the removal of geode material via the use of a De Soutter saw (A2+A3, B2+B3, C2+C3). Boxed area in B1 displays a sub-chondral cyst (geode) highlighted by the dark colour exhibited by the material.

2.2.3.1 Washed femoral head dissection and storage

The washed femoral heads were dissected as needed using an oscillating De Soutter saw. The washed bone material used in further experimentation was cut from washed femoral heads into $1cm^3$ bone cubes using a grid marker. These samples were snap-frozen in liquid nitrogen, and stored dry at -80°C until use.

2.2.4 Assessment of acellularity of washed bone

To support the wash efficiency data and assessment of marrow component removal from the washed femoral heads, a DNA quantification and degree of fragmentation experiment was conducted on washed bone cubes.

2.2.4.1 Residual DNA isolation

Bone cubes from unwashed fresh-frozen (N=3) and washed (N=3) femoral heads (one cube/femoral head) were snap frozen and impacted using a pre-chilled piston and cylinder to produce a fine powder. Digestion of the bone powder and subsequent DNA extraction from the digested samples, was undertaken using the DNeasy Blood & Tissue kit (69506; QIAGEN Ltd, Manchester, UK) and proteinase K (19131; QIAGEN Ltd, Manchester, UK). For each powdered block, a 100mg sample was digested in 40µl proteinase K and 360µl of pre-warmed (56°C) ATL buffer solution (final concentration 2.4mU(units)/ml) and incubated in a heat block at 56°C for 48 hours with occasional agitation. After incubation, the digest was vortexed (PV-1, Grant instruments, Shepreth, UK) and 400µl each of buffer AL and 100% ethanol added with vortexing to produce a homogenous sample.

For DNA extraction, 650µl of digest solution was pipetted into a DNeasy mini spin column and centrifuged to enable the adherence of the DNA to the membrane. This process was repeated until all the digest solution had been used. The column was then washed in accordance with the manufacturer's protocol, before the DNA was eluted with 200µl AE buffer. The elution step was repeated and the eluents combined to maximise the DNA yield from the membrane.

2.2.4.2 Assessment of DNA Concentration

The isolated DNA was concentrated using ethanol precipitation. To each 400µl extracted DNA sample, 40µl (10% v/v) of 300mM sodium acetate, 1ml (2.5x volume) of 100% ethanol and 1.5µl Glycoblue (AM9516; Life Technologies, Paisley, UK) (for improved visualisation of the pellet), were added and mixed gently together by inversion so as not to cause any accidental DNA fragmentation. This solution was then incubated at room temperature for one hour, before being centrifuged at 12,000*xg* for 30 minutes at 4°C to produce a blue pellet. The supernatant was removed from the pelleted DNA and replaced with 1ml of 75% ethanol. The pellet was carefully dislodged from the side of the microcentrifuge tubes (MCT) and washed by inverting several times. The MCT was centrifuged at 12,000*xg* at 4°C for 15 minutes and the supernatant removed to expose the pellet which was allowed to air dry for three minutes at room temperature. The dried pellet was resuspended in 20µl 1x TE buffer (93302; Sigma-Aldrich, Gillingham, UK) and incubated for one hour at 60°C on a heating block with intermittent vortexing to fully dissolve.

2.2.4.3 DNA quantification

The total DNA of each sample was quantified using a Nanodrop spectrophotometer (ND1000; Thermo Scientific, Hemel Hempstead, UK). After blanking with TE buffer, a 1µl sample was placed on to the machine and the nucleic acid programme run for DNA-50 sample types. The optical density value taken at 260nm was multiplied by a conversion factor of 50 to calculate concentration, whilst the 260/280 and 260/230 ratios were used to determine quality in regard to protein, phenol and salt contaminants. The Nanodrop pedestal was cleaned with dH_2O and wiped between each sample to prevent cross contamination.

2.2.4.4 Analysis of DNA fragmentation

To assess whether the DNA extracted from the digested bone was intact or fragmented, end-point polymerase chain reaction (PCR) using Platinum Taq DNA polymerase (10966-034; Life Technologies, Paisley, UK) was performed with primers for the gene GAPDH (Glycetaldehyde-3-phosphate dehydrogenase) (Sigma-Aldrich, Gillingham, UK) (Table 2.3). Similar methodology has been used before (Ma *et al*., 2013) and the technique has been shown to amplify only intact DNA.

Table 2.3: List of primers used for PCR amplification of GAPDH

Target Gene	Forward Primer (5'>3')	Reverse Primer (5'>3')	Gene variants	Accession no. (Gene bank)	Product Size (bp)
GAPDH	GGG CTG CTT TTA ACT CTG GT	GCA GGT TTT TCT AGC CGG	GAPDH Variant 1	NM_002046.4	700
			GAPDH Variant 2	NM_001256799.1	700

The extracted DNA (described in section 2.2.4.3) was diluted using molecular grade water (455847D; VWR, Lutterworth, UK) to a final concentration of 1ng/µl. A 1µl (1ng DNA) volume of each diluted sample was then mixed with 24µl Master Mix (Table 2.4). Reactions were then performed on an MJ research PTC-200 Thermocycler (GMI Inc, Minnesota, USA).

Table 2.4: Conventional PCR using Platinum® Taq master mix reaction

PCR Master Mix reagent	Volume of reagents (µl)	Final concentrations
10x PCR buffer -$MgCl_2$ (10966-034 kit)	2.5	1x
50mM $MgCl_2$ (10966-034 kit)	0.75	1.5mM
5nM dNTP mix (18427088; Life Technologies, Paisley, UK)	1	0.2mM
100µM Forward primer	0.25	1µM
100µM Reverse primer	0.25	1µM
Platinum® Taq DNA polymerase enzyme (10966-034 kit)	0.125	2.5U/rxn
Molecular grade water (VWR)	19.125	NA

An optimisation study was conducted for both annealing temperature and cycle number to ensure amplification of a single fragment of the intended molecular weight within the exponential phase of the reaction. A range of annealing temperatures from 54°C to 62°C were tested, increasing in 2°C increments, as well as the number of reaction cycles from 20 to 34, increasing in 2 cycle increments. For this study, 22 cycles of an end-point PCR program (Table 2.5) using 60°C annealing temperature was found to be optimal for visualisation of product.

Table 2.5: Thermocycler conditions for conventional PCR reaction

Step	Temperature (°C)	Time length (Minutes)	Cycle details
1 – Activation step	94	1:30	
2 – Denaturation	94	0:30	Step 2–4 repeated for 22 cycles
3 – Annealing	60	0:30	
4 – Extension	72	1:20	
5 – Finish	4	∞	

2.2.4.5 Agarose gel DNA electrophoresis

To visualise amplified DNA, agarose gel electrophoresis was used to separate the DNA fragments by size. A 2% (w/v) agarose gel was produced by dissolving 1g of agarose powder (A9414, Sigma-Aldrich, Gillingham, UK) in 50ml 1x TAE (Tris-acetate EDTA) buffer (BDHA443847D, VWR, Lutterworth, UK) with 5µl of GelRed (730-2956P; VWR, Lutterworth, UK) to enable visualisation of the DNA under fluorescence (302nm). Two microlitres of DNA orange (R0631; Thermo Scientific, Hemel Hempstead, UK) was added to 10µl of each sample and mixed before being pipetted into lane wells. A 100bp DNA ladder (N0467; New England Biolabs, Hitchin, UK) was included on the gel for size comparison. The agarose gel was submerged in TAE buffer and run in an electrophoresis gel tank (Mini-Sub®; BIO-RAD, Hemel Hempstead, UK) at 100V (PPV 300/200.4; Northumbria Biologicals Ltd, Cramlington, UK), until the dye front had migrated to the end of the gel (approx. 45 minutes). Gels were transferred to a transilluminator gel analyser for visualisation and image capture (GeneGenious Bio Imaging stem; Syngene, Cambridge, UK). Images were viewed using Gensnap imaging software (Syngene, Cambridge, UK).

2.2.5 Histological assessment of washed bone cubes

2.2.5.1 Processing bone samples to paraffin wax

Cubed bone samples from the unwashed fresh-frozen (N=2) and washed bone (N=2) were fixed in 50ml formal saline (4% (v/v) formaldehyde, 0.9% (w/v) sodium chloride) at room temperature for in excess of 48 hours, then decalcified in 20% (v/v) EDTA (pH 7.4), which was replaced every three to four days to prevent saturation. X-ray radiographs (43855A Fixatron X-ray system; Hewlett Packard) were taken (50mA, 10 seconds) of each sample and

used to determine levels of decalcification. Once decalcified, bone samples were drained and washed for 24 hours in fresh running water to remove traces of EDTA.

Bone samples underwent automated chemical dehydration and wax fixation (Shandon: Citadel 2000; Thermo Scientific, Paisley, UK) using industrial methylated spirits (IMS) (11442874; Fischer Scientific, Loughborough, UK) and xylene (10418473; Fischer Scientific, Loughborough, UK) according to a programed schedule (Table 2.6).

Table 2.6: Automatic wax processing schedule for bone cubes

Processing fluid	Time length (Hours)
50% IMS	5
70% IMS	5
99% IMS	5
99% IMS	5
99% IMS	5
99% IMS	5
99% IMS	5
Xylene	5
Xylene	5
Xylene	5
Molten wax	5
Molten wax	11

Samples were removed to a vacuum oven (VDL 53; Binder, Tuttlinger, DE) for two hours to remove all traces of xylene and ensure full wax penetration, before being embedded in histological paraffin wax blocks. All embedded samples were cut to 5µM sections using a Microtome (Shandon Finesse 325; Thermo Scientific, Paisley, UK) and mounted onto positively charged glass slides (4951PLUS4 Superfrost® Plus; Thermo Scientific, Paisley, UK).

2.2.5.2 Histological staining

2.2.5.2.1 Masson's trichrome

To perform a Masson trichrome (MTC) stain the mounted bone cube sections were de-waxed by emersion in xylene, four times for five minutes, and rehydrated by emersion in 99% IMS, four times for five minute each time.

Equal volumes of Weigerts iron Haematoxylin A (HS375; TCS Biosciences, Buckingham, UK) and B (HS380; TCS Biosciences, Buckingham, UK) were mixed to produce a working stain. Slides were soaked in dH_2O for five minutes before approximately 200µl of the Weigerts iron Haematoxylin stain was added carefully in a drop wise manner onto each section and incubated for 10 minutes at room temperature. After being rinsed with deionised water, the slides were soaked for five minutes in running tap water. Sections were then stained in 200µl of Ponceau acid fuchsin solution (RRSP131-c; Biostain, Manchester, UK) and incubated for 10 minutes, before being soaked in running water for five minutes or until excess stain was removed. Sections were drained of water then differentiated in 200µl phosphomolybdic acid solution (RRSP172-c; Biostain, Manchester, UK) for 10 minutes.

Slides were washed in dH_2O for five minutes and drained, before 200µl Masson Aniline blue (SP972; GCC diagnostics, Deeside, UK) was added and incubated for five minutes. Slides were drained and without being washed, 200µl acetic acid was added (UN:3265; GCC Diagnostics, Deeside, UK) for five minutes. Finally, slides were washed in dH_2O until leaching of blue colour had ceased. The slides underwent 4x five minute emersions in 99% IMS to dehydrate them, before being cleared 3x five minutes in xylene. Slides were sealed and mounted in Pertex. All images were acquired on a Leitz DMRB microscope (Leica Microsystems, Milton Keynes, UK) using Deltapix Infinity X and supporting software (Deltapix, Maalov Beyvej, Denmark).

2.2.5.2.2 Haematoxylin and eosin

For haematoxylin and eosin (H&E) staining, mounted sections were de-waxed in xylene, and rehydrated in alcohols and deionised water as described previously (2.2.5.2.1). Samples were placed in Mayer's haematoxylin solution (HST011; Solmedia, Shrewsbury, UK) for three minutes, rinsed in running tap water for five minutes and placed in eosin for 10 seconds. Slides were then dehydrated, cleared through xylene and had cover slips sealed on using Pertex.

2.2.5.2.3 Fluorescence staining of nucleic acids

Fluorescence staining of cellular DNA using DAPI (4',6-diamidino-2-phenylindole) was undertaken for better visualisation of potential cell nuclei. Dewaxed and rehydrated mounted sections were incubated with mounting solution containing DAPI (H-1200; Vector Laboratories, Peterborough, UK). Images were captured in fluorescence and visible light using an Olympus Bx51 (Olympus, Southend-on-Sea, UK) microscope equipped with a U-RFL-T mercury lamp. Images were acquired using a Retiga-SRV Fast 1394 camera with QCapture suite image capture software (QImaging, Surrey, Ca).

2.2.5.3 Immunohistochemical staining for immunogenic antigen MHC I

The human variant of the MHC class I antigen, HLA, has 3 major gene products termed HLA A, B and C. As all three of these antigens are able to activate $CD8^+$ T cells, causing an immune response, an antibody was chosen which was able to bind all three. Mounted sections of unwashed fresh-frozen (N=3) and washed bone (N=3) were dewaxed and rehydrated (2.2.5.2.1). The endogenous peroxidase was blocked by incubating for 30 minutes at room temperature in 300ml IMS containing 3% hydrogen peroxide and 200µl hydrochloric acid.

This was rinsed off by washing once in dH_2O and twice in Tris-buffered Saline (TBS) for five minutes each time. Sections were then immersed in TBS for five minutes at 37°C before being transferred to an enzymatic antigen retrieval solution containing 0.01% (w/v) chymotrypsin (C4129; Sigma-Aldrich, Gillingham, UK) and 0.1% (w/v) calcium chloride dihydrate in 300ml TBS, for 20 minutes. The slides were washed in TBS at room temperature to stop the reaction.

Non-specific binding sites were blocked by incubating sections in 200µl 25% (v/v) normal goat serum in TBS at room temperature for 30 minutes. The blocking solution was tapped off and the samples were incubated overnight at 4°C in primary HLA Class 1 ABC [EMR8-5] mouse monoclonal antibody (ab70328; Abcam, Cambridge, UK) diluted 1/200 in TBS containing 1% BSA (w/v). Following overnight incubation, the samples were drained of primary antibody and washed in TBS three times for five minutes each. Sections were then incubated for 30 minutes with the biotinylated secondary goat anti-mouse immunoglobulin G (IgG) antibody diluted 1/200 in TBS containing 1% BSA (sc-3795; SantaCruz Biotechnology, Heidelberg, Germany).

Antibody binding was visualised by incubating with streptavidin-biotin-HRP (horseradish peroxidase) complex (PK-7100; Vector Laboratories, Peterborough, UK) for 30 minutes. The sections were again washed in TBS three times for five minutes and stained using 3',3-diaminobenzidine tetrahydrochloride (DAB) (H-2200; Vector Laboratories, Peterborough, UK) for 10 minutes. Finally the sections were rinsed using tap water and counter stained in Mayers haematoxylin for one minute, before being rinsed in running tap water for five minutes. The stained sections were dehydrated in IMS, cleared using xylene, and sealed with Pertex, and mounted with coverslips.

2.2.6 Biocompatibility assessment of washed and unwashed fresh-frozen bone

2.2.6.1 Primary cell extraction and general cell culture

Primary human BM-MSCs were isolated from bone marrow aspirates and reamings removed with full consent from patients undergoing hip replacement surgery. Samples initially arrived in 180ml specimen pots (SP422; Appleton woods, Birmingham, UK) in 75ml collection solution, which contained 20U of heparin/ml of Hanks balanced salt solution (HBSS) (H8264; Sigma-Aldrich, Gillingham, UK) and 7,000U penicillin, 18µg/ml streptomycin, 38ng/ml amphotericin B (A5955; Sigma-Aldrich, Gillingham, UK).

Upon arrival, samples were transferred to 50ml Falcon tubes (352070; BD Bioscience, Oxford, UK) and centrifuged at 500*xg* for 10 mins (Universal 320, rotor: 1619; Hettish Zentrifugen, Newport Pagnell, UK). The supernatant was removed and the pellet resuspended in 5ml standard medium comprised of α-modified Eagle's medium (αMEM) (M4526; Sigma-Aldrich, Gillingham, UK), 10% foetal calf serum (FCS) (10270; Sigma-Aldrich, Gillingham, UK), 10µM ascorbate-2-phosphate (A8960-5G; Sigma-Aldrich, Gillingham, UK), 2mM GlutaMAX (35050-038; Life Technologies, Paisley, UK) and combined antibiotic/antimycotic solution (50,000U penicillin, 100 µg/ml streptomycin, 250ng/ml amphotericin B) (A5955; Sigma-Aldrich, Gillingham, UK). The resuspended pellet was then transferred to one or more 15ml centrifuge tubes (35-2097; BD Bioscience, Oxford, UK) depending on the size of the pellet, and each tube made up to 5ml with fresh medium. To each 15ml tube, 250µl of RosetteSep (15128/15168; Stem Cell Technologies, Manchester, UK) was added and incubated for 20 minutes at room temperature. Five millilitres of HBSS containing 2% FCS and 1mM EDTA (E9884; Sigma-Aldrich, Gillingham, UK) were then added, and the solution gently mixed. The solution was then layered over 5ml Histopaque

1077 (H8889; Sigma-Aldrich, Gillingham, UK) and centrifuged at 300*xg* for 30 minutes to separate cells by density gradient. After centrifugation the interface layer was removed (Figure 2.4) and transferred to a 25cm^2 (T25) culture flask (35-3014; BD Bioscience, Oxford, UK) and cultured in standard medium containing 20% FCS. Media was changed every five to seven days until 70-80% confluence was achieved at which point cells were passaged.

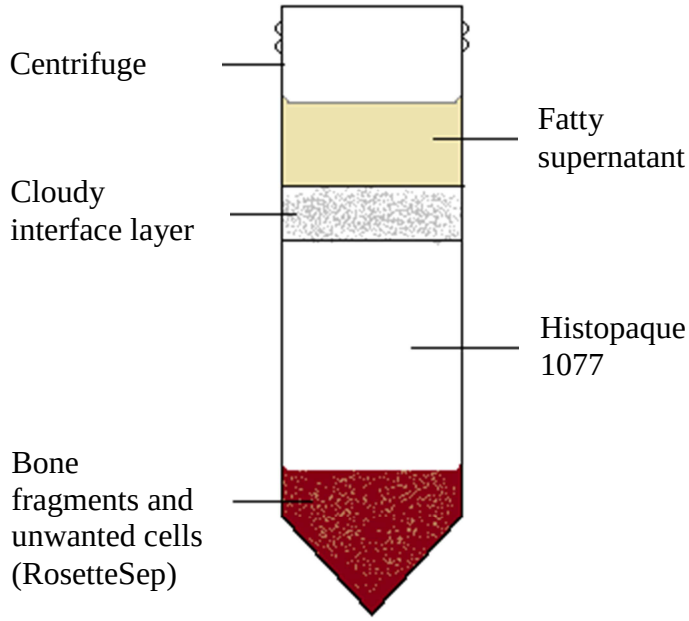

Figure 2.4: Diagram of post centrifuge histopaque 1077 for cell isolation. Fractions of bone marrow sample with RosetteSep are separated by density. The fraction of coagulated cells and bone fragments are denser than the 1.077g/ml histopaque and sediment to the bottom of the Falcon tube; while the lighter mononuclear cells float above the histopaque, and are topped by the most buoyant material, the fatty supernatant.

2.2.6.1.1 Cell expansion

In this study both MG-63 osteosarcoma and processed BM-MSCs were used to assess the cytotoxic potential of both washed and unwashed fresh-frozen bone. Cell cultures were grown in vented 150cm^2 (T150) culture flasks (35-5000; BD Bioscience, Oxford, UK) at 37°C and 5% CO_2 in standard medium, changed every five to seven days until 70–80% confluence was achieved. Confluent flasks were drained of media and washed using phosphate-buffered saline (PBS) (D8537; Sigma-Aldrich, Gillingham, UK) to remove traces of FCS from the flasks. The PBS was aspirated and the flasks were incubated for 10 minutes with 6ml of 0.25% (w/v) trypsin enzyme/EDTA (T4174; Sigma-Aldrich, Gillingham, UK) to dissociate cells from the tissue culture plastic. After incubation an equal volume (6ml) of standard medium was used to stop the enzymatic action and the solution removed to a centrifuge tube. The solution was centrifuged at 400*xg* for five minutes to pellet the cells, after which the supernatant was discarded and replaced with an adequate volume of fresh standard medium before being vortexed to mix well.

A 10µl aliquot was used to assess cell density through use of a haemocytometer (Improved Neubauer; Weber Scientific, Teddington, UK). Cells were counted using a light microscope (Labonet; Lieca Microsystems, Milton Keynes, UK) in four grid locations and used to derive an average which was converted to cells per ml. The suspended cell solution was then split between new T150 culture flasks (400,000/flask) with an aliquot frozen for potential future use.

2.2.6.1.2 Cell cryopreservation

Suspended cells were counted using a haemocytometer (2.2.6.1.1) and centrifuged to form a cell pellet. The pellet was resuspended in Recovery™ Cell Culture Freezing Media

containing 10% DMSO (dimethylsulfoxide) (12648-010; Life Technology, Paisley, UK) to give a cell concentration below $2x10^6$ cells per ml. This mixture was aliquoted into labelled CryoTubes (368632 Nunc CryoTube; Thermo Scientific, Hemel Hempstead, UK) and frozen at -1°C/min using a Mr Frosty™ freezing container (5100-0001; Thermo Scientific, Hemel Hempstead, UK), placed in a -80°C freezer, and stored overnight. Frozen cells were then transferred to liquid nitrogen for long-term storage.

2.2.6.2 Proximity cytotoxicity of wash bone

Cubes of unwashed fresh-frozen (N=4) and washed bone (N=4) were fixed into position on a 6-well plate (35-3046; BD Bioscience, Oxford, UK) using hypoallergenic silicone adhesive (MED1137; NuSil, High Wycombe, UK), and allowed to cure for approximately one hour. Separate samples of silicone adhesive, and known cytotoxic agent cyanoacrylate glue (P01174; Ultraloc™, Bradford, UK), were also included as controls.

MG-63 osteosarcoma cells were grown to 70–80% confluence, and incubated at 37°C, 5% CO_2 in standard medium. Cells were dissociated from tissue culture flasks by incubation with trypsin, centrifuged at 400*xg*, and resuspended and counted in fresh standard medium. The MG-63 cells were pelleted again and resuspended in standard medium to give a working cell concentration of $6.5x10^3$ cells per ml. From this solution a 2ml aliquot was added to each well containing fixed bone samples or control wells. This gave approximately 50% confluence for a $10cm^2$ growth area and an initial cell number of 130,000 cells per well. Control cubes of washed or unwashed fresh-frozen bone were fixed to 6-well plates and cultured with standard medium only, to assay for any potential cells still alive within the bone structure. Cultures were incubated for 72 hours at 37°C, 5% CO_2, to allow cell migration and proliferation.

2.2.6.2.1 Giemsa staining and visualisation

All media was aspirated from culture wells, which were then washed twice with PBS to remove traces of FCS. To each well, 2ml of 50% ethanol was added and incubated at room temperature for five minutes. The 50% ethanol was then removed and replaced with 2ml of 70% ethanol. After five minutes the wells were aspirated dry and 2ml of 100% ethanol added. After a five minute period the wells were again aspirated and left for 10 minutes to dry completely. Giemsa stain (32884; Sigma-Aldrich' Gillingham, UK) was diluted to 20% (v/v) in PBS and 2ml added to each well and left to stain for five minutes before being removed. All wells were rinsed briefly with dH_2O and allowed to air dry before microscopy.

Images were captured in fluorescence and visible light using an Olympus Bx51 (Olympus, Southend-on-Sea, UK) microscope equipped with a U-RFL-T mercury lamp. Images were acquired using a Retiga-SRV Fast 1394 camera with QCapture suite image capture software (QImaging, Surrey, Ca).

2.2.6.3 Extract cytotoxicity of washed bone

2.2.6.3.1 Production of bone extract conditioned media

Unwashed fresh-frozen (N=3) and washed (N=3) bone samples were snap frozen in liquid nitrogen and powdered using a solid metal cylinder and fitting punch rod, which were chilled to -80°C prior to use. Snap frozen bone samples were loaded into the cylinder, followed by the fitting rod and hammered sharply to produce a powdered sample. The powdered samples were weighed and soaked in five times their own weight in standard culture medium for 72 hours at 37°C under constant agitation (ISO 10993-5, 2009). The solution was centrifuged at 400*xg* for five minutes to remove large bone fragments and at 10875*xg* (Rotina 35R, rotor: 1789-L; Hettish Zentrifugen, Newport Pagnell, UK) for 10 minutes to remove finer bone

particles. The resulting supernatant was used as extract conditioned media in the extract cytotoxicity assays on BM-MSCs.

2.2.6.3.2 Effect of extract conditioned media on BM-MSC metabolic activity

Human BM-MSCs were isolated from bone marrow (55 YOA female), with ethical approval using established methodology (section 2.2.6.1). Cells were expanded in standard culture medium until passage two, whereby BM-MSCs were seeded into 96-well plates at $3.3x10^4$ cells/cm^2 then incubated for 24 hours. After initial incubation, standard medium was replaced with 100µl of extract conditioned media and cells incubated for a further 24 hours. Cell viability was assessed by adding 5µl of WST-1 (05015944001; Roche, Welwyn Garden City, UK) to each well. The culture plates were incubated for four hours, at 37°C and 100µl of supernatant read at absorbance 450nm/620nm (Multiscan FC; Thermo Scientific, UK). All raw data values had the blank control value removed, before being divided by the average of standard medium control to give fold-change in relation to standard medium only control.

2.2.6.3.3 Effect of extract conditioned media on total BM-MSC number

After supernatant was removed for WST-1 assay, cells remaining in the 96-well culture plate were rinsed with PBS twice and lysed with 100µl, 2% Triton X-100 (X100; Sigma-Aldrich, Gillingham, UK) in PBS. A Lactate dehydrogenase (LDH) Master Mix was produced from a kit (MAK066; Sigma-Aldrich, Gillingham, UK) by first reconstituting one vial of LDH substrate mix in 1ml dH_2O. This was mixed well before 400µl was diluted in to 9.6ml of pre-warmed LDH buffer to produce the LDH reagent. To each well 100µl of LDH reagent was added and incubated at room temperature for 30 minutes. Plates were then read at absorbance 485nm/620nm using a spectrophotometer. All raw data values had the blank control value

removed, before being divided by the average of standard medium control to give fold-change in relation to standard medium.

2.2.7 Direct contact biocompatibility assessment of washed bone allograft

2.2.7.1 Seeding method and ability of cells to adhere to washed bone

Washed bone cubes were removed from -80°C storage and soaked in PBS under agitation at 37°C for 30 minutes to defrost and remove dust caused by cutting. This dust was removed to prevent cells adhering to small bone fragments, which may then be inadvertently removed through rinsing and media changes. The defrosted cubes were then centrifuged in bespoke holders (Figure 2.5) at 400*xg* for five minutes to remove all liquid, and individually placed in separate wells of 24-well plates (35-3047; BD Bioscience, Oxford, UK).

MG-63 cells were cultured in standard medium as described previously (2.2.6.1.1). At 70–80% confluence cells were trypsinised, counted and resuspended at $4x10^6$/ml in standard medium. To each bone cube, 250µl of resuspended cells ($1x10^6$ cells) were added carefully in a drop wise manner from approximately 2cm above the cube surface, and incubated for 1, 5, 10, 20, 40, 60 or 120 minutes, before being washed three times in 2ml PBS. The cubes were then removed from the wells, and replaced with 1ml 0.25% (w/v) trypsin/EDTA. The 24-well plates were then incubated at 37°C for 10 minutes and the enzyme process stopped by adding 1ml standard medium. Meanwhile, the bone cubes were centrifuged at 400*xg* for five minutes to remove all liquid, which was vortexed to resuspend any pelleted cells. This was combined with the trypsin and PBS washes, and centrifuged again at 400*xg* for five minutes to pellet all cells. These were counted and termed non-adherent cells.

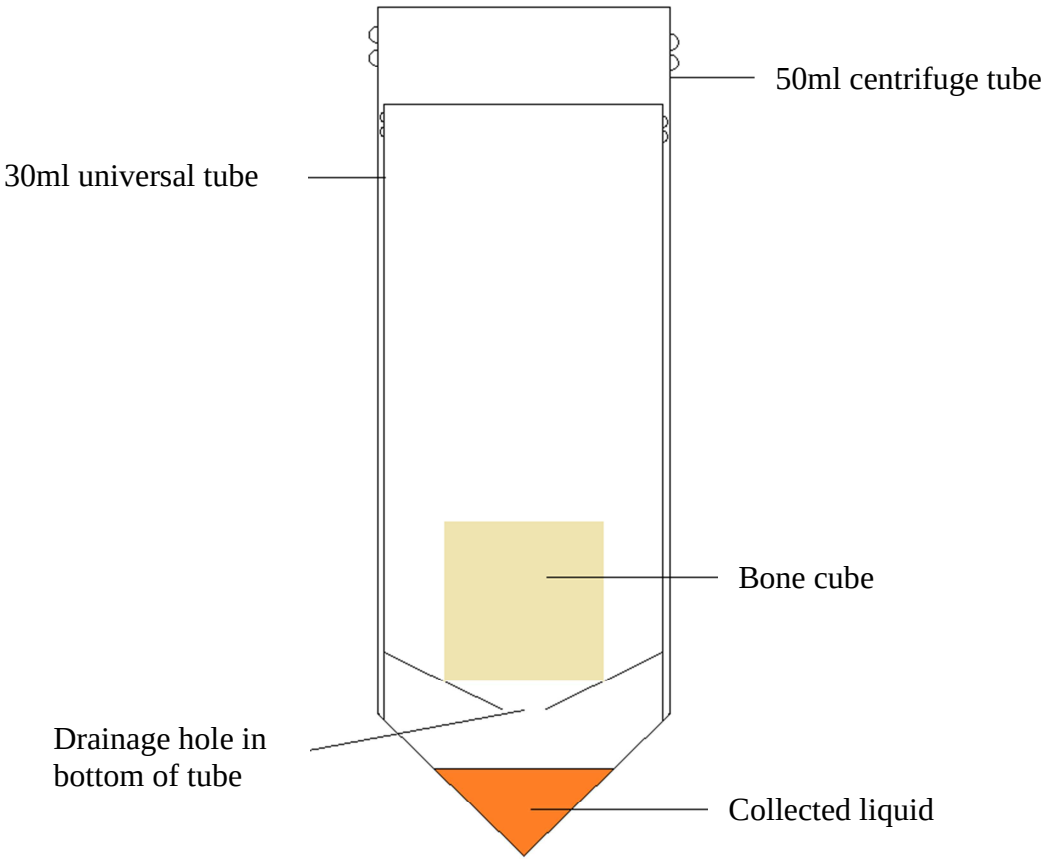

Figure 2.5: Diagram of specialised centrifuge device. A hole was produced in the bottom of a universal tube, which was subsequently placed inside of a 50ml Falcon centrifuge tube, thereby elevating the bone from any liquid removed by centrifugation.

2.2.7.2 Direct contact compatibility of washed bone cubes

Bone cubes taken from a washed femoral head (457 344, 78 YOA female) were defrosted and placed into separate wells of a 24-well plate. BM-MSCs from a 50 YOA male were cultured in standard medium as previously described (2.2.6.1.1). Cells were removed from TCP using trypsin/EDTA (2.2.7.1) and resuspended at $4x10^6$ cells/ml in standard medium. The cell suspension was used to seed bone cubes (n=5) with $1x10^6$ cells (250µl) each, which were then incubated for one hour at 37°C, 5% CO_2. Non-adherent cells were collected as described

previously (2.2.7.1) and used to determine the number of adhered cells. The seeded bone cubes were transferred to 2ml fresh standard medium containing 5% alamarBlue (DAL1025; Life Technologies, UK). After two and a half hour incubation a 100µl sample was measured using an absorbance plate reader at 540/620nm. The bone cubes were transferred to a fresh 24-well plate washed twice with PBS then incubated at 37°C, 5% CO_2 in 2ml fresh standard medium. Media was changed every two to three days until seven days, at which point the seeded cubes were tested for cell metabolic activity using the alamarBlue assay (2.2.7.2).

2.2.7.3 CFDA-SE visualisation of BM-MSCs seeded on to washed bone cubes

Prior to seeding, cells were labelled with the intracellular vital dye carboxyfluorescein diacetate succinimidyl ester (CFDA-SE) (V12883; Life Technologies, Paisley, UK). Briefly, 90µl of DMSO (supplied in kit) was added to one vial of lyophilised Vybrant® CFDA-SE powder, to create a 10mM stock solution. A 10µl aliquot was diluted in 10ml PBS to give a working CFDA-SE reagent solution at a concentration of 10µM (Richardson *et al.*, 2006).

BM-MSCs (WH106, 73 YOA male) were trypsinised and pelleted using previously described culture techniques (2.2.7.1). The cell pellet was washed twice in PBS to remove traces of serum and resuspended in 10ml CFDA-SE reagent, then incubated for 30 minutes in the dark at 37°C.

The cells were centrifuged at 400*xg* for five minutes to form a cell pellet then resuspended in standard medium and incubated for a further 30 minutes. Finally the cells were counted and resuspended to give a cell concentration of $4x10^6$ cells/ml. Defrosted bone cubes (2.2.7.1) from three different donors were seeded with $0.5x10^6$ cells (in 125µl) and incubated for one hour, before being washed with PBS, centrifuged to remove liquid and then incubated in fresh standard medium for 72 hours. After incubation, bone cubes were washed twice in PBS

and placed in histology cassettes with sponges to maintain correct orientation. The cubes were then fixed and processed to wax blocks as described previously (2.2.5.1).

2.2.7.3.1 Immunohistochemical staining of CFDA-SE stained cells

Embedded bone cubes seeded with CFDA-SE labelled cells were sectioned as described previously (2.2.5.1) and mounted on slides. Sections were blocked in normal goat serum (G9023; Sigma-Aldrich, Gillingham, UK), immunohistochemically stained using 1/300 dilution, mouse anti-fluorescein biotinylated antibody (ab6655; Abcam, Cambridge, UK) and visualised with 1/300 dilution goat anti mouse secondary antibody and DAB, using the methodology described in section 2.2.5.3. Images were captured in fluorescence and visible light using an Olympus Bx51 (Olympus, Southend-on-Sea, UK) microscope equipped with a U-RFL-T mercury lamp. Images were acquired using a Retiga-SRV Fast 1394 camera with QCapture suite image capture software (QImaging, Surrey, Ca).

2.2.7.4 Statistical analysis of data

Mann Whitney non-parametric analysis was conducted on data recorded from extract media cytotoxicity assays. For all cases N is the number of biological repeats (number of biological donors), whilst n is the number of technical/ experimental repeats.

2.3 Results

2.3.1 Evaluation of the efficiency of the novel human bone wash process

The results indicated a large proportion of the soluble marrow components had been removed leading up to the chemical sterilisation at step 10, with a cumulative removal value of 93.2% (±3.9), 95% (±2.1) and 96.7% (±4.4) recorded for DNA, protein and haemoglobin respectively (N=14). After the completion of the 14 step wash process, total removal percentages of 96.4% (±2.4), 98.3% (±0.67) and 99.3% (±0.84) for DNA, soluble protein and haemoglobin respectively were calculated to have been removed, with an average total of 98% (±1.4) for the total removal of all detected soluble factors.

Comparative studies on both the intact femoral head halves and excised trabecular material with an extended residual step process were used to scrutinise samples for residual contamination. The results showed a wash efficiency of 92.8% (±1.3), a significant decrease from the previous wash efficiency result of 98% (±1.4). However, the trabecular only material had an average contamination removal of 99.5% (±0.15), with removal of 99.45% (±0.1) of recorded DNA, 99.3% (±0.2) of soluble protein and 99.8% (±0.1) of haemoglobin (N=3).

2.3.1.1 Quantification of residual DNA contamination

The washed material was then lysed and a quantitative measurement taken of the DNA trapped within the structure after washing. The results of this DNA extraction showed a residual DNA concentration of 16.9ng (±3.9) DNA/100mg of dry bone material in the

washed trabecular bone (n=9). The unwashed fresh-frozen material contained 100.3ng (±35) of DNA material in a 100mg sample (n=9). These are not directly comparable as the unwashed sample contained a portion of marrow, therefore decreasing the relative volume of bone. The agarose gel electrophoresis results of the PCR amplified DNA samples displayed viable DNA in all samples, both washed and unwashed, indicated by the appearance of bands at the 700bp region of the gel, as designated by the 100bp DNA ladder (Figure 2.6).

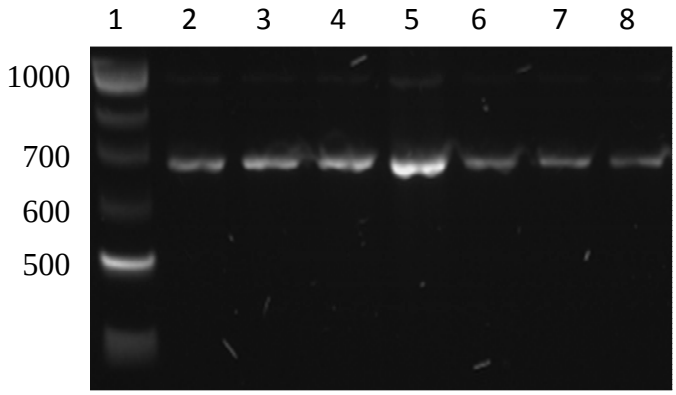

Figure 2.6: Analysis of DNA viability in unwashed fresh-frozen and washed bone cubes. Cubes were powdered and lysed to extract DNA. Image displays agarose visualisation of DNA products from PCR reaction using GAPDH primers. Lanes are as follows: 1) 100bp ladder, 2-4) unwashed samples (N=3), 5) positive control (total human DNA), 6-8) washed samples (N=3).

2.3.2 Histological analysis of marrow removal from the bone

H&E staining of unwashed fresh-frozen bone (N=2) showed large quantities of soft marrow and cells present in the marrow ECM within the marrow space of the trabecular structure

(Figure 2.7 A and C). Encapsulated osteocytes in their lacunae were also evident, as too were cells adhered to the bone surface in a thin layer evident of an endosteal type structure.

A fine meshwork, indicative of lysed adipose and marrow tissue, was still present in the washed bone material (N=2) (Figure 2.7 B); however this was almost completely untethered from the trabeculae. Additionally, there was a substantially diminished cell presence both in the marrow space and anchored to the bone surface, with no obvious endosteum. A small number of osteocytes were still present encapsulated in lacunae, as displayed by DAPI staining (Figure 2.7 D).

In addition to cellular staining by H&E, MTC staining was used to identify any changes in bone morphology. The MTC stain also identified a large decrease in soft tissue histology (Figure 2.7 E and F), with stained osteocytes present in the lacunae. However, similar morphological staining of newer osteoid (red) and older more dense mineralised (ossified) (blue) matrix was evident between washed and unwashed bone samples.

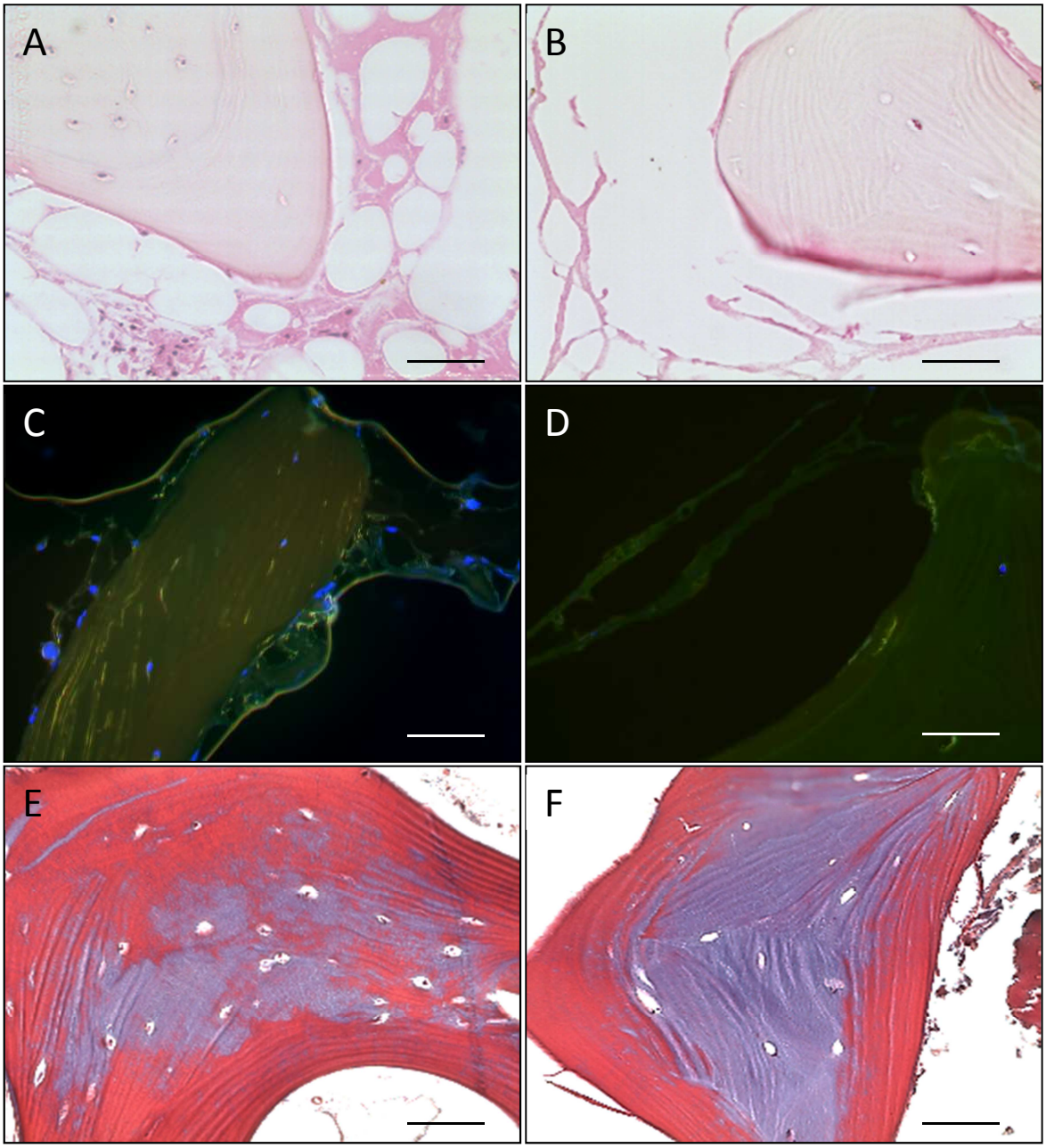

Figure 2.7: Histological staining of unwashed (A, C, E) and washed (B, D, F) allograft bone. Images display H&E staining (A, B), DAPI (C, D) and MTC (E, F). Scale bars represent 50µm at x300 magnification. Images clearly display a substantial decrease in immunogenic cellular content and soft tissue, whilst maintaining bone morphology.

2.3.3 Biocompatibility assessment

2.3.3.1 Immunogenicity of washed bone

As MHC antigens are used to recognise foreign material, samples were immunohistochemically stained for HLA serotypes A, B and C. The unwashed material was heavily stained, including endosteum, soft marrow tissue containing fat cells, stromal cells and osteocytes (Figure 2.8 A). In comparison, washed bone displayed little or no immunopositivity for the HLA ABC antibody (Figure 2.8 B).

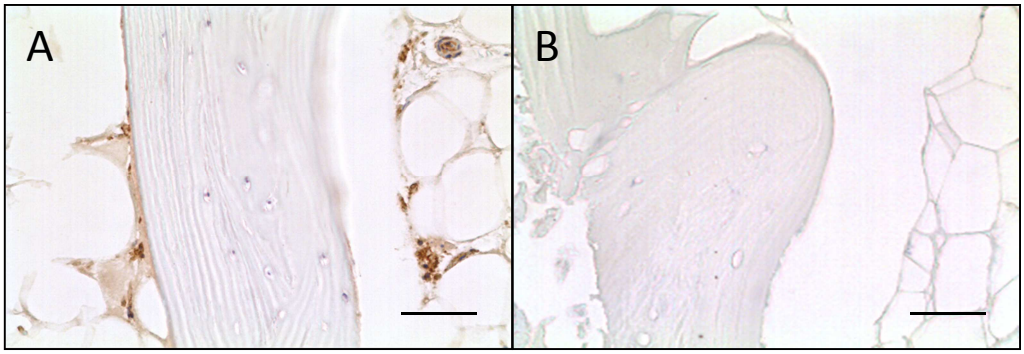

Figure 2.8: HLA class 1 ABC antibody immunohistological staining of unwashed fresh-frozen (A) and washed bone (B). Images clearly display a substantial decrease in immunogenic cellular content and soft tissue, whilst maintaining bone morphology. Scale bars represent 50µm at x150 magnification.

2.3.3.2 Phase contrast microscope analysis of proximity cytotoxicity assay

In vitro proximity cytotoxicity testing was conducted on both washed and unwashed fresh-frozen material. The cell only control (Figure 2.9 A) showed normal attachment to the TCP by the MG-63 cell line; additionally the silicone adhesive-containing wells caused no change to normal cell adhesion or presence, with cells only prohibited by the physical boundary of the control substance (Figure 2.9 B).

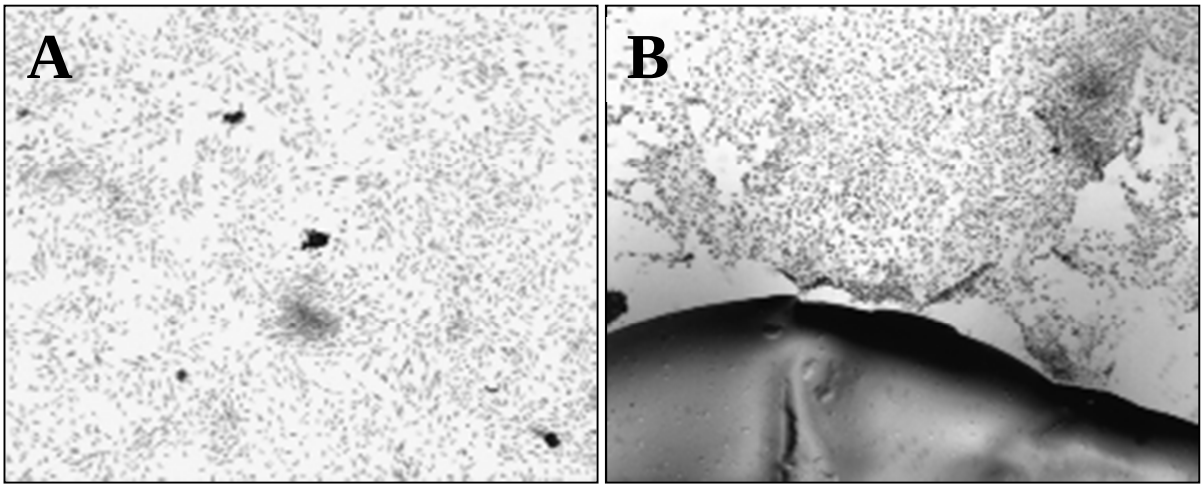

Figure 2.9: Phase contrast images displaying cultured cells in direct contact cytotoxicity assays with controls; no material (A) and silicone adhesive (B). Images were taken at x150 magnification.

In culture wells containing the unwashed fresh-frozen bone samples (N=4) a “boundary” like area was evident in which the MG-63 cells were either sparsely populated or absent (Figure 2.10). This boundary was noticeable in all samples (Figure 2.10 A, B, C and D); however in cases where cells were present at the bone edge, they exhibited a rounded and more compact morphology.

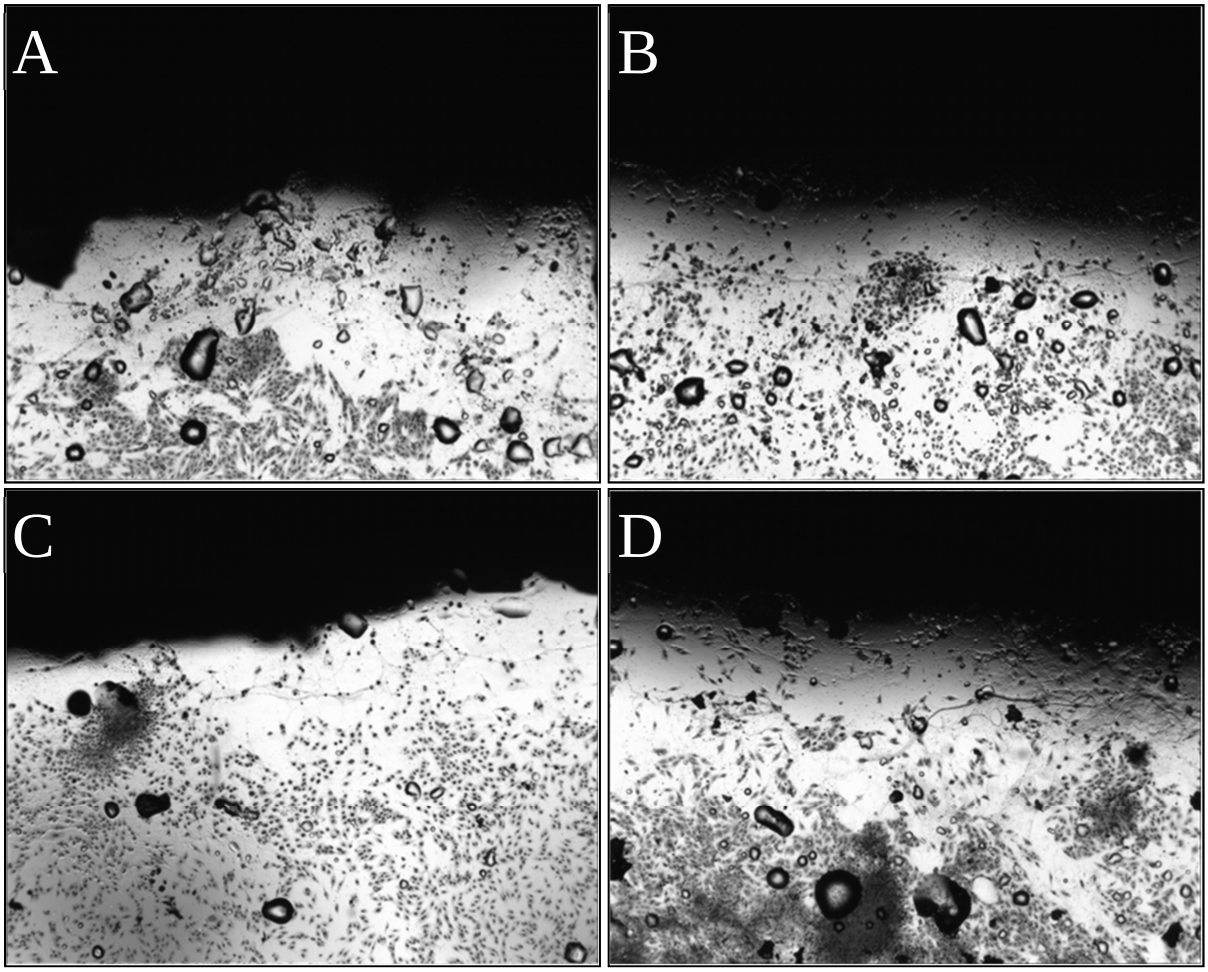

Figure 2.10: Proximity cytotoxicity of human unwashed fresh-frozen bone. Phase contrast images display the presence of osteosarcoma MG-63 cells culture for 72 hours in the vicinity of unwashed fresh-frozen bone samples (N=4), seen as regions of black at the top of images. All samples stained using Giemsa staining and images taken using light microscopy. Images were taken at x150 magnification.

For washed bone sample (N=4) there were a large number of cells present around the washed bone material, which did not display a distinct boundary-like appearance (Figure 2.11). These cells appeared able to grow up to, and be in contact with, the bone material as displayed prominently in Figure 2.11 D. All cells exhibited an elongated and flattened morphology.

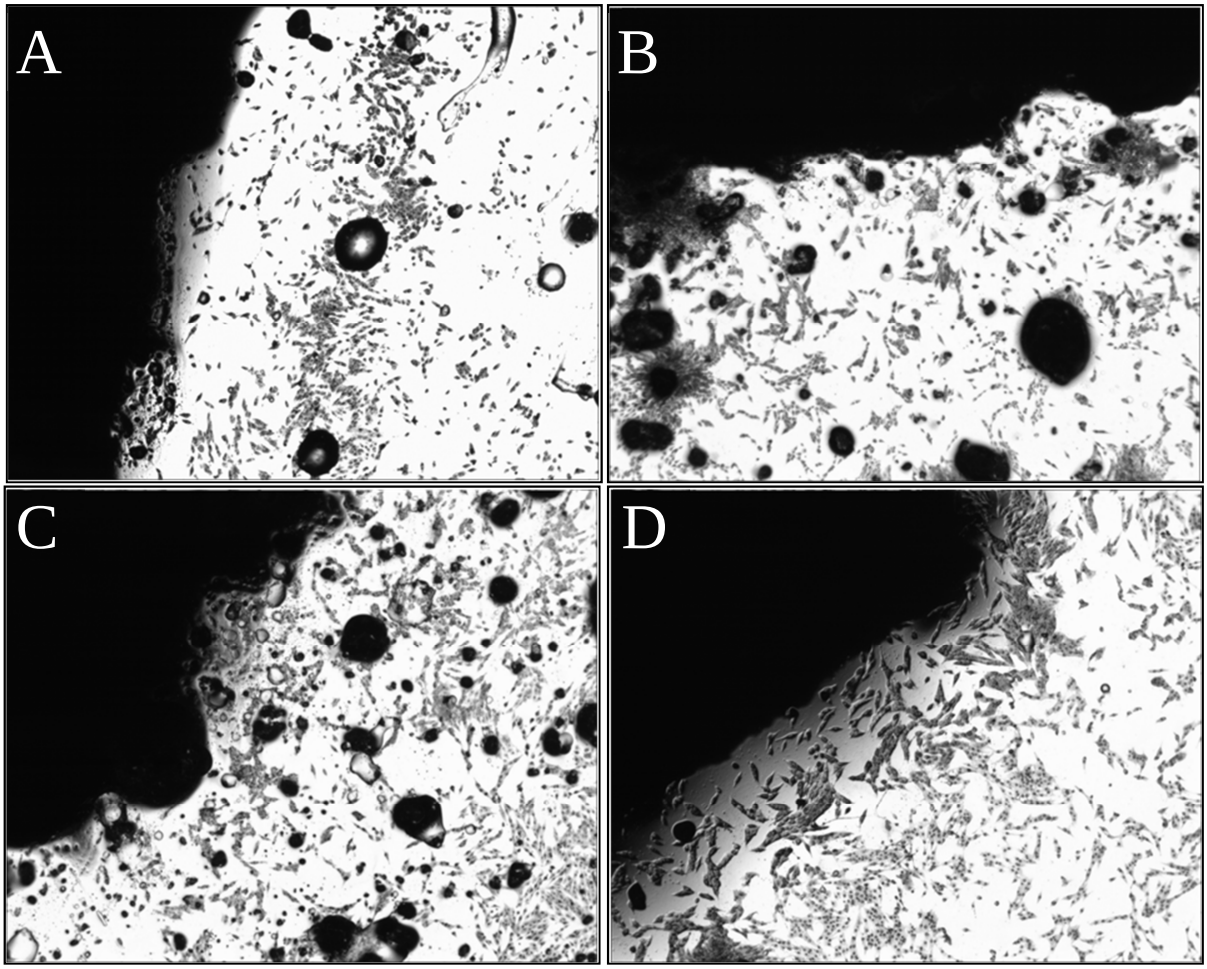

Figure 2.11: Proximity cytotoxicity of human washed bone. Phase contrast images display the presence of osteosarcoma MG-63 cells cultured for 72 hours in the vicinity of washed bone samples (N=4), seen as regions of black at the top of images. All samples stained using Giemsa staining and taken with light microscopy. Images were taken at x150 magnification.

2.3.3.2.1 Giemsa stained fluorescence images of proximity cytotoxicity assays

Observable areas of diminished cell growth similar to the unwashed bone samples were present in some of the washed samples (Figure 2.11 A). However these areas were sporadic and were often accompanied by adjacent cell growth up to and under the bone sample itself. Therefore fluorescence imaging of Giemsa stained wells was used to visualise the underside of the bone. Similar to phase contrast images for unwashed fresh-frozen bone samples, there was a diminished cell presence around the bone, especially around areas where the bone was in contact with the culture plate (Figure 2.12 A1, A2 and A3). Additionally there were no signs of a cell presence underneath the unwashed fresh-frozen bone samples (N=3). In contrast MG-63 cells grown in the proximity of washed bone samples (N=3) displayed a cell presence at the bone's boundaries (Figure 2.12 B1, B2 and B3), even colonising the TCP underneath the sample (Figure 2.12 B2 and B3).

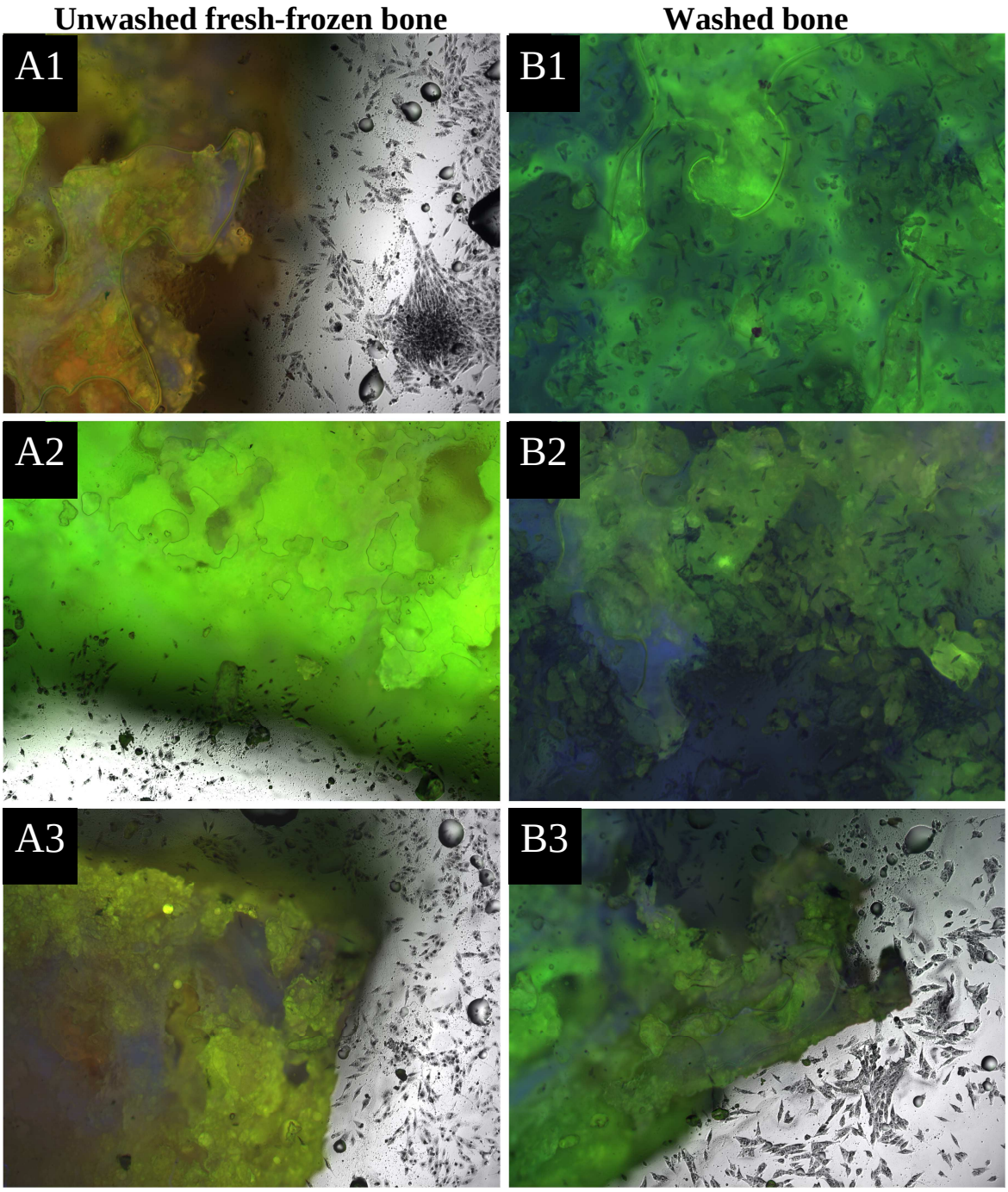

Figure 2.12: Proximity cytotoxicity of unwashed fresh-frozen (A1, A2, A3) and washed (B1, B2, B3) human bone cubes (N=3, respectively) cultured with MG-63 osteosarcoma cells. Samples were cultured for 72 hours, then fixed and stained using Giemsa stain. The bone's natural auto fluorescence (visualised as green or orange/yellow, depending on marrow content) was utilised as a background for visualisation of Giemsa stained cells (blue). Images are composite of light and fluorescent microscopy and taken at x150 magnification.

2.3.3.3 Extract cytotoxicity of washed bone

Extract cytotoxicity assays were conducted using extract media from either washed or unwashed samples (N=3 for both), treated in accordance with ISO 10993 standards for medical devices. BM-MSC cultures subjected to washed bone extract conditioned medium (WBCM) displayed a significant increase in cellular metabolic activity of 10.6% (±4.4) ($p \leq 0.05$) compared to a standard medium growth control, indicated by an increase in reduced WST-1 (Figure 2.13 A). In contrast, unwashed fresh-frozen bone extract conditioned medium (FFCM) caused a significant 32% (±13.8) ($p \leq 0.05$) decrease in WST-1 reduction compared to standard conditions and was significantly less than the WBCM samples ($p \leq 0.05$) (Figure 2.13 A).

The LDH assays, designed to ascertain the number of total live cells present at the end of culture, indicated no significant increase in total cell number in WBCM cultures (Figure 2.13 B). However, in FFCM cultures, similar to the WST-1 assay, there was a significant 20% (±9.03) decrease in total cell number compared to standard medium cultures ($p \leq 0.05$).

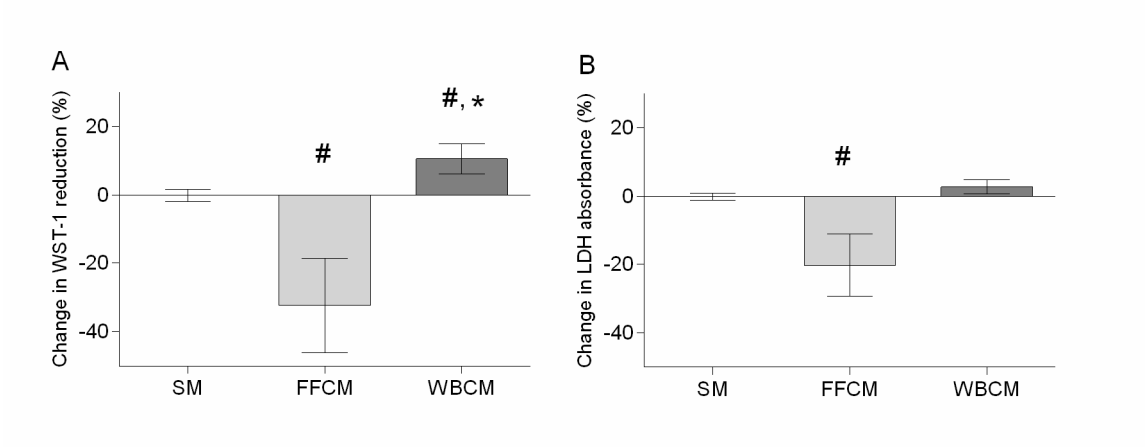

Figure 2.13: Biocompatibility of extract media produced from unwashed fresh-frozen and washed bone cubes (N=3 for both). Analysis of cell activity and viability assessed using (A) WST-1 assay and (B) LDH assays respectively. Cells were incubated in standard medium (SM), fresh-frozen extract conditioned medium (FFCM) or washed bone extract conditioned medium (WBCM) and cultured for 72 hours. Results from FFCM or WBCM were averaged and normalised to SM and displayed as percentage change ± SE. #, indicates significant difference with respect to standard medium ($p \leq 0.05$). *, indicates significant difference ($p \leq 0.05$) between FFCM and WBCM.

2.3.4 Analysis of direct contact biocompatibility of washed bone scaffold by analysis of cell adherence and viability

Results of cell seeding indicated MG-63 cells were able to adhere to the washed bone scaffold with a fast rate of adherence. An optimal adherence time of 60 minutes resulted in 91% (± 1.3) of the seeded cells adhering to the structure, with 90% (±1.4) adherent at 120 minutes adherence time (Figure 2.14).

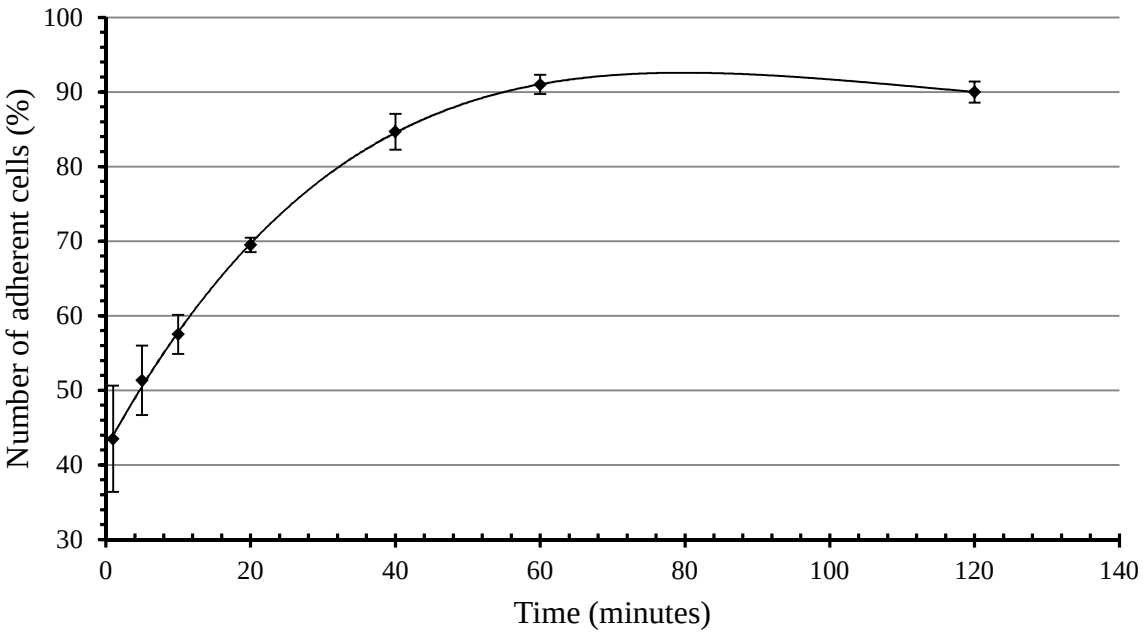

Figure 2.14: The adherence efficiency of MG-63 cells seeded onto washed bone scaffolds at 1, 5, 10, 20, 40, 60 and 120 minutes (n=3 for each time point). Data displayed as percentage of total seeded ($1x10^6$) ± SE.

In the assessment of direct contact adhesion of primary BM-MSCs, cells were able to adhere to the washed bone with adherence efficiency after one hour of 89.5% (±2.15) respectively. AlamarBlue cell health assay indicated a 2.2-fold (±0.10) increase in metabolic activity of BM-MSCs, seeded on the washed bone scaffold, indicative of sustained cell viability.

2.3.4.1 CFDA-SE labelling of mesenchymal stem cells for visualisation of cells

MSCs labelled with CFDA-SE were visualised adhered to the washed human bone scaffold (N=3), including the bone surface and marrow ECM (Figure 2.15 A, B and C). There were no unstained cells present in the structure. Non-seeded and isotype monolayer controls (Figure 2.15 D and E) displayed no staining, though staining was evident in the positive control (Figure 2.15 F).

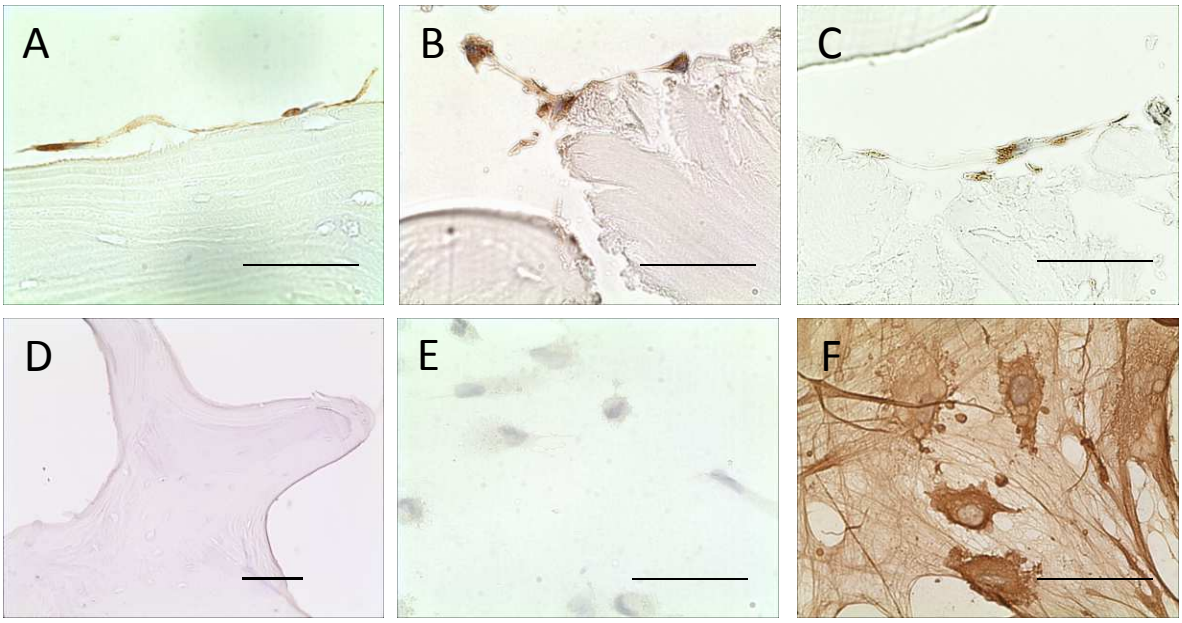

Figure 2.15: Immunohistochemical visualisation of CFDA–SE labelled BM-MSC (WH106) seeded on human washed bone scaffold (N=3), visualised using biotin conjugated anti-fluorescein antibody and DAB counterstained with haematoxylin. Samples displayed for three different bone donors (A, B, and C), as well as a non-seeded control (D). Monolayer IgG negative control and monolayer CFDA-SE stained cell positive control are also displayed (E and F respectively). Scale bars represent 50µm. All images were captured at x300 magnification except D, which was captured at x150.

2.4 Discussion and Conclusion

Bone graft material is an extremely important tool in the surgical treatment of bone loss. Whilst autograft is the gold standard and the most osteogenic material, it is extremely limited in volume and so human allograft bone is often required instead. However, the bone marrow it contains is potentially detrimental to the osseointegration of an allograft in the recipient (Burwell, 1985; Burwell, 1962). The large cellular component of the marrow, bound by a protein extracellular mesh in a haematopoietic environment, is able to initiate an immune response, activating T–lymphocytes and leading to the grafts rejection. So too can bacterial and viral diseases, such as Hepatitis C, which may be present within it, leading to further complications to the recipients health. It is therefore of great importance to remove as much of this potentially harmful material as possible, though it is also essential that any sterilisation technique used is not detrimental to the scaffolds biocompatibility, such as inferring a cytotoxic quality as this would diminish the bones' feasibility as a scaffold in tissue engineering.

This part of the study aimed to assess the feasibility of using a novel wash process to produce an acellular material, and the biocompatible nature of the acellular material produced.

2.4.1 Efficiency of sterilisation process

Here, the soluble factors; DNA, soluble protein and haemoglobin were used as indicators of bone marrow, with the removal of these factors from the whole femoral head signifying the removal of cellular material and blood products contained in the marrow.

The use of the wash protocol on whole femoral heads resulted in a 98% average removal efficiency of these soluble factors, all of which followed a similar trend in their removal. A greater amount of haemoglobin than DNA or protein was removed during the sterilisation process. This was to be expected as red blood cells lyse quickly and are not bound to an ECM. This large removal of marrow may increase the perfusion of the PAA-ethanol solution into the structure, thereby increasing its efficiency as concluded by Pruss *et al.* (2003).

The 98% removal efficiency, although high, was lower than the expected value, which was based on preliminary work conducted by both Rooney *et al.* (2006) and Board *et al.* (2006a), who recorded removal efficiencies in excess of 99% on pre-cut material. Although this discrepancy is small, it represents a potentially large difference in the removal of harmful biological pathogens. A larger percentage (up to 99.99% efficiency), indicates a greater dilution of virus concentration to below that of its minimal infection titre. Whilst the current study did not observe the viral particle content of the washes, Pruss *et al.* (2003) demonstrated the reliability of PAA-ethanol at denaturing viral particles to levels well below those of their minimal titre. A potential limitation to the form of analysis used in this study, and a possible cause of this discrepancy, is the relation of the percentage efficacies to a residual contamination value. Femoral heads were washed whole; however for the residual wash they were bisected. This process potentially unlocks trapped material such as sub-chondral cysts (termed geodes), which were previously inaccessible. Geodes containing soft tissue such as marrow may appear in femoral heads which have severe damage to their cartilage (Resnick *et al.,* 1977), and as the samples used for this study have been retrieved from patients undergoing hip replacement surgery, the majority of the femoral heads had geodes present.

As the percentage removal values are related back to the residual value, percentage removals are vulnerable to changes caused by the release of this previously inaccessible marrow material from the geode, which is highlighted by the results of the excised trabecular material comparative study. Once this geode material was removed, an improved removal efficiency of 99.5% for soluble protein, DNA and haemoglobin trapped in the trabecular structure of the femoral head was achieved. This higher level of marrow removal, particularly soluble protein (98.9%), is equatable to that reported by Yates *et al.* (2005) (98.7%) and Lomas *et al.* (2000) (96.4%), and superior in the removal of soluble protein and DNA (99.2%) to Ibrahim *et al.* (2012) (70.5% and 68.4% respectively). Importantly, the studies by Yates and Lomas utilised whole femoral heads in their wash processes as opposed to the morcilised bone used by Ibrahim, or smaller pre-cut shapes used by Rooney *et al.* (2006), Board *et al.* (2006a), and Hashimoto *et al.* (2011). Though geodes may cause issues, by using whole femoral heads, large intact volumes of decellularised trabecular material can be obtained, which enables surgeons to create bespoke structures, as required.

The marrow components remaining in the material have the potential to initiate a cytotoxic response, and may alter the behaviour of cells. Therefore, in addition to the assessment of remaining marrow components by percentage efficiency, alternate assessments of marrow removal were undertaken to determine whether the material could be deemed acellular. The large scale removal of marrow from the whole femoral heads resulted in a material with a low DNA value (16.9ng DNA/mg dry material), which histologically displayed very little to no cells present within its structure, similar to decellularised samples produced in publications by Dutra and French (2010) and Hashimoto *et al.* (2011). However, whilst these studies claimed decellularisation, neither was able to successfully produce acellular material in accordance with the standards proposed by Crapo *et al.* (2011) for the evaluation of a decellularised soft tissue (Choi *et al.,* 2011; Ma *et al.*, 2013). For ECM to be classed as

acellular according to these criteria, the material must have a DNA value of less than 50ng DNA/mg dry material, have little to no cells visible histologically, and no DNA fragments greater than 200 base pairs. The washed human bone material produced in this study met both the DNA value and histological criteria; however there were DNA fragments large enough for PCR amplification. This was most likely due to DNA from osteocytes trapped within the ECM matrix. It is important to note however that these criteria were defined for soft not hard tissue which has extremely difficult to reach encapsulated cell types such as osteocytes.

2.4.2 Immunogenicity and cytotoxicity

The removal of the marrow material from the whole femoral heads is particularly important in reducing the immunogenic load placed on the patient. However, even decellularised material has the potential to contain material which can illicit an immune response by the host (Markel *et al.,* 2012), potentially due to remaining soluble proteins (VandeVord *et al.,* 2005). Other ECM decellularisation studies have determined the immunogenicity of a sample based on its MHC class I and II profile, displaying decreases in the staining of these antigens after processing. As such, the MHC class I antibody was selected for this study as it represented the majority of potential tissue present (Feng *et al.,* 2012). Though there was initial staining for the HLA class I antigens in unwashed fresh-frozen samples, after the wash process, the human bone matrix displayed no antigen presenting immunogenic material.

Whilst the material may not cause direct activation of immune cells through antigen presentation, any cytotoxic effect by the bone material or bacterial contaminates could still cause damage to the host and affect cell adherence (Bonsignore *et al.,* 2013). The results of both the proximity and extract cytotoxicity assays demonstrated the biocompatible nature of the washed material, with cells migrating underneath and remaining in contact with the

structure, whilst being able to proliferate and maintain viability in its vicinity. In contrast to the washed material, the unwashed fresh-frozen bone caused a significant reduction in cell viability and total number in extract conditions, with proximity cytotoxicity analysis displaying clear boundaries around the samples, which were devoid of cells. These results therefore suggest the novel wash process removes the cytotoxic effect of unwashed fresh-frozen bone, and importantly there were similar result for both BM-MSC and MG-63 cell types. The effects of the unwashed fresh-frozen material are unlikely to be caused by retained viable cells. Though studies by Simpson *et al.* (2007) and Heyligers and Klein-Nulend (2005) have both demonstrated live, metabolically active cells in unwashed fresh-frozen bone, the results of the alamarBlue assays undertaken on unwashed fresh-frozen bone in the current study were not supportive of these finds, with no metabolic activity measured.

Importantly, the biocompatibility data is supported by previous work by Board *et al.* (2009), which demonstrated a comparable cytotoxic effect by unwashed fresh-frozen bone on osteogenic cells, and identified zones of decreased cell presence around bone samples, as well as a cytotoxic effect, assayed for by MTT (3-(4,5-Dimethylthiazol-2-yl)-2,5-Diphenyltetrazolium Bromide) testing. The cell number and viability data presented by this current study, whilst not directly comparable, also provides evidence for the negative effect of unwashed fresh-frozen bone on cell activity.

In this current study, powdered bone samples were utilised in extract conditioned media, increasing the available surface area of the material as well as displaying previously trapped material more in keeping with ISO guidelines, thereby decreasing the likelihood of discrepancies in results (Fawzi-Grancher *et al.*, 2009). Studies by Bormann *et al.* (2010) and Coquelin *et al.* (2012) have also shown a negative effect on cell viability by fresh-frozen bone, with Kluger *et al.* (2003) demonstrating a deceased osteogenic activity of cells in contact with frozen bone compared to fresh. The cytotoxic effect by the fresh-frozen bone is

potentially due to the peroxidation of lipids (Parhami *et al.*, 1997), which have been found in fresh-frozen bone allograft, even at -70°C (Laitinen *et al.*, 2006).

Importantly, whilst fresh-frozen material displays good long term healing (Buttaro *et al.*, 2012), the potential for cytotoxic factors to leach into surrounding tissue from this material could be detrimental to patient health; however, currently there are no reports of clinical trials comparing the outcomes of fresh-frozen versus washed allograft, and as such *in vivo* trials to assess this are required.

In addition to extract and proximity cytotoxicity assays, this study highlighted the successful seeding of the washed human bone scaffold with BM-MSCs, with an increase in their metabolic activity after 7 days, suggesting viability and proliferation. To seed the washed human bone cubes, a direct scaffold seeding method was utilised, which has been adopted in both biological (Stiehler *et al.*, 2010; Shi *et al.*, 2012; Tayton *et al.*, 2012; Weszl *et al.*, 2012; Schubert *et al.*, 2011; Seebach *et al.*, 2010; Fawzi-Grancher *et al.*, 2009) and synthetic graft studies (Barbanti Brodano *et al.*, 2012; Nukavarapu and Amini, 2011; Niemeyer *et al.*, 2010). This method removes the need for complex equipment and culturing methods, seen in more intricate methods (for example bioreactors) (Haykal *et al.*, 2014), and which have not shown to be any more efficient (Weinand *et al.*, 2009). The static loading method used still resulted in a high percentage seeding efficiency using the washed human bone (90% after one hour), which is superior to other synthetic and biologically derived products as reported by Seebach *et al.* (2010). Importantly, whilst this group was seeded with 250,000 cells, MTT levels indicated the highest cell retention number was only approximately 20,000 cells (8%).

Whilst non-adherent cells were collected in similar ways between our study and others (Shi *et al.*, 2012), these non-adherent cells were directly counted whilst other groups have utilised PicoGreen assays to determine cell number within their scaffolds (Bolland *et al.*, 2006; Tilley

et al., 2006; Tayton *et al.,* 2012; Hashimoto *et al.,* 2011; Stiehler *et al.,* 2010). Whilst this method is less laborious, the presence of DNA, however low, within our washed structure may have altered results and as such was deemed unsuitable. Furthermore, by only counting non-adhered cells, the seeded bone cubes could be used in further examination, as a sample sacrifice was not required. In addition to cell seeding efficiency, the actual presence of adhered seeded cells within the scaffold was visualised through immunohistological staining of CFDA-SE labelled cells. This staining determined that seeded cells were adhering to the structure and were not merely trapped within the matrix. Whilst studies have also utilised a similar method of determining cell adhesion through histology (Shi *et al.,* 2012; Frith *et al.,* 2010; Gao *et al.,* 2012; Boo *et al.,* 2002), by using labelled cells, similar to Lo *et al.* (2011), this study helped identify seeded cells specifically, eliminating the possibility of counting native cells not removed by the wash process. The adhered cells were also shown to be metabolically active, by assessment with alamarBlue.

2.4.3 Effect of wash process sterilants on bone allograft material

The sterilant PAA has the potential to cause cell damage and death; however the results have demonstrated this novel wash method does not produce cytotoxic material. Lomas *et al.* (2004) also utilised PAA as a sterilant, ultimately noting no cytotoxic affect after its use. However, the study by Lomas *et al.* (2004) also demonstrated that a final PAA concentration greater than 0.003% had the potential to reduce cell number, and below 0.0015% did not affect cell viability. Additionally, Bormann *et al.* (2010) noted an initial cytotoxic effect of an extract media created with their PAA sterilised material; however this cytotoxic effect was not present after an additional extraction process, suggesting the initial extraction process had reduced the PAA remaining in the material to safe levels.

Importantly, as there was no decreases in cell viability or cell number from incubation with washed bone extract media in the current study, it would suggest that despite using relatively high, 0.02% PAA for sterilisation purposes, the level of residual PAA was below a cytotoxic limit. In addition to the use of PAA, hydrogen peroxide was used simultaneously in the novel wash method to ensure denaturation and removal of as much material as possible. The detrimental nature of hydrogen peroxide alone has been displayed by DePaula *et al.* (2005) and Kluger *et al.* (2003). However, the study by DePaula *et al*. (2005) concluded that hydrogen peroxides effect was dependent on the time the bone was in contact with it, concluding that bone retained its osteoinductive capacity when in contact with hydrogen peroxide for no longer than 1h, which is a greater timepoint than the 15 minutes the bone was in contact with hydrogen peroxide in the current study. Furthermore, no PAA was use in their study, ruling it out as a potential cause of any effect. The biocompatible nature of the novel washed material produced in this study would therefore suggest appropriate removal of PAA and hydrogen peroxide from the system, and that they are no longer able to cause any cytotoxic effects.

A potential limitation of the contact cytotoxicity study is the lack of uniformity in bone cube porosity. The porous structure of the fresh-frozen bone is filled by the marrow component, which prevents cells from penetrating into and under the structure. Removal of this marrow by the novel wash process allows cells to enter this cavity, and may influence the distribution of cells once added to the growth wells. This may explain why cells were present directly under the bone cube in novel washed samples, and not in unwashed fresh-frozen, although it does not explain why cells were unable to grow up to the bone boundary.

This study did not examine the effect of gamma irradiation on cell viability in addition to native and washed samples. Moreau *et al.* (2000) displayed gamma irradiated samples as causing a cytotoxic boundary to cell growth, caused by the peroxidation of lipids. Therefore

possible further work could be undertaken to include such samples, to determine whether there is any alteration in biocompatibility between the two sterilisation methods.

2.4.4 Conclusions

The analysis of the cellular nature of the bone shows extensive removal of marrow components, leading to a metabolically inactive, acellular material. This acellular bone is more biocompatible compared to unwashed fresh-frozen, and would suggest that a marrow component is responsible for causing a cytotoxic effect. In addition, the removal of the marrow enabled cells to remain viable when in contact with the material, with BM-MSCs able to adhere and proliferate on the washed bone structure. These results highlight the efficacy of the wash process to produce a biocompatible material, suitable as a scaffold for use in further investigations into the assessment of osteogenic properties.

Chapter 3

Assessing the effect of the wash process on the biomechanical properties of bone

3.1 Introduction

The primary function of human bone allograft material is as a stable platform for osseointegration, adequately filling a bone void whilst being able to support some mechanical load. Failure of grafts to withstand mechanical load can lead to non-unions and subsidence, and ultimately leads to revision surgery (Berner *et al.,* 2012; Ateschrang *et al.,* 2009) which is technically more complex with an increased chance of further failure and associated patient morbidity (Pekkarinen *et al.,* 2000).

In addition to being able to withstand load, the strength, rigidity, and architecture of the bone are also important in directing cell differentiation and ultimately activity, which has led to synthetic materials being modified to exhibit these properties (Binulal *et al.,* 2010). The porosity of the material is believed to be essential in a grafts osteogenic ability, as highly porous materials present a larger surface area available to adherent cells. This ultimately increases the total number of cells able to inhabit a graft (Tayton *et al.,* 2012), whilst decreasing the diffusion path for nutrients and new blood vessel formation, which potentially improves cell viability (Fawzi-Grancher *et al.,* 2009).

Importantly, the force applied to the structure may also prove beneficial to osteogenic activity, activating osteogenic cells and triggering tissue regeneration through mechanical force transduction (Robling *et al.,* 2008; Kelly and Jacobs, 2010), with evidence suggesting this is a clear regulator of genetic precursors (Haudenschild *et al.,* 2009) and may well lead to quicker cell specialisation (Sen *et al.,* 2011). The conservation of these properties would therefore be beneficial in the clinical application of bone graft material, not only in terms of force distribution but also as a regulator of osteogenic activity.

Currently, the most widely used allograft material in the UK is fresh-frozen human allograft bone, which despite freeze-thawing before use, still retains its structural and biomechanical properties (Reikeras, 2010; Shaw *et al.,* 2012). However, this material poses serious issues with safety and efficacy in a clinical setting. Though processing methods have been developed which may improve the safety of this material, they may inadvertently detrimentally affect its biomechanical properties. In particular, though gamma irradiation has been demonstrated to successfully denature biological particles and improve safety, the process may also alter the biomechanical stability, and therefore the latent osteoconductivity of the material (Nguyen *et al.,* 2007). While 25kGy of gamma irradiation is the recommended level of irradiation to guarantee safety, levels as low as 17kGy can cause significant changes in the "final strength" of the allograft (Currey *et al.,* 1997), with research by Cornu *et al.* (2000), demonstrating a decrease of as much as 71% in overall strength after gamma irradiation. This decrease in mechanical strength is most likely due to the denaturing mechanism of gamma irradiation, and the production of free radicals from water radiolysis. These free radicals are responsible for denaturing the viral and bacterial particles; however they may also denature collagen within bone material (Hamer *et al.,* 1999; Hamer *et al.,* 1996). This allows unhindered fracture propagation, dramatically decreasing the resistance of the structure (Mitchell *et al.,* 2004), and in a practical situation suggests irradiated bones are more likely to develop large fractures leading to premature failure under load (Dux *et al.,* 2010). The failure in mechanical property has serious clinical implications; with one post-operative study by Hassaballa *et al.* (2009) demonstrating an implant subsidence of greater than 5mm in 21.7% of patients, with larger subsidence occurring in patients who had received higher dose irradiated bone grafts, and resulted in decreased bone repair rate of 30% with no trabecular bone remodelling.

Using alternative processing techniques offers the opportunity to remove the potentially harmful marrow components without the production of free radicals and the destruction of the collagen microstructure. However, alternate processing techniques may also have a negative effect on the biomechanical stability of the material, with both deproteinisation and demineralisation, and the removal of the mineral from the osseous tissue, eliminating the crucial mechanical properties of the bone (Chen and McKittrick, 2011).

Research into combination wash steps involving PAA-ethanol sterilisation has also shown an effect on the biomechanical properties of bone (Rauh *et al.*, 2014); however other studies utilising this sterilisation method (Haimi *et al.*, 2009; Pruss *et al.*, 2003), do not report any alteration of the mechanical properties of bone in such a severe manner as gamma irradiation. The discrepancy in results, similar to gamma irradiation, may be dependent on the concentration of sterilant (Pruss *et al.*, 2003) and exposure time (DePaula *et al.*, 2005). Furthermore, biomechanical research conducted using washes, gamma irradiation or a combination of the two, have shown no significant difference between treatment groups suggesting chemical sterilisation is no more or less damaging than irradiation (Mikhael *et al.*, 2008; Schwiedrzik *et al.*, 2011).

3.1.1 Aims

The mechanical stability of the bone allograft is important not only in its clinical use, but also in the maintenance of the porous 3D structure which can ultimately affect the osteogenic activity of any cells seeded into its structure. For this study the mechanical stability of the structure was assessed to determine whether the novel wash process had altered its biomechanical properties. The aims of this investigation were to: (i) using mirrored samples assess whether the wash process had an effect on the bone's biomechanical properties

compared to unwashed and, (ii) in a clinical compression model compare the wash process to gamma irradiation sterilisation to assess the effect on the bone mechanical stability.

3.2 Materials and Methods

3.2.1 Uniaxial mirrored samples compression testing

To assess the comparable biomechanical stability of washed and unwashed fresh-frozen bone material, a uniaxial model was used with location mapped samples to reduce variance between femoral heads and location of material taken. Whole fresh-frozen femoral heads from male and female donors aged 70 YOA and above (N=15; 70-90, mean 77.9 YOA) (Table 3.1), were laterally bisected along the coronal plane to produce two equal halves. One half was retained whilst the other was washed according to the method described previously (2.2.1.2). The two halves were grid marked along their axis of normal compression and cut into $1cm^3$ cubes (n=216) and labelled with orientation and designated coordinates in the X, Y and Z axis (Figure 3.1). Cubes from geode locations along with their mirrored sample were not included in the study.

Table 3.1: Femoral head sample details for uniaxial mirrored biomechanical compression testing

Sample ID	Sex	Age (Years)
450 389	Male	70
458 473	Male	72
451 104	Male	73
457 291	Male	74
458 309	Male	76
160 267	Male	76
443 659	Female	76
159 922	Male	77
450 583	Female	77
456 822	Male	79
454 750	Female	80
449 713	Female	81
160 731	Female	83
449 028	Male	85
450 223	Female	90

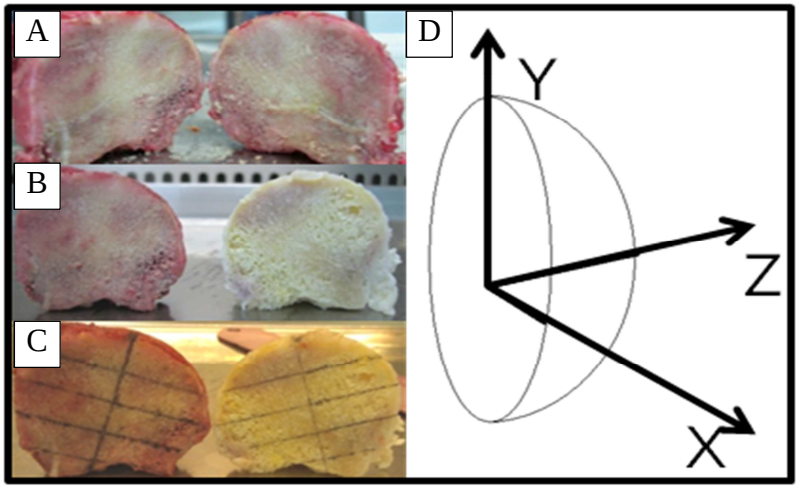

Figure 3.1: Diagram displays the process of producing location mapped samples for uniaxial mirrored sample compression testing. Femoral heads were first halved (A) before one half was washed using the novel wash process (B). The two halves were then marked for cutting (C) and designated X, Y and Z axis coordinates (D).

Cubes were loaded onto a compression testing machine (LRX Plus; Lloyd Instruments, Sussex, UK) and subjected to one round of compression to failure with the settings: preload 0.2N, maximum deflection of 3mm and maximum load of 5KN at a speed of 5mm/minute. Using the NEXYGEN*plus* software, data was recorded for the parameters of:

- Young's modulus (Pa): A measure of the materials elasticity up to the point of yield, measured by the gradient (stress / strain) of the stress strain curve during this period. This is a measure of the materials stiffness / rigidity in relation to its geometrical parameters.
- Load (N): The force the material was burdened with at point of recording.
- Stress (Pa): The intensity of pressure the entire volume of the material was subject to, at point of recording. This is equal to the force exerted on the sample/ the samples surface area.

- Deflection (mm): The deformation of the material from its original height, at point of recording.
- Work (J): The energy absorbed by the material, at the point of recording.

All data sets were taken during the elastic period, at the point of yield and the maximum point on the stress strain curve termed point of failure (Figure 3.2).

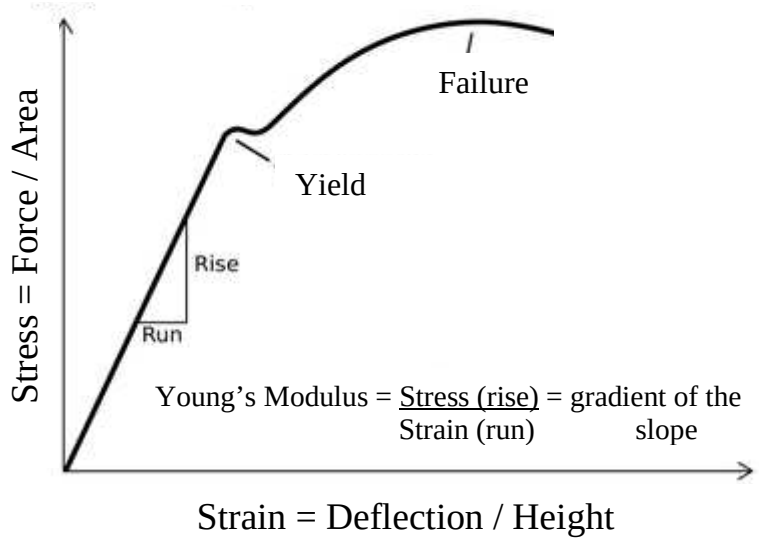

Figure 3.2: Stress strain curve representative of trabecular bone under compression. Diagram depicts points of yield and failure of the trabecular material. (Diagram adapted from original: http://www.naturalheightgrowth.com/wp-content/uploads/2013/04/stress-strain-curve.png)

3.2.2 Orientated vs random orientated uniaxial compression testing

For the comparison of orientated and random orientated biomechanical values, a cohort of three femoral heads were split as previously described (2.2.3.1) (Table 3.2). The two halves were cut into 1cm^3 cubes, with one half being marked for orientated uniaxial compression, and the other unmarked so as to not cause bias. The two groups were compressed as described previously (3.2.1). Data was recorded for parameters of elasticity, yield and failure. In addition to standard error (SE), the coefficient of variation was produced so as to

normalise the dispersion of the frequency distribution of the data and as such measure the extent of the variability. The coefficient of variation is defined as the ration of standard deviation to the mean of the data set.

Table 3.2: Femoral head sample details for orientated vs random orientated compression testing

Sample ID	Sex	Age (Years)
454 608	Female	77
162 509	Female	81
458 642	Female	84

3.2.3 Clinical compression model of biomechanical stability

For use in clinical model biomechanical testing, $1cm^3$ bone cubes were cut from 22 femoral heads, both washed (N=10, 72 cubes) and unwashed fresh-frozen (N=12, 128 cubes) (Table 3.3 for more details) using a De Soutter saw and grid line. Half the bone cubes from each femoral head were irradiated (25KGy, Cobalt 60 gamma irradiation, Applied Sterilisation Technologies) to produce unwashed fresh-frozen gamma irradiated and washed gamma irradiated samples. The cubes were made as level as possible and loaded onto a compression testing machine and subjected to one round of compression to failure as previously described (3.2.1). Data was recorded using NEXYGEN*plus* software.

Samples were retained for unwashed fresh-frozen young (n=28) and old (n=37) and washed young (n=18) and old (n=16) cubes. Samples of both unwashed fresh-frozen and washed bone cubes were irradiated to produce young and old unwashed fresh-frozen irradiated (n=12 and n=10; respectively) and washed irradiated (n=18 for both young and old). These samples were subject to mechanical testing for biomechanical comparison.

Table 3.3: Femoral head details for compression testing using clinical compression model

Sample ID	Sex	Age (Years)	Material Type/ Additional Use
457 356	Male	38	Washed
457 282	Male	41	Washed
458 034	Female	42	Washed
455 354	Male	43	Washed
447 995	Male	46	Washed
156 251	Male	77	Washed
449 505	Female	77	Washed
457 447	Male	78	Washed
455 486	Male	79	Washed
458 330	Male	82	Washed
488 577	Female	44	Fresh-Frozen (comparison of age)
453 071	Male	47	Fresh-Frozen (comparison of age)
459 458	Male	48	Fresh-Frozen (comparison of age)
456 299	Male	48	Fresh-Frozen (comparison of age)
458 463	Female	50	Fresh-Frozen (comparison of age)
536 083	Female	50	Fresh-Frozen (comparison of age)
157 565	Female	70	Fresh-Frozen (comparison of age)
156 862	Male	72	Fresh-Frozen (comparison of age)
450 023	Male	73	Fresh-Frozen (comparison of age)
449 400	Male	74	Fresh-Frozen (comparison of age)
161 055	Female	74	Fresh-Frozen (comparison of age)
161 334	Female	78	Fresh-Frozen (comparison of age)

3.2.4 Statistical analysis

Statistical analysis was conducted using Origin Pro (Origin Pro 8.5; Silverdale Scientific Ltd, Stoke Mandeville, UK). Paired t-test analysis was conducted on paired mirrored orientated samples, Wilcoxon non-parametric paired statistical analysis was performed on orientated vs random orientation sample compression data, whilst a Mann-Whitney non-parametric statistical analysis was performed to compare mechanics data from young and old donor material in clinical model, as well as between unwashed fresh-frozen, washed, and gamma irradiation treated samples. Significance was accepted for $p \leq 0.05$.

3.3 Results

3.3.1 Mirrored uniaxial compression data

There was a significant increase in Young's modulus between the unwashed fresh-frozen and washed bone material, with washed bone displayed a Young's modulus of 84.6MPa (±3.6) compared to unwashed 75.9MPa (±3.4) ($p \leq 0.05$) (Figure 3.3).

Figure 3.3: Compression testing results of Young's modulus, recorded during the elastic period, for 1cm^3 bone cubes from both unwashed fresh-frozen (n=108) and washed (n=108) bone cubes taken from mirrored locations of halved femoral heads. Data is displayed as mean ± SE. * Symbol denotes a significant difference ($p \leq 0.05$) between unwashed fresh-frozen and washed bone data sets.

The result at the point of yield indicated no significant differences between the two data sets for the parameters load at yield, stress at yield or work at yield (Figure 3.4). There was a significant decrease in the deflection at yield of the washed bone material compared to unwashed fresh-frozen with a decrease from 1.49mm (±0.04) to 1.35mm (±0.04) ($p \leq 0.01$) (Figure 3.4 B), suggesting the washed materials' height was compressed less at the point it lost its elasticity. There were also no significant differences between unwashed fresh-frozen and washed bone cubes at the parameters of failure (Figure 3.5).

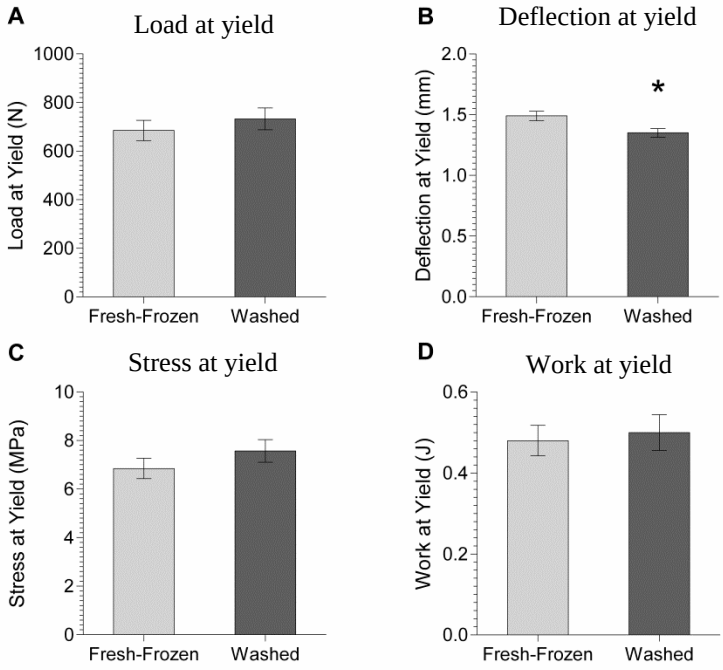

Figure 3.4: Compression testing results at the point of yield for $1cm^3$ bone cubes from unwashed fresh-frozen and washed femoral heads. Graphs display averaged results for load at yield (A), deflection at yield (B), stress at yield (C) and work at yield (D) for both unwashed fresh-frozen (n=108) and washed (n=108) bone cubes taken from mirrored locations of halved femoral heads (N=15). Data is displayed as mean ± SE. *, indicates significant difference ($p \leq 0.05$) between unwashed fresh-frozen and washed.

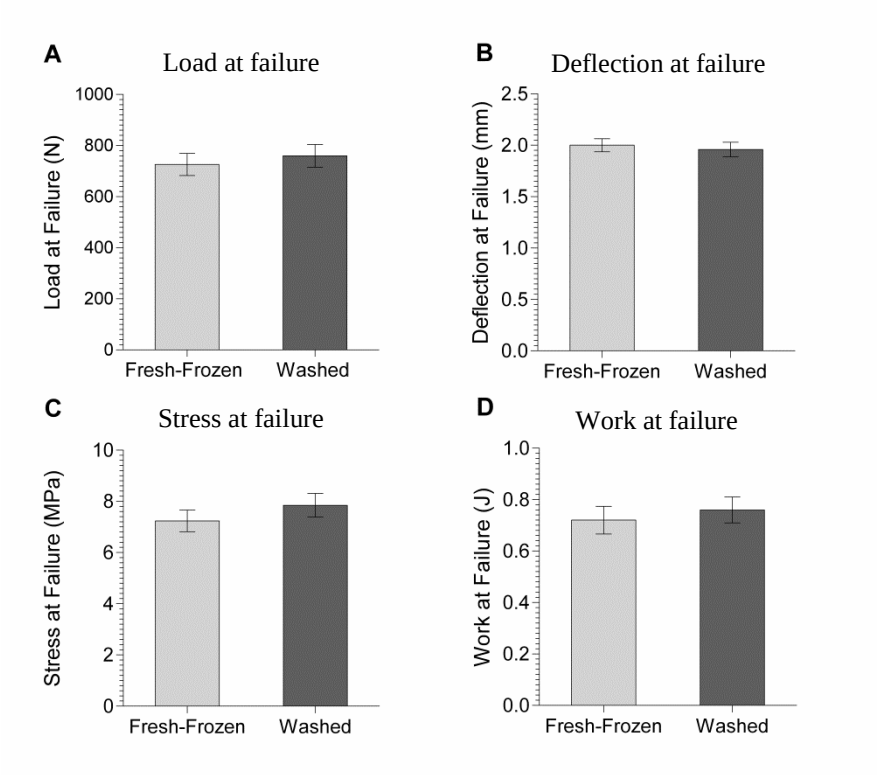

Figure 3.5: Compression testing results at the point of failure for 1cm^3 bone cubes from unwashed fresh-frozen and washed femoral heads. Graphs display averaged results for load at failure (A), deflection at failure (B), stress at failure (C) and work at failure (D) for both unwashed fresh-frozen (n=108) and washed (n=108) bone cubes taken from mirrored locations of halved femoral heads. Data is displayed as mean ± SE.

3.3.2 Mechanical compression of orientated vs random orientated unwashed fresh-frozen samples

Mechanical testing of orientated vs random orientated samples was undertaken to assess any large changes in biomechanical strength caused by not compressing the bone in the normal direction of load. There was no significant difference between the standard coefficient of variation for intra-head and inter-sample under all compression parameters at orientated or

random orientation (see section 8.1: Appendix I-Table 8.1). Similarly there was no statistical significance between the coefficient of variation for randomly orientated and orientated samples at any parameter. The results of this compression testing demonstrated no significant changes in any parameters during the elastic period (Figure 3.6), parameters at the point of yield (Figure 3.7) or failure (Figure 3.8) between the orientated and random orientation samples.

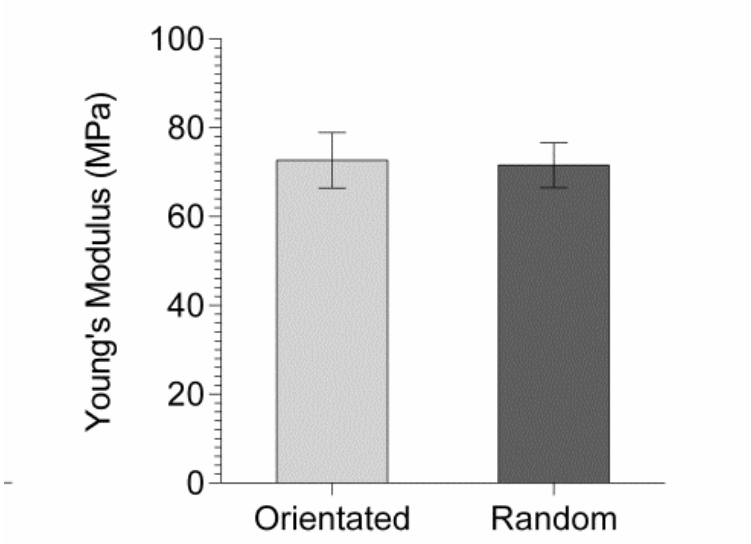

Figure 3.6: Compression testing results of Young's modulus, recorded during the elastic period, for 1cm^3 bone cubes biomechanically tested at orientated (n=15) and random orientated (n=15) taken from halved femoral heads (N=3). Data is displayed as mean ± SE.

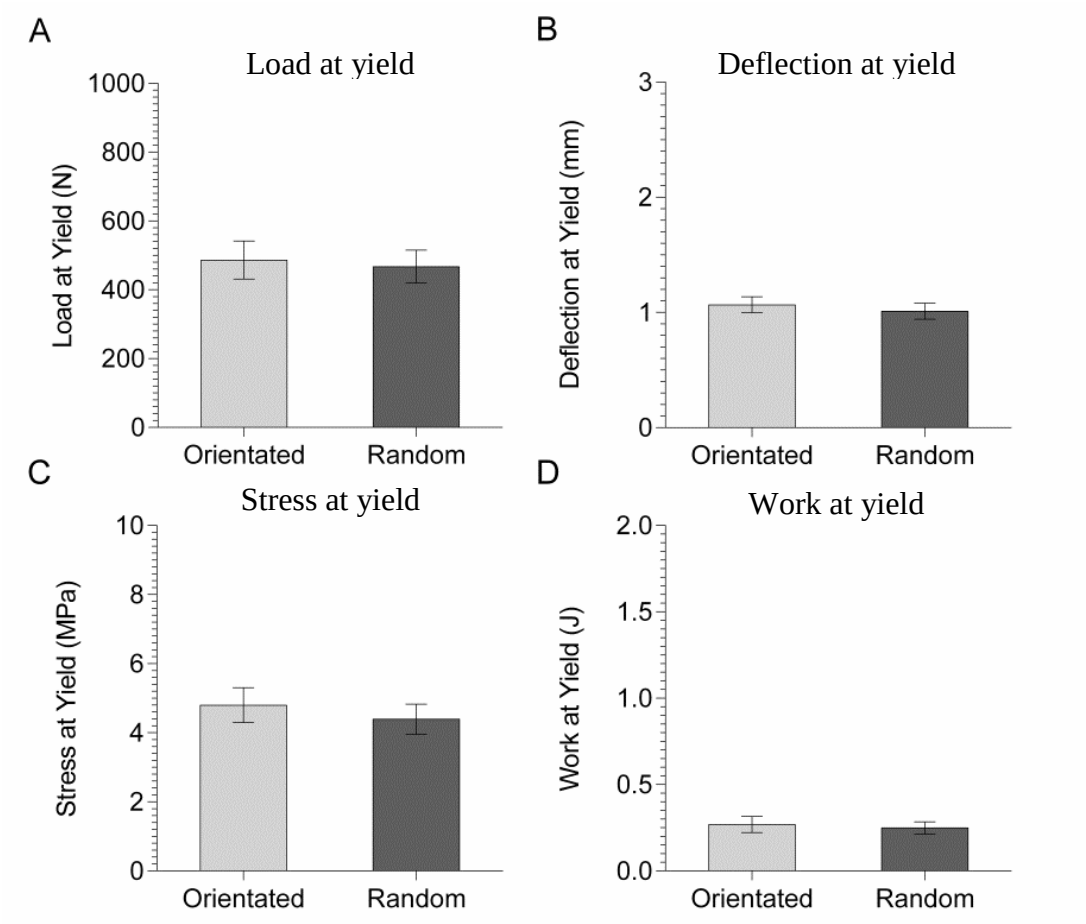

Figure 3.7: Compression testing results at the point of yield for 1cm^3 bone cubes biomechanically tested at orientated (n=15) and random orientated (n=15) taken from halved femoral heads (N=3). Graphs display averaged results for load at yield (A), deflection at yield (B), stress at yield (C) and work at yield (D). Data is displayed as mean ± SE.

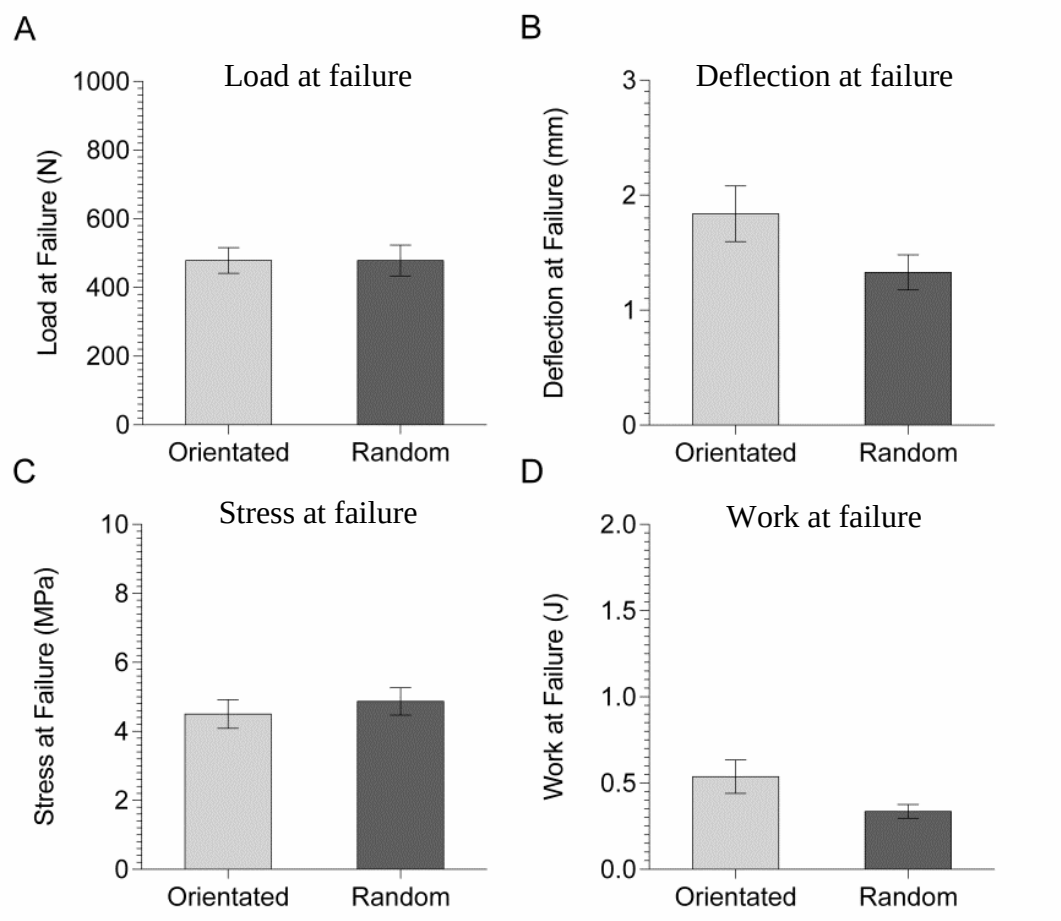

Figure 3.8: Compression testing results at the point of failure for 1cm^3 bone cubes biomechanically tested at orientated (n=15) and random orientated (n=15) taken from halved femoral heads (N=3). Graphs display averaged results for load at failure (A), deflection at failure (B), stress at failure (C) and work at failure (D). Data is displayed as mean ± SE.

3.3.3 Mechanical compression of samples from young (≤50 YOA) and old (≥70 YOA) bone donors using clinical compression model

A cohort of 12 femoral heads (Table 3.3 comparison of age samples) were split between ≤50 YOA (N=6) and ≥70 YOA (N=6) and cut into 1cm^3 cubes (n=28 and n=37; respectively). Half the samples underwent mechanical compression to failure, while the other half were gamma irradiated first (see section 3.3.4). Though values were consistently larger for younger samples, there was no statistically significant difference for the Young's modulus between the old (≥70 YOA) and young (≤50 YOA) aged donor material (Figure 3.9). Neither were there any statistically significant differences for any parameter at the point of yield (Figure 3.10).

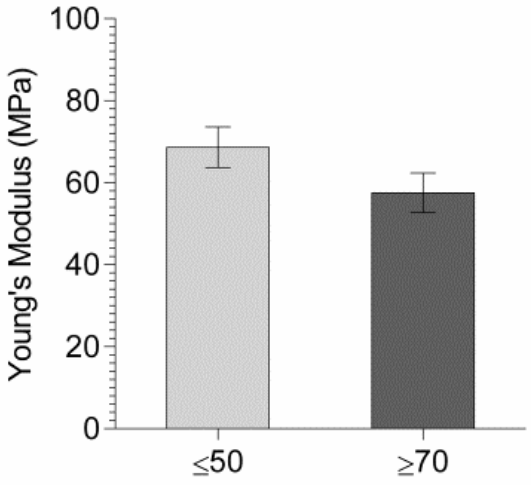

Figure 3.9: Compression testing results of Young's modulus, recorded during the elastic period, for 1cm^3 bone cubes from unwashed fresh-frozen femoral heads from young (≤50 YOA, n=28) and old (≥70 YOA, n=37) bone donors. Data is displayed as mean ± SE. The absence of a * symbol denotes no significant differences between unwashed fresh-frozen young and old bone.

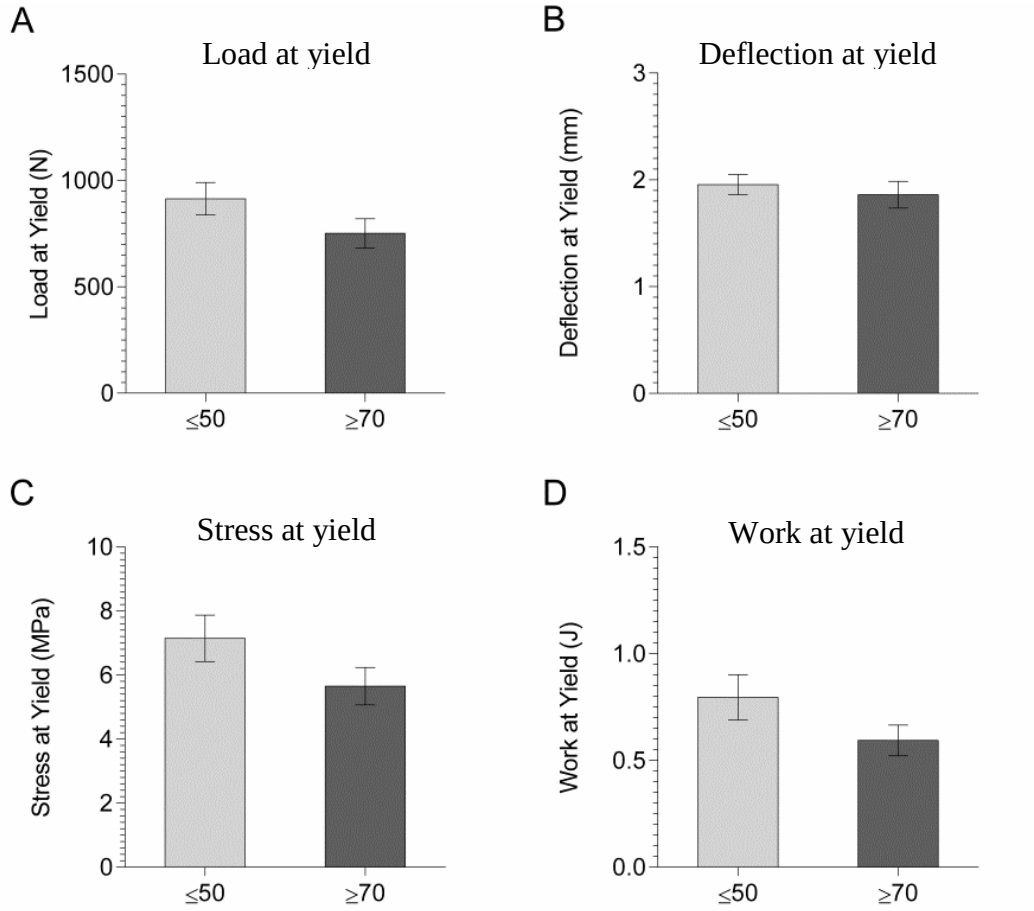

Figure 3.10: Compression testing results at the point of yield for 1cm^3 bone cubes samples from unwashed fresh-frozen femoral heads from young (≤50 YOA, n=28) and old (≥70 YOA, n=37) bone donors. Graphs display the averaged results for parameters load to yield (A), deflection at yield (B), stress at yield (C) and work at yield (D). Data is displayed as mean ± SE. The absence of a * symbol denotes no significant differences between unwashed fresh-frozen young and old bone data sets.

Comparisons of the results at point of failure between the old and young material demonstrated statistical differences between the two sample groups. Younger material had a significantly higher load at failure (1073N±84.2) compared to old (821N±70.2) ($p \leq 0.05$), as well as an increased stress at failure (7.7MPa±0.61 compared to 5.8MPa±0.49) ($p \leq 0.05$). The younger material also had a work at failure reading of 1.13J (±0.11), which was significantly larger than old material (0.83J±0.08) ($p \leq 0.05$) (Figure 3.11).

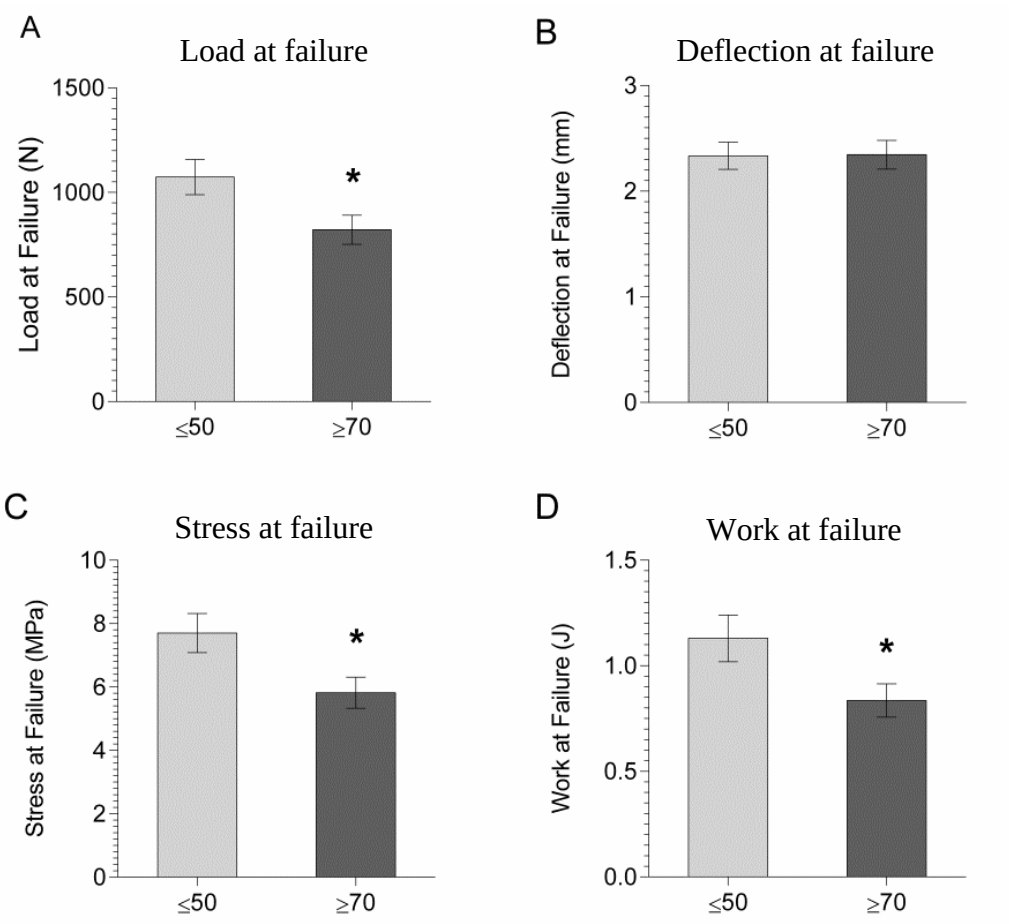

Figure 3.11: Compression testing results at the point of failure for 1cm^3 bone cubes samples from unwashed fresh-frozen femoral heads from young (≤50 YOA, n=28) and old (≥70 YOA, n=37) bone donors. Graphs display averaged results for load at failure (A), deflection at failure (B), stress at failure (C) and work at failure (D). Data is displayed as mean ± SE. * Symbol denotes a significant difference ($p \leq 0.05$) between unwashed fresh-frozen young and old bone data sets.

3.3.4 Mechanical compression of unwashed fresh-frozen, washed, unwashed fresh-frozen irradiated and washed irradiated bone samples

In addition to the unwashed fresh-frozen samples used in section 3.3.3, a further 10 femoral heads, five in the ≤50 YOA group and five in the ≥70 YOA group (Table 3.3), were washed and used to produce 1cm^3 cubes. The elasticity parameter of Young's modulus was not significantly different between unwashed fresh-frozen and washed samples before or after irradiation of the material. (Figure 3.12)

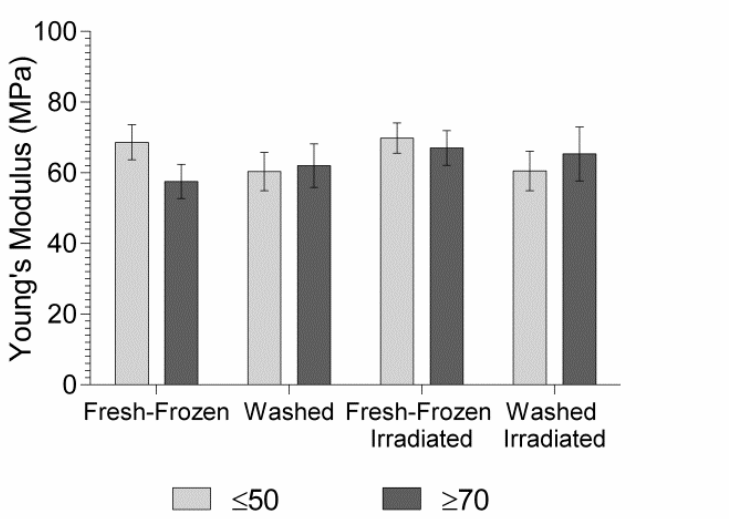

Figure 3.12: Compression testing results of Young's modulus, recorded during the elastic period, for 1cm^3 bone cubes from young (≤50 YOA) and old (≥70 YOA) age groups for unwashed fresh-frozen (n=28 and n=37; respectively), washed (n=18 and n=16; respectively), unwashed fresh-frozen irradiated (n=12 and n=10; respectively) and washed irradiated material (n=18 for both). Data is displayed as mean ± SE.

At the point of yield, young (≤50 YOA) bone samples indicated significantly lower readings for washed bone compared to unwashed fresh-frozen samples for the parameters of load, stress ($p \leq 0.01$) and work ($p \leq 0.05$); however these results were not evident between old (≥70 YOA) unwashed fresh-frozen and washed bone (Figure 3.13). There was also no significant difference in the deflection of this material. In comparison, after irradiation, deflection at yield was significantly decreased in old (≥70 YOA) unwashed fresh-frozen irradiated bone compared to unwashed fresh-frozen ($p \leq 0.05$). However, irradiation of washed bone caused a significant decrease at deflection at yield for both young and old samples (Figure 3.13 C). As previously recorded, there was no statistically significant difference between ages in any parameter at yield after washing; this was also true after irradiation.

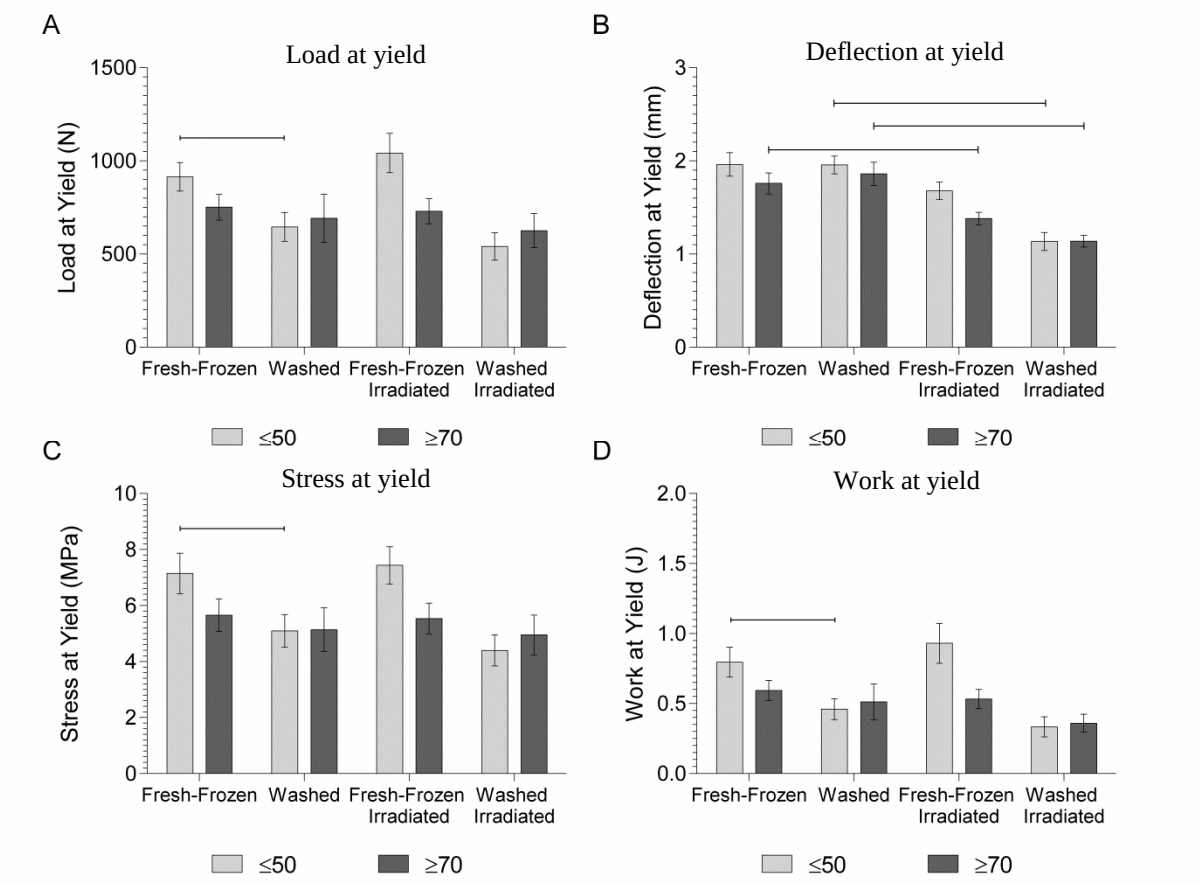

Figure 3.13: Compression testing results at the point of yield for 1cm^3 bone cubes from young (≤50 YOA) and old (≥70 YOA) age groups for unwashed fresh-frozen (n=28 and n=37; respectively), washed (n=18 and n=16; respectively), unwashed fresh-frozen irradiated (n=12 and n=10; respectively) and washed irradiated material (n=18 for both). Graphs display the averaged results for parameters load to yield (A), deflection at yield (B), stress at yield (C) and work at yield (D). Data is displayed as mean ± SE. Line denotes significance ($p \leq 0.05$) between samples.

At the point of failure, the statistical significant differences in load, stress and work previously reported between age groups in unwashed samples were also present in unwashed fresh-frozen irradiated samples (Figure 3.14 A, C and D).

The significant differences seen between young and old unwashed fresh-frozen samples were not present after washing. Instead, there was a statistically significant decrease after washing in the parameters of work at failure and load at failure ($p \leq 0.01$) as well as stress at failure ($p \leq 0.05$) for young (≤50 YOA) samples only. The irradiation of samples caused no loss to the biomechanical properties of the material at any parameter, other than deflection; however this was only significant in samples which were washed prior to irradiation.

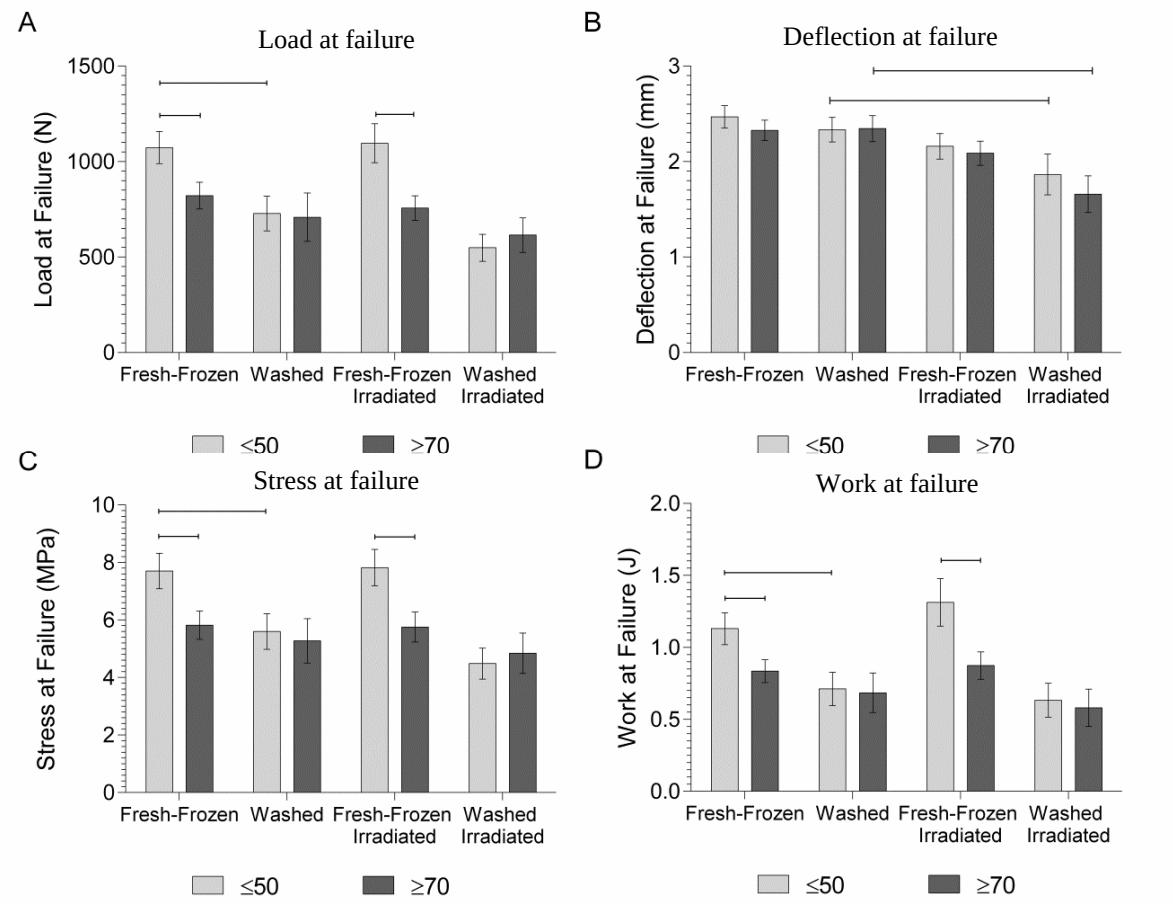

Figure 3.14: Compression testing results at the point of failure for 1cm^3 bone cubes from young (≤50 YOA) and old (≥70 YOA) age groups for unwashed fresh-frozen (n=28 and n=37; respectively), washed (n=18 and n=16; respectively), unwashed fresh-frozen irradiated (n=12 and n=10; respectively) and washed irradiated material (n=18 for both). Graphs display averaged results for load at failure (A), deflection at failure (B), stress at failure (C) and work at failure (D). Data is displayed as mean ± SE. Line denotes significance ($p \leq 0.05$) between samples.

3.4 Discussion and Conclusion

Determining the mechanical stability of any graft material is important in assessing its potential use in load bearing or force distributing situations. The stability of a material can determine its ability to support its 3D architecture under compressive force such as in a clinical setting (Berner *et al.,* 2012; Ateschrang *et al.,* 2009), and which can ultimately determine how cells not only react to the material, but which may also help in their regeneration of a damaged site through osteogenic stimulation via mechano-transduction (Robling *et al.,* 2008; Haudenschild *et al.,* 2009). Whilst bone strength may be determined easily though bone mineral density (BMD), this method may be ineffective in assessing the true mechanical stability, as up to 40% of a bones strength is determined by non-mineral factors such as architecture, porosity, thickness and protein ECM constituents (Ammann and Rizzoli, 2003). As such, a compressive model was utilised, examining the materials mechanical characteristics at the parameters of yield and failure.

3.4.1 Effect of novel wash process on compressive properties of human bone in uniaxial compression, mirrored location model

Compression testing of the washed human bone demonstrated comparable biomechanical stability to unwashed fresh-frozen for parameters at both the points of yield and failure. Though there were small increases in Young's modulus and a reduction displacement at yield, the resulting increase in rigidity had no effect on the overall structural stability of the washed material, with no significant differences recorded in the parameters at the point of failure. The increase in Young's modulus seen after the removal of marrow has also been documented by Halgrin *et al.* (2012), who concluded that the marrow, present in the fresh-

frozen bone, had caused increased transverse pressure and local stress on trabeculae, causing it to fail prematurely. Additionally, the results also suggest that the material was not demineralised by the wash process, as this would have compromised the biomechanical stability of the bone (Currey, 1988; Chen and McKittrick, 2011).

This study utilised 1:1 (height:width) ratio bone cubes for compression experiments (the shape used in cell culture methods), which have been demonstrated to be extremely efficient in compression testing (Ang *et al.,* 2012). Whilst cylindrical cores are more generally used in compression models (Mikhael *et al.,* 2008), the use of trabecular cores does not account for the intra-femoral head variability caused by the differing compressive and tensile structures of the trabeculae (Martens *et al.,* 1983), and as such aspects of the femoral head such as size and shape, which greatly affect the overall strength of the trabecular sample are not accounted for, leading to large inter patient variability (Aleixo *et al.,* 2013). This variation may also arise through changes in sex, age, weight or even disease state (Green *et al.,* 2011; Homminga *et al.,* 2002). Similarly, use of halved femoral heads and mirrored sample locations eliminates inter-patient variance, and whilst left and right femoral heads from the same patient show similar mechanical strength (Banse *et al.,* 1996), high variability between patient sides may arise through limp, gate or walking aids (Smith and Smith, 1976; Weaver and Chalmers, 1966). This would suggest that intra-femoral head samples with matched locations allow for changing mechanical distribution, and is therefore a strong mechanical compression model (Brown and Shaw, 1983; Brown and Ferguson, 1980; Vastel *et al.,* 2004).

3.4.1.1 Evaluation of mirrored location compression model

Whilst orientated uniaxial compression is routinely used for biomechanical strength, it is unrepresentative of the trabecular material when used in a clinical setting. Surgeons creating bespoke shapes will be unaware of load orientation, and so force may be applied to the material in a non-orientated fashion. As such, the testing of load orientation on femoral head trabecular structures was undertaken to determine whether a more relevant clinical compression model could be successfully utilised.

Results of orientated vs random orientated samples suggested that a random orientation model is representative of the whole femoral heads biomechanical properties. Orientated and non-orientated samples displayed similar averages and coefficient of variation, with no statistically significant difference between them for any compression parameter. This is in accordance with results recorded in a previous study by Cornu *et al.* (2000), even suggesting agreeable inter-head variation in results; however this is only applicable for stress. The data from the current study suggests that "general" loading of the trabecular material is comparable to "linear loading". This may be explained by the internal structure of the femoral head, which allows for the distribution of structural forces in both compression and tension (Figure 3.15) (Martens *et al.*, 1983). Specific alignments of trabeculae dissipate the load throughout the whole head, directing it towards the femur through the neck.

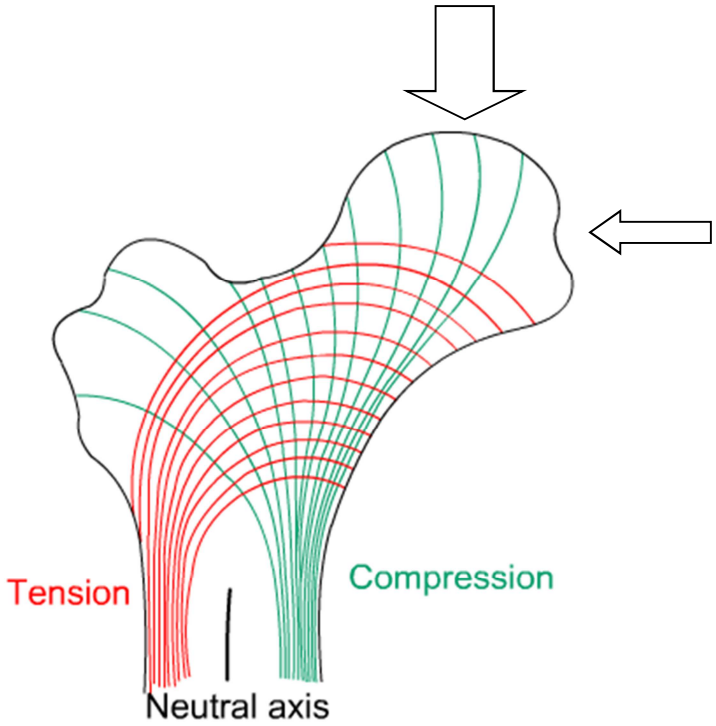

Figure 3.15: Diagram displaying the constant compressive and tensile stresses within the femoral head which dictate trabecular distribution and alignment. Arrows depict the relative direction and size of force that the femoral head is subjected to, via its contact with the acetabulum in the hip joint (Image adapted from original: http://www.doitpoms.ac.uk/tlplib/bones/structure.php).

3.4.2 Compression of human bone material in a clinical model

3.4.2.1 Effect of gamma irradiation on the compressive properties of human bone in a clinical model

The majority of research suggests a detrimental action by gamma irradiation to the mechanical properties of bone (Akkus *et al.*, 2005; Hamer *et al.*, 1996; Hamer *et al.*, 1999; Mitchell *et al.*, 2004; Dux *et al.*, 2010), with clinical analysis of IBG using irradiated samples resulting in a reduction in mechanical stability, thereby leading to complications (Hassaballa

et al., 2009). In this current study, gamma irradiation of unwashed fresh-frozen trabecular bone did not cause any change in any biomechanical parameter; however it is important to note that the majority of studies in the literature are undertaken in cortical strut material, which is biomechanically different to trabecular bone (Martens *et al.,* 1983; Turunen *et al.,* 2013), and once washed, treatment with gamma irradiation significantly changed the stress at yield and stress at failure. Although no other parameter significantly changed, the work at failure, work to yield as well as the stress and load at failure were all slightly diminished. This would suggest that the material required less energy and displacement to reach yield and subsequently failure. As this is only apparent in irradiated washed samples, it is likely to be caused by the decrease in the volume of the material increasing the relative concentration of radiation absorbed (Cornu *et al.,* 2000). This may be due to the differences in the volume of material, with the washed material having a decreased mass to energy ratio due to the removal of the marrow, therefore absorbing relatively larger amounts of irradiation (Currey *et al.,* 1997). In addition, Nguyen *et al.* (2013) have also noted that by reducing the radiation dose, many of the negative effects of gamma irradiation are prevented; however this drastically diminished the sterilisation ability with increased bacterial titres present.

3.4.2.2 Effect of novel wash process on the compressive properties of human bone in a clinical model

The results of the biomechanical testing show that the unwashed fresh-frozen samples ≤50 YOA exhibited a superior biomechanical ability in trabeculae yield and point of failure compared to the ≥70 YOA group. This change in age has been noted by other groups in relation to fracture propagation (Nagaraja *et al.,* 2007) as well as the ability to withstand the strain and stresses associated with compression (Green *et al.,* 2011). Normally this would

suggest the trabeculae of young bone are able to withstand greater loads until they become ductile and are able to withstand that load for longer before fracturing completely. This process may be explained by decreased non-enzymatic collagen cross-linking (Turunen *et al.*, 2013), increased porosity and collagen denaturation (Wang *et al.*, 2002), leading to a loss of bone strength.

The lack of change between samples after washing may therefore be due to the disease state of the material. The majority of bone samples are obtained from diseased individuals with osteoporosis, which has been identified as having decreasing mechanical strength through changes in architecture (Homminga *et al.*, 2002) or simply a premature loss of bone material (Li and Aspden, 1997).

Strong oxidising agents, such as the hydrogen peroxide used in the novel wash procedure, have been demonstrated to remove minor mineral aspects of bone (Dumas *et al.,* 2006). However, the histological assessment of washed material in this study demonstrated a lack of change in bone morphology as opposed to the severe changes seen in a study by Dumas *et al.* (2006). Furthermore, the wash process did not change the elastic modulus of the material in either age groups, suggesting that the initial difference between the age groups in native samples was not due to alterations in bone structure density, as there was no change in stiffness, or mineral content (Currey, 1988; Currey, 1968). Additional testing for mineral content before and after the novel wash process would be required to confirm the lack of mineral leaching.

The differences present between age groups may also be, in part, due to changes in the ability of the material to distribute force, or mineral fluidity (Davies *et al.,* 2014); however the results instead support a contribution by the bone marrow to improving the structural fragility of the trabecular bone in young samples. Though this does not seem to corroborate previous

findings on old bone, or Halgrin *et al.* (2012), and the removal of marrow improving the mechanical stability, the difference in sample ages may explain the altered results.

Importantly, there was no change in the relative amount of DNA or protein removed from the young or old femoral heads, suggesting that any change in the removed marrow between these groups is unlikely to be an increase in ECM protein or cellular component. This contribution may instead be due to the load distribution by fluid dynamics (Simkin, 2004; Ochoa *et al.,* 1991), with a difference in marrow viscosity between young and old patients causing a change in the distribution of force throughout the structure. Interestingly, studies have demonstrated a difference in the marrow composition between young and old bone, with increases in adipose cells (Justesen *et al.,* 2001) and decreases in pressure (Shaw, 1963). An increase in yellow fat in older patients may decrease the marrows viscosity and load bearing capability (Tavassoli and Yoffey, 1983), as red bone marrow is denser than yellow ($1.06 g/cm^3$ compared to $0.89 g/cm^3$) (Gurkan and Akkus, 2008). A change in the fluid properties of different marrow compositions has been reported by Davis and Praveen (2006), in which a normal red cell rich marrow displayed non-Newtonian properties, increasing its viscosity with increasing force, which was not apparent in yellow fat cell rich marrow. This would correspond with the large change in the strength of the material between ages which was removed by the wash. A non-Newtonian fluid would, under a large amount of pressure, act to increase its resistance to deformity, potentially alleviating the trabeculae from further damaging loads.

Although the results suggest an effect in the bone, with a change in ≤50 YOA groups, this is not reciprocated by ≥70 YOA bone samples. Together with no alteration to the Young's

modulus of this material, this would suggest a change in marrow composition causing the change in behaviour between age groups.

A potential limitation to this model is the lack of compensation for the Poisson effect by not containing the bone during biomechanical testing. The bone is therefore able to expand in a multi directional force, releasing pressure through bending and bulging. This is not representative of its normal mechanic-environment, where the material would be braced by adjacent material, and therefore able to distribute the force to surrounding structures. As such, this may limit the available strength of the material, and allow fracture propagation by flex and distortion of the materials shape.

3.4.3 Conclusion

Accurate determination of the biomechanical strength of the washed bone material is important in its eventual use, either directly as a surgical allograft, or as a scaffold for MSC-based tissue engineering. The 3D structure itself is thought to influence the activity of osteogenic cells, through mechano-transduction (Kilian *et al.*, 2010; Shih *et al.*, 2011) or simply through shear force (Yourek *et al.*, 2010). The mirrored biomechanical compression results therefore suggest that the washed bone is mechanically comparable to commonly used fresh-frozen allograft material at both yield and failure. Importantly, the yield point denotes the point at which the trabeculae are no longer able to continue resisting the force applied on them in an elastic manner. At this point the trabeculae are deforming in a plastic permanent fashion towards a point of fracture, which relates to the initial buckling on the trabeculae at yield and their resistant to fracture.

The failure point of the bone in this study was used to assess the fracturing of the trabeculae denoting their quality, and together with yield, these two points can determine the rigidity and fragility of the structure. Maintenance of rigidity and an appropriate porous 3D architecture is essential for osteoconductivity and new bone infiltration (Tagil *et al.*, 2000), and further analysis of the bones ability to support osteogenic activity is therefore essential. The results of the clinical loading model denoted differences in the effect of the wash on young and old samples, but ultimately showed that the washed bone was a mechanically stable scaffold, comparable to currently used old donor fresh-frozen allograft material.

The data presented on mechanical testing therefore suggests that the novel wash process does not affect the integrity of the scaffold material, similar to the findings of Mroz *et al.* (2006) and Haimi *et al.* (2008). Ultimately the results of the compression testing show the washed bone material as able to support its 3D architecture under compression comparable to currently used fresh-frozen allograft, and would therefore be suitable as a scaffold in clinical use and further experiments assessing its capability for BTE.

Chapter 4

Assessing the osteoinductive properties of the washed bone, and the effect of cell and bone donor age on osteogenic differentiation/activity

4.1 Introduction

In tissue engineering, scaffolds act as 3D structures, supporting cell attachment and localisation, and as a replacement of lost matrix to fill voids. The potential of bone wash procedures to remove the immunogenic cellular components of marrow tissue has led to their use becoming more prevalent in the production of scaffolds, derived from fresh-frozen allograft bone, for use in BTE (Hashimoto *et al.,* 2011; Dutra and French, 2010). The introduction of pre-osteogenic cells, such as BM-MSC's to bone matrix can improve the osteogenic capacity of the graft and its clinical outcome (Supronowicz *et al.,* 2013; Ateschrang *et al.,* 2009; Hibi *et al.,* 2006; Quarto *et al.,* 2001; Mesimaki *et al.,* 2009), showing improved integration, bone density and site vascularisation compared to graft material alone; all essential processes in graft incorporation (Runyan *et al.,* 2010; Di Bella *et al.,* 2010a).

The BM-MSCs are commonly isolated from bone marrow tissue and separated from other cell types by their ability to adhere to TCP. These adherent BM-MSCs are characterised by the presence of CD markers on their surface, such as CD44, CD73 and CD105, an ability to self-renew, as well as being multipotent with the potential to differentiate along the three mesenchymal cell type lineages of adipogenesis, chondrogenesis and osteogenesis (Domonici et al., 2006) (Figure 4.1). It is this self-renewal and multipotentiality which makes these cells desirable for bone tissue engineering, and means large numbers of unspecialised cells can be grown before being differentiated and used to colonize the BTE scaffolds to aid in osseointegration.

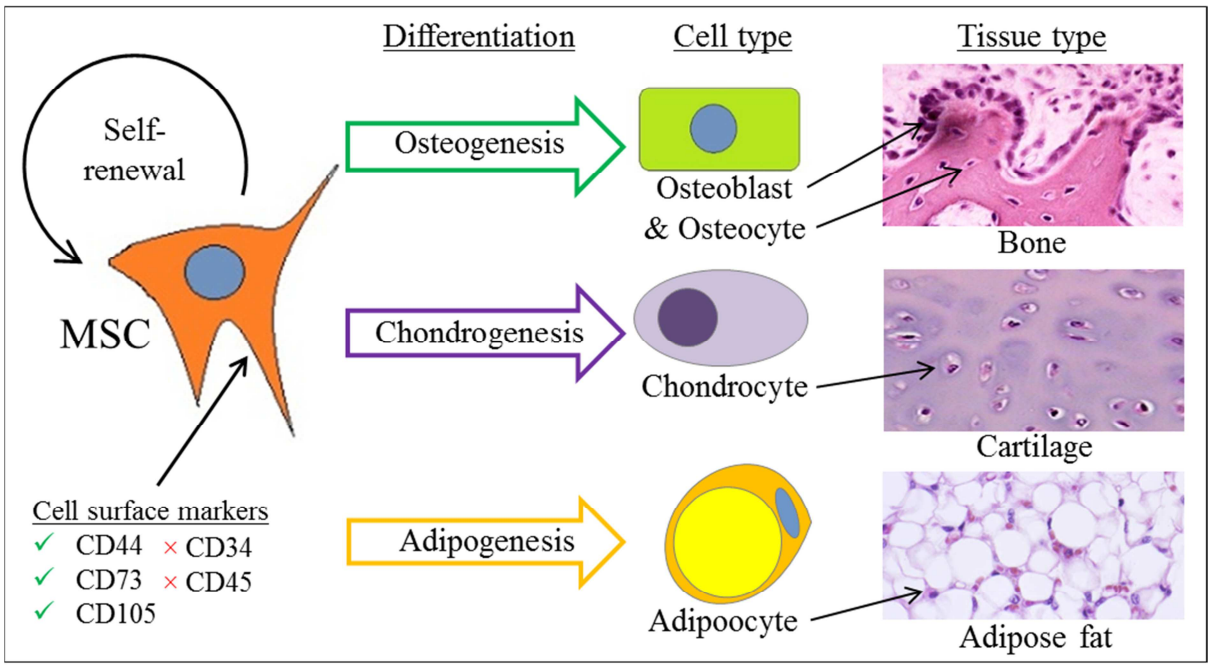

Figure 4.1 Definition and characterisation of MSCs. MSCs are firstly characterised by their plastic adherence and self-renew. They must also express specific cell surface CD markers. Finally MSCs must retain their ability to differentiate down three different lineages; osteogenesis (bone), chondrgenesis (cartilage) and adipogenesis (adipose fat).

Importantly, scaffolds used in BTE should be osteoinductive and osteoconductive, promoting the specialisation and activity of progenitor cells and supporting new bone growth on their surface (Smith *et al.*, 2011; Huang *et al.*, 2007). Together, these abilities can influence the osteogenic capacity of a graft and are determined by the microenvironment of the material. However, whilst wash techniques are required to produce such scaffolds, they may also affect the latent abilities of the graft itself (Bormann *et al.*, 2010; Huang *et al.*, 2012), with the routinely used sterilisation techniques gamma irradiation and demineralisation leading to decreased osteoinductive qualities (Nguyen *et al.*, 2007; Robinson *et al.*, 2002; Cuomo *et al.*, 2009).

As previously discussed, the architecture and mechanical stability of the structure can have a large influence on the osteogenic activity of cells, with geometry (Ang *et al.,* 2012), porosity, surface roughness (Deligianni *et al.,* 2001), as well as the transduction of mechanical force (Shih *et al.,* 2011; Yourek *et al.,* 2010) influencing the cell adhesion and potential activation (see Chapter 3). However, the biochemical nature of the graft material can also dictate cell behaviour and as such is of great importance (Kilian *et al.,* 2010). The biochemical nature of a natural bone graft is dictated by the composition of its ECM, and the combination of structural proteins and mineral phase, which can profoundly influence the cell attachment behaviour and differentiation of osteogenic cells, and ultimately osteogenesis (Mathieu and Loboa, 2012; Hidalgo-Bastida and Cartmell, 2010; Polini *et al.,* 2011).

Furthermore, the age of the stem cell donor also represents a potential limiting factor to their osteogenic ability, with cells from aged donors exhibiting a reduction in the functionality, and being less likely to differentiate given the same signals as young equivalents (Mueller and Glowacki, 2001; Wagner *et al.,* 2009; Stenderup *et al.,* 2003). However, research by Sun *et al.* (2011) has demonstrated the potential of the ECM to promote better osteogenic properties in aged MSCs, though, as with cell ageing, bone also ages with changes in the matrix proteins incorporated into its structure (Fedarko *et al.,* 1992; Ingram *et al.,* 1994), its mineral phase (Handschin and Stern, 1994), and ultimately its architecture, due to alterations in cell activity (Turunen *et al.,* 2013; Lochmuller *et al.,* 2008). This influence of ageing on several features, thought to determine osteogenic function, may therefore have a large impact on the resultant osteogenic activity.

4.1.1 Aims

The application of stem cells direct to (Hart *et al.*, 2014; Smith *et al.*, 2014b), or in conjunction with scaffolds (Hernigou *et al.*, 2014; Stiehler *et al.*, 2010; Foschi *et al.*, 2012), has demonstrated improvements to non-healing sites; with good healing times and *de novo* bone production. The osteoinductive capacity of a matrix to support such osteogenic activity is an important function if it is to be successfully utilised as a structure in tissue engineering, and although fresh-frozen allograft bone displays a reduced osteogenic capacity in comparison to autograft, it still retains these latent osteoinductive abilities. As such, any negative effect to this ability by the wash process should be avoided, and would only increase the costs needed to reinstate this function.

Therefore, the aims of this investigation were to: i) assess whether the washed bone was able to support the proliferation of BM-MSCs, and ii) induce the differentiation of these cells, independent of an osteogenic stimulant.

Additionally, as ageing causes changes in both the activity of cells and the composition and structure of bone, and as the majority of bone donor material is supplied and received by elderly patients, an investigation was undertaken to assess whether the age of cell donor or bone allograft donor was important in determining the level of osteogenic activity. In particular, the study hypothesised that young donor cells would be better able to osteogenically differentiate than old donor cells, and that young donor bone would be better able to direct /support osteogenic activity.

4.2 Materials and Methods

4.2.1 Osteoinductive capacity of washed bone

BM-MSC samples from two donors (female 67 YOA and male 72 YOA) were used to seed 1cm^3 cubes of washed bone material with 0.5x10^6 BM-MSCs, in 125µl standard medium. Each BM-MSC sample was cultured on bone cubes from three different donors (all ≥70 YOA). After seeding, cubes were incubated for one hour at 37°C, washed three times in PBS and centrifuged at 400*xg* for five minutes to remove non-adherent cells as described previously (2.2.7.1).

The BM-MSC seeded bone cubes were either cultured in standard or osteogenic differentiation medium (standard medium supplemented with 10mM beta glycerophosphate (G9891; Sigma-Aldrich, Gillingham, UK), 100µM ascorbate-2-phosphate (A8960; Sigma-Aldrich, Gillingham, UK) and 1x10^{-7}M Dexamethasone (D8893; Sigma-Aldrich, Gillingham, UK)) and cultured for up to 28 days in 24-well plates. At 0, 14 and 28 day timepoints, cell viability was assessed using an alamarBlue assay. Briefly, the culture media was replaced with 2 ml of 5% alamarBlue in relevant medium as defined in section 2.2.7.2; however after incubation samples were measured using a fluorescence plate reader (FLx800, Biotek, UK), detecting at 540nm with excitation at 600nm. This method was used instead of absorbance, as it requires less calculation, is a more adapted and simplified method (Perrot *et al.*, 2003). This data was analysed using the previously described methodology for alamarBlue (2.2.7.2).

At timepoints 0, 14 and 28 days the media were removed from the bone cubes by centrifugation at 400*xg* for five minutes. Bone cubes were transferred to clean wells and 1ml TRIzol reagent (AM9738; Ambion, Life Technologies, Paisley, UK) was added, before being incubated for five minutes with constant agitation. After incubation, bone cubes were

centrifuged at 400*xg* for five minutes to remove all TRIzol reagent using specialised collection tubes (Figure 2.5 in section 2.2.7.1).

4.2.1.1 RNA extraction

TRIzol reagent containing RNA (ribonucleic acid) was transferred to a 1.5ml MCT and centrifuged at 12,000*xg* for 15 minutes at 4°C to remove bone fragments and debris. The supernatant was transferred to a new 1.5ml MCT and 100µl of BCP (1-bromo-3-chloropropane) was added and mixed through vortexing for 20 seconds. This mixture was incubated at room temperature for three minutes then centrifuged at 12,000*xg* for 15 minutes at 4°C. The clear aqueous phase supernatant was carefully removed from the tube and transferred to a new 1.5ml MCT. To this, 2µl of Glycoblue and 500µl isopropanol (AM9515; Life Technologies, Paisley, UK) were added and mixed through inverting 10 times, before incubating at room temperature for 10 minutes. After centrifuging at 12,000*xg* for 20 minutes at 4°C, the supernatant was removed and discarded to expose the small blue pellet. This pellet was washed with 1ml, ice cold 75% ethanol by vortexing, and then pelleted again by centrifuging at 12,000*xg* for five minutes at 4°C. The ethanol was removed and the pellet allowed to air dry under supervision to prevent over-drying, before being resuspended in 21.2µl TE buffer.

4.2.1.1.1 RNA quantification

A 1.2µl sample of extracted RNA was quantified using the quantification methodology described in section 2.2.4.3; however samples were quantified using the RNA-40 sample type settings instead.

4.2.1.2 Reverse transcription of mRNA to cDNA

Extracted RNA samples, containing messenger RNA (mRNA) were reverse transcribed into complementary DNA (cDNA) using a High Capacity cDNA Reverse Transcription kit (4368814; ABI, Life Technologies, Paisley, UK). RNA samples were diluted using molecular grade water (BP 2819-10; Fisher Scientific, Loughborough, UK) to give a final concentration of 200ng/µl. A 10µl sample was then combined with 10µl of 2x reverse transcription master mix, as shown in Table 4.1.

Table 4.1: High capacity cDNA reverse transcription PCR 2x master mix

RT-PCR Master Mix reagent	Volume of reagents (µl)	Final concentration
10x RT-PCR buffer	2	1x
25x (100mM) dNTP mix	0.8	1x
10x RT random primers	2	1x
Multiscribe™ Reverse Transcriptase	1	50U
RNAse inhibitor	1	20U
Molecular grade water	3.2	NA

The 20µl reaction mixture was pipetted into reaction tubes (PCR-02-C (AXYGEN ™); Fischer Scientific, Loughborough, UK) and mixed by vortexing, then centrifuged to pool the sample. The reaction tubes were entered into the thermocycler using the program detailed in Table 4.2.

Table 4.2: Thermocycler conditions for RT reaction

Step	Temperature (°C)	Time length
1	25	10 minutes
2	37	120 minutes
3	85	5 seconds
4	4	∞

After the reaction process, samples were diluted to 5ng/µl with molecular grade water and stored at -20°C until required.

4.2.1.3 Quantitative real time PCR (QRT-PCR) for osteogenic gene expression

Samples for use in QRT-PCR gene transcriptional analysis were run in triplicate. All genes assayed for (full details in Table 4.3) were normalised to the housekeeping gene (HKG) mitochondrial ribosome protein 19 (MRPL19). This HKG was previously identified within the laboratory as the most stably expressed HKG in BM-MSCs in both monolayer expansion and under osteogenic conditions (unpublished data).

Table 4.3: All primer and probe sequences for use in QRT-PCR

Target Gene	Accession ID (Gene bank)	Forward primer seq.	Reverse primer seq.	Probe sequence	Working conc. of primer (nM)
MRPL19	NM_014763	CCA CAT TCC AGA GTT CTA	CCG AGG ATT ATA AAG TTC AAA	CAA ATC TCG ACA CCT TGT CCT TCG	900
RUNX2	NM_001024630	CGC TGC AAC AAG ACC	CGC CAT GAC AGT AAC C	TGG CCT TCA AGG TGG TAG CCC TC	900
Osteopontin (OPN)	NM_000582	CTG ACA TCC AGT ACC CTG	CAG CTG ACT CGT TTC ATA	CTG TCC TTC CCA CGG CTG TC	600
Osteocalcin (OC)	NM_199173	CCG CAC TTT GCA TCG	GCC ATT GAT ACA GGT AGC	CCA GGC AGG TGC GAA GCC C	600
Alkaline phosphatase (ALPL)	NM_000478	ACG TCT TCA CAT TTG GTG	GGT AGT TGT TGT GAG CAT A	ACT CTA TCT TTG GTC TGG CCC C	450
VEGFα	NM_001025366	GTA CCC TGA TGA GAT CGA	ATC CGC ATA ATC TGC ATG	ACA TCT TCA AGC CAT CCT GTG T	300

The QRT-PCR assay was performed on samples using Lumino-Ct qPCR ReadyMix (l6669; Sigma-Aldrich, Gillingham, UK), prepared using primers and FAM-BHQ1 (6-carboxyfluorescein-Black Hole Quencher®) probes (all from Sigma-Aldrich, Gillingham, UK) (Table 4.3). A 2µl volume of each cDNA sample was assayed in triplicate in a 96-well PCR plate (E1403; Star lab, Milton Keynes, UK) and mixed with 8µl of PCR Master Mix (Table 4.4).

Table 4.4: QRT-PCR master mix for use with FAM-BHQ1 primers and probes		
QRT-PCR Master Mix reagent	**Volume of reagents (µl)**	**Final concentration**
2x Lumino CT qPCR Readymix	5	1x
40x ROX solution (diluted 100x stock)	0.5	1x
3-9µM Forward primer (See Table 4.3)	1	0.3-0.9µM
3-9µM Reverse primer (See Table 4.3)	1	0.3-0.9µM
5µM FAM-MGB probe	0.5	0.25µM

The laden PCR plates were sealed with clear polyolefin film (E2796-9795; Star lab, Milton Keynes, UK), mixed through inversion and centrifuged at 500*xg* for one minute at room temperature to collect the sample at the bottom of the well. The plates were run on a StepOnePlus real time PCR system (4376600; Life Technologies, Paisley, UK) using the cycle conditions detailed in Table 4.5.

Table 4.5: Thermocycler conditions for RealTime QRT-PCR			
Step	**Temp (°C)**	**Time length**	**Cycle details**
1	50	2 minutes	
2	95	10 minutes	
3	95	15 seconds	Steps 3-4
4	60	1 minute	repeated 39 times

4.2.1.3.1 QRT-PCR data analysis

CT value data was collected from the StepOnePlus PCR machine in Microsoft Excel. The gene expression level of the constitutively expressed HKG was used to normalise against, for all genes of interest expression levels, to give the relative gene expression levels, termed ΔCT. The power of this value ($2^{-\Delta CT}$) displays the change in normalised gene expression relative to the HKG (normalised expression level). To measure the change compared to both the normalising reference (HKG), and a calibrator (day 0), the normalised gene expression levels (ΔCT) of sample groups were compared to a normalised control (day 0) (ΔΔCT), with the power of the change ($2^{-\Delta\Delta CT}$) termed the fold change. See Table 4.6 for details of this process, (Minogue *et al.*, 2010; Livak and Schmittgen, 2001).

Table 4.6: Calculation process for analysis of QRT-PCR data	
Step	**Process**
1	ΔCT of target gene calculated: = Ct of target gene- Ct of HKG (Mrpl19)
2	Average of ΔCT triplicate for each sample
3	Average of sample groups ΔCTs e.g. controls / condition
4	Calculate SE for sample group mean: (standard deviation of group / square root of the number) =STDEV (ΔCTs of sample group)/ SQRT(N)
5	ΔΔCT of sample group calculated: = ΔCT of sample group- ΔCT of control
6	Calculate the relative fold change $2^{-\Delta\Delta CT}$: = POWER (2,- ΔΔCT)
7	Calculate positive error bar: Pos = $(2^{-\Delta\Delta CT}$-SE)-$(2^{-\Delta\Delta CT})$
8	Calculate negative error bar: Neg = $(2^{-\Delta\Delta CT})$-$(2^{-\Delta\Delta CT}$+SE)

4.2.2 Age-related changes in osteogenic potential of cells seeded on washed bone

BM-MSCs from donors aged ≤50 YOA (N=4) and ≥70 YOA (N=3) (Table 4.7) were expanded in culture as detailed previously (2.2.7.1). The cells were trypsinised and resuspended to a concentration of $4x10^6$ cells/ ml in osteogenic medium and 125µl of this cell suspension was seeded onto defrosted washed bone cubes (2.2.7.1) from donors ≤50 YOA (N=7) and ≥70 YOA (N=9) (Table 4.8 for full details). Samples were created for PCR analysis at days 0, 14 and 28 (4.2.1.3), histological analysis at day 28 (2.2.5) and for ALP activity assays at days 0, 14 and 28.

Table 4.7: BM-MSC samples for use in age-related changes in osteogenic potential experiment

Sample ID.	Sex	Age (years)
WH113	Male	44
WH124	Female	44
WH110	Male	44
WH096	Female	49
WH101	Female	72
WH106	Male	73
WH097	Female	81

Table 4.8: Washed bone samples for use in age-related changes in osteogenic potential experiment

Sample ID.	Sex	Age (years)
170 212	Male	34
469 467	Male	39
470 480	Female	45
473 662	Male	45
170 211	Male	48
464 295	Female	49
472 268	Female	49
167 027	Female	72
455 700	Female	73
457 066	Female	75
459 319	Female	75
452 284	Male	76
160 949	Female	76
458 531	Male	82
160 289	Female	83
452 277	Male	84

4.2.2.1 ALP activity assay

ALP enzyme activity was measured by its hydrolytic cleavage of p-Nitrophenyl phosphate (p-NPP) to release p-Nitrophenol (p-NP), which in alkaline conditions causes a yellow colour change detectable at 410nm. The intensity of the yellow pertains to the amount of p-NP produced.

Seeded bone cubes samples for days 0, 14 and 28 were removed from culture media and rinsed in PBS to remove traces of serum. The cubes were then submerged in 2ml of ALP lysis buffer containing 5mM $MgCl_2$ and 0.5% Triton X-100 diluted in PBS. The cubes were incubated on ice for 10 minutes then entered into two freeze-thaw cycles, after which the cubes were centrifuged dry using the specialised centrifuge tube (Figure 2.5 in section 2.2.7.1). The lysis solution was then centrifuged at 13,000rpm for 10 minutes at 4°C to remove fine particles which could affect the assay. The lysate supernatant was carefully transferred to a fresh 1.5ml MCT and kept on ice to run fresh in the assay.

An ALP substrate solution containing 5mM p-NPP (P5896; Sigma-Aldrich, Gillingham, UK), 150mM AMP buffer (A9226; Sigma-Aldrich, Gillingham, UK) and 5mM $MgCl_2$ in dH_2O was produced for use in the ALP activity assay. A standard curve was produced by first diluting p-NP 10µmol/ml stock (N7660; Sigma-Aldrich, Gillingham, UK) to 1µmol/ml in lysis buffer. Serial dilution of this top standard (0.5µmol/ml after addition of substrate) was used to achieve an 8 point standard curve (0.5, 0.25, 0.125, 0.0625, 0.03125, 0.015625 and 0.0078µmol/ml) including lysis buffer blank.

Using neat samples, a 50µl volume was loaded in triplicate into wells of a 96-well plate alongside the standard curve and 50µl of substrate solution added to each well. The plate was run on an absorbance reader at 420nm with readings performed immediately and then again at five minute intervals until 30 minutes, thereby ensuring results could be taken during the exponential phase. Additional 50µl samples were loaded into wells of a 96-well plate and a PicoGreen assay run for quantification of DNA material (as detailed in section 2.2.2.1.1). Similar to the quantification of DNA, the equation of the trend-line for the standard curve was used to determine the actual concentration of p-NP from raw values. ALP activity was referred back to total DNA, therefore giving results as µmol p-NP/µl/minute/ng DNA using the equation:

$$Enzyme\ activity = \frac{(t30 - t0) \div (v\ x\ t)}{DNA\ (ng)}$$

Where: *t30* is the value after 30 minutes

t0 is the initial value at 0 minutes

v is the volume being read

t is the time between readings (30 minutes)

DNA (ng) is the DNA material in 50µl in ng from PicoGreen assay

Enzyme activity was then normalised to day 0 controls to display results as fold increase.

4.2.2.2 Histological analysis of cell seeded bone

Histological sections were stained with H&E and MTC using the methods described previously (2.2.5). Immunohistochemical staining was undertaken to support QRT-PCR assessment of osteogenic differentiation and activity, using previously described methodology (2.2.5.3). Briefly, a rabbit anti-ALP antibody was diluted to 1/200 in TBS containing 1% BSA (ab108337; Abcam, Cambridge, UK) for use on mounted samples which had undergone heat-mediated antigen retrieval in Citrate Buffer Solution (10mM citric acid (251275; Sigma-Aldrich, Gillingham, UK) in dH_2O, pH 6) for 15 minutes in a steamer (366815-3668; TEFAL, Windsor, UK), using a goat-anti-rabbit secondary antibody at 1/300 dilution (sc-3840; Santa Cruz Biotechnology, Heidelberg, DE). Staining was visualised with DAB as described previously (2.2.5.3).

4.2.3 Assessment of osteogenic differentiation of BM-MSC samples in monolayer

BM-MSC samples used in the assessment of cell age on osteogenic activity on bone were cultured in monolayer at 25,000/well in a 6-well plate and incubated for one hour. The media were then removed and the cells washed in PBS twice before 2ml of 5% alamarBlue was added, and then incubated for two and a half hours with media replaced with fresh standard or osteogenic media (as described in section 2.2.7.2). At 14 and 28 day timepoints, alamarBlue assays were used to assess cell metabolic activity and samples were removed for PCR and ALP activity assays as described in sections 4.2.1.3 and 4.2.2.2.

4.2.3.1 Alizarin red

At day 28, Alizarin red staining was used to visually determine the mineralisation state of monolayer BM-MSCs after culture in standard and osteogenic medium. Two grams of Alizarin red S (A5533; Sigma-Aldrich, Gillingham, UK) was dissolved in 100ml dH_2O, and adjusted to pH 4.2 with hydrochloric acid. This solution was filtered before use.

Monolayer cells were fixed in 4% neutral buffered formalin for a minimum of one hour then washed three times in PBS and rinsed in water to remove all traces of fixative. The fixed monolayer was then incubated in the Alizarin red solution for one minute. The solution was removed and well rinsed in distilled water to remove excess stain, then air dried. Images were taken using a light microscope as described in section 2.2.5.2.1.

4.2.3.2 ALP staining

Alkaline phosphatase activity was visually assessed using a 5-bromo-4-chloro-3'-indolyphosphate p-toluidine/ nitro-blue tetrazolium chloride (BCIP/NBT) substrate, staining cells blue-violet when active ALP is present. One BCIP/NBT tablet (SigmaFast™ BCIP/NBT; Sigma-Aldrich, Gillingham, UK) was dissolved in 10ml of dH_2O to prepare the substrate solution. This photosensitive solution was kept in the dark to prevent breakdown. Monolayer cells were washed in PBS containing 0.05% Tween 20 (P9416; Sigma-Aldrich, Gillingham, UK), which was aspirated off carefully so as not to disturb the fragile monolayer structure. The wash solution was removed and the monolayer was covered in 4% neutral buffered formalin, and incubated for one minute. The fixative was carefully removed and the monolayer washed using the wash buffer. Finally, the wash buffer was aspirated carefully and sufficient substrate solution added to cover the monolayer (approx. 0.5ml). The plate was incubated in darkness at room temperature for 10 minutes. The substrate solution was removed and the monolayer washed one last time in wash buffer. Images were taken to evaluate staining results using a light microscope as previously described (2.2.5.2.1).

4.2.4 Assessment of bone mineral crystallinity

The phase structure and crystallinity of hydroxyapatite in the bone was measured by X-ray defraction (XRD). Samples were placed in a Philips X'Pert-MPD (PW 3040; Phillips, UK) and measured in 2-Theta (2Θ) with a step size of 0.008 2θ/second and a scan range of 10 to 70°. Measurements were analysed using OriginPro 8.1 (OriginLab, Stoke Mandeville, UK) with phase determinations made using standard card; JCPDS 74-0565, from the International Centre for Diffraction Data (ICDD) (Whiteside *et al.,* 2010).

Additionally, samples were analysed by X-ray fluorescence (XRF) to determine chemical composition and assess mineralisation by a measurement of the calcium to phosphate (Ca/P) ratio. Samples were excited with high energy X-rays using a Minipal 4 EDXRF (Panalytical, Cambridge, UK). Measurements were retrieved in chemical compound percentage concentration. The value for calcium was then divided by the phosphorous value to give a Ca/P ratio.

4.3 Results

4.3.1 Osteoinductive capacity of washed human bone allograft

4.3.1.1 Culture of BM-MSCs in 3D on washed human bone scaffold with and without osteogenic medium

Metabolic activity was assessed through reduction of alamarBlue, with increased reduction potentially resulting from cell proliferation. This change in fluorescent signature occurs as its constituent chemical resazurin is converted to resorufin by cytochrome a3 by the cells mitochondria. The results for BM-MSCs seeded on washed bone showed significant fold changes in metabolic activity after 14 days, with increases of 3-fold in standard medium and 3.49-fold in osteogenic medium compared to day 0 controls ($p \leq 0.001$ for both). At the day 28 timepoint, metabolic activity had significantly increased 4.98-fold in standard medium and 4.63-fold in osteogenic medium compared to initial day 0 readings ($p \leq 0.001$ for both). This increase was also significantly higher compared to day 14 readings ($p \leq 0.05$) (Figure 4.2 A). There were no detectable readings for non-seeded washed bone controls at day 0, 14 or 28.

The osteoinductive potential of the washed bone material, and its ability to support osteogenic differentiation was assessed through the analysis of osteogenic gene expression in BM-MSCs seeded on washed bone, cultured in either standard or osteogenic medium. Osteogenic markers for initial differentiation (RUNX2), immature osteoblast gene (OPN) and mature osteoblast gene (OC) were used to determine both osteogenesis and the extent of cell maturation. Non-seeded, washed bone material was also included in the PCR analysis and revealed no detectable expression for any of the genes studied.

Expression of the early osteogenic gene RUNX2 by BM-MSCs seeded on washed bone (Figure 4.2 B) was significantly increased at day 14 compared to day 0 in both standard and osteogenic medium (2.62-fold, $p \leq 0.001$ and 4.2-fold, $p \leq 0.001$; respectively), with significantly larger increases noted in osteogenic medium compared to standard medium ($p \leq 0.01$). By day 28, RUNX2 expression by BM-MSCs in standard medium had returned to day 0 control levels, whereas expression in osteogenic medium remained significantly higher than both day 0 controls (2.7-fold, $p \leq 0.001$) and in comparison to standard medium at day 28 ($p \leq 0.001$).

Expression of the immature osteoblast marker gene OPN (Figure 4.2 C) was also significantly increased by day 14 in both standard and osteogenic medium compared to day 0 controls (13.1-fold, $p \leq 0.001$ and 5.4-fold, $p \leq 0.001$; respectively). However, levels were significantly lower in osteogenic medium compared to standard medium at day 14 ($p \leq 0.01$). By day 28, expression of OPN remained significantly higher than day 0 controls in both medium types (6.2-fold, $p \leq 0.001$ and 4.3-fold, $p \leq 0.001$ in standard and osteogenic medium; respectively), with no significant difference noted between culture media.

Expression of the mature osteoblast marker gene OC (Figure 4.2 D) was upregulated to similar extents at day 14 in both standard and osteogenic medium compared to day 0 controls (3.3-fold and 4.43-fold; respectively, both $p \leq 0.001$). Expression was further increased in both medium types by day 28 relative to day 0 (5.6-fold in standard and 8.1-fold osteogenic medium, both $p \leq 0.001$) and in standard and osteogenic medium relative to the same medium type at day 14 (both $p \leq 0.01$), with a small but significant increase noted in osteogenic medium compared to standard medium at day 28 ($p \leq 0.01$).

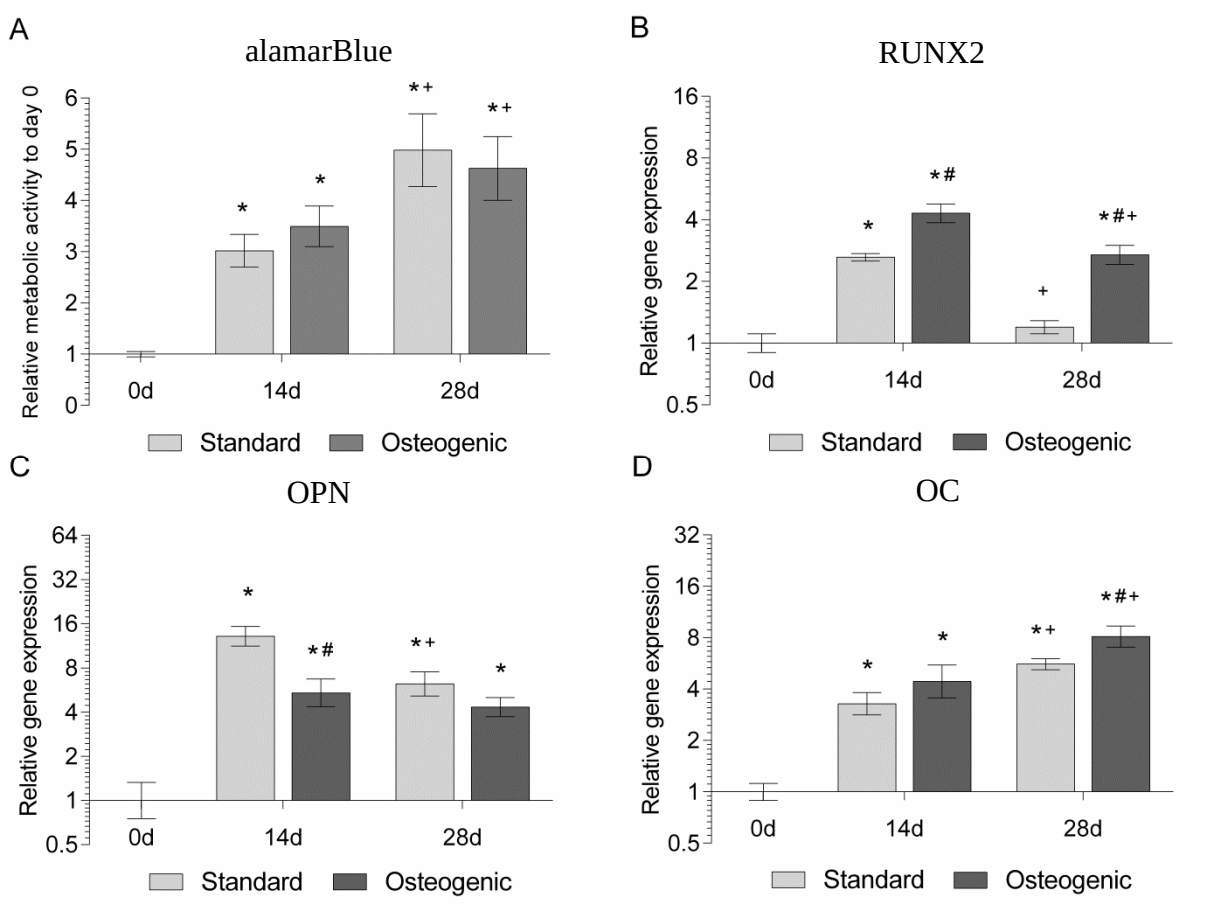

Figure 4.2: AlamarBlue metabolic activity and QRT-PCR for osteogenic marker gene expression of BM-MSCs seeded on washed bone scaffolds (n=6) and cultured for 14 or 28 days in either standard medium or osteogenic medium containing dexamethasone. Relative metabolic activity (A) was normalised to non-seeded bone controls and day 0 readings whilst gene expression of RUNX2 (B), OPN (C) and OC (D) was normalised to the HKG MRPL19 and day 0 controls ($2^{-\Delta\Delta CT}$). Data represent mean ± SE. *, significant difference with respect to 0d control ($p \leq 0.05$). #, indicates significant difference between standard and osteogenic medium ($p \leq 0.05$). +, indicates significant difference between 14d and 28d in the same medium type ($p \leq 0.05$).

4.3.2 Influence of cell donor age on the osteogenic differentiation of BM-MSCs cultured on the washed human bone scaffold

4.3.2.1 QRT-PCR analysis of osteogenic gene expression in BM-MSCs cultured on the washed human bone allograft

Metabolic activity, measured by alamarBlue reduction, was significantly increased compared to day 0 controls, for cells from both young (≤50 YOA) and old (≥70 YOA) donors, with 2.1-fold and 2.2-fold increases at day 14 and 2.7-fold and 2.0-fold at day 28 respectively ($p \leq 0.01$ for all values) (Figure 4.3 A). There was no significant difference between young and old samples at either day 14 or 28 timepoints.

The osteogenic transcription factor RUNX2 was significantly increased at day 14 for cells from both young and old donors (2.4-fold, $p \leq 0.001$ and 1.4-fold, $p \leq 0.01$; respectively) compared to day 0; however levels at day 28 were only significantly increased for young donor cells and not old (1.9-fold, $p \leq 0.001$) (Figure 4.3 B). At both timepoints, RUNX2 was significantly higher in the young cell donor samples compared to old cell donor samples ($p \leq 0.001$).

At both day 14 and 28 there was a significant increase in OPN transcription levels for young (6.2-fold, $p \leq 0.001$ and 5-fold, $p \leq 0.001$; respectively) and old (4.3-fold, $p \leq 0.001$ and 2.6-fold, $p \leq 0.05$; respectively) donor cells in comparison to day 0 controls, with significant differences between the two groups at both timepoints ($p \leq 0.001$) (Figure 4.3 C). In contrast, OC transcription levels varied greatly between the two age groups (Figure 4.3 D). There were significant increases in OC transcription levels for young donor cells at 14 and 28 days in comparison to day 0 controls (2.6-fold, $p \leq 0.01$ and 2.5-fold, $p \leq 0.001$; respectively); however there was no statistical difference at day 14 for old donor cells, and a statistically significantly

decrease in OC at day 28 (0.44-fold, $p \leq 0.05$). At both 14 and 28 days, young donor cells had significant higher OC transcription levels than old cells ($p \leq 0.001$ for both).

Tissue non-specific ALPL transcription was only significantly upregulated for young donor cells at day 28 (1.6-fold, $p \leq 0.01$), and was significantly different to old donor cells at this timepoint ($p \leq 0.001$) (Figure 4.3 E) when compared to day 0. There were no other significant differences at 14 days for young cells or at either timepoint for old donor cell samples.

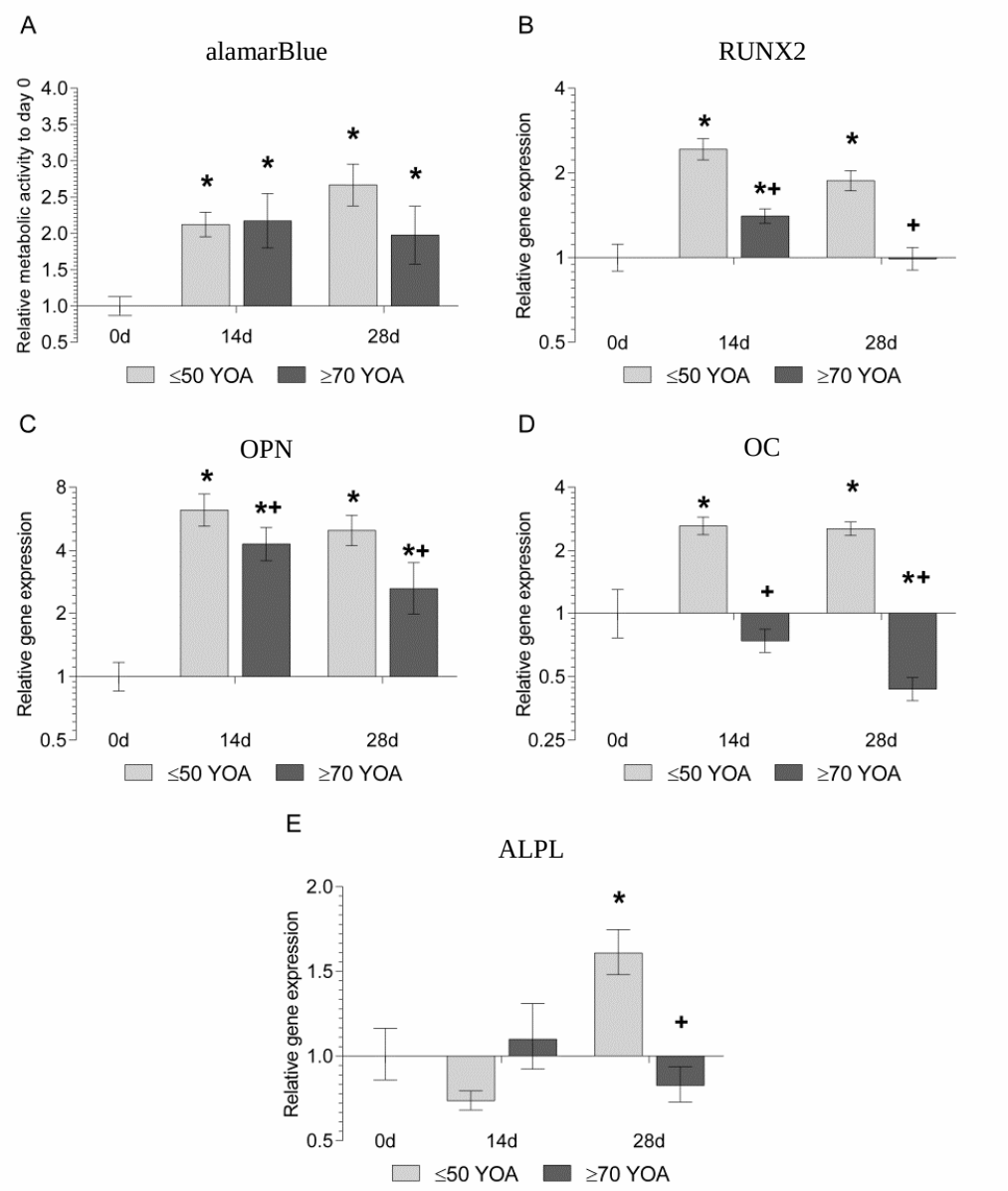

Figure 4.3: AlamarBlue metabolic activity and QRT-PCR gene expression in BM-MSCs isolated from young (≤50 YOA) (n=24) and old (≥70 YOA) (n=18) donors seeded on washed bone scaffolds. Seeded cubes were cultured in osteogenic medium for 14 or 28 days, and cell gene expression assessed. Relative metabolic activity (A) was normalised to non-seeded bone controls and day 0 readings whilst relative gene expression of osteogenic markers RUNX2 (B), OPN (C), OC (D) and ALPL (E) were normalised to the HKG MRPL19 and day 0 controls ($2^{-\Delta\Delta CT}$). Data represent mean ± SE. *, significant difference with respect to 0d control ($p \leq 0.05$). +, indicates significant difference between young and old samples at the same timepoint ($p \leq 0.05$).

4.3.2.2 Quantitative assessment of tissue non-specific enzyme activity

Alkaline phosphatase activity was quantitatively assessed through the lysis of substrate pNPP to pNP by the enzyme, and its subsequent colourimetric change. This raw value was normalised to the DNA content to give relative changes in enzymatic activity compared to day 0. Results indicated a significant increase in enzymatic activity in all samples (Figure 4.4). Young and old donor samples were significantly higher at day 14 and 28 compared to day 0 (2.4, $p \leq 0.01$ and 1.9, $p \leq 0.01$; respectively), (2.1-fold, $p \leq 0.05$ and 2.6, $p \leq 0.01$; respectively); however there was no statistical difference between age groups at either timepoint, or any statistical differences between 14 and 28 day timepoints in either age group.

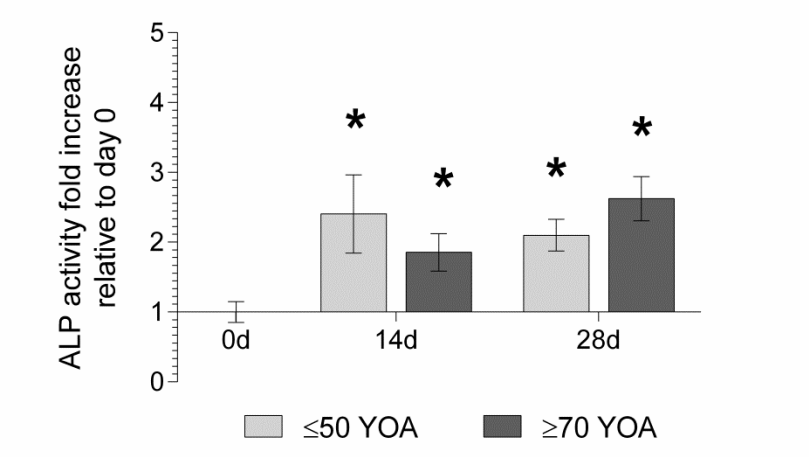

Figure 4.4: Alkaline phosphatase enzyme activity of BM-MSCs isolated from young (≤50 YOA) (n=6) and old (≥70 YOA) (n=6) donors and seeded on washed bone scaffolds measured through pNPP lysis to pNP and subsequent colourimetric change. Seeded bone scaffolds were cultured for 14 or 28 days in osteogenic medium and enzyme retrieved through cell lysis. Relative enzymatic activity was normalised to non-seeded bone controls, DNA content and day 0 readings. Data represent mean ± SE. *, significant difference with respect to 0d control ($p \leq 0.05$). +, indicates significant difference between young and old samples at the same timepoint ($p \leq 0.05$).

4.3.2.3 Influence of cell donor age on the osteogenic differentiation of BM-MSCs cultured in monolayer

The influence of cell donor age on osteogenic differentiation of bone marrow BM-MSCs was re-assessed in monolayer to ensure all cell samples were able to undergo osteogenic differentiation in standardised conditions.

Results of the alamarBlue cell metabolic assay for monolayer cultures indicated significant increases for both young (≤50 YOA) and old (≥70 YOA) donor cells at day 14 (4.6-fold, $p \leq 0.001$ and 4.8, $p \leq 0.001$; respectively) and day 28 (7.8-fold, $p \leq 0.001$and 7-fold, $p \leq 0.001$; respectively) in comparison to day 0 controls (Figure 4.5 A). There was no statistical difference between the two age groups at either timepoint.

Expression levels of osteogenic transcription factor RUNX2 were significantly increased in young donor cells at both 14 and 28 days (3.3-fold and 2.0-fold; respectively, both $p \leq 0.001$) in comparison to standard controls at the same timepoint (Figure 4.5 B). However, RUNX2 was only increased significantly at day 14 for old donor cells (1.5-fold, $p \leq 0.05$). At both 14 and 28 days, expression levels were significantly higher in young donor cells compared to old ($p \leq 0.01$ and $p \leq 0.05$; respectively).

OPN and OC levels were significantly decreased compared to standard controls for young donor cell samples at day 14 (0.48-fold and 0.66-fold; respectively, $p \leq 0.01$ for both) and day 28 (0.47-fold, $p \leq 0.05$ and 0.40-fold, $p \leq 0.001$; respectively) (Figure 4.5 C and D). However, there was no significant difference at either timepoint for OPN and significance only at day 14 for OC (0.63-fold, $p \leq 0.01$) in old donor cells samples compared to standard controls. There was also no significant difference between the two age groups at either timepoint other than day 28 for OC ($p \leq 0.01$).

In monolayer culture, the relative expression levels of ALP were significantly increased at both 14 and 28 days compared to day 0 controls, for young (18.6-fold, $p \leq 0.001$ and 4.2, $p \leq 0.001$; respectively) and old donor cells (3-fold, $p \leq 0.001$ and 2.7, $p \leq 0.01$; respectively) (Figure 4.5 E); however at both timepoints young donor cells expressed significantly higher levels than old ($p \leq 0.001$ at day 14 and $p \leq 0.05$ at day 28).

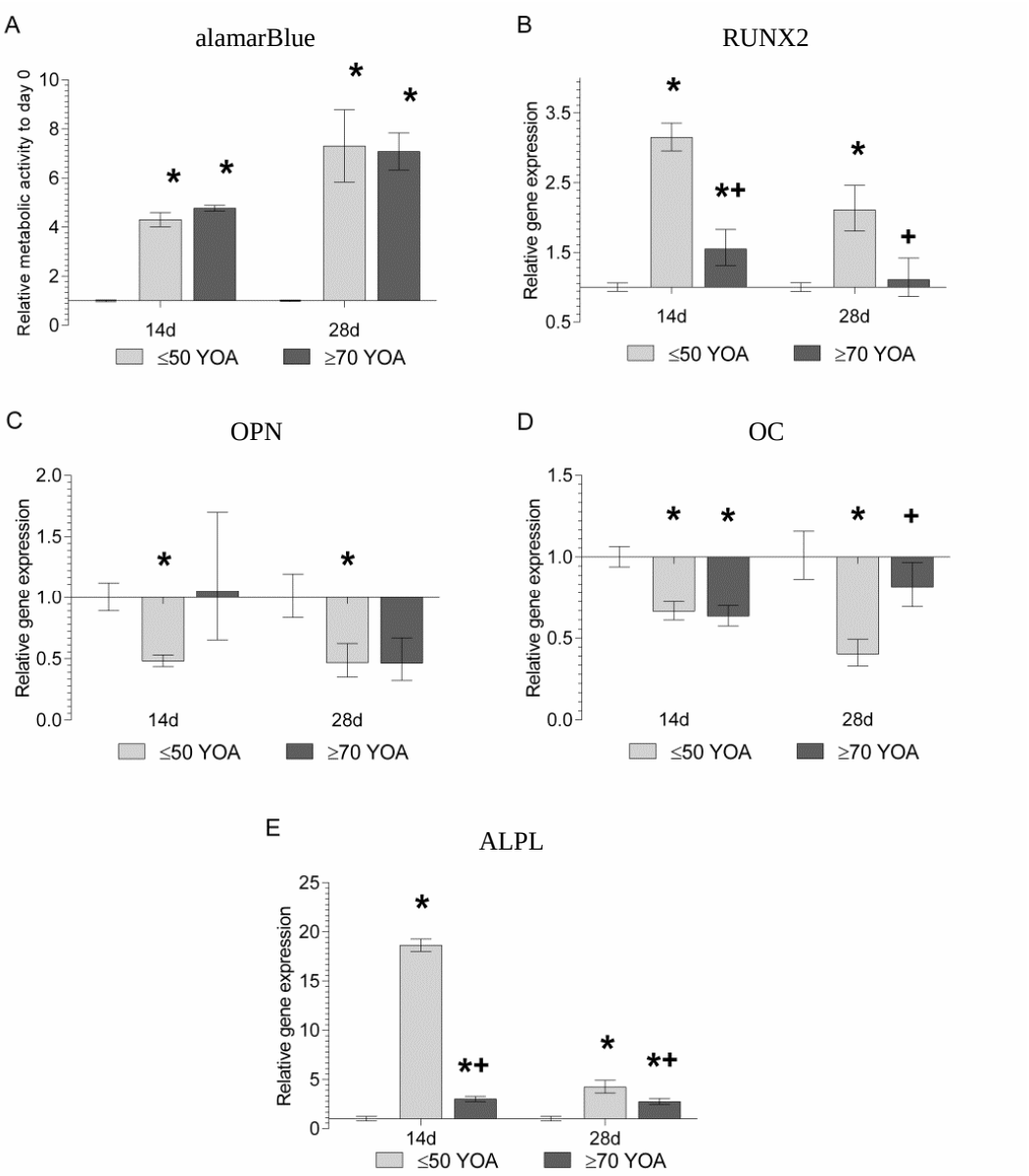

Figure 4.5: AlamarBlue metabolic activity and QRT-PCR gene expression in BM-MSCs isolated from young (≤50 YOA) and old (≥70 YOA) donors seeded in monolayer (n=9 for both). Cells were cultured in osteogenic medium for 14 or 28 days and samples retrieved through RNA extraction and reverse transcription. Relative metabolic activity (A) was normalised to non-seeded bone controls and day 0 readings whilst relative gene expression of osteogenic markers RUNX2 (B), OPN (C), OC (D) and ALPL (E) were normalised to the HKG MRPL19 and day 0 controls ($2^{-\Delta\Delta CT}$). Data represent mean ± SE. *, significant difference with respect to standard medium control at same timepoint ($p \leq 0.05$). +, indicates significant difference between young and old samples at the same timepoint ($p \leq 0.05$).

4.3.2.3.1 Histology staining of mineralised matrix in monolayer cultures

BM-MSCs were seeded at low cell concentrations for monolayer cultures, to avoid the cells becoming over confluent during the long culture period; however, this initial low cell number resulted in ALP activity assays becoming impractical and resulting in unreadable data. As such, ALP staining and alizarin red calcium deposition stains were used to view mineralisation in the monolayer cultures instead.

The results of BCIP/NBT staining for active ALP in monolayer cultured cells indicate minimal activity in young donor cells cultured for 28 days in standard medium (Figure 4.6 A, B and C). In contrast, all young donor cell samples cultured in osteogenic medium readily stained positive (blue) for active ALP (Figure 4.6 D, E and F). Alizarin red staining of partner cultures indicated no calcium deposition in standard medium cultures (Figure 4.7 A, B and C), with large amounts of red-orange alizarin S-calcium staining in osteogenic medium cultures (Figure 4.7 D, E and F).

ALP staining of old donor cell monolayer samples cultured in standard medium displayed varied staining (Figure 4.8 A, B and C). One sample in particular (Figure 4.8 B) displayed a large amount of ALP staining, though the other two were minimal. Whilst there was staining in standard conditions, this was visibly different to cells cultured in osteogenic medium, in which all samples had dense blue stained matrices (Figure 4.8 D, E and F). Alizarin red staining of old donor cell monolayer cultures also displayed no staining in standard conditions (Figure 4.9 A, B and C) similar to young donor cell samples. However, osteogenic medium cultured samples had varied staining, ranging from complete (Figure 4.9 D) to sparse (Figure 4.9 F).

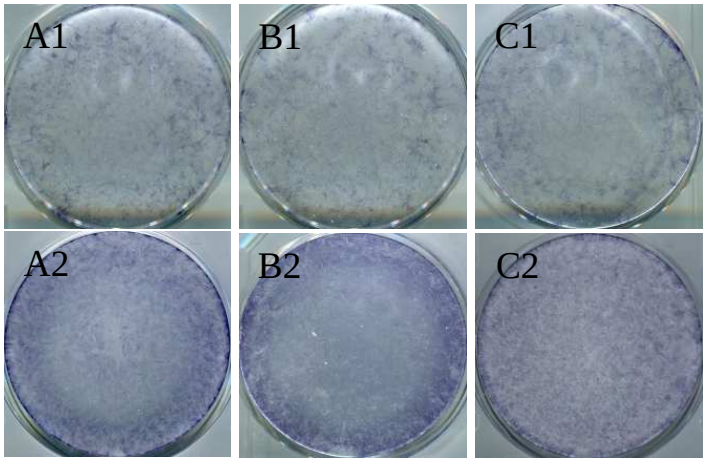

Figure 4.6: Images represent the BCIP/NBT substrate staining of active ALP in BM-MSCs isolated from three different young cell donors ≤50 YOA (A, B and C), cultured in monolayer in either standard (A1, B1, C1) or osteogenic medium (A2, B2, C2) for 28 days. Blue colouring represents active enzyme.

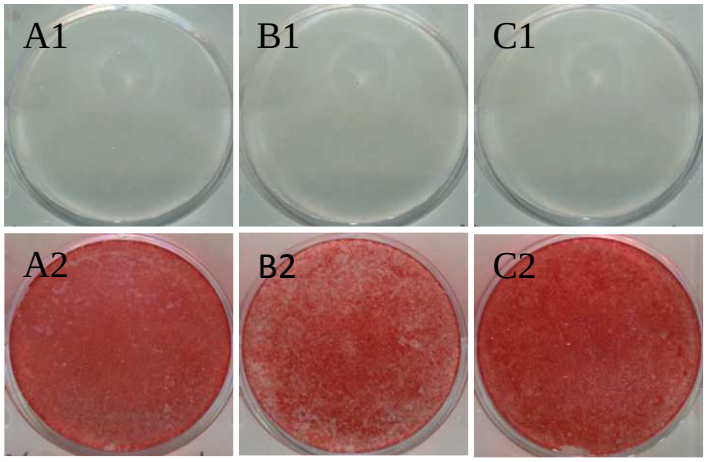

Figure 4.7: Images represent the alizarin red staining of calcium deposition by BM-MSCs isolated from three different young cell donors ≤50 YOA (A, B, and C)), cultured in monolayer in either standard medium (A1, B1, C1) or osteogenic medium (A2,B2, C2) for 28 days. Red-orange colour represents calcium deposition, indicative of calcified matrix.

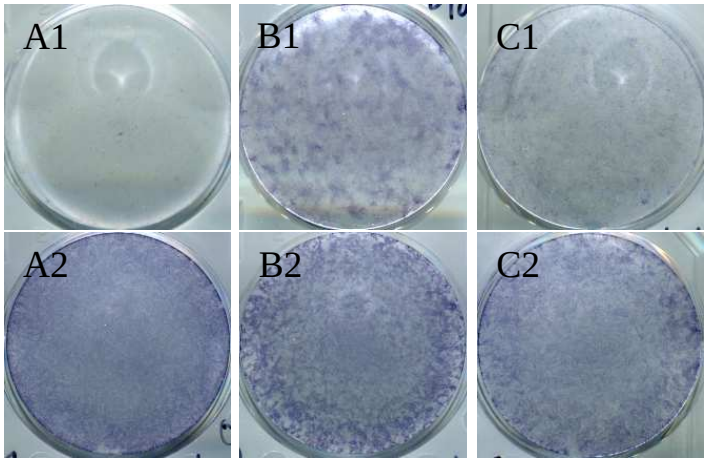

Figure 4.8: Images represent the BCIP/NBT substrate staining of active ALP in BM-MSCs isolated from three different old cell donors ≥70 YOA (A, B and Cn=9), cultured in monolayer in either standard (A1, B1, C1) or osteogenic medium (A2, B2, C2) for 28 days. Blue colouring represents active enzyme.

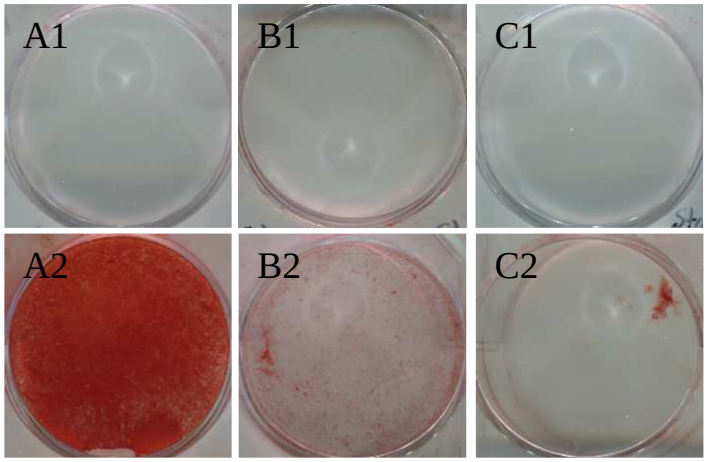

Figure 4.9: Images represent the alizarin red staining of calcium deposition by BM-MSCs isolated from three different old cell donors ≥70 YOA (A, B and C), cultured in monolayer in either standard medium (A1, B1, C1) or osteogenic medium (A2, B2, C2) for 28 days. Red-orange colour represents calcium deposition, indicative of calcified matrix.

4.3.3 Influence of bone donor age on osteogenic differentiation of BM-MSCs seeded on a washed human bone allograft

4.3.3.1 Young donor cells cultured on washed human bone allograft from young (≤50 YOA) and old (≥70 YOA) donors

The QRT-PCR expression analysis results indicate that young donor cells seeded onto either young or old donor washed bone underwent osteogenic differentiation (Figure 4.10). However, RUNX2 expression was only up regulated at day 14 for cells seeded onto young bone (1.8-fold, $p \leq 0.01$), whilst cells seeded onto old bone had increased expression at both day 14 and 28 (3.3-fold and 2.6-fold; respectively, $p \leq 0.001$ for both) (Figure 4.10 A) in comparison to day 0.

After 14 days, expression was significantly increased in cells cultured on young and old donor bone for both OPN (3.4 and 11.4; respectively, $p \leq 0.001$ for both) (Figure 4.10 B) and OC (2.1-fold, $p \leq 0.01$ and 3.3-fold, $p \leq 0.001$; respectively) when compared to day 0 controls (Figure 4.10 C). This increase in expression was sustained at 28 days for OPN (3.8-fold and 6.5; respectively, $p \leq 0.001$ for both) and OC (2.0-fold, $p \leq 0.01$ and 3.15, $p \leq 0.001$), again in comparison to day 0 controls. Expression of OPN and OC was significantly higher in cells grown on old donor bone than young donor bone at 14 days ($p \leq 0.001$ and $p \leq 0.01$; respectively), with OC also significantly higher at 28 days ($p \leq 0.01$).

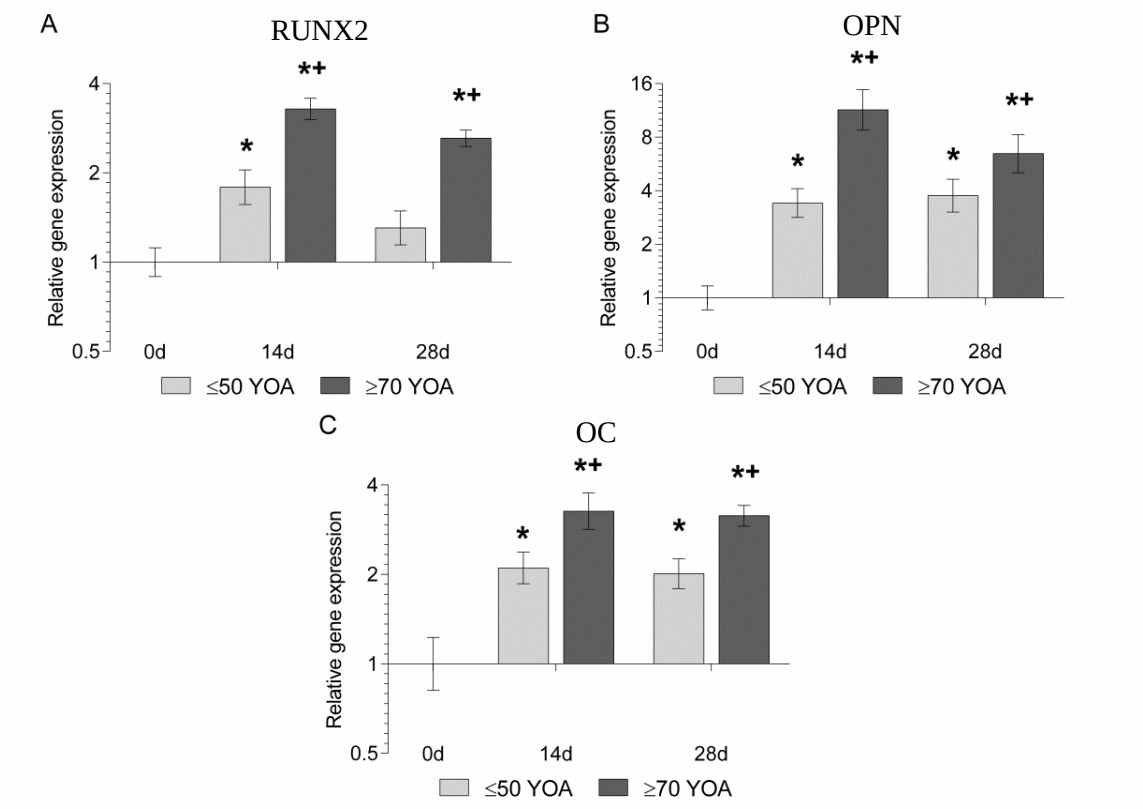

Figure 4.10: QRT-PCR gene expression in BM-MSCs isolated from young (≤50 YOA) donors seeded on washed bone scaffolds from either young (n=12) or old (n=12) bone donors. Seeded cubes were cultured in osteogenic medium for 14 or 28 days and samples retrieved through RNA extraction and reverse transcription. Relative gene expression of osteogenic markers RUNX2 (A), OPN (B) and OC (C) were normalised to the HKG MRPL19 and day 0 controls ($2^{-\Delta\Delta CT}$). Data represent mean ± SE. *, significant difference with respect to 0d control ($p \leq 0.05$). +, indicates significant difference between cells cultured on young and old bone samples at the same timepoint ($p \leq 0.05$).

4.3.3.1.1 ALP activity of young cells cultured on young and old donor bone

Alkaline phosphatase activity was significantly increased by day 14, compared to day 0 controls, for cells cultured on young and old donor bone (2.9-fold, $p \leq 0.001$ and 1.9-fold, $p \leq 0.01$; respectively), as well as at 28 days on young and old bone (2.2-fold, $p \leq 0.01$ and 2-fold, $p \leq 0.01$; respectively) (Figure 4.11). There was no significant difference between timepoints or age groups.

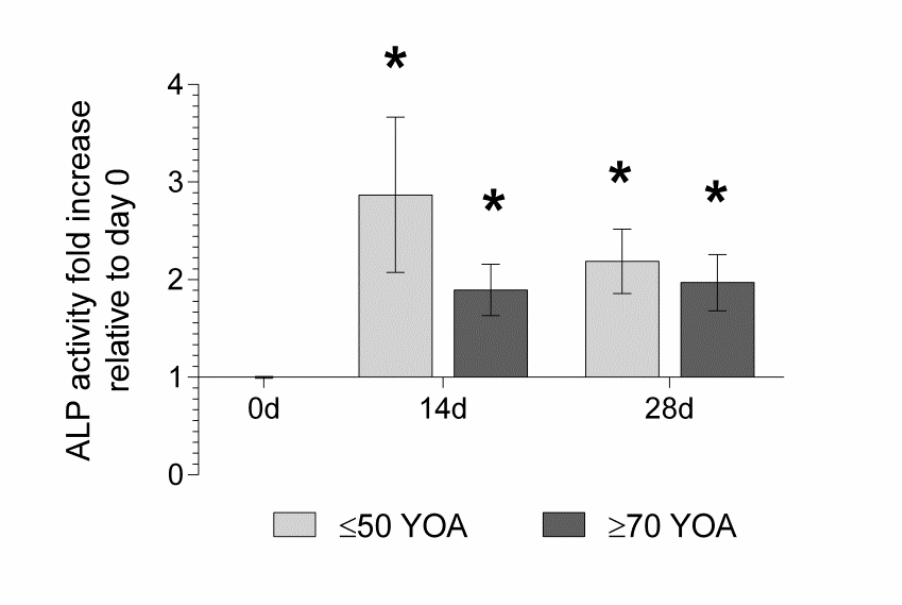

Figure 4.11: Alkaline phosphatase enzyme activity of BM-MSCs isolated from young (≤50 YOA) donors seeded on young (n=3) and old (n=3) donor washed bone scaffolds measured through pNPP lysis to pNP and subsequent colourimetric change. Seeded bone scaffolds were cultured for 14 or 28 days in osteogenic medium and enzyme retrieved through cell lysis. Relative enzymatic activity was normalised to non-seeded bone controls, DNA content and day 0 readings. Data represent mean ± SE. *, significant difference with respect to 0d control ($p \leq 0.05$). +, indicates significant difference between young and old samples at the same timepoint ($p \leq 0.05$).

4.3.3.2 Old donor cells cultured on washed human bone allograft from young (≤50 YOA) and old (≥70 YOA) donors

Expression of RUNX2 varied greatly between old donor cell samples seeded onto young and old donor bone (Figure 4.12 A). In comparison to day 0 there was no significant difference at day 14 for old cells seeded on young bone; however there was a significant decrease in the expression of RUNX2 by day 28 (0.6-fold, $p \leq 0.01$). In contrast, old cells cultured on old donor bone had significantly increased expression levels of RUNX2 at both day 14 and 28 in comparison to day 0 controls (2.0-fold, $p \leq 0.001$ and 1.9-fold, $p \leq 0.001$; respectively) and were significantly increased compared to the young bone samples ($p \leq 0.001$ for both timepoints).

In comparison to day 0 controls, samples of old cells cultured on young donor bone displayed a significant increase in OPN expression at 14 days, followed by a significant decrease at day 28 (2.0-fold, $p \leq 0.01$ and 0.5-fold, $p \leq 0.05$; respectively) (Figure 4.12 B). On old donor bone, there were significant increases in OPN expression at both day 14 and 28 compared to day 0 (10.2-fold and 17.7-fold; respectively, $p \leq 0.001$ for both), and in comparison to cells grown on young bone ($p \leq 0.001$ for both). There was no increase recorded in OC expression from day 0 (Figure 4.12 C), instead there was a significant decrease in expression levels at day 14 for cells grown on old donor bone (0.4-fold, $p \leq 0.05$) and at day 28 for cells grown on young or old donor bone (0.44-fold, $p \leq 0.01$ and 0.44-fold, $p \leq 0.05$; respectively), with a significant difference recorded between young and old donor bone at day 14 ($p \leq 0.001$).

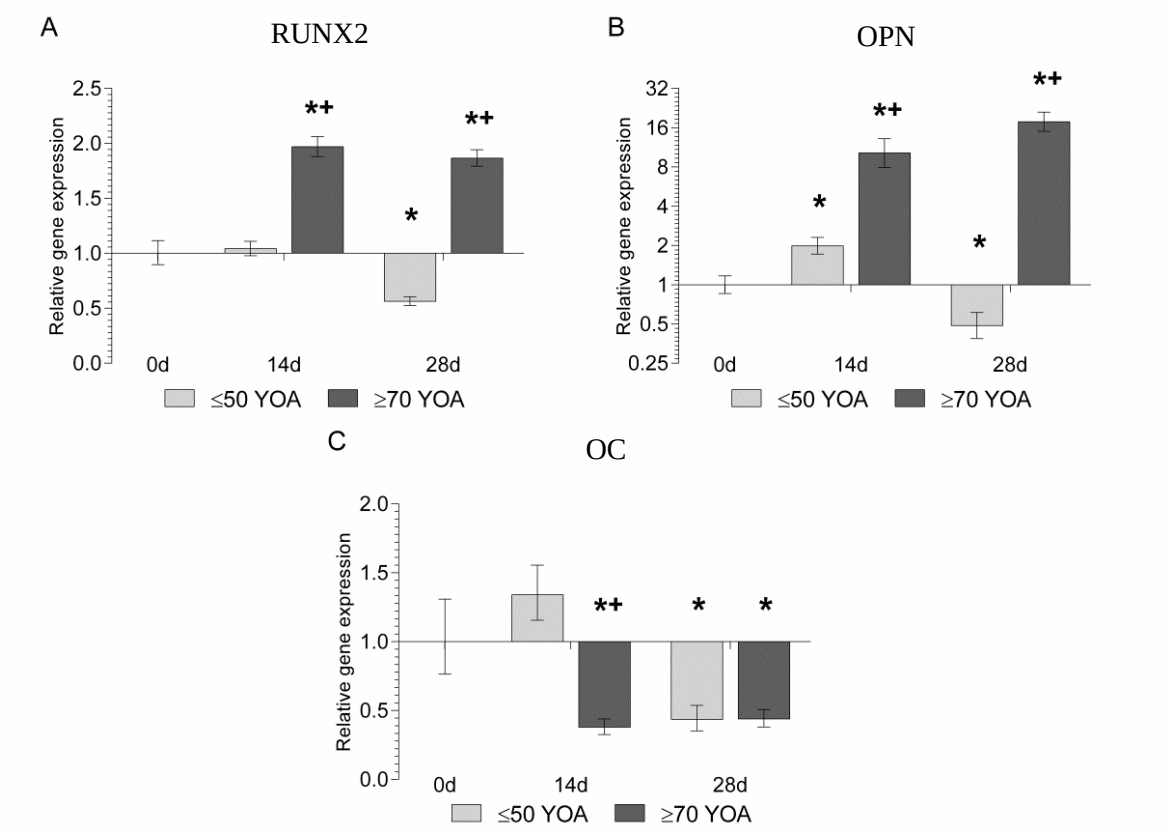

Figure 4.12: QRT-PCR gene expression in BM-MSCs isolated from old (≥70 YOA) donors seeded on washed bone scaffolds from either young (n=9) or old bone donors (n=9). Seeded cubes were cultured in osteogenic medium containing Dexamethasone for 14 or 28 days and samples retrieved through RNA extraction and reverse transcription. Relative gene expression of osteogenic markers RUNX2 (A), OPN (B) and OC (C) were normalised to the HKG MRPL19 and day 0 controls ($2^{-\Delta\Delta CT}$). Data represent mean ± SE. *, significant difference with respect to 0d control ($p \leq 0.05$). +, indicates significant difference between cells cultured on young and old bone samples at the same timepoint ($p \leq 0.05$).

4.3.3.2.1 ALP activity of old donor cells cultured on young and old donor bone

At day 14 there were significant increases in ALP activity in old cells cultured on young and old donor bone (1.8-fold, $p \leq 0.05$ and 1.9-fold, $p \leq 0.01$; respectively) compared to day 0 controls (Figure 4.13). The significant increase in activity was also seen at day 28 in cells grown on young and old donor bone (2.4-fold, $p \leq 0.001$ and 2.9-fold, $p \leq 0.001$; respectively). There was no significant difference between the age groups at either timepoint.

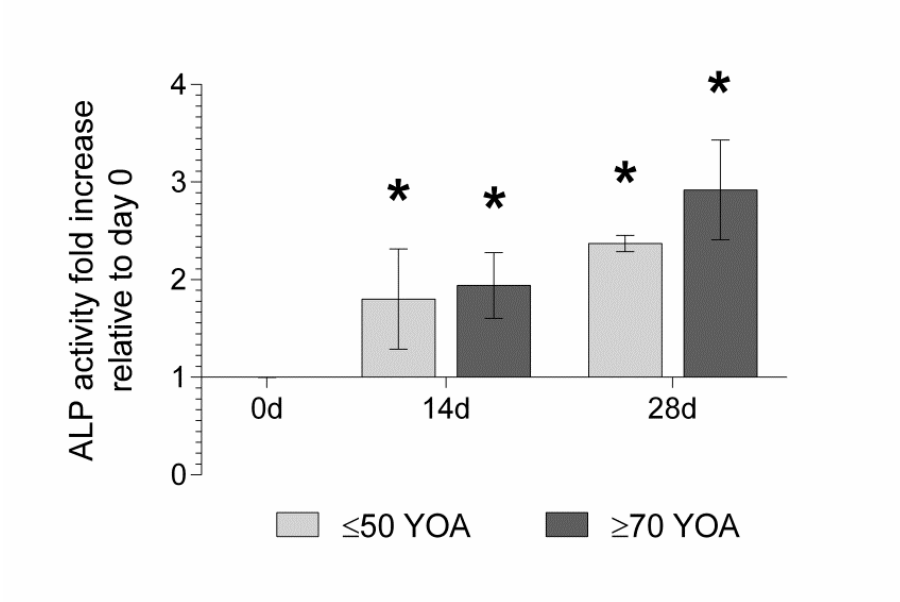

Figure 4.13: Alkaline phosphatase enzyme activity of BM-MSCs isolated from old (≥70 YOA) donors seeded on young (n=3) and old (n=3) donor washed bone scaffolds measured through pNPP lysis to pNP and subsequent colourimetric change. Seeded bone scaffolds were cultured for 14 or 28 days in osteogenic medium and enzyme retrieved through cell lysis. Relative enzymatic activity was normalised to non-seeded bone controls, DNA content and day 0 readings. Data represent mean ± SE. *, significant difference with respect to 0d control ($p \leq 0.05$). +, indicates significant difference between young and old samples at the same timepoint ($p \leq 0.05$).

4.3.3.3 Histological assessment of seeded bone cubes

Histological staining with H&E of young and old donor BM-MSCs seeded on young and old donor washed bone indicated the presence of BM-MSCs in all bone cubes (Figure 4.14 A, D, G and J). MTC staining further indicated blue staining of newly deposited connective ECM in young donor cell samples, seeded on either young or old donor bone (Figure 4.13 B, E, H and K); however young donor cells seeded on old donor bone, displayed larger areas of new matrix deposition (Figure 4.14 E) with stronger staining than cells on young donor bone (Figure 4.14 B). In comparison there was very little new ECM deposition in old donor cells seeded on either young or old donor bone (Figure 4.14 H and K).

ALPL staining was present in all bone samples, both young and old cell donor on young and old donor bone; however there was more consistent, stronger staining in young donor cells (Figure 4.14 C and F) compared to old donor cells (Figure 4.14 I and J). Additionally, there appeared to be stronger staining in old donor cells seeded on old donor bone (Figure 4.14 J) than seeded on young donor bone (Figure 4.14 I).

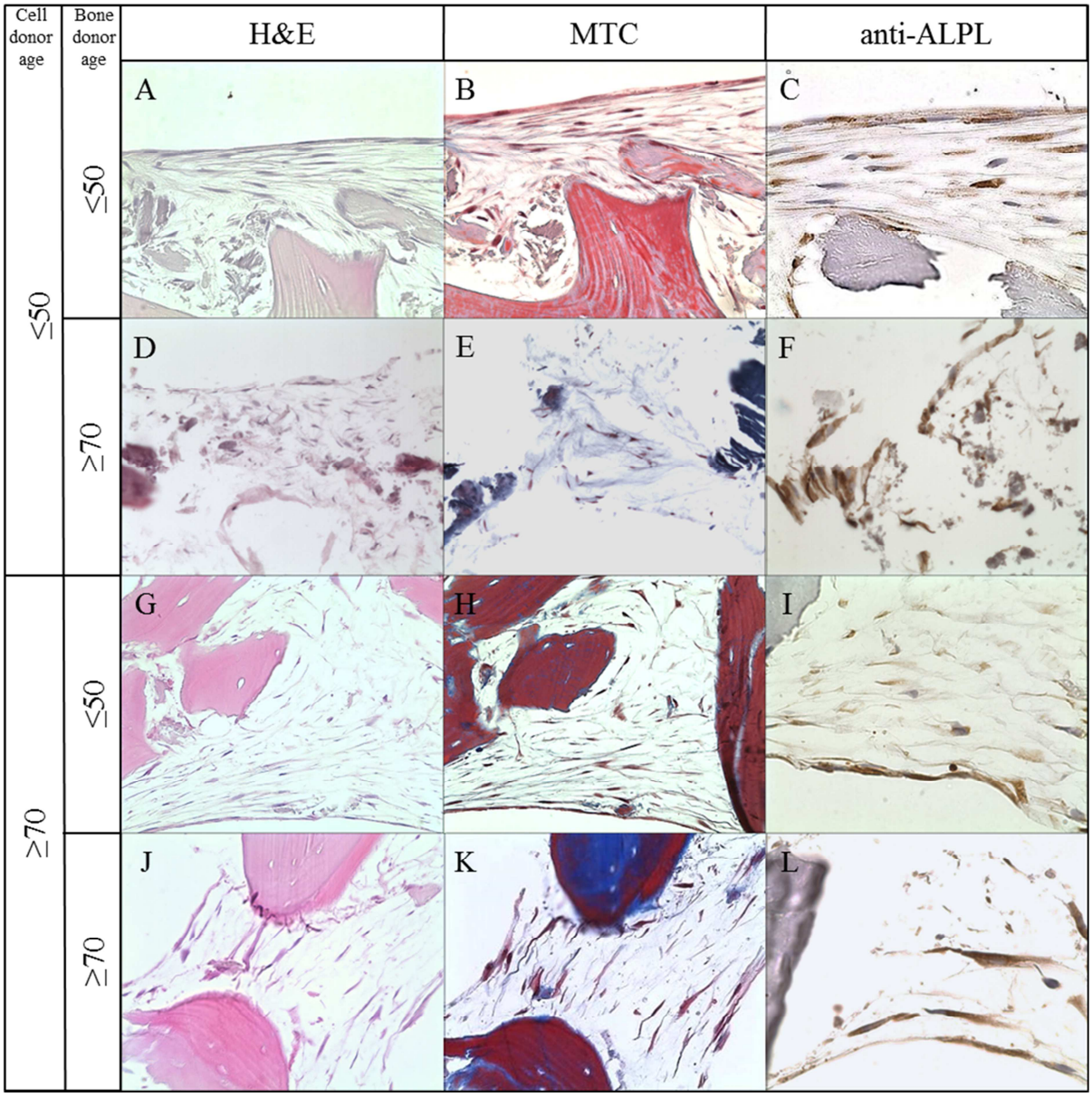

Figure 4.14: Histological assessment of young and old donor BM-MSCs seeded on either young or old donor bone material. Seeded cubes were cultured in osteogenic conditions for 28 days, then histologically fixed and sectioned. Mounted sections were stained for H&E for cell presence (nuclei blue/purple and protein pink) (A, D, G and J), MTC to distinguish cells from connective tissue (B, E, H and K), and anti-ALPL to view osteogenically differentiated cells (C, F, I and L). All images are displayed at x300 magnification except C, F, I and L which are displayed at x600 for extra clarity.

4.3.3.4 Mineralisation state of the washed bone

XRD analysis indicated that the bone contained hydroxyapatite in its structure, with a broad peak at comparable locations to the hydroxyapatite standard peaks (HA JCPDS 74-0565) (Figure 4.15). The XRD plot for young bone donor material matched closely with that of older material, with no significant difference in the peak for hydroxyapatite (position 30-35) between the two age groups. In addition, XRF data indicated a Ca/P ratio of 1:5 (±2) for young and 1:3.6 (±1) for old donor bone; with no significant difference between them.

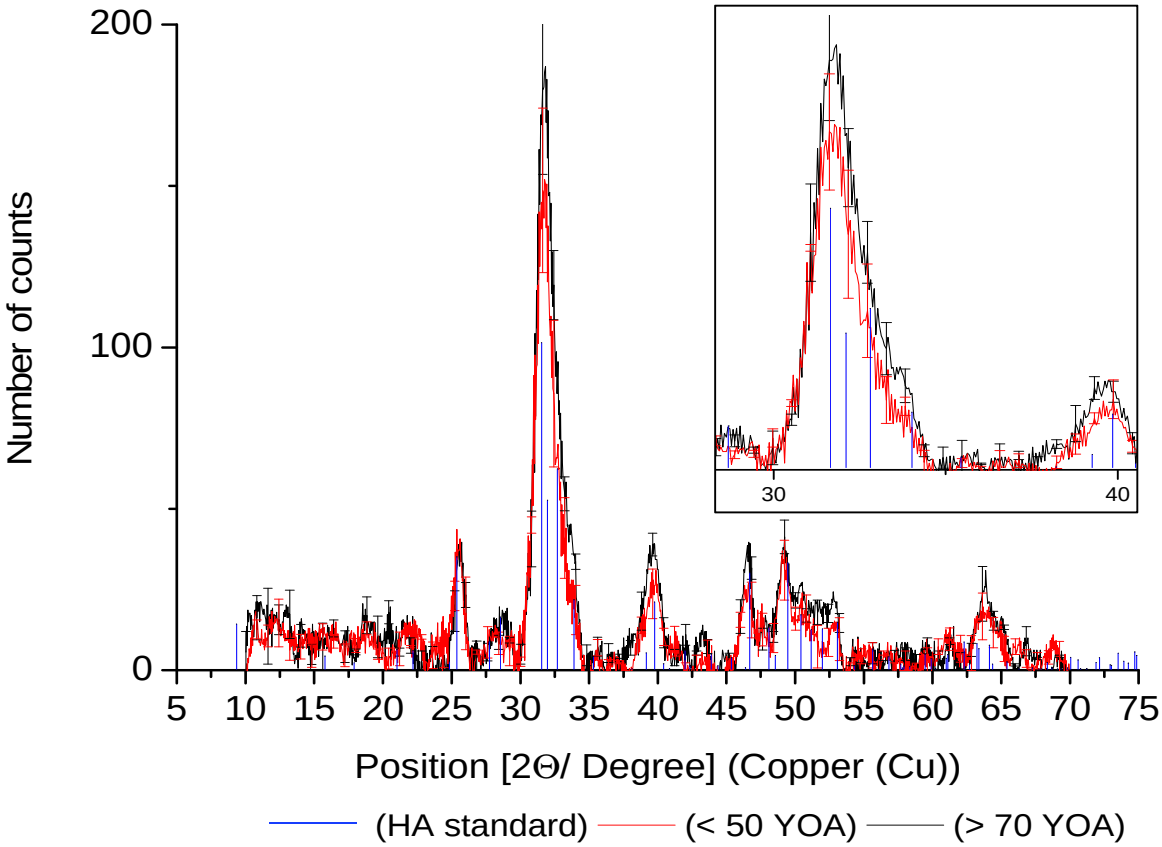

Figure 4.15: XRD patterns of signal diffraction in young (≤50 YOA) and old (≥70 YOA) donor washed bone scaffold including exploded view insert. Samples are displayed as line charts with error bars every 15 positions, for young (red) and old (black) bone with hydroxyapatite (HA) standard HA JCPDS 74-0565, displayed as line drop (blue). All measurements are in deflection angle (2-Theta (2Θ)).

4.4 Discussion and Conclusion

The addition of stem cells to bone grafting material has been shown both *in vitro* and *in vivo* to improve osteogenic ability and graft incorporation (Supronowicz *et al.,* 2013; Ateschrang *et al.,* 2009; Hibi *et al.,* 2006; Quarto *et al.,* 2001; Mesimaki *et al.,* 2009). The osteoinductive capability of the graft is of importance as it may determine the speed at which new bone may be formed, new host cells are recruited (Zhou *et al.,* 2012), and ultimately the incorporation of the graft into the host tissue (Tohma *et al.,* 2012). However, it has been shown that fresh allograft material has a low osteoinductive potential, which is further decreased by sterilisation techniques (Munting *et al.,* 1988; Coquelin *et al.,* 2012).

Ultimately, the osteoinductive abilities of these grafts are determined by their 3D structure (discussed in Chapter 3), and biochemical composition. Although the novel wash process has been shown to not detrimentally affect the mechanical properties of the bone (Chapter 3), it is unknown how it may affect the ability of the washed bone to induce the osteogenic differentiation of seeded stem cells. Therefore, this study aimed to seed isolated BM-MSCs onto the washed bone and evaluate osteogenic differentiation. Additionally, the study sought to assess the effect that the donor age of cell and bone had on any osteogenic differentiation and activity.

4.4.1 Osteoinductive assessment of washed bone

The results of this study show that the washed bone allograft was capable of initiating osteogenic differentiation of BM-MSCs seeded upon its surface in static culture, and that this occurred independent of an osteogenic medium source. Assessment of the seeded bone cubes by alamarBlue displayed significant increases in the metabolic activity of the seeded cells in

both the standard and osteogenic conditions, with no significant difference between them, therefore supporting the results for seeding and biocompatibility reported in Chapter 2. Importantly, the seeded bone cubes in both medium types had significant increases in the early transcription factor RUNX2 by day 14; however this was only maintained at day 28 in osteogenic conditions. Together with the pre-osteoblastic marker OPN being significantly higher in standard conditions, and OC being significantly higher in osteogenic, this would suggest a more mature cell type in osteogenic conditions as OC is only produced by late stage differentiated osteoblast like cells (Strauss *et al.,* 1990; Kalajzic *et al.,* 2005).

The osteogenic gene markers RUNX2, OPN and OC are widely used measures of osteogenic differentiation (Anderson *et al.,* 2011; Bassi *et al.,* 2012; Beebe *et al.,* 2009; Smith *et al.,* 2011; Huang *et al.,* 2007; Huang *et al.,* 2012; Babiker *et al.,* 2012). Although some of these studies have indicated that washed bone material is osteoinductive and able to cause the osteogenic differentiation of MSCs both *in vitro* (Evans *et al.,* 2010; Babiker *et al.,* 2013) and *in vivo* (Bolland *et al.,* 2006; Beebe *et al.,* 2009), wash procedures including PAA have shown a lack of osteoinductive capacity in the washed structures (Bormann *et al.,* 2010; Stiehler *et al.,* 2010), despite displaying good biocompatibility (Bormann *et al.,* 2010), and containing BMPs (Wildemann *et al.,* 2007).

It is considered that this osteoinductive effect by the bone is likely to occur due to its protein and mineral composition. The protein component is comprised primarily of osteoconductive type I collagen but also includes osteo-modulatory BMPs, and non–collagenous proteins such as OC, fibronectin, laminin and vitronectin (Urist *et al.,* 1983; Chaudhary *et al.,* 2004; Clough *et al.,* 2014; Nilsson *et al.,* 1998). In particular, the abundance of BMPs contained within the bone ECM structure, and their subsequent osteoinductive effect on the differentiation of MSCs, has been shown in studies which have released them from the ECM by a process of demineralisation (Supronowicz *et al.,* 2013; Supronowicz *et al.,* 2011; Mo *et*

al., 2009). However, the non-collagenous ECM molecules also have unique osteogenic promotion qualities, and adhesion of pre-osteogenic cells to these proteins may have beneficial effects on cell viability and osteogenic differentiation (Salasznyk *et al.,* 2004; Hidalgo-Bastida and Cartmell, 2010; Wang *et al.,* 2009), altering lineage specificity (Santiago *et al.,* 2009; Frith *et al.,* 2012), as well as directing the migration of MSCs (Thibault *et al.,* 2007). Differing responses to different ECM proteins, such as laminin or fibronectin, may dictate gene transcription through specific interactions with cell surface integrins (Brighton and Albelda, 1992) and downstream signalling (Gordon *et al.,* 2009), leading to cell differentiation (Au *et al.,* 2007; Jaiswal *et al.,* 2000). Results here would suggest that the wash process did not negatively affect these structural proteins or alter their functional ability, as osteogenic induction of seeded BM-MSCs was observed, although further detailed studies are required to ascertain which factors may be playing a major role in this process.

Additionally, the promotion of osteoegenic differentiation may, in part, be due to the architecture of the material, with more porous material exhibiting improved osteoinductive potential (Sicchieri *et al.,* 2012; Marcos-Campos *et al.,* 2012; Polini *et al.,* 2011), compared to cortical material which exhibits very little (Cornejo *et al.,* 2012). This innate ability of the architecture of a graft (Marcos-Campos *et al.,* 2012; Li *et al.,* 2012a), its surface roughness (Deligianni *et al.,* 2001) and mineralisation state are of importance in the osteogenic activity of seeded cells and have been discussed in Chapter 3. However, though previous results have identified the washed human bone allograft as maintaining its structural stability, additional experimentation would be required to examine the porosity of the material.

The majority of studies measuring the osteogenic capacity of their graft materials, synthetic or biological, do so in an osteogenic medium containing the powerful osteogenic differentiation inducer dexamethasone (Yamanouchi *et al.,* 1997). Importantly, by using

standard medium not containing osteoinductive factors, this study was able to highlight the innate osteoinductive potential of the bone allograft as also shown in studies by Polini *et al.* (2011) and Hashimoto *et al.* (2011). Further investigations were undertaken using osteogenic medium, as the presence of osteogenic conditions is more akin to a normal healing environment and included factors required for appropriate mineralised matrix formation in order to appropriately assess ALP transcription and activity.

4.4.2 Influence of cell donor age

The effective osteogenic differentiation and activity of stem cells is an important issue. The senescence of osteoprogenitor cells such as BM-MSCs greatly affects the intrinsic ability of cells used in tissue engineering (Sun *et al.,* 2011).

The results of this study indicated a clear difference, both in monolayer and 3D, in the ability of BM-MSCs from young and old donors to undergo osteogenic differentiation. Cells donated from individuals under the age of 50 YOA displayed statistically higher osteogenic gene transcription levels than those from older (≥70 YOA) donors. In addition to QRT-PCR analysis, ALP activity, commonly used as an osteogenic marker (Foschi *et al.,* 2012; Hashimoto *et al.,* 2011), displayed evidence of significant enzymatic activity increases compared to day 0 controls in both age groups, with Immunohistochemistry identifying staining for ALP in all samples. This would indicate that both age groups had undergone osteogenic differentiation, as ALP is unlikely to increase in non-differentiated BM-MSCs. Taken together, these result suggest that though all cells were osteogenically induced, young cells displayed a more mature cell lineage, indicated by significantly more OC being produced in young samples. There was no detectable increase in ALP activity in monolayer cultures, as a low seeding density meant there was insufficient material to accurately

determine day 0 activities. Instead, ALP and Alizarin red staining of monolayer cultures indicated inconsistent differentiation and mineralisation of the structure in old donor cell samples, whilst young donor samples displayed consistently good staining for both.

Whilst the ECM may play a large role in stem cell development, the initial ability of the cell to respond to its environment is also of importance (Erickson *et al.,* 2011; Laschober *et al.,* 2011). Similar to the results of the current study, cells from older donors have been demonstrated to have a decreased osteogenic potential in 3D culture (Mueller and Glowacki, 2001; Wagner *et al.,* 2009), as well as displaying a change in the protein synthesis (Fedarko *et al.,* 1992; Ikeda *et al.,* 1995). In particular Ingram *et al.* (1994) showed decreases in OC production in older cells compared to younger, whilst OPN expression remained relatively constant. This corroborates fully with the findings of this current study, and the significant decrease in OC gene expression levels by old donor cells compared to young.

This decrease in osteogenic ability may be caused by changes in the ageing bone marrow microenvironment in which the BM-MSCs originate (Carlson and Conboy, 2007). This ageing bone marrow niche is signified by the conversion of red marrow into yellow and an increase in the concentration of adipocytes (Justesen *et al.,* 2001), which may affect cell activity by direct interaction (Maurin *et al.,* 2000), or by limiting the exposure of BM-MSCs to required supportive cell types.

Additionally, replicative senescence through passage is a contributing factor to the decreases in proliferation, life span and activity of cells, and is thought to occur both *in vitro and in vivo* (Wagner *et al.,* 2009). Whilst the current study used cells from the same passage, the time spent in monolayer expansion may have impacted on the ability of young and old cells differently, with culture of old cells causing an acceleration of senescence, decreasing life

span and proliferative ability (Stenderup *et al.*, 2003). However there was no evidence of a decrease in proliferative ability between the young and old cells in this study.

4.4.3 Effect of bone donor age

The retention and rejuvenation of "stemness ability" by ECM may prove important in utilising an autologous osteoprogenitor source in tissue engineering (Auletta *et al.*, 2011). Research by Sun *et al.* (2011), has highlighted alterations in activity of cells grown on ECM constructed by young or old osteogenic cells, demonstrating the ability of ECM produced by young osteogenic cells to sustain cell viability and maintain, even rescue, a cells osteogenic capacity.

In the investigation into the effect of bone allograft donor age on the osteogenic capacity of both young and old donor cells, this experiment indicated, contrary to the initial hypothesis, that old donor bone was better able to support the osteogenic differentiation of BM-MSCs from either cell donor age group, with statistically higher expression of all osteogenic genes in young cells seeded on old bone compared to those seeded on young donor bone. This was also true for old donor cells; however there were no significant changes to OC production. Additionally, both ALP activity and histological staining indicated that all samples underwent osteogenic differentiation. Whilst this suggests the old bone was better able to support the innate abilities of the cells, it does not suggest that the bone can rescue osteogenic ability, such as demonstrated by Sun *et al.* (2011). However, Sun *et al.* (2011) utilised newly produced matrix structures by young and old cells, whilst the current study used actual human bone, focussing on patient age instead.

To the authors knowledge this is the first study to be undertaken to examine the effect of bone allograft donor age utilising large, non-powdered structures of human trabecular allograft bone, free from bone marrow material. Whilst previous studies have examined donor age, and indicated the superior ability of old bone material compared to young (Jergesen *et al.,* 1991; Pinholt and Solheim, 1998), they have all used powdered, demineralised bone. Of note, the study by Lohmann *et al.* (2001) also used non-demineralised material, though this was not decellularised and resulted in no reportable osteoinductive effect.

Though some studies have identified no difference between ages in osteoinductive potential (Traianedes *et al.,* 2004; Schwartz *et al.,* 1998), or clinical outcome (Delloye *et al.,* 2014), it is important to note that these did not include stem cell populations, instead relying on the healing potential of the host. These results therefore suggest that the host healing environment, such as inflammatory signals (Laschober *et al.,* 2011), is equally as important as the graft material used. This would indicate that further investigation should be undertaken into the osteogenic ability of bone marrow material, without isolation and culture expansion.

Ultimately the change in activity seen between young and old donor bone may be due to a change in composition and structural attributes, such as ECM proteins, mineralisation and architecture. As ageing occurs, osteoblasts become less numerous due to an increased rate of apoptosis (Zhou *et al.,* 2008), with any remaining cells displaying altered matrix protein output (Fedarko *et al.,* 1992; Ikeda *et al.,* 1995; Ingram *et al.,* 1994). This change in non-collagenous proteins, which are subsequently incorporated into new bone formation, may ultimately affect the binding and promotion of the pre-osteogenic cells, due to possible alterations in their bone promoting abilities. Importantly, a reduction in bone turn-over through ageing also causes changes in the collagen structure, with non-enzymatic alterations

to the collagen network potentially leading to the presentation of new binding areas which cells may then interact with (Wang *et al.,* 2002).

This decrease in osteoblastic cell number and activity impacts on structural protein maintenance and leads to changes in the microarchitecture of the ageing trabecular structure (Viguet-Carrin *et al.,* 2010; Turunen *et al.,* 2013), with decreases in trabecular plates and connectivity density (Chen *et al.,* 2008; Chen *et al.,* 2010), and increases in the thickness of remaining trabeculae struts (Lochmuller *et al.,* 2008; Fazzalari and Parkinson, 1998). This may lead to an increase in porosity and therefore a decreased BMD (Riggs *et al.,* 2004), resulting in an increased surface area within the structure for cell adhesion and/or interaction. This increase in porosity may improve osteogenic activity, with more porous material exhibiting improved osteoinductive potential (Sicchieri *et al.,* 2012; Marcos-Campos *et al.,* 2012; Polini *et al.,* 2011), and epitomised by cortical material exhibiting very little (Cornejo *et al.,* 2012).

Whilst the protein constituency and architecture are of importance to osteogenic activity, so too is the mineral phase of the structure (Shi *et al.,* 2009; Chou *et al.,* 1999; Hu *et al.,* 2014). The results of mineralisation assay XRD displayed broad peaks at locations relating to hydroxyapatite for both young and old bone samples, representing large elongated crystal of hydroxyapatite (Peters *et al.,* 2000). Together with XRF analysis, which indicated no significant difference in the mineral phase or Ca/P ratio between the young and old donor bone samples, these results suggest that there was no change in the size, morphology or crystallinity of the hydroxyapatite crystals with age (Boskey, 2003). Though previous studies have indicated that mineral crystallinity can alter with age (Smith and Smith, 1976; Handschin and Stern, 1994), this study has indicated no difference between the two bone donor age groups, and would suggest that this does not account for the differences recorded in the osteoinductive ability between young and old donor bone.

4.4.4 Conclusion

In conclusion, this study has assessed the osteoinductive potential of a human bone allograft scaffold, washed using a novel wash procedure, analysing the osteogenic differentiation of BM-MSCs seeded upon its surface. In addition, the study has also determined age specific changes in both cells and bone donated from young and old age groups.

The results of this study have demonstrated the washed human bone scaffold as being osteoinductive, independent of an osteogenic promoter such as dexamethasone, with significant increases in the transcription levels of the osteogenic differentiation related genes in seeded BM-MSCs. The results further identified clear differences in the ability of BM-MSCs from young and old donors to undergo osteogenic differentiation, given the same osteoinductive environment, with young donor cells expressing mature differentiation markers.

In addition to the influence of cell donor age, the results of this study have also highlighted the importance of bone donor age; showing that old donor bone is better than young bone in supporting the osteogenic activity of seeded BM-MSC from young and old donors. These findings are of direct clinical importance, as the majority of available bone stock from living donors is retrieved from elderly patients, and would suggest that the use of this allograft bone is not only safe and reliable, but beneficial.

Whilst this study has indicated that there are no changes in the mineral phase between young and old donor bone, further studies are required to elucidate the potential differences in ECM constitution, relative BMP availability and bone architecture, which are all important osteoinductive factors. These findings indicate the intrinsic effect of cell age on ECM production and in turn an extrinsic effect on the cell by the microenvironment. This research

highlights the need for better understanding of how unique microenvironments affect cells, with particular interest in matrix composition and recreation of an optimal healing niche.

Chapter 5

Preliminary assessment of the osteogenic potential of alternative sources of osteogenic and pre-osteogenic cells seeded on the washed bone scaffold

5.1 Introduction

Whilst BM-MSCs are the primary source of stem cells in tissue engineering, particularly BTE, the number of studies utilising alternative sources of stem cells has gradually been increasing. These include stem cells isolated from adipose tissue (Zuk *et al.,* 2002; Hattori *et al.,* 2004), dental pulp and circulating stem cells (Yamada *et al.,* 2011; Matsumoto *et al.,* 2008), together with cell concentration technologies for clinical use of bone marrow with bone grafts (Hung *et al.,* 2013; Hart *et al.,* 2014). The prevalence of these studies has increased due to the issues with the isolation of BM-MSCs; their low numbers (De Ugarte *et al.,* 2003), particularly in older individuals (Stolzing *et al.,* 2008), the effect of ageing on their activity (see Chapter 4), and the requirement for additional surgical procedures to acquire the material. This low BM-MSC concentration has historically required expensive and time consuming *in vitro* culture to expand their numbers to usable levels. This methodology may also influence BM-MSC fate (Yang *et al.,* 2014), thereby resulting in the reduction in differentiation capacity (Wagner *et al.,* 2008; Baxter *et al.,* 2004; Banfi *et al.,* 2002), and eventual osteogenic activity (Niemeyer *et al.,* 2010; Cornejo *et al.,* 2012).

Adipose tissue offers a more abundant source of stem cells than bone marrow, containing approximately between 7 to 20-fold more stem cells per gram of material. Furthermore, they are typically easier to isolate from whole tissue (De Ugarte *et al.,* 2003; Kern *et al.,* 2006) or even liposuction aspirates (Aust *et al.,* 2004). Although adipose stem cells (ASC) may display different cell surface signalling molecules (Gronthos *et al.,* 2001; Zuk *et al.,* 2001), they do express the general stromal markers (CD13, CD29, CD44, CD63, CD73, CD90, CD105 and CD166) (Zuk *et al.,* 2001; Yoshimura *et al.,* 2006; Mitchell *et al.,* 2006) and are able to undergo osteogenic differentiation when given the same stimulus as BM-MSCs (Zuk *et al.,* 2002; Wall *et al.,* 2007; Gupta *et al.,* 2007; De Ugarte *et al.,* 2003; Hattori *et al.,* 2004),

displaying successful osseointegration when used in combination with multiple types of bone grafts (Runyan *et al.,* 2010; Schubert *et al.,* 2011; Shi *et al.,* 2012; Lu *et al.,* 2013; Declercq *et al.,* 2013). Additionally, in comparison to BM-MSCs, the proliferation and osteogenic differentiation ability of ASCs is less affected by the processes of ageing and multiple passages (Chen *et al.,* 2012b; Wu *et al.,* 2013; Shi *et al.,* 2005; Kern *et al.,* 2006).

Though the use of ASCs and BM-MSCs is beneficial to BTE and subsequent graft integration, their isolation and culture expansion through serial passaging is expensive, time consuming and may cause issues with loss of cell differentiation capacity. As such, techniques which can be used during surgery, without a prior operation and minimal invasive procedures, would be of great benefit in the use of BTE scaffolds. The direct use of bone marrow material to aid *de novo* bone formation has long been used in surgery (Tiedeman *et al.,* 1991; Gangji *et al.,* 2011), combining the marrow removed to create space for prosthetics, such as a stem in hip surgery, with allograft in an attempt to promote its osseointegration (Brodke *et al.,* 2006; Babiker *et al.,* 2012; Deakin and Bannister, 2007). This reamed marrow material has the benefit of containing multiple cell types including pre-osteogenic cells and BM-MSCs, and in greater numbers than can be isolated from iliac crest aspirations, a common form of autograft material (Cox *et al.,* 2011).

However, bone marrow material, such as aspirates and reamings, still contains a relative low concentration of BM-MSCs and pre-osteogenic cells, whilst containing large concentrations of non-required cells such as erythrocytes, haematopeotic progenitor cells, and immune cell such as monocytes and macrophage. Therefore, rapid isolation and concentration techniques can be used to isolate mononucleur cells, characterised by a non-granular cytoplasm and a unilobulated nuclei, which are collectively termed BM-MNCs. This BM-MNC fraction contains an increased concentration of pre-osteogenic cells and BM-MSCs which are able to adhere to the graft, as well as the non-osteogenic cells such as pericytes, vascular endothelial

cells and haemopoietic stem cells, which may be important in supporting the “stemness” and later differentiation of the BM-MSCs (Bianco, 2011; Augello *et al.,* 2010; Di Nardo and Parker, 2011). Such isolation systems, though varying in efficiency, are commercially available (Hegde *et al.,* 2014), and are FDA (Federal Drug Administration) approved for the production, and immediate use of, concentrated cell fractions at the time of surgery. These cells may then be used in conjunction with allografts (Hung *et al.,* 2013; Vulcano *et al.,* 2013; Scaglione *et al.,* 2014; Ginis *et al.,* 2012), displaying improved bone production and integration over allograft alone (Hart *et al.,* 2014; Kretlow *et al.,* 2010).

Importantly, the inclusion of additional cell types such as endothelial cells may lead to the production of angiogenic growth factors such as VEGFa, which promotes revascularisation and the formation of new blood vessels. This revascularisation of a graft is important in its osseointegration. In addition to promoting new blood vessel formation the angiogenic growth factor VEGFa may also encourage *de novo* bone production, and aid the incorporation of a graft into the host (Street *et al.,* 2002; Huang *et al.,* 2005). Indeed clinically, the inclusion of endothelial cells with a graft material has been identified as being beneficial to its integration into the host (Thebaud *et al.,* 2012).

5.1.1 Aims

Due to cost, low stem cell density and the implications of long culture periods on BM-MSC proliferation and differentiation ability, alternative sources of MSCs are being assessed for use in BTE. ASCs in particular offer an abundant, easy to acquire, alternative source to BM-MSCs, exhibiting a comparable ability to undergo osteogenic differentiation and resulting in positive clinical outcomes. Importantly, it has also been demonstrated that these cells do not undergo age-related changes in differentiation capacity as dramatically as BM-MSC,

maintaining their osteogenic differentiation ability after multiple passages in culture expansion. In contrast, by removing the need for culture altogether, the use of BM-MNC concentration methods at the time of surgery may offer a relatively cheaper, faster and less processed source of osteogenic cells for BTE and ultimately clinical application.

As such this study aimed to:

(i) Compare the ability of patient-matched ASCs and BM-MSCs, cultured on the washed bone, to undergo osteogenic differentiation in either standard or osteogenic conditions. This aim hypothesised that ASCs seeded on the washed bone, similar to the BM-MSCs, would undergo osteogenic differentiation;

(ii) Assess the osteogenic potential of minimally processed BM-MNCs in conjunction with the washed bone, and their potential as an alternative osteogenic cell source in comparison to highly processed, monoculture expanded BM-MSCs. This aim hypothesised that the washed bone material would induce the osteogenic activity of the pre-osteogenic cells and BM-MSCs contained in the BM-MNC mixed cell type fraction, despite it containing relatively low numbers.

5.2 Materials and Methods

5.2.1 Comparison of the efficacy and differentiation potential of BM-MSC and ASCs from patient-matched samples seeded on washed bone

5.2.1.1 Isolation of stem cells

BM-MSCs and ASCs were isolated from a 73 YOA male, with BM-MSCs isolated using previously described methodology (2.2.6.1). Adipose tissue was removed from tissue surrounding the joint and cut into small pieces, which were digested in 15ml digestion buffer containing 15mg/ml collagenase type 1 (17100-017; Gibco, Life Technologies, Paisley, UK) and 2mM calcium chloride (C7902; Sigma-Aldrich, Gillingham, UK) in HBSS (H9394, Sigma-Aldrich, Gillingham, UK). This solution was incubated at 37°C with constant agitation for two hours. The digestion solution was passed through a 100µm filter (352360; BD Bioscience, Oxford, UK) to remove non-digested particles before enzyme activity was neutralised with 15ml of standard medium. The mixture was then centrifuged at 500*xg* for five minutes, with enough supernatant aspirated to leave a 5ml reservoir. An additional 7ml of culture medium was added and cells were cultured in monolayer.

5.2.1.2 Seeding of cells on washed (allograft) bone

ASCs and BM-MSCs were cultured until sufficient cells were recovered for experimental use (Passage 4), then seeded onto bone cubes from three bone donors (all ≥70 YOA), as described previously (2.2.7.1). The bone cubes were cultured for 0, 14 and 28 days in either standard or osteogenic medium. AlamarBlue cell health indicator was used to ascertain cell

metabolic activity (2.2.7.2). Samples were removed at 0, 14 and 28 days for RNA extraction and QRT-PCR analysis of osteogenic gene activity as described in section 4.2.1.

5.2.2 Assessment of the osteogenic potential of concentrated mononuclear cells seeded on washed bone

5.2.2.1 Isolation of BM-MNCs from human bone marrow reamings

Bone marrow reamings from a 76 YOA female was treated as described in section 2.2.6.1. The bone marrow aspirate was separated into two fractions; one underwent the normal Rosettesep treatment while the other was pipetted over Histopaque 1077 without Rosettesep treatment. Non-Rosettesep treated cells were recovered from the interphase layer of the Histopaque. These cells were termed BM-MNC. The other fraction underwent normal BM-MSC isolation (2.2.6.1), and adherent cells were cultured in monolayer until sufficient BM-MSCs were expanded for experimental use.

5.2.2.2 Seeding of bone cubes with BM-MNCs and BM-MSCs

The BM-MNC fraction and isolated BM-MSCs were both counted and resuspended to $4x10^6$/ml in fresh medium. A 250µl aliquot containing $0.5x10^6$ cells was used to seed defrosted bone cubes, which were cultured in osteogenic medium, with cell viability assessed using alamarBlue (2.2.7.2). Cubes were produced for 0 and 28 day samples for PCR analysis of osteogenic gene expression as described previously (4.2.1).

5.3 Results

5.3.1 Comparison of osteogenic potential of patient-matched BM-MSCs and ASCs

5.3.1.1 Culture of ASC-seeded bone cubes in standard and osteogenic medium

Expression levels of RUNX2 in ASCs seeded onto washed bone (n=3) were significantly increased in both standard and osteogenic medium at day 14 (8.1-fold and 8.9-fold; respectively, $p \leq 0.001$ for both) and day 28 (8.6-fold and 7.3-fold; respectively, $p \leq 0.001$ for both) compared to day 0 controls (Figure 5.1 A). However, there was no significant increase from day 14 to day 28, and no significant difference between conditions at either timepoint.

At day 14, there were no significant differences in OPN expression levels when compared to day 0 controls for samples cultured in either standard osteogenic media; however there was a significant difference between culture conditions, with osteogenic medium cultured samples displaying higher expression levels than standard medium cultured ($p \leq 0.01$) (Figure 5.1 B). Additionally, in standard medium, OPN levels were significantly decreased at day 28 compared to day 0 (0.1-fold, $p \leq 0.001$), while in osteogenic medium, OPN expression was significantly increased (2.5-fold, $p \leq 0.01$), with a significant difference between culture conditions ($p \leq 0.001$).

In comparison, the transcription levels of OC were significantly increased in both standard and osteogenic medium at day 14 (4.4-fold and 12.2-fold; respectively, $p \leq 0.001$ for both) and day 28 (6.7-fold and 9.3-fold; respectively, $p \leq 0.001$ for both) compared to day 0 controls; however there was a significant decrease from day 14 to 28 in osteogenic medium cultured

samples ($p \leq 0.01$) (Figure 5.1 C). There was a significant difference between the two culture conditions at day 14 ($p \leq 0.001$), but not day 28.

The gene transcription levels for ALPL were also significantly increased at day 14 and 28 compared to day 0 for both standard (7.6-fold and 8.4; respectively, $p \leq 0.001$ for both) and osteogenic medium (5.6-fold and 4.9-fold; respectively, $p \leq 0.001$ for both) (Figure 5.1 D). There were no significant differences for either culture condition between day 14 and 28; however there was significantly lower transcription levels in osteogenic medium at day 28 than in standard ($p \leq 0.001$).

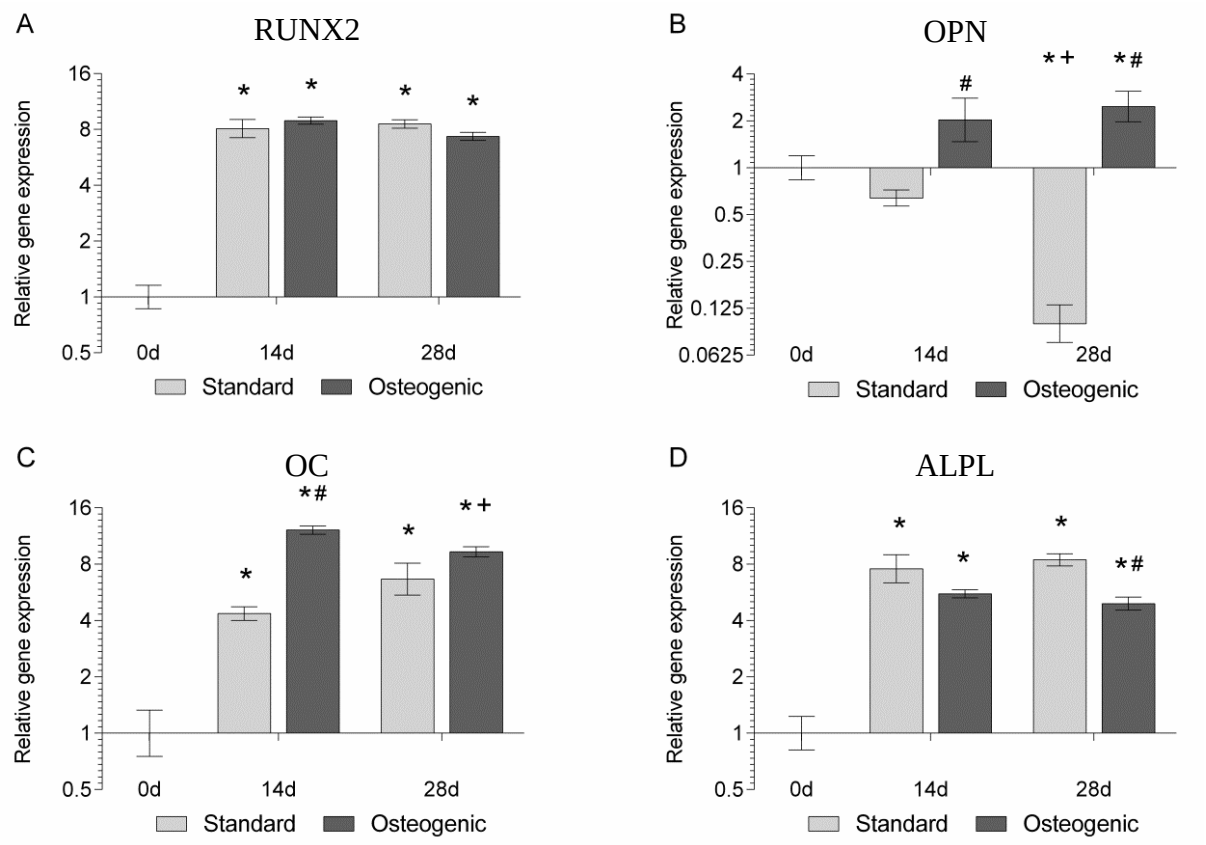

Figure 5.1: QRT-PCR gene expression in ASCs isolated from a 73 YOA donor (WH106) seeded on washed bone scaffolds (n=3). Seeded cubes were cultured in either standard or osteogenic medium for 14 or 28 days and samples retrieved through RNA extraction and reverse transcription. Relative gene expression of osteogenic markers RUNX2 (A), OPN (B), OC (C), and ALPL (D) were normalised to the housekeeping gene MRPL19 and day 0 controls ($2^{-\Delta\Delta CT}$). Data represent mean ± SE. *, significant difference with respect to 0d control ($p \leq 0.05$). +, indicates significant difference between 14d and 28d ($p \leq 0.05$). #, indicates significant difference between cells cultured in standard or osteogenic medium at the same timepoint ($p \leq 0.05$).

5.3.1.2 Culture of BM-MSC seeded bone cubes in standard and osteogenic medium

RUNX2 transcription levels in BM-MSC seeded on washed bone cubes (n=3) were increased significantly at day 14 and 28 in both standard (2.2-fold and 3.5-fold; respectively, $p \leq 0.001$ for both) and osteogenic conditions compared to day 0 controls (4.1-fold and 5.8-fold; respectively, $p \leq 0.001$ for both) (Figure 5.2 A). No significant difference between day 14 and 28 was recorded in standard medium; however there was a significant increase in osteogenic medium cultures ($p \leq 0.01$). There were also significantly higher expression levels of RUNX2 in osteogenic medium at day 28 than in standard medium ($p \leq 0.001$).

The increases in OPN expression followed those of RUNX2, with significant increases in both standard and osteogenic medium at day 14 (7.7-fold and 32.2-fold; respectively, $p \leq 0.001$ for both) and day 28 in comparison to day 0 (26.2-fold and 60-fold; respectively, $p \leq 0.001$ for both) (Figure 5.2 B). As with RUNX2, there was only a significant increase from day 14 to day 28 in osteogenic medium ($p \leq 0.01$); however at both timepoints, expression levels were significantly higher in osteogenic medium ($p \leq 0.001$ for both).

There was no significant change in OC expression from day 0 in BM-MSC seeded bone cubes in standard conditions at either timepoint (Figure 5.2 C). In contrast, there were significant increases at both day 14 and 28 compared to day 0, in osteogenic medium cultured samples (3.7-fold and 4.7-fold; respectively, $p \leq 0.01$ for both). There was also significantly higher expression in osteogenic conditions than standard at both 14 and 28 days ($p \leq 0.01$ for both). In comparison to levels at day 0, ALPL expression was significantly increased at day 14 in standard medium (2.3-fold, $p \leq 0.001$), though there was no significant difference at day 28. However, expression at day 28 was significantly decreased in comparison to that of day 14 ($p \leq 0.001$) (Figure 5.2 D). At both day 14 and 28, expression levels were significantly

decreased in osteogenic medium compared to day 0 (0.51-fold, $p \leq 0.001$ and 0.52-fold, $p \leq 0.01$), as well as compared to levels in standard medium ($p \leq 0.001$ and $p \leq 0.01$ respectively).

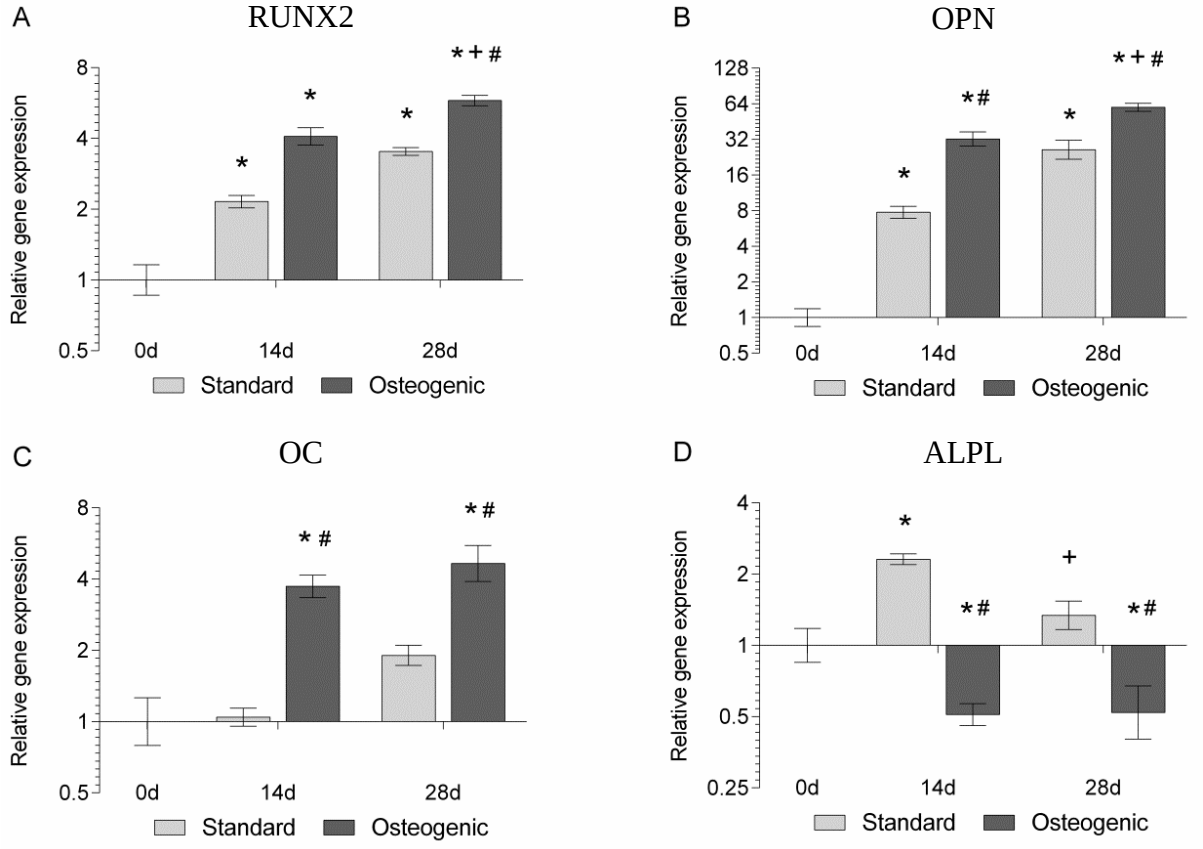

Figure 5.2: QRT-PCR gene expression in BM-MSCs isolated from a 73 YOA donor (WH106) seeded on washed bone scaffolds (n=3). Seeded cubes were cultured in either standard or osteogenic medium for 14 or 28 days and samples retrieved through RNA extraction and reverse transcription. Relative gene expression of osteogenic markers RUNX2 (A), OPN (B), OC (C), and ALPL (D) were normalised to the housekeeping gene MRPL19 and day 0 controls ($2^{-\Delta\Delta CT}$). Data represent mean ± SE. *, significant difference with respect to 0d control ($p \leq 0.05$). +, indicates significant difference between 14d and 28d ($p \leq 0.05$). #, indicates significant difference between cells cultured in standard or osteogenic medium at the same timepoint ($p \leq 0.05$).

5.3.1.3 Comparison of patient-matched ASCs and BM-MSCs cultured on bone cubes in standard and osteogenic conditions

Assessment by alamarBlue indicated that at day 14 in standard conditions, there were significant increases in relative metabolic activity in both ASC and BM-MSC samples compared to day 0, of 1.6-fold (±0.09) and 1.9-fold (±0.11) respectively ($p \leq 0.001$ for both) (Figure 5.3 A). Relative metabolic activity was also significantly increased at day 28 compared to day 0, in both ASCs (1.7-fold ±0.03) and BM-MSCs (2.15-fold ±0.08) ($p \leq 0.001$ for both). There was no significant fold-change in alamarBlue reduction between day 14 and day 28 for either ASCs or BM-MSCs; however, both at day 14 and day 28 timepoints, BM-MSC fold change was significantly larger than ASCs ($p \leq 0.05$).

In osteogenic conditions, relative metabolic activity was significantly increased in both ASCs and BM-MSCs at day 14 (1.7-fold ±0313, and 2.15-fold ±0.19; respectively, $p \leq 0.001$ for both) compared to day 0; however the fold change in BM-MSCs was significantly larger than in ASCs ($p \leq 0.05$) (Figure 5.3 B). At day 28, both ASC and BM-MSC metabolic activity was significant increase compared to day 0; by 1.92-fold (±0.05) and 2.0-fold (±0.05) respectively ($p \leq 0.001$ for both), with no significant increase compared to day 14, or difference between cell types.

Additionally, there were no significant differences in metabolic activity between standard and osteogenic conditions for ASCs or BM-MSCs at either 14 or 28 days.

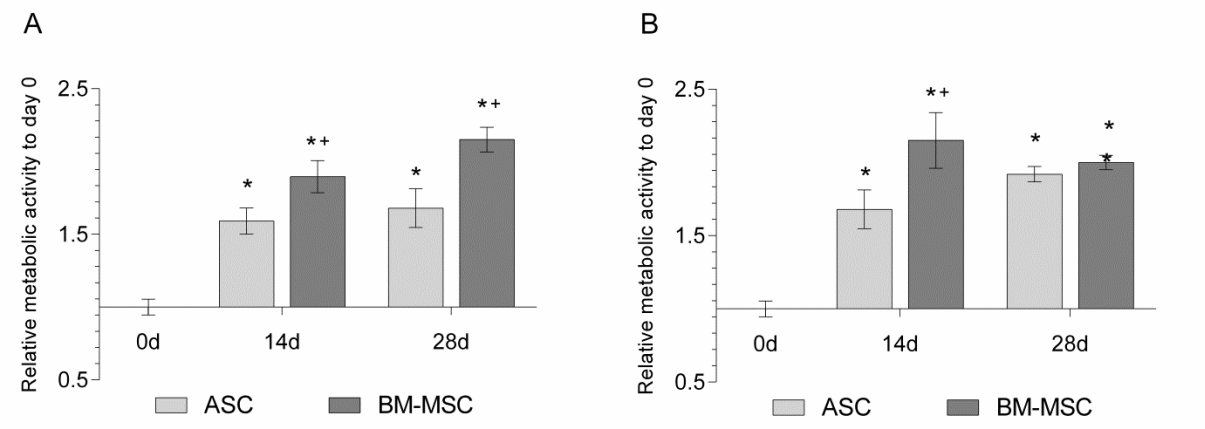

Figure 5.3: AlamarBlue metabolic activity for ASCs and BM-MSCs isolated from a 73 YOA donor (WH106), and cultured on washed bone scaffolds (n=3). Seeded cubes were cultured in either standard medium (A) or osteogenic medium (B) for 14 or 28 days with metabolic activity normalised to day 0 controls. Data represent mean ± SE. *, significant difference with respect to 0d control ($p \leq 0.05$). +, indicates significant difference between ASCs and BM-MSCs at the same timepoint ($p \leq 0.05$). #, indicates significant difference between 14d and 28d in the same medium type ($p \leq 0.05$).

QRT-PCR data presented clear variances in the osteogenic differentiation profiles of ASCs and BM-MSCs seeded on washed bone cultured in standard conditions. Expression levels of RUNX2 were significantly higher in ASCs at both 14 and 28 days compared to BM-MSCs ($p \leq 0.001$ for both) whilst there were no significant differences at day 0 levels (Figure 5.4 A). OPN expression was also not significantly different at day 0; however at day 14 and 28, BM-MSC samples produced significantly higher transcription levels than ASCs ($p \leq 0.001$ for both) (Figure 5.4 B). Initial OC expression levels were significantly higher in BM-MSC samples than ASCs ($p \leq 0.01$); however by day 28 there were significantly higher expression levels in ASCs ($p \leq 0.05$) (Figure 5.4 C). There were no significant differences in ALPL

expression at day 0; however at both day 14 and 28 there was significantly higher expression levels in ASCs than BM-MSCs ($p \leq 0.001$ for both) (Figure 5.4 D).

In osteogenic culture conditions, RUNX2 expression was still significantly higher in ASCs than BM-MSCs at both day 14 and 28 ($p \leq 0.001$ and $p \leq 0.01$; respectively), but not significantly different at day 0 (Figure 5.5 A). OPN levels were not significantly different between ASC and BM-MSC samples at day 0; however at day 14 and 28, expression was significantly higher in BM-MSC samples than ASCs ($p \leq 0.1$ and $p \leq 0.001$; respectively) (Figure 5.5 B). As with standard conditions, basal levels of OC at day 0 were significantly higher in BM-MSCs than in ASCs ($p \leq 0.01$) (Figure 5.5 C); however, at day 14 OC expression was significantly higher in ASCs than BM-MSCs ($p \leq 0.001$), though at day 28 there were no significant differences. ALPL expression was not statistically different at day 0, but was significantly higher at both day 14 and 28 in ASC samples, compared to BM-MSCs at the same timepoint ($p \leq 0.001$) (Figure 5.5 D).

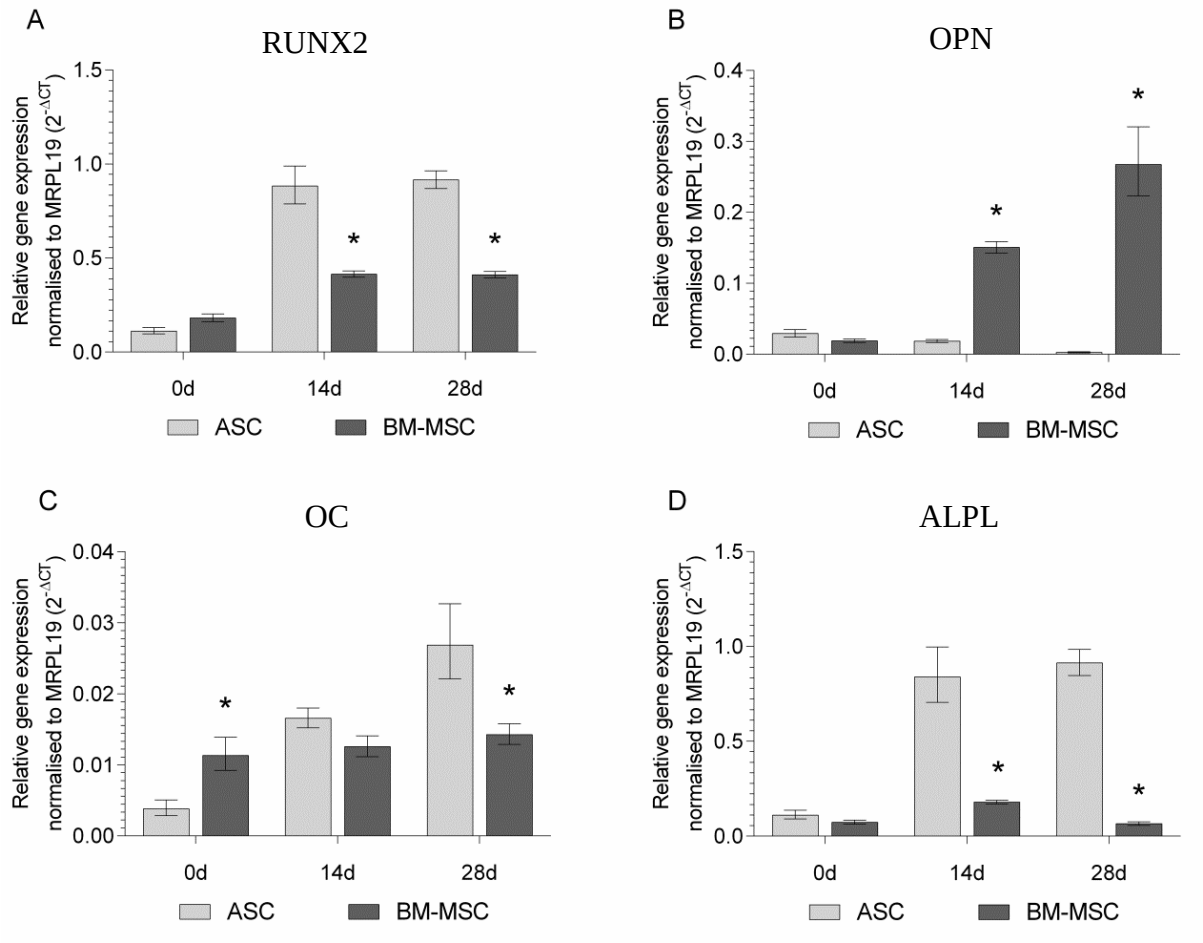

Figure 5.4: QRT-PCR gene expression in patient-matched ASCs and BM-MSCs isolated from a 73 YOA donor (WH106), and cultured on washed bone scaffolds in standard medium (n=3 for both). Seeded cubes were cultured in standard medium for 14 or 28 days and samples retrieved through RNA extraction and reverse transcription. Relative gene expression of osteogenic markers RUNX2 (A), OPN (B), OC (C), and ALPL (D) were normalised to the housekeeping gene MRPL19 ($2^{-\Delta CT}$). Data represent mean ± SE. *, indicates significant difference between ASCs and BM-MSCs at the same timepoint ($p \leq 0.05$).

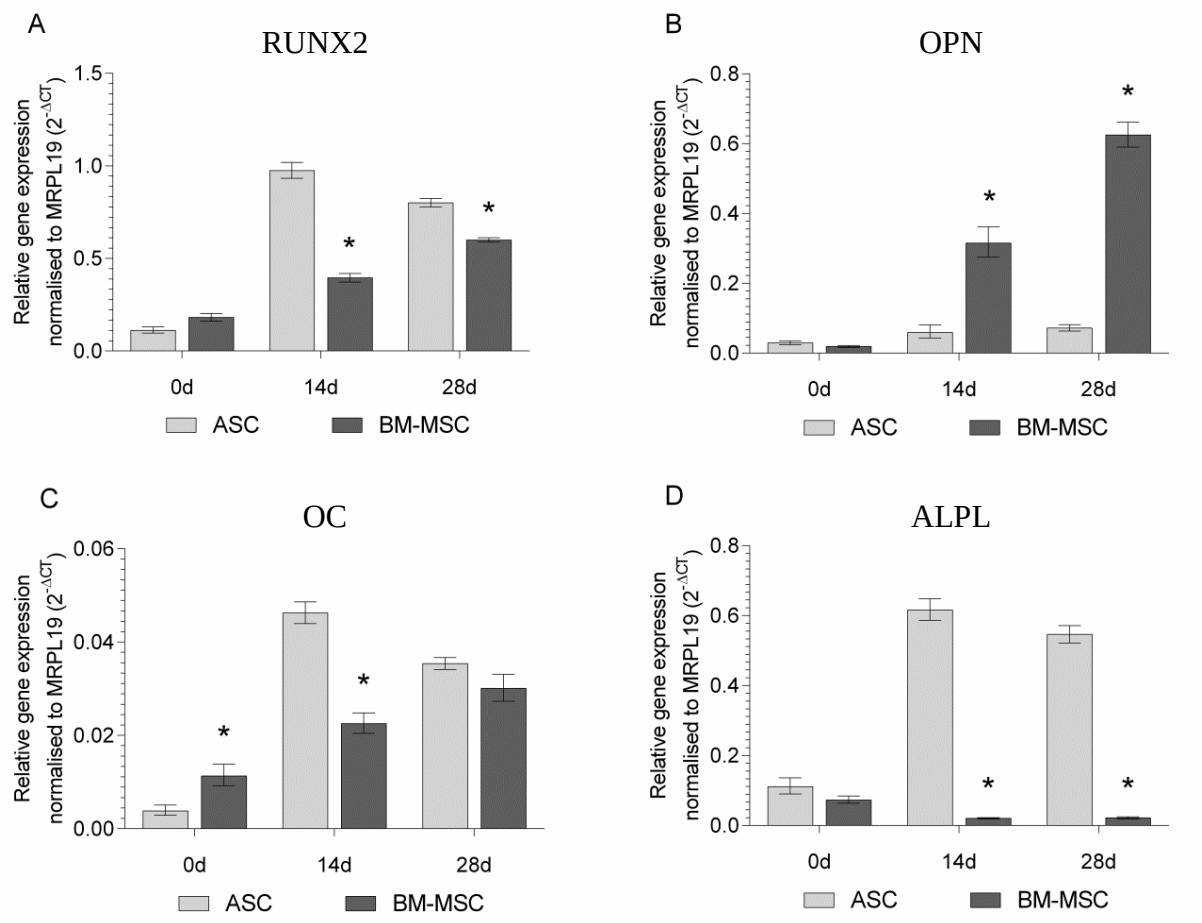

Figure 5.5: QRT-PCR gene expression in patient-matched ASCs and BM-MSCs isolated from a 73 YOA donor (WH106) (n=3 for both), and cultured on washed bone scaffolds in osteogenic medium. Seeded cubes were cultured in osteogenic medium for 14 or 28 days and samples retrieved through RNA extraction and reverse transcription. Relative gene expression of osteogenic markers RUNX2 (A), OPN (B), OC (C), and ALPL (D) were normalised to the housekeeping gene MRPL19 ($2^{-\Delta CT}$). Data represent mean ± SE. *, indicates significant difference between ASCs and BM-MSCs at the same timepoint ($p \leq 0.05$).

5.3.2 Osteogenic differentiation of BM-MSC and BM-MNCs cultured on washed human bone allograft

Culture of BM-MSCs on washed bone (n=3) resulted in significant increases in expression levels of RUNX2 (2.47-fold, $p \leq 0.01$) and OPN (12.8-fold, $p \leq 0.01$) (Figure 5.6 A and B) at day 28, when compared to day 0. In contrast, while expression levels of OC were not significantly changed at day 28 compared to day 0 controls, the expression levels of ALPL and the angiogenic factor VEGFα were significantly down-regulated (0.06-fold, $p \leq 0.01$ and 0.77-fold, $p \leq 0.05$; respectively) (Figure 5.6 C, D and E).

BM-MNCs cultured on the washed bone (n=3) had significant increases in RUNX2 (1.54-fold, $p \leq 0.05$) and OC (4.9-fold, $p \leq 0.05$) at day 28 in comparison to day controls (Figure 5.7 A and C). In contrast, OPN expression at day 28 was significantly down-regulated compared to day 0 (0.03, $p \leq 0.001$). Additionally, whilst ALPL levels were not significantly different when compared to day 0, expression of VEGFα was significantly increased after the 28 day culture period (12.1-fold, $p \leq 0.001$) (Figure 5.7 B, D and E). In addition, there was a significant, 5.6-fold (±0.95) increase in relative metabolic activity after 28 days in culture in the BM-MNCs compared to day 0 ($p \leq 0.001$).

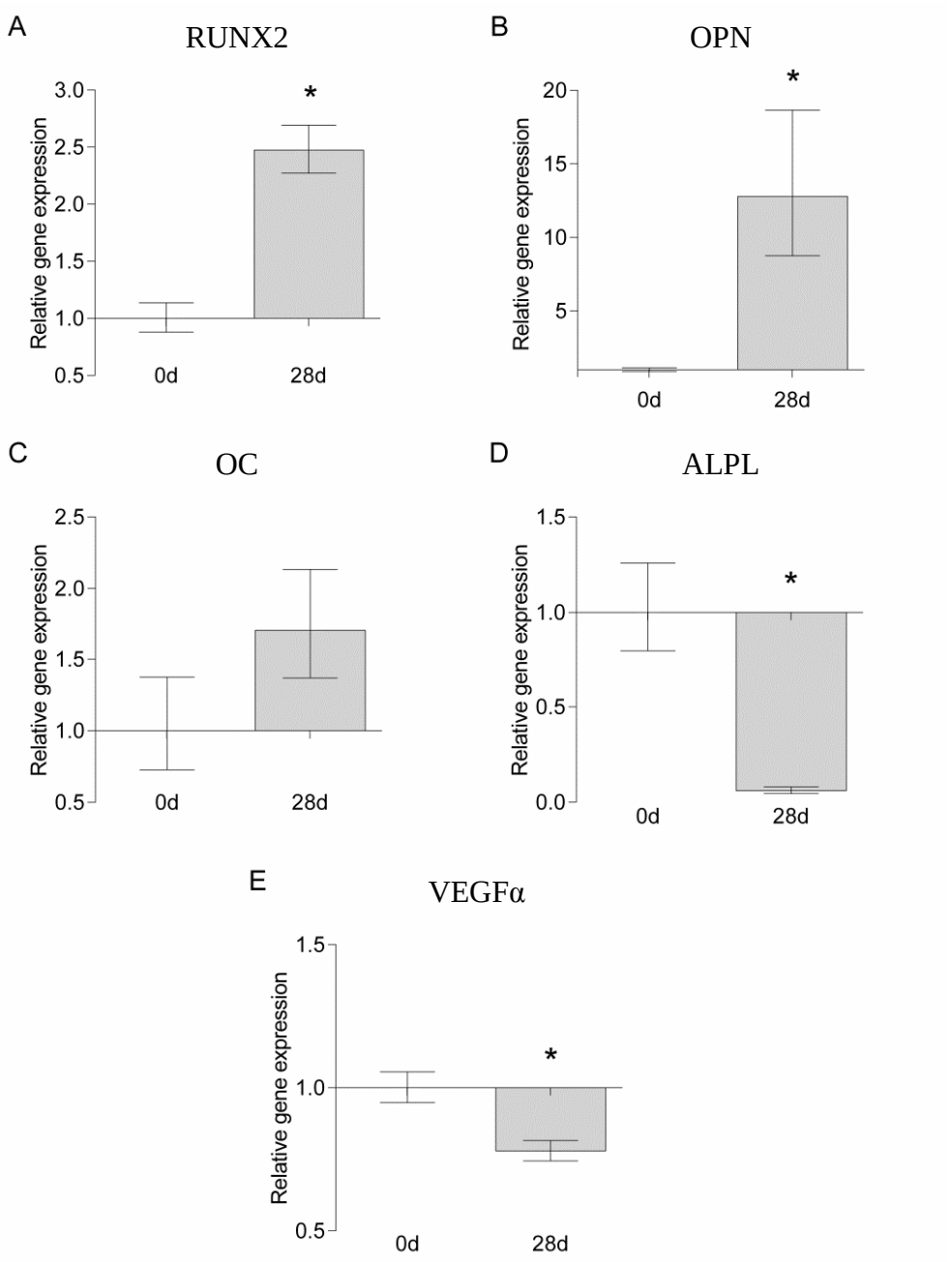

Figure 5.6: QRT-PCR gene expression in BM-MSCs isolated from a 76 YOA donor (WH129) seeded on washed bone scaffolds (n=3). Seeded cubes were cultured in osteogenic medium for 28 days and samples retrieved through RNA extraction and reverse transcription. Relative gene expression of osteogenic markers RUNX2 (A), OPN (B), OC (C), and ALPL (D) and angiogenesis marker VEGFα (E) were normalised to the housekeeping gene MRPL19 and day 0 controls ($2^{-\Delta\Delta CT}$). Data represent mean ± SE. *, significant difference with respect to 0d control ($p \leq 0.05$).

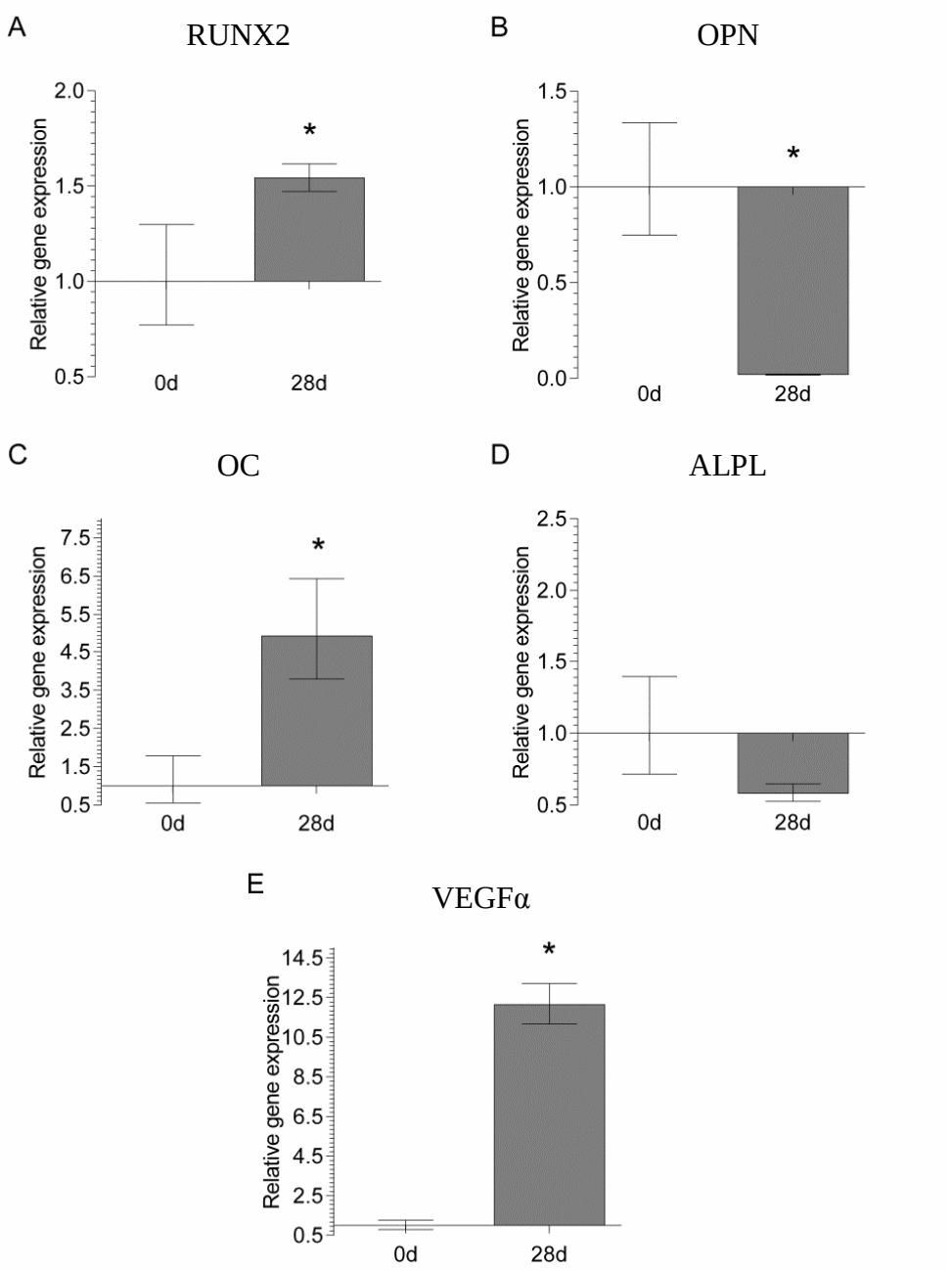

Figure 5.7: QRT-PCR gene expression in BM-MNCs isolated from a 76 YOA donor (WH129) seeded on washed bone scaffolds (n=3). Seeded cubes were cultured in osteogenic medium for 28 days and samples retrieved through RNA extraction and reverse transcription. Relative gene expression of osteogenic markers RUNX2 (A), OPN (B), OC (C), and ALPL (D) and angiogenesis marker VEGFα (E) were normalised to the housekeeping gene MRPL19 and day 0 controls ($2^{-\Delta\Delta CT}$). Data represent mean ± SE. *, significant difference with respect to 0d control ($p \leq 0.05$).

5.4 Discussion and Conclusion

Although BM-MSCs are currently the most widely used source for BTE, their low abundance, difficult isolation and high cost due to additional surgical procedures and culture expansion, has meant the number of studies utilising alternative sources of stem cells has increased. Two of the most promising sources are ASCs and BM-MNCs. Whilst ASCs are in relatively high abundance in tissue, they still require some culture expansion; conversely, BM-MNCs require no monolayer expansion or separate isolation procedures and can be used directly in theatre. Therefore this preliminary study aimed to determine whether such cells were able to undergo osteogenic differentiation once seeded onto the washed bone allograft which has previously been shown to be osteoconductive and osteoinductive (Chapter 4).

As these were preliminary experiments using a small n value, it is important to interpret their results with caution. As such, while they test the basic hypothesis, additional experimentation using a larger cohort of patient-matched samples and a wider range of techniques, such enzyme activity or protein expression, are required in order to reproducibly, and clearly evaluate whether (i) the relatively more abundant ASCs are equivalent to BM-MSCs in their ability to undergo osteogenic differentiation when cultured on the washed bone, and (ii) whether culture of minimally processed BM-MNCs results in increased expression of osteogenic markers (thereby depicting osteogenic differentiation of such cells).

5.4.1 Culture of ASCs on the washed bone allograft

The results show that ASCs isolated from an elderly donor underwent osteogenic differentiation independent of osteogenic medium, as did the BM-MSC (similar to previous findings with BM-MSCs) (Chapter 4). However, there were differences in transcription levels

of osteogenic genes between the two cell groups. ASCs expressed significantly higher levels of RUNX2 and OC compared to their bone marrow equivalents, in both standard and osteogenic conditions, whilst expressing less OPN. Importantly, the ALPL expression levels were also significantly increased in the ASC population compared to their BM-MSC counterparts. These results suggest that, whilst the two stem cell groups were both able to undergo osteogenic differentiation, the ASCs were further differentiated than their bone marrow derived counterparts. Interestingly, the higher expression of late stage marker OCN, together with significantly higher ALPL expression by the ASCs, is similar to the expression profiles of young donor BM-MSCs, previously shown in this study (Chapter 4).

A difference in osteogenic activity of ASC and BM-MSCs has previously been documented by Noel *et al.* (2008) and Schubert *et al.* (2011), who also noted similar increases in OC and ALPL to those recorded in the current investigation. Interestingly, studies into the comparative effect of ageing on the osteogenic activity of ASCs and BM-MSCs have indicated that ASCs are not as dramatically affected as BM-MSCs (Shi *et al.,* 2012; Wu *et al.,* 2013; Chen *et al.,* 2012b). In particular, the study by Chen *et al.* (2012b) reported increased expression of RUNX2, OC and ALPL in old donor ASCs compared to patient-matched BM-MSCs, whilst the old BM-MSCs displayed increased expression in senescence markers (p21 and β-glactosidase activity) compared to ASCs group. However, the same group also determined that the young donor BM-MSCs group outperformed their ASC counterparts. As such, the osteogenic differentiation of ASCs may differ with age, and would suggest that, in addition to experimental repeats; this study should be replicated using cells from young donors, to better understand the influence of age on the osteogenic differentiation of ASCs seeded on the washed bone.

There have been multiple studies indicating the successful incorporation and osteogenic differentiation of ASCs in BTE, both *in vivo* (Runyan *et al.,* 2010; Fan *et al.,* 2014) and *in*

vitro (Desai *et al.*, 2013; Mihaila *et al.*, 2014; Shi *et al.*, 2012; Haimi *et al.*, 2009; Noel *et al.*, 2008). In particular, the use of ASCs in conjunction with washed bone allograft material has shown positive results (Runyan *et al.*, 2010; Shi *et al.*, 2012; Kloeters *et al.*, 2011); however they are routinely used in combination with factors such as platelet rich plasma (PRP), which contain numerous growth factors, or osteogenic factors (e.g. BMP-2). In comparison, the current study has displayed induction independent of an osteogenic growth factor source. As previously discussed in Chapter 4, this is most likely to be due to the material attributes of both rigidity and biochemical qualities that have also been recognised as important cues for the osteogenic differentiation of ASCs (Li *et al.*, 2014; Haimi *et al.*, 2009). Importantly, the current experiment only utilised bone material retrieved from old donors (≥70 YOA), which has previously been identified by this study (Chapter 4) as being the most able to induce the osteogenic differentiation of seeded BM-MSCs. As such, additional experiments should incorporate young donor bone material, and assess the influence of bone donor age on the osteogenic differentiation of seeded ASCs.

5.4.2 Use of BM-MNCs for Bone Tissue Engineering

The results of the BM-MNC seeded bone cube experiments suggest that, despite there being a relatively low concentration of BM-MSCs and presence of other non-osteogenic cells, the BM-MNC fraction was still able to undergo osteogenic differentiation, with significant increases in osteogenic gene transcription levels of RUNX2 and late stage marker OC. Furthermore, alamarBlue results indicated the presence and proliferation of cells adhered to the washed bone.

Additionally, the transcription levels of VEGFα were significantly increased in BM-MNC, whilst being down-regulated in BM-MSCs. These results imply that in addition to the

osteogenic differentiation of cells within the BM-MNC fraction to a mature osteoblast phenotype, the powerful angiogenic growth factor VEGFα was also expressed, which may be beneficial to the osseointegration of a bone tissue engineered graft into the host. The increase in VEGFα gene transcription by the BM-MNCs may be of clinical significance, as expression of this angiogenic factor has been identified as being beneficial to the bone healing environment, through both increasing cell proliferation as well as attracting host BM-MSCs and osteoblasts (Fiedler *et al.,* 2005; Mayr-Wohlfart *et al.,* 2002). This activity may lead to increases in *de novo* bone production (Street *et al.,* 2002), and when used by itself or in combination with other osteogenic factors, may benefit the incorporation of a graft into the host (Huang *et al.,* 2005).

Unlike processed and monoculture expanded BM-MSC, the minimal processing required to produce BM-MNCs retains non–osteogenic supportive cells, such as endothelial cells and pericytes. These cell types have been identified as supporting the osteogenic ability of the BM-MSCs (Bianco 2011; Augello *et al.,* 2010; Di Nardo and Parker, 2011), either by the promotion of BM-MSC (and pre-osteogenic cell) adhesion to the bone surface, or through prolonged cross-talk and interaction between the different cell types (Hammoudi *et al.,* 2012). Indeed the presence of endothelial cells in particular may account for the expression of VEGFα by the BM-MNC fraction. Indeed this may be of benefit, as the use of endothelial cells in combination with stem cell tissue engineered bone graft has been shown to greatly aid in the incorporation of graft material *in vivo* (Thebaud *et al.,* 2012; Cornejo *et al.,* 2012). As such, by seeding BM-MNCs directly onto the bone, cell types which would normally have been removed during processing to BM-MSCs, such as the endothelial cells, may have been able to adhere to the washed bone structure and support osteogenic differentiation and the production of angiogenic factors. However, this study did not ascertain the relative concentration of BM-MSCs and other cells types which were present in the BM-MNC

fraction, or their biological necessity. Additionally, once seeded, the distribution of these different cells types within the scaffold was not assessed histologically, and would be of interest regarding potential cell-cell interactions.

Ultimately, utilising cells concentrated from bone marrow reamings reduces the costs of additional surgical procedures required to procure BM-MSCs and laboratory time needed for culture expansion. In addition, the use of BM-MNCs as an alternative to BM-MSCs enables the production of an autologous source of osteogenic cells, including BM-MSCs, at the time of surgery (Scaglione *et al.*, 2014; Hermann *et al.*, 2008) and has shown positive clinical results (Hung *et al.*, 2013; Vulcano *et al.*, 2013; Scaglione *et al.*, 2006; Ginis *et al.*, 2012; Hart *et al.*, 2014; Kretlow *et al.*, 2010). Importantly, the FDA approval for the use of concentrated BM-MNCs at the time of surgery, may expedite the production of osteogenic grafts (Scaglione *et al.*, 2006; Chatterjea *et al.*, 2012), potentially allowing clinical translation without intervening use of animal models.

5.4.3 Conclusion

The use of long culture periods to expand isolated BM-MSCs, due to their low abundance, increases the cost involved with BTE and has the potential to alter their later osteogenic differentiation and functional ability. Consequently, the use of alternative sources of MSCs, such as the use of ASCs and minimally processed BM-MNCs, is increasing.

This preliminary study has identified the potential use of alternative sources of stem cells for use in BTE, with both ASCs and BM-MNCs able to undergo osteogenic differentiation on the washed bone. The results also suggested that given the same osteoinductive cues, ASCs were

further differentiated than their BM-MSC counterparts and that the BM-MNC fraction showed increased transcription levels of angiogenic factors when seeded on bone.

Although the washed bone was able to induce osteogenic differentiation of the two cell sources, the further investigation of minimally processed BM-MNCs is of greater clinical importance, and may offer more promising results.

Chapter 6

Conclusion and Future work

6.1 Conclusions of the study

Bone grafting is a crucial surgical tool for the replacement of large areas of bone which has been lost through disease, trauma or surgical procedures. Whilst autograft is considered the gold standard, it is limited in availability and its removal poses the risk of site morbidity in the patient. Although tissue engineered allografts produced from washed bone are available, they often lack the substantial osteogenic activity and consistency found in autograft material, and as such have not become ubiquitously used. Other issues affecting the use of BTE allografts include its availability, the size of material, the speed at which it can be produced, cost of production, but most importantly its osteogenic qualities.

6.1.1 The wash process produced an acellular bone scaffold, with osteogenic properties suitable for BTE

In this study a novel wash process (developed by the NHSBT) was employed to test its efficiency in producing a biocompatible, biomechanically stable washed bone allograft that could be used for BTE. Importantly this study has shown that:

i) The novel wash process is highly efficient, with both biochemical and histological evidence displaying the production of an acellular structure. Further results show this material to be biocompatible, with BM-MSCs able to colonise the structure and proliferate in culture. Conversely, the unwashed fresh-frozen bone is not biocompatible and displays cytotoxicity both in extract and proximity cytotoxicity assays.

ii) The washed material is able to withstand compressive forces and is mechanically comparable to currently used, unwashed fresh-frozen material. This is shown in both the orientated and random orientated loading models, and implies that the washed allograft bone will maintain its structural stability *in vivo*, under clinical conditions. The stability is important not only for supporting areas of load, but also in the maintenance of native architecture, which has been identified as being crucial in the formation of new bone, and which clinically may promote osseointegration.

iii) Importantly, this study also demonstrates that BM-MSCs seeded upon the washed bone undergo osteogenic differentiation, with significant increases in gene transcription levels of the osteogenic genes RUNX2, OPN and OC. In particular, BM-MSCs are able to undergo osteogenic differentiation in standard medium and independent of the osteoinductive corticosteroid dexamethasone, indicating the bone itself is osteoinductive, a crucial characteristic of a successful graft material.

iv) Taken together, though they are from *in vitro* studies, these results suggest that utilisation of the wash process would be beneficial for clinical use of human allograft bone, and that the washed acellular bone scaffold produced is suitable for direct clinical use as an allograft material.

6.1.2 Cell donor age and bone donor age are important factors which may determine the success of bone allograft applications

Having demonstrated the use of a novel wash process to produce a washed bone scaffold suitable for use in BTE, the study subsequently aimed to ascertain whether the age of cell or bone donor directly influenced the osteogenic differentiation of BM-MSCs seeded on the

washed bone scaffold. Clinically the majority of patients who receive bone allografts are elderly. This has ramifications in BTE when utilising autologous BM-MSCs, as with increasing patient age, the number and osteogenic ability of the BM-MSCs decreases. In addition, the majority of bone material is donated by elderly patients as they undergo primary hip replacements and, as with cells, there are known changes which occur in the bone structure with age which may influence cell behaviour.

The results of this particular section of the study indicate that:

i) Young donor cells are better able to undergo osteogenic differentiation when given the same cues as old donor cells, and importantly that old donor bone is better able to support this osteogenic activity. This has important implications for clinical use, as the data suggests that the current use of old donor bone may actually be beneficial to using young, but that elderly patients' cells may require additional osteogenic factors to promote and support their osteogenic activity.

Importantly, with increasing age, the number of BM-MSCs present in the bone marrow also decreases, and culture expansion to produce significant numbers may exacerbate loss of function. As such this study also utilised alternative sources of stem cells for population of the scaffold for BTE.

ii) The results of these experiments (detailed in Chapter 5), show that the washed bone is able to support the osteogenic differentiation of ASCs and BM-MNCs. In addition, the seeded BM-MNCs actively expressed the gene for the angiogenic factor VEGFα. Expression of VEGFα is important as angiogenesis is crucial in bone graft incorporation, and though this work is preliminary, it emphasises the need to understand the requirement for supportive cell types in BTE.

6.2 Future studies

This study yielded promising results for the production of a washed human biological bone scaffold from whole femoral heads (suitable for tissue engineering) using a novel wash process. It has successfully shown the osteoinductive ability of the washed bone scaffold and the osteogenic differentiation of stem cells seeded upon it, and in addition, added to the understanding of how age of cell or bone donor may influence the success of such BTE allografts in patients. As such, this study offers new avenues of research to progress the clinical application of the material and fully understand the potential of this type of bone scaffold in BTE.

To date, the data in this study has been obtained from *in vitro* experimentation, and as such there is a need to understand how this material will function *in vivo*, and how it will compare to allograft currently being used. Although the study has shown the washed bone to be biocompatible and osteoinductive, these promising results need to be assessed *in vivo* utilising appropriate animal models prior to clinical translation. These animal models may initially be undertaken in small animal studies, such as subcutaneous implantation into rats to assess biocompatibility and osteogenic potential, before developing into orthopaedic surgery models in larger mammals such as sheep or dogs. Of note, however, is the fact that a similar wash process (minus PPA and hydrogen peroxide) is already employed in the processing of deceased bone for use in surgery (Paul Rooney (NHSBT) – personal communication).

Additionally, preliminary experiments have indicated that this material can be used in conjunction with BM-MNCs, and that importantly this material invokes angiogenic gene expression. This angiogenic promotion is thought to be essential for bone osseointegration into the host without which grafts usually fail. Furthermore, the use of BM-MNCs removes

the requirement for expensive and time consuming *in vitro* expansion, and crucially, concentration techniques can be undertaken within the theatre at the time of surgery. There are a number of commercially available concentration techniques that work in an automated fashion to the methods used in this study, which are FDA approved for the production, and immediate use of, concentrated cell fractions from bone marrow. As such, the use of this source of osteogenic cells removes the regulations faced with isolated and culture expanded BM-MSCs, and may expedite the clinical translation of the washed bone allograft by withdrawing the need for animal studies. This could indicate a quick-to-use product; however the study presented here needs to be expanded to include more samples from a number of donors of varying ages, as well utilising additional experimental techniques to confirm findings.

This study has also identified age as an important factor dictating the osteoinductive capacity of the washed bone; however the basis for the difference seen between the two bone donor age groups was not studied and necessitates further investigation. Although this study indicated no mechanical difference between the young and old donor bone, the architecture is known to change with age which may have an impact on osteogenic activity. Therefore, structural imaging experiments such as µCT may be employed to determine factors such as surface area or porosity. Additionally, this study has indicated no statistic differences in mineral composition of the two age groups detected by XRD; however other biological constituents of the structure, most notably encapsulated BMPs and other growth factors (e.g IGF, TGFβ and BMP7), may change in concentration or accessibility with age. As such, further studies involving the enzymatic release of these encapsulated factors from the bone should be undertaken, with an assessment of bioavailability, identification, and total yield of growth factors. This could be achieved utilising proteolytic enzymes, such as collagenase, to breakdown the bone type I collagen structure, utilising Luminex multiplexed ELISAs

(enzyme-linked immunosorbent assay) to screen a broad panel of bioactive (growth) factors encapsulated in the structure (total content), and quantifying the presence specific growth factors (e.g. BMP2 and 7) in the lysate using ELISA at specified time points, thereby assessing rate of release of the encapsulated factors. Importantly, such experiments may provide important information on the bioavailability of osteogenic growth factors encapsulated in bone and whether this changes with age.

Additionally, the preliminary data has also shown that the washed bone scaffold is able to support ASCs, and that in comparison to patient-matched BM-MSCs, they displayed increased osteogenic differentiation. Importantly, ASCs are not thought to be affected by age as dramatically as BM-MSC, and could be a useful cell source alternative. Again, this requires further investigation to ascertain whether ASCs are indeed a suitable cell source, and whether cell donor age affects their differentiation potential and activity. The design of this study would closely follow that of experimentation undertaken in Chapter 4, instead utilising patient-matched ASCs and BM-MSCs.

Finally, although this study demonstrated the expression of both osteogenic and angiogenic genes by the seeded BM-MNCs, the relative concentration of BM-MSCs and supportive cell types it contained is unknown. As such, additional research should be undertaken to determine the relative concentration of different cell types present in the BM-MNC fraction. Using molecular biology techniques such as FACS (fluorescence-activated cell sorting) analysis, individual cell types could be identified and systematically removed, to investigate their biological activity in a BTE system. This would help isolate the crucial cell types and reduce the burden unnecessary cells would place on the limited nutrients available in the healing environment during graft incorporation.

Although this material has demonstrated good osteoinductive properties, there are still issues surrounding the use of this, and other, scaffolds in bone tissue engineering. The integration of the graft into the host is not only dependent on the ability to produce bone, but also its promotion of neovascularisation, essential if cells seeded further than 5mm into its surface are to survive and become active. The implantation of any graft is also commonly accompanied by a foreign body response by the host, which can cause severe inflammation of the area resulting in fibrous tissue enveloping the graft, further preventing blood vessel infiltration, and leading to the death of seeded stem cells. To prevent this activity, many current technologies aim at modulating the immune response of the host via the use of immunomodulatory growth factors while improving the infiltration of the vasculature network, and may be used in conjunction with this material in its eventual clinical use.

Additionally, the use of growth factors to promote the formation of new bone tissue and vascularisation is contentious, due to difficulties in localising the area they affect and using concentrations several times higher than naturally occurring, which may inadvertently affect surrounding tissue. This issue may also be overcome by improved culturing methods, and the use of *in vitro* bioreactors to culture the scaffold, seeded cells and specific growth factors, to establish cell growth and tissue maturation (including vessel formation) pre-implantation, potentially improving the integration of the graft. However, *in vitro* culture is an expensive process, and ultimately the most beneficial “bioreactor” bone healing environment is that of the host, though only if a beneficial environment can be assured. As such more efficient intraoperative cell seeding methods should be assessed, as well as technologies to control the *in vivo* environment. This may include the controlled release of growth factors into specific regions and at specific times and durations during the healing processes, by the use of tailored microparticles. In this study, the inclusion of a BM-MNC fraction to the bone scaffold promoted the expression of the angiogenic factor VEGFa by the seeded cells. The production

of VEGFa at a localised site by the cells may diminish the need for additional expensive growth factors and aid in the bone graft's integration. This improved integration may also negate the need for metal screw fixation to stabilise the graft after implantation. This crew fixation regularly results in complications relating to bending, breaking or metal-on-metal wear, which can lead to failure of the graft and revision surgery.

Also of importance is the practical clinical use of the bone material. Currently the majority of fresh-frozen bone allograft is morcellised into small fragments for use in IBG, this process is quick, but destroys much of the materials structure and mechanical stability and is an ineffective way at stabilising a structurally integral area of bone such as the acetabulum or the glenoid in the shoulder. In these cases large structural grafts are required. These structural grafts can be formed from whole femoral heads relatively easily, with the surgeon using images and moulds of the defect area to help fashion the right shape, which is implanted and stabilised with screws. The novel wash process used in this study produced whole washed femoral heads which may allow for use in both IBG, as well as the formation of structural graft. However, the formation of structural graft from the femoral head does require training, expertise and time, though from the authors own experience the removal of the cortical shell from the femoral head would allow for structures to be easily fashioned with use of a De Souter saw, and could be undertaken at the time of the wash process, in an attempt to later save the surgeon time and effort during surgery.

Chapter 7

References

2004/23/EC. Directive 2004/23/EC of the European parliament and of the council of 31 March 2004 on setting standards of quality and safety for the donation, procurement, testing, processing, preservation, storage and distribution of human tissues and cells. *Official Journal Eur Union,* 2004, 102, 48-58.

Akiyama H, Chaboissier MC, Martin JF, Schedl A, & de Crombrugghe B. The transcription factor Sox9 has essential roles in successive steps of the chondrocyte differentiation pathway and is required for expression of Sox5 and Sox6. *Genes Dev,* 2002, 16(21), 2813-2828.

Akiyama H, Lyons JP, Mori-Akiyama Y, Yang X, Zhang R, Zhang Z, Deng JM, Taketo MM, Nakamura T, Behringer RR, McCrea PD, & de Crombrugghe B. Interactions between Sox9 and beta-catenin control chondrocyte differentiation. *Genes Dev,* 2004, 18(9), 1072-1087.

Akkus O, Belaney RM, & Das P. Free radical scavenging alleviates the biomechanical impairment of gamma radiation sterilized bone tissue. *J Orthop Res,* 2005, 23(4), 838-845.

Albrektsson T, & Johansson C. Osteoinduction, osteoconduction and osseointegration. *Eur Spine J,* 2001, 10 (Suppl 2), 96-101.

Aleixo I, Vale A, Lúcio M, Amaral P, Rosa L, Caetano-Lopes J, Rodrigues A, Canhão H, Fonseca J, & Vaz MF. A method for the evaluation of femoral head trabecular bone compressive properties. *In:* Materials Science Forum, Trans Tech Publ, 2013, 3-8.

American Association of Tissue Banks. Standards for Tissue Banking 11th edition. Bethesda, MD, 2006.

Ammann P, & Rizzoli R. Bone strength and its determinants. *Osteoporos Int,* 2003, 14(Suppl 3), S13-18.

Anderson HC. Matrix vesicles and calcification. *Curr Rheumatol Rep,* 2003, 5(3)**,** 222-226.

Anderson JM, VinesJB, Patterson JL, Chen H, Javed A, & Jun HW. Osteogenic differentiation of human mesenchymal stem cells synergistically enhanced by biomimetic peptide amphiphiles combined with conditioned medium. *Acta Biomater,* 2011, 7(2)**,** 675-682.

Ang B, Tan Y, Ng Y, Ong S, Yap S, Gwee S, Chou SM, Poh C, & Yew K. The Effect of Specimen Geometry on the Mechanical Behavior of Trabecular Bone Specimens. *Solid State Phenomena,* 2012, 185**,** 129-132.

Aspenberg P, Johnsson E, & Thorngren KG. Dose-dependent reduction of bone inductive properties by ethylene oxide. *J Bone Joint Surg Br,* 1990, 72(6)**,** 1036-1037.

Ateschrang A, Ochs BG, Ludemann M, Weise K, & Albrecht D. Fibula and tibia fusion with cancellous allograft vitalised with autologous bone marrow: first results for infected tibial non-union. *Arch Orthop Trauma Surg,* 2009, 129(1)**,** 97-104.

Au A, Boehm CA, Mayes AM, Muschler GF, & Griffith LG. Formation of osteogenic colonies on well-defined adhesion peptides by freshly isolated human marrow cells. *Biomaterials,* 2007, 28(10)**,** 1847-1861.

Augello A, Kurth TB, & De Bari C. Mesenchymal stem cells: a perspective from *in vitro* cultures to *in vivo* migration and niches. *Eur Cell Mater,* 2010, 20**,** 121-133.

Auletta JJ, Zale EA, Welter JF, & Solchaga LA. Fibroblast Growth Factor-2 Enhances Expansion of Human Bone Marrow-Derived Mesenchymal Stromal Cells without Diminishing Their Immunosuppressive Potential. *Stem Cells Int,* 2011**,** Article ID 235176 doi: 10.4061/2011/235176.

Aust L, Devlin B, Foster SJ, Halvorsen YD, Hicok K, du Laney T, Sen A, Willingmyre GD, & Gimble JM. Yield of human adipose-derived adult stem cells from liposuction aspirates. *Cytotherapy,* 2004, 6(1)**,** 7-14.

Babiker H, Ding M, & Overgaard S. Demineralized bone matrix and human cancellous bone enhance fixation of porous-coated titanium implants in sheep. *J Tissue Eng Regen Med,* 2013, 24(10).

Babiker H, Ding M, Sandri M, Tampieri A, & Overgaard S. The effects of bone marrow aspirate, bone graft, and collagen composites on fixation of titanium implants. *J Biomed Mater Res B Appl Biomater,* 2012, 100(3)**,** 759-766.

Banfi A, Bianchi G, Notaro R, Luzzatto L, Cancedda R, & Quarto R. Replicative aging and gene expression in long-term cultures of human bone marrow stromal cells. *Tissue Eng,* 2002, 8(6)**,** 901-910.

Banse X, Delloye C, Cornu O, & Bourgois R. Comparative left-right mechanical testing of cancellous bone from normal femoral heads. *J Biomech,* 1996, 29(10)**,** 1247-1253.

Bao CLM, Teo EY, Chong MS, Liu Y, Choolani M & Chan JK. "Advances in bone tissue engineering." *Regenerative medicine and tissue engineering.* Rijeka: Intech, 2013, 599-614.

Barbanti Brodano G, Mazzoni E, Tognon M, Griffoni C, & Manfrini M. Human mesenchymal stem cells and biomaterials interaction: a promising synergy to improve spine fusion. *Eur Spine J,* 2012, 21(Suppl 1)**,** S3-9.

Bassi A, Gough J, & Downes S. A novel phosphonate for the repair of critical size bone defects. *J Tissue Eng Regen Med,* 2012, 6(10)**,** 833-840.

Baxter MA, Wynn RF, Jowitt SN, Wraith JE, Fairbairn LJ, & Bellantuono I. Study of telomere length reveals rapid aging of human marrow stromal cells following *in vitro* expansion. *Stem Cells,* 2004, 22(5)**,** 675-682.

Beebe KS, Benevenia J, Tuy BE, DePaula CA, Harten RD, & Enneking WF. Effects of a new allograft processing procedure on graft healing in a canine model: a preliminary study. *Clin Orthop Relat Res,* 2009, 467(1)**,** 273-280.

Bergmann G, Deuretzbacher G, Heller M, Graichen F, Rohlmann A, Strauss J, & Duda GN. Hip contact forces and gait patterns from routine activities. *J Biomech,* 2001, 34(7)**,** 859-871.

Berner A, Reichert JC, Muller MB, Zellner J, Pfeifer C, Dienstknecht T, Nerlich M, Sommerville S, Dickinson IC, Schutz MA, & Fuchtmeier B. Treatment of long bone defects and non-unions: from research to clinical practice. *Cell Tissue Res,* 2012, 347(3)**,** 501-519.

Bianco P. Minireview: The stem cell next door: skeletal and hematopoietic stem cell "niches" in bone. *Endocrinology,* 2011, 152(8)**,** 2957-2962.

Bilezikian JP, Raisz LG, & Martin TJ. *Principles of Bone Biology: Two-Volume Set*: Academic Press, 2008.

Binulal NS, Deepthy M, Selvamurugan N, Shalumon KT, Suja S, Mony U, Jayakumar R, & Nair SV. Role of nanofibrous poly(caprolactone) scaffolds in human mesenchymal stem cell attachment and spreading for *in vitro* bone tissue engineering--response to osteogenic regulators. *Tissue Eng Part A*, 2012, 16(2)**,** 393-404.

Board T, Mann J, Rooney P, Eagle M, Hogg P, Kay P, & Kearney J. P62 Processing of Whole Femoral Head Allografts: Efficacy and Biological Compatability of a New Procesing Technique. *Transfusion Medicine*, 2006a, 16(s1)**,** 51-51.

Board TN, Brunskill S, Doree C, Hyde C, Kay PR, Meek RD, Webster R, & Galea G. Processed versus fresh frozen bone for impaction bone grafting in revision hip arthroplasty. *Cochrane Database Syst Rev*, 2009, 7(4)**,** CD006351.

Board TN, Rooney P, Kearney JN, & Kay PR. Impaction allografting in revision total hip replacement. *J Bone Joint Surg Br*, 2006b, 88(7)**,** 852-857.

Boden SD. Overview of the biology of lumbar spine fusion and principles for selecting a bone graft substitute. *Spine (Phila Pa 1976)*, 2002, 27(16-Suppl 1)**,** S26-31.

Boden SD, Schimandle JH, & Hutton WC. An experimental lumbar intertransverse process spinal fusion model. Radiographic, histologic, and biomechanical healing characteristics. *Spine (Phila Pa 1976)*, 1995, 20(4)**,** 412-420.

Bolder SB, Schreurs BW, Verdonschot N, van Unen JM, Gardeniers JW, & Slooff TJ. Particle size of bone graft and method of impaction affect initial stability of cemented cups: human cadaveric and synthetic pelvic specimen studies. *Acta Orthop Scand*, 2003, 74(6)**,** 652-657.

Bolland BJ, Partridge K, Tilley S, New AM, Dunlop DG, & Oreffo RO. Biological and mechanical enhancement of impacted allograft seeded with human bone marrow stromal cells: potential clinical role in impaction bone grafting. *Regen Med*, 2006, 1(4)**,** 457-467.

Bonewald LF. The amazing osteocyte. *Journal of Bone and Mineral Research*, 2011, 26(2)**,** 229-238.

Bonsignore LA, Anderson JR, Lee Z, Goldberg VM, & Greenfield EM. Adherent lipopolysaccharide inhibits the osseointegration of orthopedic implants by impairing osteoblast differentiation. *Bone*, 2003, 52(1)**,** 93-101.

Boo JS, Yamada Y, Okazaki Y, Hibino Y, Okada K, Hata K, Yoshikawa T, Sugiura Y, & Ueda M. Tissue-engineered bone using mesenchymal stem cells and a biodegradable scaffold. *J Craniofac Surg*, 2002, 13(2)**,** 231-239.

Bormann N, Pruss A,Schmidmaier G, & Wildemann B. *In vitro* testing of the osteoinductive potential of different bony allograft preparations. *Arch Orthop Trauma Surg*, 2010, 130(1)**,** 143-149.

Borrelli J, Prickett WD, & Ricci WM. Treatment of nonunions and osseous defects with bone graft and calcium sulfate. *Clin Orthop Relat Res*, 2003, June(411)**,** 245-254.

Bos GD, Goldberg VM, Zika JM, Heiple KG, & Powell AE. Immune responses of rats to frozen bone allografts. *J Bone Joint Surg Am*, 1983, 65(2)**,** 239-246.

Boskey A. Bone mineral crystal size. *Osteoporos Int*, 2003, 14(Suppl 5)**,** S16-21.

Bostrom MP, & Seigerman DA. The clinical use of allografts, demineralized bone matrices, synthetic bone graft substitutes and osteoinductive growth factors: a survey study. *HSS J*, 2005, 1(1)**,** 9-18.

Boyle WJ, Simonet WS, & Lacey DL. Osteoclast differentiation and activation. *Nature,* 2003, 423(6937)**,** 337-342.

Brighton CT, & Albelda SM. Identification of integrin cell-substratum adhesion receptors on cultured rat bone cells. *J Orthop Res,* 1992, 10(6)**,** 766-773.

Brighton CT, & Hunt RM. Early histological and ultrastructural changes in medullary fracture callus. *J Bone Joint Surg Am,* 1991, 73(6)**,** 832-847.

Brodke D, Pedrozo HA, Kapur TA, Attawia M, Kraus KH, Holy CE, Kadiyala S, & Bruder SP. Bone grafts prepared with selective cell retention technology heal canine segmental defects as effectively as autograft. *J Orthop Res,* 2006, 24(5)**,** 857-866.

Brown JP, Delmas PD, Malaval L, Edouard C, Chapuy MC, & Meunier PJ. Serum bone Gla-protein: a specific marker for bone formation in postmenopausal osteoporosis. *Lancet,* 1984, 1(8386)**,** 1091-1093.

Brown TD, & Ferguson AB, Jr. The effects of hip contact aberrations on stress patterns within the human femoral head. *Ann Biomed Eng,* 1980, 8(1)**,** 75-92.

Brown TD, & Shaw DT. *In vitro* contact stress distributions in the natural human hip. *J Biomech,* 1983, 16(6)**,** 373-384.

Buckwalter JA, Glimcher MJ, Cooper RR, & Recker R. Bone biology. I: Structure, blood supply, cells, matrix, and mineralization. *Instr Course Lect,* 1996a, 45**,** 371-386.

Buckwalter JA, Glimcher MJ, Cooper RR, & Recker R. Bone biology. II: Formation, form, modeling, remodeling, and regulation of cell function. *Instr Course Lect,* 1996b, 45**,** 387-399.

Burchardt H, & Enneking WF. Transplantation of bone. *Surg Clin North Am,* 1978, 58(2)**,** 403-427.

Burdick JA, & Anseth KS. Photoencapsulation of osteoblasts in injectable RGD-modified PEG hydrogels for bone tissue engineering. *Biomaterials,* 2002, 23(22)**,** 4315-4323.

Burwell RG. Studies of the primary and the secondary immune responses of lymph nodes draining homografts of fresh cancellous bone (with particular reference to mechanisms of lymph node reactivity). *Ann N Y Acad Sci,* 1962, 99**,** 821-860.

Burwell RG. The function of bone marrow in the incorporation of a bone graft. *Clin Orthop Relat Res,* 1985, Nov(200)**,** 125-141.

Buttaro MA, Costantini J, Comba F, & Piccaluga F. The use of femoral struts and impacted cancellous bone allograft in patients with severe femoral bone loss who undergo revision total hip replacement: a three- to nine-year follow-up. *J Bone Joint Surg Br,* 2012, 94(2)**,** 167-172.

Carlson ME, & Conboy IM. Loss of stem cell regenerative capacity within aged niches. *Aging Cell,* 2007, 6(3)**,** 371-382.

Castillo Diaz LA, Saiani A, Gough JE, & Miller AF. Human osteoblasts within soft peptide hydrogels promote mineralisation *in vitro*. *Journal of Tissue Engineering,* 2014, 5, doi: 10.1177/2041731414539344.

Catone GA, Reimer BL, McNeir D, & Ray R. Tibial autogenous cancellous bone as an alternative donor site in maxillofacial surgery: a preliminary report. *J Oral Maxillofac Surg,* 1992, 50(12)**,** 1258-1263.

Chalmers J. Transplantation immunity in bone homografting. *J Bone Joint Surg Br,* 1959, 41-B(1)**,** 160-179.

Chatterjea A, Renard AJ, Jolink C, van Blitterswijk CA, & de Boer J. Streamlining the generation of an osteogenic graft by 3D culture of unprocessed bone marrow on ceramic scaffolds. *J Tissue Eng Regen Med,* 2012, 6(2)**,** 103-112.

Chaudhary LR, Hofmeister AM, & Hruska KA. Differential growth factor control of bone formation through osteoprogenitor differentiation. *Bone,* 2004, 34(3)**,** 402-411.

Chen G, Deng C, & Li YP. TGF-beta and BMP signaling in osteoblast differentiation and bone formation. *Int J Biol Sci,* 2012a, 8(2)**,** 272-288.

Chen H, Shoumura S, Emura S, & Bunai Y. Regional variations of vertebral trabecular bone microstructure with age and gender. *Osteoporos Int,* 2008, 19(10)**,** 1473-1483.

Chen H, Zhou X, Shoumura S, Emura S, & Bunai Y. Age- and gender-dependent changes in three-dimensional microstructure of cortical and trabecular bone at the human femoral neck. *Osteoporos Int,* 2010, 21(4)**,** 627-636.

Chen HT, Lee MJ, Chen CH, Chuang SC, Chang LF, Ho ML, Hung SH, Fu YC, Wang YH, Wang HI, Wang GJ, Kang L, & Chang JK. Proliferation and differentiation potential of human adipose-derived mesenchymal stem cells isolated from elderly patients with osteoporotic fractures. *J Cell Mol Med,* 2012b, 16(3)**,** 582-593.

Chen L, Jacquet R, Lowder E, & Landis WJ. Refinement of collagen-mineral interaction: A possible role for osteocalcin in apatite crystal nucleation, growth and development. *Bone,* 2015, 71, 7-16.

Chen PY, & McKittrick J. Compressive mechanical properties of demineralized and deproteinized cancellous bone. *J Mech Behav Biomed Mater,* 2011, 4(7)**,** 961-973.

Chenu C, Colucci S, Grano M, Zigrino P, Barattolo R, Zambonin G, Baldini N, Vergnaud P, Delmas PD, & Zallone AZ. Osteocalcin induces chemotaxis, secretion of matrix proteins, and calcium-mediated intracellular signaling in human osteoclast-like cells. *J Cell Biol,* 1994, 127(4)**,** 1149-1158.

Choi JS, Kim BS, Kim JY, Kim JD, Choi YC, Yang HJ, Park K, Lee HY, & Cho YW. Decellularized extracellular matrix derived from human adipose tissue as a potential scaffold for allograft tissue engineering. *J Biomed Mater Res A,* 2011, 97(3)**,** 292-299.

Chou L, Marek B, & Wagner WR. Effects of hydroxylapatite coating crystallinity on biosolubility, cell attachment efficiency and proliferation *in vitro*. *Biomaterials,* 1991, 20(10)**,** 977-985.

Clough BH, McCarley MR, Krause U, Zeitouni S, Froese JJ, McNeill EP, Chaput CD, Sampson HW, & Gregory CA. Bone Regeneration with Osteogenically Enhanced Mesenchymal Stem Cells and Their Extracellular Matrix Proteins. *J Bone Miner Res,* 2014, doi: 10.1002/jmbr.2320.

Coquelin L, Fialaire-Legendre A, Roux S, Poignard A, Bierling P, Hernigou P, Chevallier N, & Rouard H. *In vivo* and *in vitro* comparison of three different allografts vitalized with human mesenchymal stromal cells. *Tissue Eng Part A,* 2012, 18(17-18)**,** 1921-1931.

Cornejo A, Sahar DE, Stephenson SM, Chang S, Nguyen S, Guda T, Wenke JC, Vasquez A, Michalek JE, Sharma R, Krishnegowda NK, & Wang, H. T. Effect of adipose tissue-derived osteogenic and endothelial cells on bone allograft osteogenesis and vascularization in critical-sized calvarial defects. *Tissue Eng Part A*, 2012, 18(15-16)**,** 1552-1561.

Cornu O, Banse X, Docquier PL, Luyckx S, & Delloye C. Effect of freeze-drying and gamma irradiation on the mechanical properties of human cancellous bone. *J Orthop Res*, 2000, 18(3)**,** 426-431.

Costain DJ, & Crawford RW. Fresh-frozen vs. irradiated allograft bone in orthopaedic reconstructive surgery. *Injury*, 2009, 40(12)**,** 1260-1264.

Cox G, McGonagle D, Boxall SA, Buckley CT, Jones E, & Giannoudis PV. The use of the reamer-irrigator-aspirator to harvest mesenchymal stem cells. *J Bone Joint Surg Br*, 2011, 93(4)**,** 517-524.

Crapo PM, Gilbert TW, & Badylak SF. An overview of tissue and whole organ decellularization processes. *Biomaterials*, 2011, 32(12)**,** 3233-3243.

Cuomo AV, Virk M, Petrigliano F, Morgan EF, & Lieberman JR. Mesenchymal stem cell concentration and bone repair: potential pitfalls from bench to bedside. *J Bone Joint Surg Am*, 2009, 91(5)**,** 1073-1083.

Currey J. The structure and mechanics of bone. *Journal of Materials Science*, 2012, 47(1)**,** 41-54.

Currey JD. The adaptation of bones to stress. *J Theor Biol*, 1968, 20(1)**,** 91-106.

Currey JD. The effect of porosity and mineral content on the Young's modulus of elasticity of compact bone. *J Biomech*, 1988, 21(2)**,** 131-139.

Currey JD. *Bones: structure and mechanics*: Princeton University Press. 2002.

Currey JD, Foreman J, Laketic I, Mitchell J, Pegg DE, & Reilly GC. Effects of ionizing radiation on the mechanical properties of human bone. *J Orthop Res*, 1997, 15(1)**,** 111-117.

Czitrom AA, Axelrod T, & Fernandes B. Antigen presenting cells and bone allotransplantation. *Clin Orthop Relat Res*, 1985, (197)**,** 27-31.

Damien CJ, & Parsons JR. Bone graft and bone graft substitutes: a review of current technology and applications. *J Appl Biomater*, 1991, 2(3)**,** 187-208.

Davies E, Muller KH, Wong WC, Pickard CJ, Reid DG, Skepper JN, & Duer MJ. Citrate bridges between mineral platelets in bone. *Proc Natl Acad Sci U S A*, 2014, 111(14)**,** E1354-1363.

Davis BL, & Praveen SS. Nonlinear versus linear behavior of calcaneal bone marrow at different shear rates. *American Society of Biomechanics Annual Meeting, Blacksburg, VA. 2006.*

Day TF, Guo X, Garrett-Beal L, & Yang Y. Wnt/beta-catenin signaling in mesenchymal progenitors controls osteoblast and chondrocyte differentiation during vertebrate skeletogenesis. *Dev Cell*, 2005, 8(5)**,** 739-750.

De Long WG, Einhorn TA, Koval K, McKee M, Smith W, Sanders R, & Watson T. Bone grafts and bone graft substitutes in orthopaedic trauma surgery. A critical analysis. *J Bone Joint Surg Am*, 2007, 89(3)**,** 649-658.

De Ugarte DA, Morizono K, Elbarbary A, Alfonso Z, Zuk PA, Zhu M, Dragoo JL, Ashjian P, Thomas B, Benhaim P, Chen I, Fraser J, & Hedrick MH. Comparison of multi-lineage cells from human adipose tissue and bone marrow. *Cells Tissues Organs,* 2003, 174(3)**,** 101-109.

Deakin DE, & Bannister GC. Graft incorporation after acetabular and femoral impaction grafting with washed irradiated allograft and autologous marrow. *J Arthroplasty,* 2007, 22(1)**,** 89-94.

Declercq HA, De Caluwe T, Krysko O, Bachert C, & Cornelissen MJ. Bone grafts engineered from human adipose-derived stem cells in dynamic 3D-environments. *Biomaterials,* 2013, 34(4)**,** 1004-1017.

Deirmengian GK, Zmistowski B, O'Neil JT, & Hozack WJ. Management of acetabular bone loss in revision total hip arthroplasty. *J Bone Joint Surg Am,* 2011, 93(19)**,** 1842-1852.

Deligianni DD, Katsala ND, Koutsoukos PG, & Missirlis YF. Effect of surface roughness of hydroxyapatite on human bone marrow cell adhesion, proliferation, differentiation and detachment strength. *Biomaterials,* 2001, 22(1)**,** 87-96.

Delloye C, Cornu O, Druez V, & Barbier O. Bone allografts: What they can offer and what they cannot. *J Bone Joint Surg Br,* 2007, 89(5)**,** 574-579.

Delloye C, van Cauter M, Dufrane D, Francq BG, Docquier PL, & Cornu O. Local complications of massive bone allografts: an appraisal of their prevalence in 128 patients. *Acta Orthop Belg,* 2014, 80(2)**,** 196-204.

DePaula CA, Truncale KG, Gertzman AA, Sunwoo MH, & Dunn MG. Effects of hydrogen peroxide cleaning procedures on bone graft osteoinductivity and mechanical properties. *Cell Tissue Bank,* 2005, 6(4)**,** 287-298.

Desai HV, Voruganti IS, Jayasuriya C, Chen Q, & Darling EM. Live-cell, temporal gene expression analysis of osteogenic differentiation in adipose-derived stem cells. *Tissue Eng Part A,* 2013, 19(1-2)**,** 40-48.

Di Bella C, Aldini NN, Lucarelli E, Dozza B, Frisoni T, Martini L, Fini M, & Donati D. Osteogenic protein-1 associated with mesenchymal stem cells promote bone allograft integration. *Tissue Eng Part A,* 2010a, 16(9)**,** 2967-2976.

Di Bella C, Dozza B, Frisoni T, Cevolani L, & Donati D. Injection of demineralized bone matrix with bone marrow concentrate improves healing in unicameral bone cyst. *Clin Orthop Relat Res,* 2010b, 468(11)**,** 3047-3055.

Di Nardo P, & Parker GC. Stem cell standardization. *Stem Cells Dev,* 2011, 20(3)**,** 375-377.

Dominici M, Le Blanc K, Mueller I, Slaper-Cortenbach I, Marini F, Krause D, Deans R, Keating A, Prockop D, & Horwitz E. Minimal criteria for defining multipotent mesenchymal stromal cells. The International Society for Cellular Therapy position statement. *Cytotherapy,* 2006, 8(4)**,** 315-317.

Donati D, Di Liddo M, Zavatta M, Manfrini M, Bacci G, Picci P, Capanna R, & Mercuri M. Massive bone allograft reconstruction in high-grade osteosarcoma. *Clin Orthop Relat Res,* 2000, (377)**,** 186-194.

Donati D, Zolezzi C, Tomba P, & Vigano A. Bone grafting: historical and conceptual review, starting with an old manuscript by Vittorio Putti. *Acta Orthop,* 2007, 78(1)**,** 19-25.

Dorr LD, Ranawat CS, Sculco TA, McKaskill B, & Orisek BS. Bone graft for tibial defects in total knee arthroplasty. 1986. *Clin Orthop Relat Res,* 2006, 446**,** 4-9.

Ducy P, Desbois C, Boyce B, Pinero G, Story B, Dunstan C, Smith E, Bonadio J, Goldstein S, Gundberg C, Bradley A, & Karsenty G. Increased bone formation in osteocalcin-deficient mice. *Nature,* 1996, 382(6590)**,** 448-452.

Ducy P, Zhang R, Geoffroy V, Ridall AL, & Karsenty G. Osf2/Cbfa1: a transcriptional activator of osteoblast differentiation. *Cell,* 1997, 89(5)**,** 747-754.

Dufrane D, Cornu O, Verraes T, Schecroun N, Banse X, Schneider YJ, & Delloye C. *In vitro* evaluation of acute cytotoxicity of human chemically treated allografts. *Eur Cell Mater,* 2001, 1**,** 52-58.

Dumas A, Gaudin-Audrain C, Mabilleau G, Massin P, Hubert L, Basle MF, & Chappard D. The influence of processes for the purification of human bone allografts on the matrix surface and cytocompatibility. *Biomaterials,* 2006, 27(23)**,** 4204-4211.

Dutra TF, & French SW. Marrow stromal fibroblastic cell cultivation *in vitro* on decellularized bone marrow extracellular matrix. *Exp Mol Pathol,* 2010, 88(1)**,** 58-66.

Dux SJ, Ramsey D, Chu EH, Rimnac CM, & Hernandez CJ. Alterations in damage processes in dense cancellous bone following gamma-radiation sterilization. *J Biomech,* 2010, 43(8)**,** 1509-1513.

Dziedzic-Goclawska A, Kaminski A, Uhrynowska-Tyszkiewicz I, & Stachowicz W. Irradiation as a safety procedure in tissue banking. *Cell Tissue Bank,* 2005, 6(3)**,** 201-219.

Ebraheim NA, Elgafy H, & Xu R. Bone-graft harvesting from iliac and fibular donor sites: techniques and complications. *J Am Acad Orthop Surg,* 201, 9(3)**,** 210-218.

Einhorn TA. The cell and molecular biology of fracture healing. *Clin Orthop Relat Res,* 1998, 355 (Suppl)**,** S7-21.

Einhorn TA & Gerstenfeld LC. Fracture healing: mechanisms and inteventions. *Nat Rev Rheomatol,* 2015, 11(1), 45-54.

Erickson IE, van Veen SC, Sengupta S, Kestle SR, & Mauck RL. Cartilage matrix formation by bovine mesenchymal stem cells in three-dimensional culture is age-dependent. *Clin Orthop Relat Res,* 2011, 469(10)**,** 2744-2753.

Ern C, Krump-Konvalinkova V, Docheva D, Schindler S, Rossmann O, Bocker W, Mutschler W, & Schieker M. Interactions of human endothelial and multipotent mesenchymal stem cells in cocultures. *Open Biomed Eng J,* 2010, 4**,** 190-198.

Eswarakumar VP, Monsonego-Ornan E, Pines M, Antonopoulou I, Morriss-Kay GM, & Lonai P. The IIIc alternative of Fgfr2 is a positive regulator of bone formation. *Development,* 2002, 129(16)**,** 3783-3793.

Evans ND, Gentleman E, Chen X, Roberts CJ, Polak JM, & Stevens MM. Extracellular matrix-mediated osteogenic differentiation of murine embryonic stem cells. *Biomaterials,* 2010, 31(12)**,** 3244-3252.

Fan J, Park H, Lee MK, Bezouglaia O, Fartash A, Kim J, Aghaloo T, & Lee M. Adipose-Derived Stem Cells and BMP-2 Delivery in Chitosan-Based 3D Constructs to Enhance Bone Regeneration in a Rat Mandibular Defect Model. *Tissue Eng Part A,* 2014, 20(15-16)**,** 2169-2179.

Fawzi-Grancher S, Goebbels RM, Bigare E, Cornu O, Gianello P, Delloye C, & Dufrane D. Human tissue allograft processing: impact on *in vitro* and *in vivo* biocompatibility. *J Mater Sci Mater Med,* 2009, 20(8)**,** 1709-1720.

Fazzalari NL, & Parkinson IH. Femoral trabecular bone of osteoarthritic and normal subjects in an age and sex matched group. *Osteoarthritis Cartilage,* 1998, 6(6)**,** 377-382.

Fedarko NS, Vetter UK, Weinstein S, & Robey PG. Age-related changes in hyaluronan, proteoglycan, collagen, and osteonectin synthesis by human bone cells. *J Cell Physiol,* 1992, 151(2)**,** 215-227.

Feng W, Fu L, Liu J, & Li D. The expression and distribution of xenogeneic targeted antigens on porcine bone tissue. *Transplant Proc,* 2012, 44(5)**,** 1419-1422.

Fiedler J, Leucht F, Waltenberger J, Dehio C, & Brenner RE. VEGF-A and PlGF-1 stimulate chemotactic migration of human mesenchymal progenitor cells. *Biochem Biophys Res Commun,* 2005, 334(2)**,** 561-568.

Foschi F, Conserva E, Pera P, Canciani B, Cancedda R, & Mastrogiacomo M. Graft materials and bone marrow stromal cells in bone tissue engineering. *J Biomater Appl,* 2012, 26(8)**,** 1035-1049.

Friedenstein, A. J., Chailakhyan, R. K. & Gerasimov, U. V. (1987). Bone marrow osteogenic stem cells: *in vitro* cultivation and transplantation in diffusion chambers. *Cell Tissue Kinet,* 20(3)**,** 263-272.

Friedenstein AJ, Piatetzky S, & Petrakova KV. Osteogenesis in transplants of bone marrow cells. *J Embryol Exp Morphol,* 1966, 16(3)**,** 381-390.

Frith JE, Mills RJ, Hudson JE, & Cooper-White JJ. Tailored integrin-extracellular matrix interactions to direct human mesenchymal stem cell differentiation. *Stem Cells Dev,* 2012, 21(13)**,** 2442-2456.

Frith JE, Thomson B, & Genever PG. Dynamic three-dimensional culture methods enhance mesenchymal stem cell properties and increase therapeutic potential. *Tissue Eng Part C Methods,* 2010, 16(4)**,** 735-749.

Frost HM. Wolff's Law and bone's structural adaptations to mechanical usage: an overview for clinicians. *Angle Orthod,* 1994, 64(3)**,** 175-188.

Gangji V, De Maertelaer V, & Hauzeur JP. Autologous bone marrow cell implantation in the treatment of non-traumatic osteonecrosis of the femoral head: Five year follow-up of a prospective controlled study. *Bone,* 2011, 49(5)**,** 1005-1009.

Gao C, Seuntjens J, Kaufman GN, Tran-Khanh N, Butler A, Li A, Wang H, Buschmann MD, Harvey EJ, & Henderson JE. Mesenchymal stem cell transplantation to promote bone healing. *J Orthop Res,* 2012, 30(8)**,** 1183-1189.

Giannoudis PV, Einhorn TA, & Marsh D. Fracture healing: the diamond concept. *Injury,* 2007, 38(Suppl 4)**,** S3-6.

Ginis I, Weinreb M, Abramov N, Shinar D, Merchav S, Schwartz A, & Shirvan M. Bone progenitors produced by direct osteogenic differentiation of the unprocessed bone marrow demonstrate high osteogenic potential *in vitro* and *in vivo*. *Biores Open Access,* 2012, 1(2)**,** 69-78.

Gordon JA, Hunter GK, & Goldberg HA. Activation of the mitogen-activated protein kinase pathway by bone sialoprotein regulates osteoblast differentiation. *Cells Tissues Organs,* 2009, 189(1-4)**,** 138-143.

Green JO, Nagaraja S, Diab T, Vidakovic B, & Guldberg RE. Age-related changes in human trabecular bone: Relationship between microstructural stress and strain and damage morphology. *J Biomech,* 2011, 44(12)**,** 2279-2285.

Gronthos S, Franklin DM, Leddy HA, Robey PG, Storms RW, & Gimble JM. Surface protein characterization of human adipose tissue-derived stromal cells. *J Cell Physiol,* 2001, 189(1)**,** 54-63.

Gupta A, Leong DT, Bai HF, Singh SB, Lim TC, & Hutmacher DW. Osteo-maturation of adipose-derived stem cells required the combined action of vitamin D3, beta-glycerophosphate, and ascorbic acid. *Biochem Biophys Res Commun,* 2007, 362(1)**,** 17-24.

Gurkan UA, & Akkus O. The mechanical environment of bone marrow: a review. *Ann Biomed Eng,* 2008, 36(12)**,** 1978-1991.

Haimi S, Suuriniemi N, Haaparanta AM, Ella V, Lindroos B, Huhtala H, Raty S, Kuokkanen H, Sandor GK, Kellomaki M, Miettinen S, & Suuronen R. Growth and osteogenic differentiation of adipose stem cells on PLA/bioactive glass and PLA/beta-TCP scaffolds. *Tissue Eng Part A,* 2009, 15(7)**,** 1473-1480.

Haimi S, Vienonen A, Hirn M, Pelto M, Virtanen V, & Suuronen R. The effect of chemical cleansing procedures combined with peracetic acid-ethanol sterilization on biomechanical properties of cortical bone. *Biologicals,* 2008, 36(2)**,** 99-104.

Halgrin J, Chaari F, & Markiewicz E. On the effect of marrow in the mechanical behavior and crush response of trabecular bone. *J Mech Behav Biomed Mater,* 2012, 5(1)**,** 231-237.

Hamer AJ, Stockley I, & Elson RA. Changes in allograft bone irradiated at different temperatures. *J Bone Joint Surg Br,* 1999, 81(2)**,** 342-344.

Hamer AJ, Strachan JR, Black MM, Ibbotson CJ, Stockley I, & Elson RA. Biochemical properties of cortical allograft bone using a new method of bone strength measurement. A comparison of fresh, fresh-frozen and irradiated bone. *J Bone Joint Surg Br,* 1996, 78(3)**,** 363-368.

Hammoudi TM, Rivet CA, Kemp ML, Lu H, & Temenoff JS. Three-dimensional *in vitro* tri-culture platform to investigate effects of crosstalk between mesenchymal stem cells, osteoblasts, and adipocytes. *Tissue Eng Part A,* 2012, 18(15-16)**,** 1686-1697.

Handschin RG, & Stern WB. Crystallographic and chemical analysis of human bone apatite (Crista Iliaca). *Clin Rheumatol,* 1994, 13(Suppl 1)**,** 75-90.

Hart R, Komzak M, Okal F, Nahlik D, Jajtner P, & Puskeiler M. Allograft alone versus allograft with bone marrow concentrate for the healing of the instrumented posterolateral lumbar fusion. *Spine J,* 2014, 14(7)**,** 1318-1324.

Hashimoto Y, Funamoto S, Kimura T, Nam K, Fujisato T, & Kishida A. The effect of decellularized bone/bone marrow produced by high-hydrostatic pressurization on the osteogenic differentiation of mesenchymal stem cells. *Biomaterials,* 2011, 32(29)**,** 7060-7067.

Hassaballa M, Mehendale S, Poniatowski S, Kalantzis G, Smith E, & Learmonth ID. Subsidence of the stem after impaction bone grafting for revision hip replacement using irradiated bone. *J Bone Joint Surg Br,* 2009, 91(1)**,** 37-43.

Hattori H, Sato M, Masuoka K, Ishihara M, Kikuchi T, Matsui T, Takase B, Ishizuka T, Kikuchi M, Fujikawa K, & Ishihara M. Osteogenic potential of human adipose tissue-derived stromal cells as an alternative stem cell source. *Cells Tissues Organs,* 2004, 178(1)**,** 2-12.

Haudenschild AK, Hsieh AH, Kapila S, & Lotz JC. Pressure and distortion regulate human mesenchymal stem cell gene expression. *Ann Biomed Eng,* 2009, 37(3)**,** 492-502.

Hauschka PV, Lian JB, Cole DE, & Gundberg CM. Osteocalcin and matrix Gla protein: vitamin K-dependent proteins in bone. *Physiol Rev,* 1989, 69(3)**,** 990-1047.

Hayes WC, Swenson LW, & Schurman DJ. Axisymmetric finite element analysis of the lateral tibial plateau. *J Biomech,* 1978, 11(1-2)**,** 21-33.

Haykal S, Salna M, Zhou Y, Marcus P, Fatehi M, Frost G, Machuca T, Hofer SO, & Waddell TK. Double-chamber rotating bioreactor for dynamic perfusion cell seeding of large-segment tracheal allografts: comparison to conventional static methods. *Tissue Eng Part C Methods,* 2014, 20(8)**,** 681-692.

Hegde V, Shonuga O, Ellis S, Fragomen A, Kennedy J, Kudryashov V, & Lane JM. A prospective comparison of 3 approved systems for autologous bone marrow concentration demonstrated nonequivalency in progenitor cell number and concentration. *J Orthop Trauma,* 2014, 28(10)**,** 591-598.

Henthorn PS, & Whyte MP. Missense mutations of the tissue-nonspecific alkaline phosphatase gene in hypophosphatasia. *Clin Chem,* 1992, 38(12)**,** 2501-2505.

Hermann PC, Huber SL, Herrler T, von Hesler C, Andrassy J, Kevy SV, Jacobson MS, & Heeschen C. Concentration of bone marrow total nucleated cells by a point-of-care device provides a high yield and preserves their functional activity. *Cell Transplant,* 2008, 16(10)**,** 1059-1069.

Hernigou P, Pariat J, Queinnec S, Homma Y, Lachaniette CH, Chevallier N, & Rouard H. Supercharging irradiated allografts with mesenchymal stem cells improves acetabular bone grafting in revision arthroplasty. *Int Orthop,* 2014, 38(9)**,** 1913-1921.

Hernigou P, Poignard A, Beaujean F, & Rouard H. Percutaneous autologous bone-marrow grafting for nonunions. Influence of the number and concentration of progenitor cells. *J Bone Joint Surg Am,* 2005, 87(7)**,** 1430-1437.

Hessle L, Johnson KA, Anderson HC, Narisawa S, Sali A, Goding JW, Terkeltaub R, & Millan JL. Tissue-nonspecific alkaline phosphatase and plasma cell membrane glycoprotein-1 are central antagonistic regulators of bone mineralization. *Proc Natl Acad Sci U S A,* 2002, 99(14)**,** 9445-9449.

Heyligers IC, & Klein-Nulend J. Detection of living cells in non-processed but deep-frozen bone allografts. *Cell Tissue Bank,* 2005, 6(1)**,** 25-31.

Hibi H, Yamada Y, Ueda M, & Endo Y. Alveolar cleft osteoplasty using tissue-engineered osteogenic material. *Int J Oral Maxillofac Surg,* 2006, 35(6)**,** 551-555.

Hidalgo-Bastida LA, & Cartmell SH. Mesenchymal stem cells, osteoblasts and extracellular matrix proteins: enhancing cell adhesion and differentiation for bone tissue engineering. *Tissue Eng Part B Rev,* 2010, 16(4)**,** 405-412.

Hildebrand T, Laib A, Muller R, Dequeker J, & Ruegsegger P. Direct three-dimensional morphometric analysis of human cancellous bone: microstructural data from spine, femur, iliac crest, and calcaneus. *J Bone Miner Res,* 1999, 14(7)**,** 1167-1174.

Hill NM, Horne JG, & Devane PA. Donor site morbidity in the iliac crest bone graft. *Aust N Z J Surg,* 1999, 69(10)**,** 726-728.

Hill TP, Spater D, Taketo MM, Birchmeier W, & Hartmann C. Canonical Wnt/beta-catenin signaling prevents osteoblasts from differentiating into chondrocytes. *Dev Cell,* 2005, 8(5)**,** 727-738.

Hoang QQ, Sicheri F, Howard AJ, & Yang DS. Bone recognition mechanism of porcine osteocalcin from crystal structure. *Nature,* 2003, 425(6961)**,** 977-980.

Holm E, Gleberzon JS, Liao Y, Sorensen ES, Beier F, Hunter GK, & Goldberg HA. Osteopontin mediates mineralization and not osteogenic cell development *in vitro*. *Biochem J,* 2014, doi10.1042/BJ20140702.

Homminga J, McCreadie BR, Ciarelli TE, Weinans H, Goldstein SA, & Huiskes R. Cancellous bone mechanical properties from normals and patients with hip fractures differ on the structure level, not on the bone hard tissue level. *Bone,* 2002, 30(5)**,** 759-764.

Hu H, Hilton MJ, Tu X, Yu K, Ornitz DM, & Long F. Sequential roles of Hedgehog and Wnt signaling in osteoblast development. *Development,* 2005, 132(1)**,** 49-60.

Hu J, Zhou Y, Huang L, Liu J, & Lu H. Effect of nano-hydroxyapatite coating on the osteoinductivity of porous biphasic calcium phosphate ceramics. *BMC Musculoskelet Disord,* 15(114)**,** 2014, 1471-1474.

Huang YC, Kaigler D, Rice KG, Krebsbach PH, & Mooney DJ. Combined angiogenic and osteogenic factor delivery enhances bone marrow stromal cell-driven bone regeneration. *J Bone Miner Res,* 2005, 20(5)**,** 848-857.

Huang YZ, Cai JQ, Xue J, Chen XH, Zhang CL, Li XQ, Yang ZM, Huang YC, & Deng L. The poor osteoinductive capability of human acellular bone matrix. *Int J Artif Organs,* 2012, 35(12)**,** 1061-1069.

Huang Z, Nelson ER, Smith RL, & Goodman SB. The sequential expression profiles of growth factors from osteoprogenitors [correction of osteroprogenitors] to osteoblasts *in vitro*. *Tissue Eng,* 2007, 13(9)**,** 2311-2320.

Hung BP, Salter EK, Temple J, Mundinger GS, Brown EN, Brazio P, Rodriguez ED, & Grayson WL. Engineering bone grafts with enhanced bone marrow and native scaffolds. *Cells Tissues Organs,* 2013, 198(2)**,** 87-98.

Hunter GK, Hauschka PV, Poole AR, Rosenberg LC, & Goldberg HA. Nucleation and inhibition of hydroxyapatite formation by mineralized tissue proteins. *Biochem J,* 1996, 317(Pt 1)**,** 59-64.

Hutmacher DW. Scaffolds in tissue engineering bone and cartilage. *Biomaterials,* 2000, 21(24)**,** 2529-2543.

Ibrahim T, Qureshi A, McQuillan TA, Thomson J, Galea G, & Power RA. Intra-operative washing of morcellised bone allograft with pulse lavage: how effective is it in reducing blood and marrow content? *Cell Tissue Bank,* 2012, 13(1)**,** 157-165.

Ijiri S, Yamamuro T, Nakamura T, Kotani S, & Notoya K. Effect of sterilization on bone morphogenetic protein. *J Orthop Res,* 1994, 12(5)**,** 628-636.

Ikeda T, Nagai Y, Yamaguchi A, Yokose S, & Yoshiki S. Age-related reduction in bone matrix protein mRNA expression in rat bone tissues: application of histomorphometry to in situ hybridization. *Bone,* 1995, 16(1)**,** 17-23.

Ingram RT, Park YK, Clarke BL, & Fitzpatrick LA. Age- and gender-related changes in the distribution of osteocalcin in the extracellular matrix of normal male and female bone. Possible involvement of osteocalcin in bone remodeling. *J Clin Invest,* 1994, 93(3)**,** 989-997.

Iorio R, Robb WJ, Healy WL, Berry DJ, Hozack WJ, Kyle RF, Lewallen DG, Trousdale RT, Jiranek WA, Stamos VP, & Parsley BS. Orthopaedic surgeon workforce and volume assessment for total hip and knee replacement in the United States: preparing for an epidemic. *J Bone Joint Surg Am,* 2008, 90(7)**,** 1598-1605.

ISO 10993-5. Biological evaluation od medical devices. Part 5: Test for cytotoxicity: *In vitro* methods. *International Organization for Standardization,* Geneva, 2009.

Jaiswal RK, Jaiswal N, Bruder SP, Mbalaviele G, Marshak DR, & Pittenger MF. Adult human mesenchymal stem cell differentiation to the osteogenic or adipogenic lineage is regulated by mitogen-activated protein kinase. *J Biol Chem,* 2000, 275(13)**,** 9645-9652.

Jeffery M, Scott G, & Freeman M. Failure of an uncemented non-porous metal-backed prosthesis with augmentation using impacted allograft for acetabular revision 12- to 17-year results. *J Bone Joint Surg Br,* 2003, 85(2)**,** 182-186.

Jergesen HE, Chua J, Kao RT, & Kaban LB. Age effects on bone induction by demineralized bone powder. *Clin Orthop Relat Res,* 1991, Jul(268)**,** 253-259.

Justesen J, Stenderup K, Ebbesen EN, Mosekilde L, Steiniche T, & Kassem M. Adipocyte tissue volume in bone marrow is increased with aging and in patients with osteoporosis. *Biogerontology,* 2001, 2(3)**,** 165-171.

Kalajzic I, Staal A, Yang WP, Wu Y, Johnson SE, Feyen JH, Krueger W, Maye P, Yu F, Zhao Y, Kuo L, Gupta RR, Achenie LE, Wang HW, Shin DG, & Rowe DW. Expression profile of osteoblast lineage at defined stages of differentiation. *J Biol Chem,* 2005, 280(26)**,** 24618-24626.

Kark LR, Karp JM, & Davies JE. Platelet releasate increases the proliferation and migration of bone marrow-derived cells cultured under osteogenic conditions. *Clin Oral Implants Res,* 2006, 17(3)**,** 321-327.

Kelly DJ, & Jacobs CR. The role of mechanical signals in regulating chondrogenesis and osteogenesis of mesenchymal stem cells. *Birth Defects Res C Embryo Today,* 2010, 90(1)**,** 75-85.

Kern S, Eichler H, Stoeve J, Kluter H, & Bieback K. Comparative analysis of mesenchymal stem cells from bone marrow, umbilical cord blood, or adipose tissue. *Stem Cells,* 2006, 24(5)**,** 1294-1301.

Kilian KA, Bugarija B, Lahn BT, & Mrksich M. Geometric cues for directing the differentiation of mesenchymal stem cells. *Proc Natl Acad Sci U S A,* 2010, 107(11)**,** 4872-2877.

Klees RF, Salasznyk RM, Vandenberg S, Bennett K, & Plopper GE. Laminin-5 activates extracellular matrix production and osteogenic gene focusing in human mesenchymal stem cells. *Matrix Biol,* 2007, 26(2)**,** 106-114.

Kloeters O, Berger I, Ryssel H, Megerle K, Leimer U, & Germann G. Revitalization of cortical bone allograft by application of vascularized scaffolds seeded with osteogenic induced adipose tissue derived stem cells in a rabbit model. *Arch Orthop Trauma Surg*, 2011, 131(10)**,** 1459-1466.

Kluger R, Bouhon W, Freudenberger H, Kroner A, Engel A, & Hoffmann O. Removal of the surface layers of human cortical bone allografts restores *in vitro* osteoclast function reduced by processing and frozen storage. *Bone*, 2003, 32(3)**,** 291-296.

Ko E, & Cho SW. Biomimetic polymer scaffolds to promote stem cell-mediated osteogenesis. *Int J Stem Cells*, 2013, 6(2)**,** 87-91.

Kojimoto H, Yasui N, Goto T, Matsuda S, & Shimomura Y. Bone lengthening in rabbits by callus distraction. The role of periosteum and endosteum. *J Bone Joint Surg Br*, 1988, 70(4)**,** 543-549.

Komori T. Regulation of skeletal development by the Runx family of transcription factors. *J Cell Biochem*, 2005, 95(3)**,** 445-453.

Komori T, Yagi H, Nomura S, Yamaguchi A, Sasaki K, Deguchi K, Shimizu Y, Bronson RT, Gao YH, Inada M, Sato M, Okamoto R, Kitamura Y, Yoshiki S, & Kishimoto T. Targeted disruption of Cbfa1 results in a complete lack of bone formation owing to maturational arrest of osteoblasts. *Cell*, 1997, 89(5)**,** 755-764.

Kong YY, Yoshida H, Sarosi I, Tan HL, Timms E, Capparelli C, Morony S, Oliveira-dos-Santos AJ, Van G, Itie A, Khoo W, Wakeham A, Dunstan CR, Lacey DL, Mak TW, Boyle WJ, & Penninger JM. OPGL is a key regulator of osteoclastogenesis, lymphocyte development and lymph-node organogenesis. *Nature*, 1999, 397(6717)**,** 315-323.

Krečič Stres H, Krkovič M, Koder J, Maličev E, Marolt D, Drobnic M, & Kregar-Velikonja N. (2007). Mesenchymal Stem Cells: a Modern Approach to Treat Long Bones Defects. *11th Mediterranean Conference on Medical and Biomedical Engineering and Computing 2007. IFMBA Proceedings*, 2007, 16, 253-256.

Kretlow JD, Spicer PP, Jansen JA, Vacanti CA, Kasper FK, & Mikos AG. Uncultured marrow mononuclear cells delivered within fibrin glue hydrogels to porous scaffolds enhance bone regeneration within critical-sized rat cranial defects. *Tissue Eng Part A*, 2010, 16(12)**,** 3555-3568.

Kurtz S, Ong K, Lau E, Mowat F, & Halpern M. Projections of primary and revision hip and knee arthroplasty in the United States from 2005 to 2030. *J Bone Joint Surg Am*, 207, 89(4)**,** 780-785.

Kwong LM, Jasty M, & Harris WH. High failure rate of bulk femoral head allografts in total hip acetabular reconstructions at 10 years. *J Arthroplasty*, 1993, 8(4)**,** 341-346.

Laitinen M, Kivikari R, & Hirn M. Lipid oxidation may reduce the quality of a fresh-frozen bone allograft. Is the approved storage temperature too high? *Acta Orthop*, 2006, 77(3)**,** 418-421.

Lansford TJ, Burton DC, Asher MA, & Lai SM. Radiographic and patient-based outcome analysis of different bone-grafting techniques in the surgical treatment of idiopathic scoliosis with a minimum 4-year follow-up: allograft versus autograft/allograft combination. *Spine J*, 2013, 13(5)**,** 523-529.

Laschober GT, Brunauer R, Jamnig A, Singh S, Hafen U, Fehrer C, Kloss F, Gassner R, & Lepperdinger G. Age-specific changes of mesenchymal stem cells are paralleled by upregulation of CD106 expression as a response to an inflammatory environment. *Rejuvenation Res,* 2011, 14(2)**,** 119-131.

Lee EJ, Song DH, Kim YJ, Choi B, Chung YH, Kim SM, Koh JM, Yoon SY, Song Y, Kang SW, & Chang EJ. PTX3 stimulates osteoclastogenesis by increasing osteoblast RANKL production. *J Cell Physiol,* 2014, 229(11)**,** 1744-1752.

Lee NK, Sowa H, Hinoi E, Ferron M, Ahn JD, Confavreux C, Dacquin R, Mee PJ, McKee MD, Jung DY, Zhang Z, Kim JK, Mauvais-Jarvis F, Ducy P, & Karsenty G. Endocrine Regulation of Energy Metabolism by the Skeleton. *Cell,* 2007, 130(3)**,** 456-469.

Li B, & Aspden RM. Composition and mechanical properties of cancellous bone from the femoral head of patients with osteoporosis or osteoarthritis. *J Bone Miner Res,* 1997, 12(4)**,** 641-651.

Li B, Liao X, Zheng L, Zhu X, Wang Z, Fan H, & Zhang X. Effect of nanostructure on osteoinduction of porous biphasic calcium phosphate ceramics. *Acta Biomater,* 2012a, 8(10)**,** 3794-3804.

Li X, Huang Y, Zheng L, Liu H, Niu X, Huang J, Zhao F, & Fan Y. Effect of substrate stiffness on the functions of rat bone marrow and adipose tissue derived mesenchymal stem cells *in vitro*. *J Biomed Mater Res A,* 2014, 102(4)**,** 1092-1101.

Li ZC, Dai LY, Jiang LS, & Qiu S. Difference in subchondral cancellous bone between postmenopausal women with hip osteoarthritis and osteoporotic fracture: implication for fatigue microdamage, bone microarchitecture, and biomechanical properties. *Arthritis Rheum,* 2012b, 64(12)**,** 3955-3962.

Livak KJ, & Schmittgen TD. Analysis of relative gene expression data using real-time quantitative PCR and the 2(-Delta Delta C(T) Method. *Methods,* 2001, 25(4)**,** 402-408.

Lo KW, Ashe KM, Kan HM, Lee DA, & Laurencin CT. Activation of cyclic amp/protein kinase: a signaling pathway enhances osteoblast cell adhesion on biomaterials for regenerative engineering. *J Orthop Res,* 2011, 29(4)**,** 602-608.

Lochmuller EM, Matsuura M, Bauer J, Hitzl W, Link TM, Muller R, & Eckstein F. Site-specific deterioration of trabecular bone architecture in men and women with advancing age. *J Bone Miner Res,* 2008, 23(12)**,** 1964-1973.

Lohmann CH, Andreacchio D, Koster G, Carnes DL, Cochran DL, Dean DD, Boyan BD, & Schwartz Z. Tissue response and osteoinduction of human bone grafts *in vivo*. *Arch Orthop Trauma Surg,* 2001, 121(10)**,** 583-590.

Lomas R, Drummond O, & Kearney JN. Processing of whole femoral head allografts: a method for improving clinical efficacy and safety. *Cell Tissue Bank,* 2000, 1(3)**,** 193-200.

Lomas RJ, Jennings LM, Fisher J, & Kearney JN. Effects of a peracetic acid disinfection protocol on the biocompatibility and biomechanical properties of human patellar tendon allografts. *Cell Tissue Bank,* 2004, 5(3)**,** 149-160.

Lu Z, Wang G, Dunstan CR, Chen Y, Lu WY, Davies B, & Zreiqat H. Activation and promotion of adipose stem cells by tumour necrosis factor-alpha preconditioning for bone regeneration. *J Cell Physiol,* 2013, 228(8)**,** 1737-1744.

Luria EA, Owen ME, Friedenstein AJ, Morris JF, & Kuznetsow SA. Bone formation in organ cultures of bone marrow. *Cell Tissue Res,* 1987, 248(2)**,** 449-454.

Ma R, Li M, Luo J, Yu H, Sun Y, Cheng S, & Cui P. Structural integrity, ECM components and immunogenicity of decellularized laryngeal scaffold with preserved cartilage. *Biomaterials,* 2013, 34(7)**,** 1790-1798.

Mankin HJ, Gebhardt MC, Jennings LC, Springfield DS, & Tomford WW. Long-term results of allograft replacement in the management of bone tumors. *Clin Orthop Relat Res,* 1996, Mar(324)**,** 86-97.

Marcos-Campos I, Marolt D, Petridis P, Bhumiratana S, Schmidt D, & Vunjak-Novakovic G. Bone scaffold architecture modulates the development of mineralized bone matrix by human embryonic stem cells. *Biomaterials,* 2012, 33(33)**,** 8329-8342.

Markel DC, Guthrie ST, Wu B, Song Z, & Wooley PH. Characterization of the inflammatory response to four commercial bone graft substitutes using a murine biocompatibility model. *J Inflamm Res,* 2012, 5**,** 13-18.

Martens M, Van Audekercke R, Delport P, De Meester P, & Mulier JC. The mechanical characteristics of cancellous bone at the upper femoral region. *J Biomech,* 1983, 16(12)**,** 971-983.

Martin RB. Porosity and specific surface of bone. *Crit Rev Biomed Eng,* 1984, 10(3)**,** 179-222.

Martin RB. Determinants of the mechanical properties of bones. *J Biomech,* 1991, 24(supplt 1)**,** 79-88.

Mathieu PS, & Loboa EG. Cytoskeletal and focal adhesion influences on mesenchymal stem cell shape, mechanical properties, and differentiation down osteogenic, adipogenic, and chondrogenic pathways. *Tissue Eng Part B Rev,* 2012, 18(6)**,** 436-444.

Matsumoto T, Kuroda R, Mifune Y, Kawamoto A, Shoji T, Miwa M, Asahara T, & Kurosaka M. Circulating endothelial/skeletal progenitor cells for bone regeneration and healing. *Bone,* 2008, 43(3)**,** 434-439.

Matsuo K, & Irie N. Osteoclast-osteoblast communication. *Arch Biochem Biophys,* 2008, 473(2)**,** 201-209.

Maurin AC, Chavassieux PM, Frappart L, Delmas PD, Serre CM, & Meunier PJ. Influence of mature adipocytes on osteoblast proliferation in human primary cocultures. *Bone,* 2000, 26(5)**,** 485-489.

Mayr-Wohlfart U, Waltenberger J, Hausser H, Kessler S, Gunther KP, Dehio C, Puhl W, & Brenner RE. Vascular endothelial growth factor stimulates chemotactic migration of primary human osteoblasts. *Bone,* 2002, 30(3)**,** 472-477.

McNamara IR. Impaction bone grafting in revision hip surgery: past, present and future. *Cell Tissue Bank,* 2010, 11(1)**,** 57-73.

Megas P. Classification of non-union. *Injury,* 2005, 36(Suppl 4)**,** S30-37.

Merry K, Dodds R, Littlewood A, & Gowen M. Expression of osteopontin mRNA by osteoclasts and osteoblasts in modelling adult human bone. *J Cell Sci,* 1993, 104 (Pt 4)**,** 1013-1020.

Mesimaki K, Lindroos B, Tornwall J, Mauno J, Lindqvist C, Kontio R, Miettinen S, & Suuronen R. Novel maxillary reconstruction with ectopic bone formation by GMP adipose stem cells. *Int J Oral Maxillofac Surg,* 2009, 38(3)**,** 201-209.

Mihaila SM, Gaharwar AK, Reis RL, Khademhosseini A, Marques AP, & Gomes ME. The osteogenic differentiation of SSEA-4 sub-population of human adipose derived stem cells using silicate nanoplatelets. *Biomaterials,* 2014, 35(33)**,** 9087-9099.

Mikhael MM, Huddleston PM, Zobitz ME, Chen Q, Zhao KD, & An KN. Mechanical strength of bone allografts subjected to chemical sterilization and other terminal processing methods. *J Biomech,* 2008, 41(13)**,** 2816-2820.

Miller L, & Block J. Perspectives on the clinical utility of allografts for bone regeneration within osseous defects: a narrative review. *Orthopedic Research and Reviews,* 2011, 3**,** 31-37.

Minogue BM, Richardson SM, Zeef LA, Freemont AJ, & Hoyland JA. Transcriptional profiling of bovine intervertebral disc cells: implications for identification of normal and degenerate human intervertebral disc cell phenotypes. *Arthritis Res Ther,* 2010, 12(1)**,** R22.

Miron RJ, Hedbom E, Saulacic N, Zhang Y, Sculean A, Bosshardt DD, & Buser D. Osteogenic potential of autogenous bone grafts harvested with four different surgical techniques. *J Dent Res,* 2011, 90(12)**,** 1428-1433.

Mitchell EJ, Stawarz AM, Kayacan R, & Rimnac CM. The effect of gamma radiation sterilization on the fatigue crack propagation resistance of human cortical bone. *J Bone Joint Surg Am,* 2004, 86-A(12)**,** 2648-2657.

Mitchell JB, McIntosh K, Zvonic S, Garrett S, Floyd ZE, Kloster A, Di Halvorsen Y, Storms RW, Goh B, Kilroy G, Wu X, & Gimble JM. Immunophenotype of human adipose-derived cells: temporal changes in stromal-associated and stem cell-associated markers. *Stem Cells,* 2006, 24(2)**,** 376-385.

Mitton D, Rappeneau J, & Bardonnet R. Effect of a supercritical CO2 based treatment on mechanical properties of human cancellous bone. *European Journal of Orthopaedic Surgery & Traumatology,* 2005, 15(4)**,** 264-269.

Mo XT, Yang ZM,. & Qin TW. Effects of 20% demineralization on surface physical properties of compact bone scaffold and bone remodeling response at interface after orthotopic implantation. *Bone,* 2009, 45(2)**,** 301-308.

Moreau MF, Gallois Y, Basle MF, & Chappard D. Gamma irradiation of human bone allografts alters medullary lipids and releases toxic compounds for osteoblast-like cells. *Biomaterials,* 2000, 21(4)**,** 369-376.

Morris DC, Masuhara K, Takaoka K, Ono K, & Anderson HC. Immunolocalization of alkaline phosphatase in osteoblasts and matrix vesicles of human fetal bone. *Bone Miner,* 1992, 19(3)**,** 287-298.

Mroz TE, Lin EL, Summit MC, Bianchi JR, Keesling JE, Roberts M, Vangsness CT, & Wang JC. Biomechanical analysis of allograft bone treated with a novel tissue sterilization process. *Spine J,* 2006, 6(1)**,** 34-39.

Mueller SM, & Glowacki J. Age-related decline in the osteogenic potential of human bone marrow cells cultured in three-dimensional collagen sponges. *J Cell Biochem,* 2001, 82(4)**,** 583-590.

Munting E, Wilmart JF, Wijne A, Hennebert P, & Delloye C. Effect of sterilization on osteoinduction. Comparison of five methods in demineralized rat bone. *Acta Orthop Scand,* 1988, 59(1)**,** 34-38.

Nagaraja S, Lin AS, & Guldberg RE. Age-related changes in trabecular bone microdamage initiation. *Bone,* 2007, 40(4)**,** 973-980.

Nakashima K, Zhou X, Kunkel G, Zhang Z, Deng JM, Behringer RR, & de Crombrugghe B. The novel zinc finger-containing transcription factor osterix is required for osteoblast differentiation and bone formation. *Cell,* 2002, 108(1)**,** 17-29.

Nam HK, Liu J, Li Y, Kragor A, & Hatch NE. Ectonucleotide pyrophosphatase/ phosphodiesterase-1 (ENPP1) protein regulates osteoblast differentiation. *J Biol Chem,* 2011, 286(45)**,** 39059-39071.

National Joint Registry. National Joint Registry 11th Annual Report, 2014, Sep.

Nefussi JR, Boy-Lefevre ML, Boulekbache H, & Forest N. Mineralization *in vitro* of matrix formed by osteoblasts isolated by collagenase digestion. *Differentiation,* 1985, 29(2)**,** 160-168.

Neve A, Corrado A, & Cantatore FP. Osteocalcin: Skeletal and extra-skeletal effects. *J Cell Physiol,* 2013, 228(6)**,** 1149-1153.

Nguyen H, Cassady AI, Bennett MB, Gineyts E, Wu A, Morgan DA, & Forwood MR. Reducing the radiation sterilization dose improves mechanical and biological quality while retaining sterility assurance levels of bone allografts. *Bone,* 2013, 57(1)**,** 194-200.

Nguyen H, Morgan DA, & Forwood MR. Sterilization of allograft bone: effects of gamma irradiation on allograft biology and biomechanics. *Cell Tissue Bank,* 2007, 8(2)**,** 93-105.

Niemeyer P, Fechner K, Milz S, Richter W, Suedkamp NP, Mehlhorn AT, Pearce S, & Kasten P. Comparison of mesenchymal stem cells from bone marrow and adipose tissue for bone regeneration in a critical size defect of the sheep tibia and the influence of platelet-rich plasma. *Biomaterials,* 2010, 31(13)**,** 3572-3579.

Nilsson SK, Debatis ME, Dooner MS, Madri JA, Quesenberry PJ, & Becker PS. Immunofluorescence characterization of key extracellular matrix proteins in murine bone marrow in situ. *J Histochem Cytochem,* 1998, 46(3)**,** 371-377.

Nishio Y, Dong Y, Paris M, O'Keefe RJ, Schwarz EM, & Drissi H. Runx2-mediated regulation of the zinc finger Osterix/Sp7 gene. *Gene,* 2006, 372**,** 62-70.

Noel D, Caton D, Roche S, Bony C, Lehmann S, Casteilla L, Jorgensen C, & Cousin B. Cell specific differences between human adipose-derived and mesenchymal-stromal cells despite similar differentiation potentials. *Exp Cell Res,* 2008, 314(7)**,** 1575-1584.

Nukavarapu SP, & Amini AR. Optimal scaffold design and effective progenitor cell identification for the regeneration of vascularized bone. *Conf Proc IEEE Eng Med Biol Soc,* 2011**,** 2464-2467.

Ochoa JA, Sanders AP, Heck DA, & Hillberry BM. Stiffening of the femoral head due to inter-trabecular fluid and intraosseous pressure. *J Biomech Eng,* 191, 113(3)**,** 259-262.

Ohgushi H. Osteogenically differentiated mesenchymal stem cells and ceramics for bone tissue engineering. *Expert Opin Biol Ther,* 2014, 14(2)**,** 197-208.

Orimo H. The mechanism of mineralization and the role of alkaline phosphatase in health and disease. *J Nippon Med Sch,* 2010, 77(1)**,** 4-12.

Ornitz DM & Marie PJ. FGF signalling pathways in endochondral and intramembranous bone development and human genetics. *Genes & Dev,* 2002, 16, 1446-1465.

Ortuno MJ, Susperregui AR, Artigas N, Rosa JL, & Ventura F. Osterix induces Col1a1 gene expression through binding to Sp1 sites in the bone enhancer and proximal promoter regions. *Bone,* 2013, 52(2)**,** 548-556.

Otto F, Thornell AP, Crompton T, Denzel A, Gilmour KC, Rosewell IR, Stamp GW, Beddington RS, Mundlos S, Olsen BR, Selby PB, & Owen MJ. Cbfa1, a candidate gene for cleidocranial dysplasia syndrome, is essential for osteoblast differentiation and bone development. *Cell,* 1997, 89(5)**,** 765-771.

Parhami F, Morrow AD, Balucan J, Leitinger N, Watson AD, Tintut Y, Berliner JA, & Demer LL. Lipid oxidation products have opposite effects on calcifying vascular cell and bone cell differentiation. A possible explanation for the paradox of arterial calcification in osteoporotic patients. *Arterioscler Thromb Vasc Biol,* 1997, 17(4)**,** 680-687.

Patil N, Hwang K, & Goodman SB. Cancellous impaction bone grafting of acetabular defects in complex primary and revision total hip arthroplasty. *Orthopedics,* 2012, 35(3)**,** e306-312.

Pekkarinen J, Alho A, Lepisto J, Ylikoski M, Ylinen P, & Paavilainen T. Impaction bone grafting in revision hip surgery. A high incidence of complications. *J Bone Joint Surg Br,* 2000, 82(1)**,** 103-107.

Perrot S, Dutertre-Catella H, Martin C, Warnet JM, & Rat P. A new nondestructive cytometric assay based on resazurin metabolism and an organ culture model for the assessment of corneal viability. *Cytometry A,* 2003, 55(1)**,** 7-14.

Peters F, Schwarz K, & Epple M. The structure of bone studied with synchrotron X-ray diffraction, X-ray absorption spectroscopy and thermal analysis. *Thermochimica Acta,* 2000, 361(1–2)**,** 131-138.

Pietrzak WS, Woodell-May J, & McDonald N. Assay of bone morphogenetic protein-2, -4, and -7 in human demineralized bone matrix. *J Craniofac Surg,* 2006, 17(1)**,** 84-90.

Pinholt EM, & Solheim E. Osteoinductive potential of demineralized rat bone increases with increasing donor age from birth to adulthood. *J Craniofac Surg,* 1998, 9(2)**,** 142-146.

Phillips AM. Overview of the fracture healing cascade. *Injury, Int J Care injured,* 2005, 36S, S5-S7.Polini A, Pisignano D, Parodi M, Quarto R, & Scaglione S. Osteoinduction of human mesenchymal stem cells by bioactive composite scaffolds without supplemental osteogenic growth factors. *PLoS One,* 2011, 6(10)**,** 12.

Poundarik AA, Diab T, Sroga GE, Ural A, Boskey AL, Gundberg CM, & Vashishth D. Dilatational band formation in bone. *Proceedings of the National Academy of Sciences,* 2012, 109(47)**,** 19178-19183.

Pradel W, Eckelt U, & Lauer G. Bone regeneration after enucleation of mandibular cysts: comparing autogenous grafts from tissue-engineered bone and iliac bone. *Oral Surg Oral Med Oral Pathol Oral Radiol Endod,* 2006, 101(3)**,** 285-290.

Pradel W, Tausche E, Gollogly J, & Lauer G. Spontaneous tooth eruption after alveolar cleft osteoplasty using tissue-engineered bone: a case report. *Oral Surg Oral Med Oral Pathol Oral Radiol Endod,* 2008, 105(4)**,** 440-444.

Pruss A, Gobel UB, Pauli G, Kao M, Seibold M, Monig HJ, Hansen A, & von Versen R. Peracetic acid-ethanol treatment of allogeneic avital bone tissue transplants--a reliable sterilization method. *Ann Transplant,* 2003, 8(2)**,** 34-42.

Qian X, Yuan F, Zhimin Z, & Anchun M. Dynamic perfusion bioreactor system for 3D culture of rat bone marrow mesenchymal stem cells on nanohydroxyapatite/polyamide 66 scaffold *in vitro. J Biomed Mater Res B Appl Biomater,* 2013, 101(6)**,** 893-901.

Qiu SR, Wierzbicki A, Orme CA, Cody AM, Hoyer JR, Nancollas GH, Zepeda S, & De Yoreo JJ. Molecular modulation of calcium oxalate crystallization by osteopontin and citrate. *Proc Natl Acad Sci U S A,* 2004, 101(7)**,** 1811-1815.

Quarto R, Mastrogiacomo M, Cancedda R, Kutepov SM, Mukhachev V, Lavroukov A, Kon E, & Marcacci M. Repair of large bone defects with the use of autologous bone marrow stromal cells. *N Engl J Med,* 2001, 344(5)**,** 385-386.

Rauh J, Despang F, Baas J, Liebers C, Pruss A, Gelinsky M, Gunther KP, & Stiehler M. Comparative biomechanical and microstructural analysis of native versus peracetic acid-ethanol treated cancellous bone graft. *Biomed Res Int,* 2014**,** Article ID 784702, doi: 10.1155/2014/784702.

Reikeras O. Impact of freezing on bone graft incorporation biomechanical evaluations in rats. *Clin Biomech (Bristol, Avon),* 2010, 25(2)**,** 177-180.

Reinholt FP, Hultenby K, Oldberg A, & Heinegard D. Osteopontin--a possible anchor of osteoclasts to bone. *Proc Natl Acad Sci U S A,* 1990, 87(12)**,** 4473-4475.

Resnick D, Niwayama G, & Coutts RD. Subchondral cysts (geodes) in arthritic disorders: pathologic and radiographic appearance of the hip joint. *AJR Am J Roentgenol,* 1977, 128(5)**,** 799-806.

Rho J-Y, Kuhn-Spearing L, & Zioupos P. Mechanical properties and the hierarchical structure of bone. *Medical Engineering & Physics,* 1998, 20(2)**,** 92-102.

Richardson SM, Walker RV, Parker S, Rhodes NP, Hunt JA, Freemont AJ, & Hoyland JA. Intervertebral Disc Cell–Mediated Mesenchymal Stem Cell Differentiation. *Stem Cells,* 2006, 24(3)**,** 707-716.

Riggs BL, Melton LJ, Robb RA, Camp JJ, Atkinson EJ, Peterson JM, Rouleau PA, McCollough CH, Bouxsein ML, & Khosla S. Population-based study of age and sex differences in bone volumetric density, size, geometry, and structure at different skeletal sites. *J Bone Miner Res,* 2004, 19(12)**,** 1945-1954.

Roach HI. Why does bone matrix contain non-collagenous proteins? The possible roles of osteocalcin, osteonectin, osteopontin and bone sialoprotein in bone mineralisation and resorption. *Cell Biol Int,* 1994, 18(6)**,** 617-628.

Robinson DE, Lee MB, Smith EJ, & Learmonth ID. Femoral impaction grafting in revision hip arthroplasty with irradiated bone. *J Arthroplasty,* 2002, 17(7)**,** 834-840.

Robling AG, Niziolek PJ, Baldridge LA, Condon KW, Allen MR, Alam I, Mantila SM, Gluhak-Heinrich J, Bellido TM, Harris SE, & Turner CH. Mechanical stimulation of bone *in vivo* reduces osteocyte expression of Sost/sclerostin. *J Biol Chem,* 2008, 283(9)**,** 5866-5875.

Rodriguez DE, Thula-Mata T, Toro EJ, Yeh Y-W, Holt C, Holliday LS, & Gower LB. Multifunctional role of osteopontin in directing intrafibrillar mineralization of collagen and activation of osteoclasts. *Acta Biomaterialia,* 2014, 10(1)**,** 494-507.

Rooney P, Mann J, Eagle M, Hogg P, & Kearney J. P61 Producing a Safer Bone Allograft by Procesing Single Femoral Heads. *Transfusion Medicine,* 2006, 16**,** 51-51.

Rosen CJ, Compston JE, & Lian JB. *Primer on the metabolic bone diseases and disorders of mineral metabolism*: John Wiley & Sons, 2009.

Rougraff BT, & Kling TJ. Treatment of active unicameral bone cysts with percutaneous injection of demineralized bone matrix and autogenous bone marrow. *J Bone Joint Surg Am,* 2002, 84-A(6)**,** 921-929.

Runyan, C. M., Jones, D. C., Bove, K. E., Maercks, R. A., Simpson, D. S. & Taylor, J. A. (2010). Porcine allograft mandible revitalization using autologous adipose-derived stem cells, bone morphogenetic protein-2, and periosteum. *Plast Reconstr Surg,* 125(5)**,** 1372-1382.

Russell JL, & Block JE. Surgical harvesting of bone graft from the ilium: point of view. *Med Hypotheses,* 2000, 55(6)**,** 474-479.

Ryu J, Kim HJ, Chang EJ, Huang H, Banno Y, & Kim HH. Sphingosine 1-phosphate as a regulator of osteoclast differentiation and osteoclast–osteoblast coupling. *EMBO J,* 2006, 25(24), 5840-5851.

Salasznyk RM, Williams WA, Boskey A, Batorsky A, & Plopper GE. Adhesion to Vitronectin and Collagen I Promotes Osteogenic Differentiation of Human Mesenchymal Stem Cells. *J Biomed Biotechnol,* 2004, 1**,** 24-34.

Salkeld SL, Patron LP, Barrack RL, & Cook SD. The effect of osteogenic protein-1 on the healing of segmental bone defects treated with autograft or allograft bone. *J Bone Joint Surg Am,* 2001, 83-A(6)**,** 803-816.

Sampath TK, Maliakal JC, Hauschka PV, Jones WK, Sasak H, Tucker RF, White KH, Coughlin JE, Tucker MM, & Pang RH. Recombinant human osteogenic protein-1 (hOP-1) induces new bone formation *in vivo* with a specific activity comparable with natural bovine osteogenic protein and stimulates osteoblast proliferation and differentiation *in vitro*. *Journal of Biological Chemistry,* 1992, 267(28)**,** 20352-20362.

Samuelson KM. Bone grafting and noncemented revision arthroplasty of the knee. *Clin Orthop Relat Res,* 1988, (226)**,** 93-101.

Santiago JA, Pogemiller R, & Ogle BM. Heterogeneous differentiation of human mesenchymal stem cells in response to extended culture in extracellular matrices. *Tissue Eng Part A,* 2009, 15(12)**,** 3911-3922.

Scaglione M, Fabbri L, Dell'Omo D, Gambini F, & Guido G. Long bone nonunions treated with autologous concentrated bone marrow-derived cells combined with dried bone allograft. *Musculoskelet Surg,* 2014, 98(2)**,** 101-106.

Scaglione S, Braccini A, Wendt D, Jaquiery C, Beltrame F, Quarto R, & Martin I. Engineering of osteoinductive grafts by isolation and expansion of ovine bone marrow stromal cells directly on 3D ceramic scaffolds. *Biotechnol Bioeng,* 2006, 93(1)**,** 181-187.

Schantz JT, Teoh SH, Lim TC, Endres M, Lam CX, & Hutmacher DW. Repair of calvarial defects with customized tissue-engineered bone grafts I. Evaluation of osteogenesis in a three-dimensional culture system. *Tissue Eng,* 2003, 9(Suppl 1)**,** S113-126.

Schubert T, Xhema D, Veriter S, Schubert M, Behets C, Delloye C, Gianello P, & Dufrane D. The enhanced performance of bone allografts using osteogenic-differentiated adipose-derived mesenchymal stem cells. *Biomaterials,* 2011, 32(34)**,** 8880-8891.

Schwartz Z, Somers A, Mellonig JT, Carnes DL, Dean DD, Cochran DL, & Boyan BD. Ability of commercial demineralized freeze-dried bone allograft to induce new bone formation is dependent on donor age but not gender. *J Periodontol,* 1998, 69(4)**,** 470-478.

Schwiedrzik JJ, Kaudela KH, Burner U, & Zysset PK. Fabric-mechanical property relationships of trabecular bone allografts are altered by supercritical CO(2) treatment and gamma sterilization. *Bone,* 2011, 48(6)**,** 1370-1377.

Seebach C, Schultheiss J, Wilhelm K, Frank J, & Henrich, D. Comparison of six bone-graft substitutes regarding to cell seeding efficiency, metabolism and growth behaviour of human mesenchymal stem cells (MSC) *in vitro*. *Injury,* 2010, 41(7)**,** 731-738.

Sen B, Guilluy C, Xie Z, Case N, Styner M, Thomas J, Oguz I, Rubin C, Burridge K. & Rubin J. Mechanically induced focal adhesion assembly amplifies anti-adipogenic pathways in mesenchymal stem cells. *Stem Cells,* 2011, 9(11)**,** 1829-1836.

Seppa H, Grotendorst G, Seppa S, Schiffmann E, & Martin GR. Platelet-derived growth factor in chemotactic for fibroblasts. *J Cell Biol,* 1982, 92(2)**,** 584-588.

Shapiro F. Bone development and its relation to fracture repair. The role of mesenchymal osteoblasts and surface osteoblasts. *Eur Cell Mater,* 2008, 15**,** 53-76.

Shaw JM, Hunter SA, Gayton JC, Boivin GP, & Prayson MJ. Repeated freeze-thaw cycles do not alter the biomechanical properties of fibular allograft bone. *Clin Orthop Relat Res,* 2010, 470(3)**,** 937-943.

Shaw NE. Observations on the intramedullary blood-flow and marrow-pressure in bone. *Clin Sci,* 1963, 24**,** 311-318.

Shayesteh YS, Khojasteh A, Soleimani M, Alikhasi M, Khoshzaban A, & Ahmadbeigi N. Sinus augmentation using human mesenchymal stem cells loaded into a beta-tricalcium phosphate/hydroxyapatite scaffold. *Oral Surg Oral Med Oral Pathol Oral Radiol Endod,* 2008, 106(2)**,** 203-209.

Sheng MH, Lau KH, & Baylink DJ. Role of Osteocyte-derived Insulin-Like Growth Factor I in Developmental Growth, Modeling, Remodeling, and Regeneration of the Bone. *J Bone Metab,* 2014, 21(1)**,** 41-54.

Shi Y, Niedzinski JR, Samaniego A, Bogdansky S, & Atkinson BL. Adipose-derived stem cells combined with a demineralized cancellous bone substrate for bone regeneration. *Tissue Eng Part A,* 2012, 18(13-14)**,** 1313-1321.

Shi YY, Nacamuli RP, Salim A, & Longaker MT. The osteogenic potential of adipose-derived mesenchymal cells is maintained with aging. *Plast Reconstr Surg,* 2005, 116(6)**,** 1686-1696.

Shi Z, Huang X, Cai Y, Tang R, & Yang D. Size effect of hydroxyapatite nanoparticles on proliferation and apoptosis of osteoblast-like cells. *Acta Biomater,* 2009, 5(1)**,** 338-345.

Shih YR, Tseng KF, Lai HY, Lin CH, & Lee OK. Matrix stiffness regulation of integrin-mediated mechanotransduction during osteogenic differentiation of human mesenchymal stem cells. *J Bone Miner Res,* 2011, 26(4)**,** 730-738.

Sicchieri LG, Crippa GE, de Oliveira PT, Beloti MM, & Rosa AL. Pore size regulates cell and tissue interactions with PLGA-CaP scaffolds used for bone engineering. *J Tissue Eng Regen Med,* 2012, 6(2)**,** 155-162.

Simkin PA. Hydraulically loaded trabeculae may serve as springs within the normal femoral head. *Arthritis Rheum,* 2004, 50(10)**,** 3068-3075.

Simpson D, Kakarala G, Hampson K, Steele N, & Ashton B. Viable cells survive in fresh frozen human bone allografts. *Acta Orthop,* 2007, 78(1)**,** 26-30.

Smith CB, & Smith DA. An X-ray diffraction investigation of age-related changes in the crystal structure of bone apatite. *Calcif Tissue Res,* 1976, 22(2)**,** 219-226.

Smith CA, Richardson SM, Eagle MJ, Rooney P, Board T & Hoyland JA. the use of a novel bone allograft wash process to generate a biocompatible, mechanicall stable and osteoinductive biological scaffold for use in bone tissue engineering. *J Tissue Eng Regen Med*, 2014a, doi: 10.1002/term.1934.

Smith JO, Sengers BG, Aarvold A, Tayton ER, Dunlop DG, & Oreffo RO. Tantalum trabecular metal - addition of human skeletal cells to enhance bone implant interface strength and clinical application. *J Tissue Eng Regen Med,* 2014b, 8(4)**,** 304-313.

Smith KE, Huang Z, Ma T, Irani A, Lane Smith R, & Goodman SB. Molecular profile of osteoprogenitor cells seeded on allograft bone. *J Tissue Eng Regen Med,* 2011, 5(9)**,** 704-711.

Sodek J, Ganss B. & McKee MD. (2000). Osteopontin. *Crit Rev Oral Biol Med,* 2000, 11(3)**,** 279-303.

Spilimbergo S, & Bertucco A. Non-thermal bacterial inactivation with dense CO(2). *Biotechnol Bioeng,* 2003, 84(6)**,** 627-638.

Stenderup K, Justesen J, Clausen C, & Kassem M. Aging is associated with decreased maximal life span and accelerated senescence of bone marrow stromal cells. *Bone,* 2003, 33(6)**,** 919-926.

Stiehler M, Seib FP, Rauh J, Goedecke A, Werner C, Bornhauser M, Gunther KP, & Bernstein P. Cancellous bone allograft seeded with human mesenchymal stromal cells: a potential good manufacturing practice-grade tool for the regeneration of bone defects. *Cytotherapy,* 2010, 12(5)**,** 658-668.

Stoilov I, Kilpatrick MW, & Tsipouras P. A common FGFR3 gene mutation is present in achondroplasia but not in hypochondroplasia. *Am J Med Genet,* 1995, 55(1)**,** 127-133.

Stolzing A, Jones E, McGonagle D, & Scutt A. Age-related changes in human bone marrow-derived mesenchymal stem cells: consequences for cell therapies. *Mech Ageing Dev,* 2008, 129(3)**,** 163-173.

Strauss PG, Closs EI, Schmidt J, & Erfle V. Gene expression during osteogenic differentiation in mandibular condyles *in vitro*. *J Cell Biol,* 1990, 110(4)**,** 1369-1378.

Street J, Bao M, deGuzman L, Bunting S, Peale FV, Ferrara N, Steinmetz H, Hoeffel J, Cleland JL, Daugherty A, van Bruggen N, Redmond HP, Carano RA, & Filvaroff EH. Vascular endothelial growth factor stimulates bone repair by promoting angiogenesis and bone turnover. *Proc Natl Acad Sci U S A,* 2002, 99(15)**,** 9656-9661.

Sun L, Hu Y, Ning Z, & Liang Z. The correlation between immune rejection and osteoinduction of allogeneic bone grafting. *Chin Med J (Engl),* 1998, 111(9)**,** 818-822.

Sun Y, Li W, Lu Z, Chen R, Ling J, Ran Q, Jilka RL, & Chen XD. Rescuing replication and osteogenesis of aged mesenchymal stem cells by exposure to a young extracellular matrix. *Faseb J,* 2011, 5(5)**,** 1474-1485.

Supronowicz P, Gill E, Trujillo A, Thula T, Zhukauskas R, Perry R, & Cobb RR. Multipotent adult progenitor cell-loaded demineralized bone matrix for bone tissue engineering. *J Tissue Eng Regen Med,* 2013, 15(10), doi: 10.1002/term.1706.

Supronowicz P, Gill E, Trujillo A, Thula T, Zhukauskas R, Ramos T, & Cobb RR. Human adipose-derived side population stem cells cultured on demineralized bone matrix for bone tissue engineering. *Tissue Eng Part A,* 2011, 17(5-6)**,** 789-798.

Tagil M, Jeppsson C, & Aspenberg P. Bone graft incorporation. Effects of osteogenic protein-1 and impaction. *Clin Orthop Relat Res,* 2000, (371)**,** 240-245.

Takahashi N, Akatsu T, Udagawa N, Sasaki T, Yamaguchi A, Moseley JM, Martin TJ, & Suda T. Osteoblastic cells are involved in osteoclast formation. *Endocrinology,* 1988, 123(5)**,** 2600-2602.

Takai H, Kanematsu M, Yano K, Tsuda E, Higashio K, Ikeda K, Watanabe K, & Yamada Y. Transforming Growth Factor-β Stimulates the Production of Osteoprotegerin/Osteoclastogenesis Inhibitory Factor by Bone Marrow Stromal Cells. *Journal of Biological Chemistry,* 1998, 273(42)**,** 27091-27096.

Tang Y, Wu X, Lei W, Pang L, Wan C, Shi Z, Zhao L, Nagy TR, Peng X, Hu J, Feng X, Van Hul W, Wan M, & Cao X. TGF-[beta]1-induced migration of bone mesenchymal stem cells couples bone resorption with formation. *Nat Med,* 2009, 15(7)**,** 757-765.

Tavassoli M, & Yoffey JM. *Bone marrow, structure and function.* New York, AR Liss, 1983.

Tayton E, Purcell M, Aarvold A, Smith JO, Kalra S, Briscoe A, Shakesheff K, Howdle SM, Dunlop DG, & Oreffo RO. Supercritical CO2 fluid-foaming of polymers to increase porosity: a method to improve the mechanical and biocompatibility characteristics for use as a potential alternative to allografts in impaction bone grafting? *Acta Biomater,* 2012, 8(5)**,** 1918-1927.

Thebaud NB, Siadous R, Bareille R, Remy M, Daculsi R, Amedee J, & Bordenave L. Whatever their differentiation status, human progenitor derived - or mature - endothelial cells induce osteoblastic differentiation of bone marrow stromal cells. *J Tissue Eng Regen Med,* 2012, 6(10)**,** e51-60.

Thibault MM, Hoemann CD, & Buschmann MD. Fibronectin, vitronectin, and collagen I induce chemotaxis and haptotaxis of human and rabbit mesenchymal stem cells in a standardized transmembrane assay. *Stem Cells Dev,* 2007, 16(3)**,** 489-502.

Thirunavukkarasu K, Halladay DL, Miles RR, Yang X, Galvin RJS, Chandrasekhar S, Martin TJ, & Onyia JE. The Osteoblast-specific Transcription Factor Cbfa1 Contributes to the Expression of Osteoprotegerin, a Potent Inhibitor of Osteoclast Differentiation and Function. *Journal of Biological Chemistry,* 2000, 275(33)**,** 25163-25172.

Tiedeman JJ, Connolly JF, Strates BS, & Lippiello L. Treatment of nonunion by percutaneous injection of bone marrow and demineralized bone matrix. An experimental study in dogs. *Clin Orthop Relat Res,* 1991, (268)**,** 294-302.

Tilley S, Bolland BJ, Partridge K, New AM, Latham JM, Dunlop DG, & Oreffo RO Taking tissue-engineering principles into theater: augmentation of impacted allograft with human bone marrow stromal cells. *Regen Med,* 2006, 1(5)**,** 685-692.

Tohma Y, Dohi Y, Ohgushi H, Tadokoro M, Akahane M, & Tanaka Y. Osteogenic activity of bone marrow-derived mesenchymal stem cells (BMSCs) seeded on irradiated allogenic bone. *J Tissue Eng Regen Med,* 2012, 6(2)**,** 96-102.

Traianedes K, Russell JL, Edwards JT, Stubbs HA, Shanahan IR, & Knaack D. Donor age and gender effects on osteoinductivity of demineralized bone matrix. *J Biomed Mater Res B Appl Biomater,* 2004, 70(1)**,** 21-29.

Turunen MJ, Prantner V, Jurvelin JS, Kroger H, & Isaksson H. Composition and microarchitecture of human trabecular bone change with age and differ between anatomical locations. *Bone,* 2013, 54(1)**,** 118-125.

Udagawa N, Takahashi N, Jimi E, Matsuzaki K, Tsurukai T, Itoh K, Nakagawa N, Yasuda H, Goto M, Tsuda E, Higashio K, Gillespie MT, Martin TJ, & Suda T. Osteoblasts/stromal cells stimulate osteoclast activation through expression of osteoclast differentiation factor/RANKL but not macrophage colony-stimulating factor: receptor activator of NF-kappa B ligand. *Bone,* 1999, 25(5)**,** 517-523.

Ullmark G. Bigger size and defatting of bone chips will increase cup stability. *Arch Orthop Trauma Surg,* 2000, 120(7-8)**,** 445-447.

Urist MR. Bone: Formation by Autoinduction. *Science,* 1965, 150(3698)**,** 893-899.

Urist MR, DeLange RJ, & Finerman GA. Bone cell differentiation and growth factors. *Science,* 1983, 220(4598)**,** 680-686.

Uthgenannt BA, Kramer MH, Hwu JA, Wopenka B, & Silva MJ. Skeletal self-repair: stress fracture healing by rapid formation and densification of woven bone. *J Bone Miner Res,* 2007, 22(10)**,** 1548-1556.

VandeVord PJ, Nasser S, & Wooley PH. Immunological responses to bone soluble proteins in recipients of bone allografts. *J Orthop Res,* 2005, 23(5)**,** 1059-1064.

Varettas K, & Taylor P. Bioburden assessment of banked bone used for allografts. *Cell Tissue Bank,* 2011, 12(1)**,** 37-43.

Vastel L, Meunier A, Siney H, Sedel L, & Courpied JP. Effect of different sterilization processing methods on the mechanical properties of human cancellous bone allografts. *Biomaterials,* 2004, 25(11)**,** 2105-2110.

Viguet-Carrin S, Follet H, Gineyts E, Roux JP, Munoz F, Chapurlat R, Delmas PD, & Bouxsein ML Association between collagen cross-links and trabecular microarchitecture properties of human vertebral bone. *Bone,* 2010, 46(2)**,** 342-347.

Voss P, Sauerbier S, Wiedmann-Al-Ahmad M, Zizelmann C, Stricker A, Schmelzeisen R, & Gutwald R. Bone regeneration in sinus lifts: comparing tissue-engineered bone and iliac bone. *Br J Oral Maxillofac Surg,* 2010, 48(2)**,** 121-126.

Vulcano E, Murena L, Falvo DA, Baj A, Toniolo A, & Cherubino P. Bone marrow aspirate and bone allograft to treat acetabular bone defects in revision total hip arthroplasty: preliminary report. *Eur Rev Med Pharmacol Sci,* 2013, 17(16)**,** 2240-2249.

Wagner W, Bork S, Horn P, Krunic D, Walenda T, Diehlmann A, Benes V, Blake J, Huber FX, Eckstein V, Boukamp P, & Ho AD. Aging and replicative senescence have related effects on human stem and progenitor cells. *PLoS One,* 2009, 4(6)**,** e5846.

Wagner W, Horn P, Castoldi M, Diehlmann A, Bork S, Saffrich R, Benes V, Blake J, Pfister S, Eckstein V, & Ho AD. Replicative senescence of mesenchymal stem cells: a continuous and organized process. *PLoS One,* 2008, 3(5)**,** e2213.

Wall ME, Bernacki SH, & Loboa EG. Effects of serial passaging on the adipogenic and osteogenic differentiation potential of adipose-derived human mesenchymal stem cells. *Tissue Eng,* 2007, 13(6)**,** 1291-1298.

Wang C, Gong Y, Zhong Y, Yao Y, Su K, & Wang DA. The control of anchorage-dependent cell behavior within a hydrogel/microcarrier system in an osteogenic model. *Biomaterials,* 2009, 30(12)**,** 2259-2269.

Wang X, Shen X, Li X, & Agrawal CM. Age-related changes in the collagen network and toughness of bone. *Bone,* 2002, 31(1)**,** 1-7.

Weaver JK, & Chalmers J. Cancellous bone: its strength and changes with aging and an evaluation of some methods for measuring its mineral content. *J Bone Joint Surg Am,* 1966, 48(2)**,** 289-298.

Weinand C, Xu JW, Peretti GM, Bonassar LJ, & Gill TJ. Conditions affecting cell seeding onto three-dimensional scaffolds for cellular-based biodegradable implants. *J Biomed Mater Res B Appl Biomater,* 2009, 91(1)**,** 80-87.

Weszl M, Skaliczki G, Cselenyak A, Kiss L, Major T, Schandl K, Bognar E, Stadler G, Peterbauer A, Csonge L, & Lacza Z. Freeze-dried human serum albumin improves the adherence and proliferation of mesenchymal stem cells on mineralized human bone allografts. *J Orthop Res,* 2012, 30(3)**,** 489-496.

Whiteside P, Matykina E, Gough JE, Skeldon P, & Thompson GE. *In vitro* evaluation of cell proliferation and collagen synthesis on titanium following plasma electrolytic oxidation. *J Biomed Mater Res A,* 2010, 94(1)**,** 38-46.

Whyte MP. Hypophosphorylation and the role of alkaline phosphotase in skeletal mineralization. *Endocrine Rev,* 1994, 15(4), 439-61.

Wildemann B, Kadow-Romacker A, Pruss A, Haas NP, & Schmidmaier G. Quantification of growth factors in allogenic bone grafts extracted with three different methods. *Cell Tissue Bank,* 2007, 8(2)**,** 107-114.

Wolfe SW, Pike L, Slade JF, & Katz LD. Augmentation of distal radius fracture fixation with coralline hydroxyapatite bone graft substitute. *J Hand Surg Am,* 1999, 24(4)**,** 816-827.

Wong RW, & Rabie AB. A quantitative assessment of the healing of intramembranous and endochondral autogenous bone grafts. *Eur J Orthod,* 1999, 21(2)**,** 119-126.

Wu W, Niklason L, & Steinbacher DM. The effect of age on human adipose-derived stem cells. *Plast Reconstr Surg,* 2013, 131(1)**,** 27-37.

Xian L, Wu X, Pang L, Lou M, Rosen CJ, Qiu T, Crane J, Frassica F, Zhang L, Rodriguez JP, Jia X, Yakar S, Xuan S, Efstratiadis A, Wan M, & Cao X. Matrix IGF-1 maintains bone mass by activation of mTOR in mesenchymal stem cells. *Nat Med,* 2012, 18(7)**,** 1095-1101.

Xie C, Reynolds D, Awad H, Rubery PT, Pelled G, Gazit D, Guldberg RE, Schwarz EM, O'Keefe RJ, & Zhang X. Structural bone allograft combined with genetically engineered mesenchymal stem cells as a novel platform for bone tissue engineering. *Tissue Eng,* 2007, 13(3)**,** 435-445.

Yamada Y, Ito K, Nakamura S, Ueda M, & Nagasaka T. Promising cell-based therapy for bone regeneration using stem cells from deciduous teeth, dental pulp, and bone marrow. *Cell Transplant,* 2011, 20(7)**,** 1003-1013.

Yamamoto T, Uchida K, Naruse K, Suto M, Urabe K, Uchiyama K, Suto K, Moriya M, Itoman M, & Takaso M. Quality assessment for processed and sterilized bone using Raman spectroscopy. *Cell Tissue Bank,* 2012, 13(3)**,** 409-414.

Yamanouchi K, Gotoh Y, & Nagayama M. Dexamethasone enhances differentiation of human osteoblastic cells *in vitro*. *Journal of Bone and Mineral Metabolism,* 1997, 15(1)**,** 23-29.

Yang C, Tibbitt MW, Basta L, & Anseth KS. Mechanical memory and dosing influence stem cell fate. *Nat Mater,* 2014, 13(6)**,** 645-652.

Yates P, Thomson J, & Galea G. Processing of whole femoral head allografts: validation methodology for the reliable removal of nucleated cells, lipid and soluble proteins using a multi-step washing procedure. *Cell Tissue Bank,* 2005, 6(4)**,** 277-285.

Yoshimura K, Shigeura T, Matsumoto D, Sato T, Takaki Y, Aiba-Kojima E, Sato K, Inoue K, Nagase T, Koshima I, & Gonda K. Characterization of freshly isolated and cultured cells derived from the fatty and fluid portions of liposuction aspirates. *J Cell Physiol,* 2006, 208(1)**,** 64-76.

Yourek G, McCormick SM, Mao JJ, & Reilly GC. Shear stress induces osteogenic differentiation of human mesenchymal stem cells. *Regen Med,* 2010, 5(5)**,** 713-724.

Zambonin G, & Grano M. Biomaterials in orthopaedic surgery: effects of different hydroxyapatites and demineralized bone matrix on proliferation rate and bone matrix synthesis by human osteoblasts. *Biomaterials,* 1995, 16(5)**,** 397-402.

Zhou S, Greenberger JS, Epperly MW, Goff JP, Adler C, Leboff MS, & Glowacki J. Age-related intrinsic changes in human bone-marrow-derived mesenchymal stem cells and their differentiation to osteoblasts. *Aging Cell,* 2008, 7(3)**,** 335-343.

Zhou Y, Fan W, Prasadam I, Crawford R, & Xiao Y. Implantation of osteogenic differentiated donor mesenchymal stem cells causes recruitment of host cells. *J Tissue Eng Regen Med,* 2012, 5(10), doi: 10.1002/term.1619.

Zimmermann G, & Moghaddam A. Allograft bone matrix versus synthetic bone graft substitutes. *Injury,* 2011, 42(Suppl 2)**,** S16-21.

Zuk PA, Zhu M, Ashjian P, De Ugarte DA, Huang JI, Mizuno H, Alfonso ZC, Fraser JK, Benhaim P, & Hedrick MH. Human adipose tissue is a source of multipotent stem cells. *Mol Biol Cell,* 2002, 13(12)**,** 4279-4295.

Zuk PA, Zhu M, Mizuno H, Huang J, Futrell JW, Katz AJ, Benhaim P, Lorenz HP, & Hedrick MH. Multilineage cells from human adipose tissue: implications for cell-based therapies. *Tissue Eng*, 2001, 7(2)**,** 211-228.

Chapter 8

Appendices

8.1 Appendix I

Table 8.1: Coefficient of variation for both intra-head and inter-head in orientated and non-orientated samples

Variable	Orientation	Young's Modulus (MPa)	Load at Yield (N)	Deflection at yield (mm)	Stress at Yield (MPa)	Work to Yield (J)	Load at failure (N)	Deflection at failure (mm)	Stress at failure (MPa)	Work at failure (J)
Intra-head	Non-orientated	27.823712	38.927236	25.20791	35.982754	57.086238	35.553303	33.42678	32.360923	49.678542
	Orientated	34.524995	42.829003	19.57245	41.772395	56.987396	29.979873	29.8973	34.011731	50.683394
Inter-head	Non-orientated	30.085637	39.576705	27.01869	38.627917	54.521498	36.582331	45.8869	35.669145	48.764543
	Orientated	33.131177	44.194852	24.64107	40.570227	67.52927	29.018848	51.30686	31.552679	67.447184

8.2 Appendix II

Published article:

Smith CA, Richardson SM, Eagle MJ, Rooney P, Board T, & Hoyland JA. The use of a novel bone allograft wash process to generate a biocompatible, mechanically stable and osteoinductive biological scaffold for use in bone tissue engineering. *J Tissue Eng Regen Med*, 2014, doi:10.1002/term.1934

JOURNAL OF TISSUE ENGINEERING AND REGENERATIVE MEDICINE
J Tissue Eng Regen Med (2014)
Published online in Wiley Online Library (wileyonlinelibrary.com) **DOI:** 10.1002/term.1934

RESEARCH ARTICLE

The use of a novel bone allograft wash process to generate a biocompatible, mechanically stable and osteoinductive biological scaffold for use in bone tissue engineering

C. A. Smith[1], S. M. Richardson[1], M. J. Eagle[2], P. Rooney[2], T. Board[3] and J. A. Hoyland[1,4]*
[1]*Centre for Tissue Injury and Repair, University of Manchester, UK*
[2]*National Health Service (NHS) Blood and Transplant Tissue Services, Liverpool, UK*
[3]*Wrightington Hospital, Wigan, UK*
[4]*NIHR Manchester Musculoskeletal Biomedical Research Unit, Manchester Academic Health Science Centre, Manchester, UK*

Abstract

Fresh-frozen biological allograft remains the most effective substitute for the 'gold standard' autograft, sharing many of its osteogenic properties but, conversely, lacking viable osteogenic cells. Tissue engineering offers the opportunity to improve the osseointegration of this material through the addition of mesenchymal stem cells (MSCs). However, the presence of dead, immunogenic and potentially harmful bone marrow could hinder cell adhesion and differentiation, graft augmentation and incorporation, and wash procedures are therefore being utilized to remove the marrow, thereby improving the material's safety. To this end, we assessed the efficiency of a novel wash technique to produce a biocompatible, biological scaffold void of cellular material that was mechanically stable and had osteoinductive potential. The outcomes of our investigations demonstrated the efficient removal of marrow components (~99.6%), resulting in a biocompatible material with conserved biomechanical stability. Additionally, the scaffold was able to induce osteogenic differentiation of MSCs, with increases in osteogenic gene expression observed following extended culture. This study demonstrates the efficiency of the novel wash process and the potential of the resultant biological material to serve as a scaffold in bone allograft tissue engineering. © 2014 The Authors. ***Journal of Tissue Engineering and Regenerative Medicine*** **published by John Wiley & Sons Ltd.**

Received 29 January 2014; Revised 29 April 2014; Accepted 21 May 2014

Keywords bone tissue engineering; biocompatability; mesenchymal stem cells; osteogenic differentiation; gene expression; 3D cell culture

1. Introduction

An ever-increasing need for bone graft material is placing increased pressure on its availability, quality and integration capabilities (National Joint Register, 2012). Biocompatibility, osteogenic capacity, biomechanical strength and architecture are all important factors in the successful incorporation of graft bone and can determine the speed of recovery (Marcos-Campos *et al*., 2012). As such, for clinical use it is important to use a material which encompasses these qualities.

The 'gold standard' grafting material is currently autograft bone. Sourced from the patient, this mix of mineralized extracellular matrix (ECM), bone marrow and osteogenic cells is the most osteogenic material available, with both osteoinductive and osteoconductive properties. However, the quality and volume of the material acquired is often not able to meet the demands of surgical procedures requiring large volumes, may be of substandard biomechanical stability and may contain few viable pre-osteogenic cells, e.g. mesenchymal stem cells (MSCs) (Hernigou *et al*., 2005).

Correspondence to: Judith A. Hoyland, Centre for Tissue Injury and Repair, Institute of Inflammation and Repair, Faculty of Medical and Human Sciences, University of Manchester, Room 1.538, Stopford Building, Oxford Road, Manchester M13 9PT, UK. E-mail: Judith.a.hoyland@manchester.ac.uk

Synthetic and biological alternatives are available to autografts (Kolk *et al*., 2012; Seebach *et al*., 2010); however, whilst synthetic materials aim to duplicate many of the same features found in autografts (Beswick and Blom, 2011), with post-production modifications and addition of growth factors, biological materials are still considered the most effective and are the most widely-used alternative (Zimmermann and Moghaddam, 2011).

A commonly used biological alternative to autograft is allograft bone, incorporating many of the same qualities as autograft and displaying good healing potential (Miller and Block, 2011). However, it does not include a source of viable osteogenic cells and is therefore associated with a lack of osteogenic and angiogenic stimulatory properties (prerequisite properties for clinical success). Consequently, bone tissue-engineering approaches aim to incorporate osteogenic cells into allograft scaffolds (Schubert *et al*., 2011; Aarvold *et al*., 2012; Xie *et al*., 2007) and improve the properties of this biological material. However, while allograft contains no viable cells, it does contain residual dead cell matter, which reduces the ability of progenitor or osteogenic cells to adhere to bone, may act to induce an immune response and could potentially harbour transmittable diseases (Varettas and Taylor, 2011), all of which could profoundly affect its use as a scaffold in bone tissue engineering. This potential for harmful disease transmission, albeit somewhat alleviated by stringent donor selection, virus and microbiological testing, means that it is advised that allograft material is sterilized by γ-irradiation before clinical use (American Association of Tissue Banks, 2006). γ-Irradiation involves subjecting the target material to a dose of 25 kGy whilst deep-frozen. However, this sterilization technique fails to remove the dead cell matter and marrow containing the antigenic cell types (Czitrom *et al*., 1985) and thus it can still elicit an immune response (Bos *et al*., 1983). Furthermore, this method has been demonstrated to decrease osteogenic potential by reducing biocompatibility through the production of peroxidized lipids (Moreau *et al*., 2000), as well as diminishing the biomechanical stability of the bone (Dux *et al*., 2010; Cornu *et al*., 2011).

Alternative sterilization or processing methods have been described for human bone material, either in addition to, or as a replacement for, γ-irradiation. These methods attempt to remove all soft tissue from the allograft, leaving behind a scaffold devoid of cellular material whilst retaining biocompatibility and biomechanical stability (Hassabella *et al*., 2009).

Although the addition of chemical agents, such as peracetic acid and ethanol, may reduce the osteoinductive potential of the material (Bormann *et al*., 2010), their controlled use has been shown to have a limited effect on the biomechanical stability and biocompatibility of the material (DePaula *et al*., 2005; Haimi *et al*., 2009), whilst still reducing infectious viral particles and killing harmful bacteria (Pruss *et al*., 2003). This potential for complete removal of immunogenic cellular components has led to marrow removal techniques becoming more prevalent in the production of structures required as scaffolds in tissue-engineering applications (Ma *et al*., 2013; Djouad *et al*., 2012; Hashimoto *et al*., 2011; Dutra and French, 2010).

Although tissue-engineered bone allografts offer huge potential for the improvement of bone regeneration, a method of producing a biomechanically stable and biocompatible bone allograft material that retains the bone's innate structure and osteogenic properties is still required. Furthermore, for clinical translation, the methods to produce such allografts should be rapid and require minimal processing, whilst allowing the generation of sufficiently large structures for bespoke bone void filling. Thus, this study was designed to assess the application and efficacy of a novel bone allograft wash process on human bone from whole femoral heads. This wash process was modified from that published by Yates *et al.* (2005) to be more rapid and include the chemical sterilants peracetic acid–hydrogen peroxide and ethanol and an increased number of wash/centrifugation steps. Specifically, it aimed to ascertain whether the resulting structure had any alterations to its biocompatibility, immunogenicity, osteoinductive ability or biomechanical stability, which will ultimately determine its potential as a scaffold in bone tissue-engineering applications.

2. Materials and methods

2.1. Preparation of washed bone material

2.1.1. Sample procurement

Fresh-frozen femoral heads were obtained, through ethical approval from the National Health Service Blood and Transplant Tissue Services, from consenting live donors undergoing hip replacement surgery: male, $n = 16$; aged 38–82 (mean 53) years; and female ($n = 12$; aged 42–78 (mean 41) years. Upon removal, the samples were stored at –80 °C until required.

2.1.2. Wash process

Whole femoral heads were defrosted overnight at 5 °C, then submerged in 300 ml distilled water preheated to 60 °C and sonicated for 15 min at 60 °C (F5300b; Decon, UK). The femoral heads were then drained and rinsed in 300 ml distilled water preheated to 60 °C whilst agitated on an orbital shaker at 200 rpm at 60 °C for 5 min (IOC400; Weiss-Gallenkamp, Loughborough, UK). The femoral heads underwent a wash–centrifuge combination three times, in which they were submerged in 300 ml distilled water preheated to 60 °C and agitated in an orbital shaker at 200 rpm at 60 °C for 10 min, with an initial wash of 30 min and subsequent washes 10 min. The femoral heads were then centrifuged at 1850 × *g* for 15 min at ambient temperature (Sorvall, using rotor RC3BP; Thermo-Scientific, Hemel Hempstead, UK). After three wash–centrifuge steps the femoral heads were sonicated for 10 min at 60 °C in 300 ml prewarmed (60 °C) sterilant solution containing 3% v/v

DOI: 10.1002/term

hydrogen peroxide (H3410, Sigma-Aldrich, Gillingham, UK) and 0.02% v/v peroxy-acetic acid (PAA; 77240, Sigma-Aldrich). Samples were transferred to 300 ml 70% v/v ethanol and sonicated for 10 min at 21 °C. Finally, the femoral heads underwent two washes in 300 ml distilled water and agitated at 200 rpm for 10 min at 60 °C before being centrifuged at 1850 × *g* for 15 min at ambient temperature to remove any remaining liquids. The washed, disinfected femoral heads were then dissected into 1 cm^3 bone cubes, using an oscillating saw (NS3A, De Soutter, Aston Clinton, Buckinghamshire, UK), snap-frozen and stored dry at –80°until use.

2.2. Assessment of wash efficiency

2.2.1. Biochemical assays

To assess the removal of marrow contaminants from the whole femoral head, samples of wash solutions were collected after each step of the protocol ($n = 14$). The soluble components, protein, DNA and haemoglobin, were assessed using Bradford reagent (B6916, Sigma-Aldrich); PicoGreen assay (P7589, Life Technologies, Paisley, UK) and Drabkin's reagent (D594, Sigma-Aldrich), prepared with Brij 35 solution (B4184, Sigma-Aldrich), respectively, using 50 µl aliquots and conducted according to the manufacturers' protocols.

2.2.2. Residual DNA quantification within washed bone samples

Bone cubes from three fresh-frozen and three washed femoral heads (1 cube/femoral head) were snap-frozen, impacted and ground to produce a fine coarse powder. Samples (100 mg) were predigested (56 °C for 48 h) in proteinase k solution (19131, Qiagen, Manchester, UK) before DNA was extracted using the DNeasy Blood and Tissue Kit (69506, Qiagen). Extracted DNA was concentrated using ethanol precipitation and total DNA quantified using a Nanodrop spectrophotometer (ND1000, Thermo-Scientific, Hemel Hempstead, UK).

2.2.3. Histological analysis

Cubed bone samples from the fresh-frozen ($n = 2$) and washed bone ($n = 2$) were fixed in 50 ml formal saline (4% v/v formaldehyde, 0.9% w/v sodium chloride) at room temperature for 48 h, then decalcified in 20% v/v EDTA, pH 7.4. Decalcified bone samples were embedded in paraffin wax and 5 µm sections cut and mounted. The sections were stained with haematoxylin and eosin (H&E) and Masson's trichrome (RRSP131-c, Biostain, Manchester, UK).

2.2.4. Immunohistochemical analysis

Sections of fresh-frozen ($n = 3$) and washed bone ($n = 3$) were dewaxed and rehydrated before antigen retrieval using chemotrypsin, and incubated overnight at 4 °C with primary HLA class 1 ABC (EMR8-5) antibody (ab70328; Abcam, Cambridge, UK). The samples were incubated for 30 min with the secondary antibody (sc-3795; Santa Cruz Biotechnology, Heidelberg, Germany) and antibody binding disclosed using the avidin–biotin interaction (PK-7100; Vector Laboratories, Peterborough, UK) and DAB (3,3-diaminobenzidine) staining (H-2200; Vector Laboratories). All images were acquired on a Leitz DMRB microscope (Leica Microsystems, Milton Keynes, UK), using Deltapix Infinity X and supporting software (Deltapix, Maalov Beyvej, Denmark).

2.3. Biocompatibility of washed bone

2.3.1. Production of bone extract-conditioned medium

Powder samples of bone cubes from fresh-frozen, unwashed ($n = 3$) and washed ($n = 3$) bone samples were soaked in five times their weight of standard culture medium for 72 h at 37 °C under constant agitation (ISO-10993-5, 1993E). The solution was centrifuged at 400 × *g* for 5 min and at 10875 × *g* for 10 min to remove fine bone particles. The resulting supernatant was used as extract-conditioned medium in cytotoxicity assays on MSCs.

2.3.2. Effect of extract-conditioned medium on MSC viability

Human MSCs were isolated from the bone marrow of a 55 year-old female, with ethical approval using established methodology (Strassburg *et al.*, 2010). The cells were expanded in standard culture medium containing α-modified Eagle's medium (M4526, Sigma-Aldrich), 10% fetal calf serum (FCS; 10270, Sigma-Aldrich), 10 µM ascorbate-2-phosphate (A8960-5G, Sigma-Aldrich), 2 mM GlutaMAX (35050-038, Life Technologies, Paisley, UK) and combined antibiotic–antimycotic solution (50 000 U penicillin, 100 µg/ml streptomycin, 250 ng/ml amphotericin B; A5955, Sigma-Aldrich). At passage 2, MSCs were seeded into 96-well plates at 3.3×10^4 cells/cm^2 and incubated for 24 h. The culture medium was replaced with 100 µl extract-conditioned medium. After 24 h of incubation, cell viability was assessed by adding 5 µl WST-1 (05015944001, Roche, UK) to each well. The culture plates were incubated for 4 h at 37 °C and read at absorbance 450/620 nm (Multiscan FC, Thermo Scientific, UK). Cells remaining in the 96-well culture plate were rinsed with phosphate-buffered saline (PBS) and lysed with 100 µl 2% Triton X-100. To each well, 100 µl lactate dehydrogenase (LDH) reagent (MAK066, Sigma-Aldrich) was added and incubated at room temperature for 30 min. The plates were read at absorbance 485/620 nm.

2.4. Osteoinductive capacity of washed bone

Mesenchymal stem cell samples from two donors (a female aged 67 and a male aged 72 years) were used to seed 1 cm^3

DOI: 10.1002/term

cubes of washed bone material with 5×10^5 MSCs in 250 µl standard medium. Each MSC sample was cultured on bone cubes from three different donors (all aged > 70 years). After seeding, the cubes were incubated for 1 h at 37 °C, washed three times in PBS and centrifuged at $500 \times g$ for 5 min to remove non-adherent cells. These cells were combined with residual cells trypsinized from the tissue-culture wells and counted using a haemocytometer to assess seeding efficiency. A non-cell-seeded control was run simultaneously.

MSC-seeded bone cubes were either cultured in standard or osteogenic differentiation medium (standard medium containing 10 mM β-glycerophosphate (G9891, Sigma) and 1×10^{-7} M dexamethasone (D8893, Sigma) and cultured for 28 days. At 0, 14 and 28 day time points, cell viability was assessed using an alamarBlue® assay (DAL1025, Life Technologies). Briefly, the medium was replaced with 5% alamarBlue® in relevant medium. After 2 h of incubation a 100 µl sample was measured using a fluorescence plate reader (FLx800, Biotek, UK) at 540 nm and excitation 600 nm.

2.4.1. qRT–PCR analysis of osteogenic differentiation

At time points 0, 14 and 28 days, medium was removed from bone cubes by centrifugation at $500 \times g$ for 5 min. The bone cubes were transferred to clean tubes and 1 ml TRIzol reagent (AM9738, Ambion, Life Technologies) added, then incubated for 5 min with constant agitation. After incubation, the bone cubes were centrifuged at $500 \times g$ for 5 min to remove all TRIzol reagent. RNA was extracted as previously described (Minogue *et al*., 2010), quantified using a Nanodrop and reverse-transcribed to cDNA, using a High Capacity cDNA Reverse Transcription Kit (4368814, Life Technologies). Real-time quantitative polymerase chain reaction (PCR) was performed on a StepOnePlus real-time PCR system (4376600, Life Technologies), using Lumino-Ct qPCR ReadyMix (l6669, Sigma-Aldrich). Assays were prepared using FAM-BHQ1 assays (all primers and probes from Sigma-Aldrich) for the following genes: runt-related transcription factor 2 (*RUNX2*; NM_001024630), forward CGCTGCAACAAGACC, reverse CGCCATGACAGTAACC; osteopontin (*OP*; NM_000582), forward CTGACATCCAGTACCCTG, reverse CAGCTGACTCGTTTCATA; and osteocalcin (*OC*; NM_199173), forward CCGCACTTTGCATCG, reverse GCCATTGATACAGGTAGC. Data were normalized to the housekeeping gene mitochondrial ribosome protein 19 (*MRPL19*; NM_014763), forward CCACATTCCAGAGTTCTA, reverse CCGAGGATTATAAAGTTCAAA) and displayed as $2^{-\Delta\Delta C_T}$ (Minogue *et al*., 2010; Livak and Schmittgen, 2001) relative to day 0 controls.

2.5. Biomechanical stability of washed bone

2.5.1. Compression testing

For assessment of biomechanical stability, fresh-frozen femoral heads from male [$n = 10$, aged 72–90 (mean 78.2) years] and female [$n = 5$, aged 70–85 (mean 77.4) years] donors were laterally bisected along the coronal plane to produce two equal halves. One half was retained, while the other was washed according to the method described earlier. The two halves were grid-marked along the axis of normal compression, cut into 1 cm^3 cubes ($n = 242$) and labelled with orientation and designated coordinates.

The cubes were loaded onto a compression-testing machine (LRXPlus, Lloyd Instruments, Sussex, UK) and subjected to one round of compression to failure, with the settings: preload 0.2 N, maximum deflection 3 mm, and load of 5 kN at a speed of 5 mm/min. Data were recorded for parameters of yield, elasticity and failure, using NEXYGEN*plus* software.

2.6. Statistical analysis

Statistical analysis was conducted using Origin Pro v. 8.5 (Silverdale Scientific, Stoke Mandeville, UK). Mann–Whitney non-parametric statistical analysis was performed on the WST-1, LDH, PCR and alamarBlue® results, with a paired *t*-test used on mechanics data. Significance was set at $p \leq 0.05$.

3. Results

3.1. Wash process removes marrow components

The removal of marrow components from the femoral heads was assessed by comparing soluble factors present in the spent wash solutions to samples taken from washed bone and soaked for 1 h in deionized water at 60 °C with agitation. This indicated a total removal of 99.2 ± 1.8% recorded DNA, 98.9 ± 1.5% soluble protein and 100% haemoglobin from the trabecular material, resulting in a DNA content of 16.9 ng DNA/mg dry bone material.

3.2. Histology

H&E staining of unwashed bone showed large quantities of soft marrow and cells deposited in the trabecular structure (Figure 1a). Encapsulated osteocytes and the endosteum were also evident.

A fine meshwork was still present in the washed bone material (Figure 1b); however, this was almost completely untethered from the trabeculae. Additionally, there was a diminished cell presence with no obvious endosteum, although a few osteocytes were still present encapsulated in lacunae.

In addition, Masson's trichrome staining only showed changes to soft tissue histology (Figure 1c, d), with similar morphological staining of osteoid (red) and mineralized (ossified) (blue) matrix between washed and unwashed bone.

DOI: 10.1002/term

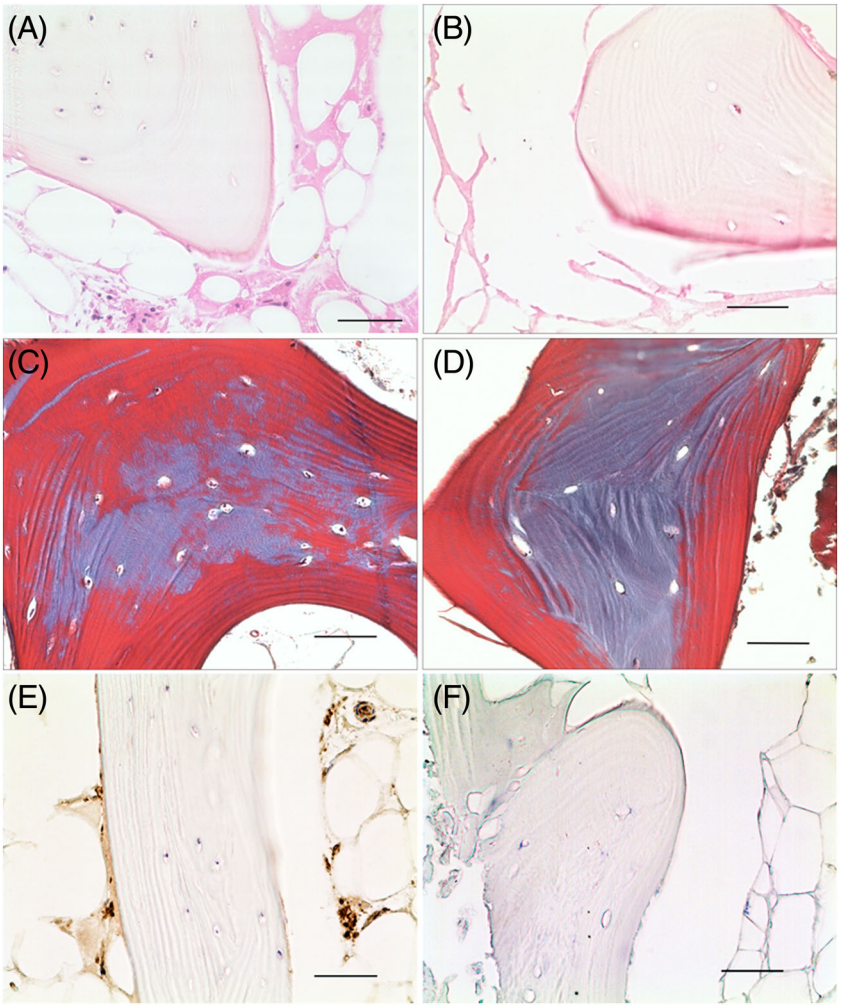

Figure 1. Histological and immunohistological staining of unwashed (A, C, E) and washed (B, D, F) allograft material. Images display H&E staining (A, B), Masson's trichrome (C, D) and HLA class 1 ABC antibody staining (E, F). All images were taken using × 600 magnification; scale bars = 50 μm. Images clearly display a significant decrease in immunogenic cellular content and soft tissue, whilst maintaining bone morphology

3.3. Immunogenicity of washed bone

As MHC antigens are used to recognize foreign material, samples were immunohistochemically stained for HLA serotypes A, B and C. The washed bone displayed little or no immunopositivity (Figure 1f). In comparison, unwashed material was heavily stained, including endosteum and soft marrow tissue containing fat cells, stromal cells and osteocytes (Figure 1e).

3.4. Biocompatibility of washed bone

MSC cultures subjected to extract-conditioned medium from washed bone material showed a significant $10.6 \pm 4.4\%$ ($p = 0.05$) increase in cellular metabolic activity (Figure 2a), with LDH assays showing a small but not significant increase in cell number (Figure 2b).

In contrast, fresh-frozen bone extract-conditioned medium caused a significant, $32 \pm 13.78\%$ ($p = 0.03$) decrease in cellular metabolic activity (Figure 2a) and a significant ($p = 0.02$) $20 \pm 9.03\%$ decrease in total cell number compared to standard culture medium.

3.5. Washed bone is osteoinductive and supports MSC osteogenic differentiation

AlamarBlue® results for MSCs seeded on washed bone displayed significant fold increases in metabolic activity at days 14 and 28 in both standard and osteogenic medium ($p < 0.001$) (Figure 3a). There was a significant increase in activity between days 14 and 28 ($p < 0.01$); however, there was no significant difference between medium types at any time point.

Osteogenic markers for initial differentiation (*RUNX2*), immature osteoblast gene (*OPN*) and mature osteoblast gene (*OCN*) were used to determine both osteogenesis and the extent of cell maturation. Non-seeded, washed bone material displayed no detectable amplification.

Expression of the early osteogenic gene *RUNX2* by MSCs seeded on washed bone (Figure 3b) was significantly increased at day 14 compared to day 0 in both

DOI: 10.1002/term

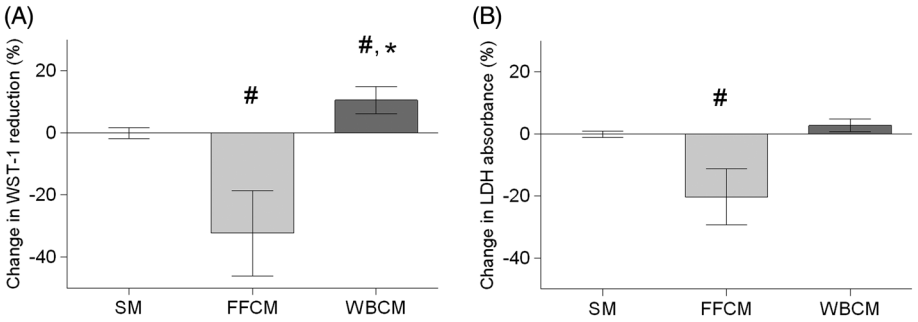

Figure 2. Analysis of MSC activity assessed using a WST-1 assay (A) and viability assessed using an LDH assay (B) after incubation in standard medium (SM), fresh-frozen extract-conditioned medium (FFCM) and washed bone extract-conditioned medium (WBCM). Results from FFCM or WBCM were averaged and normalized to SM and displayed as percentage change ± SE; #, significant difference with respect to SM ($p \leq 0.05$); *, significant difference ($p \leq 0.05$) between FFCM and WBCM

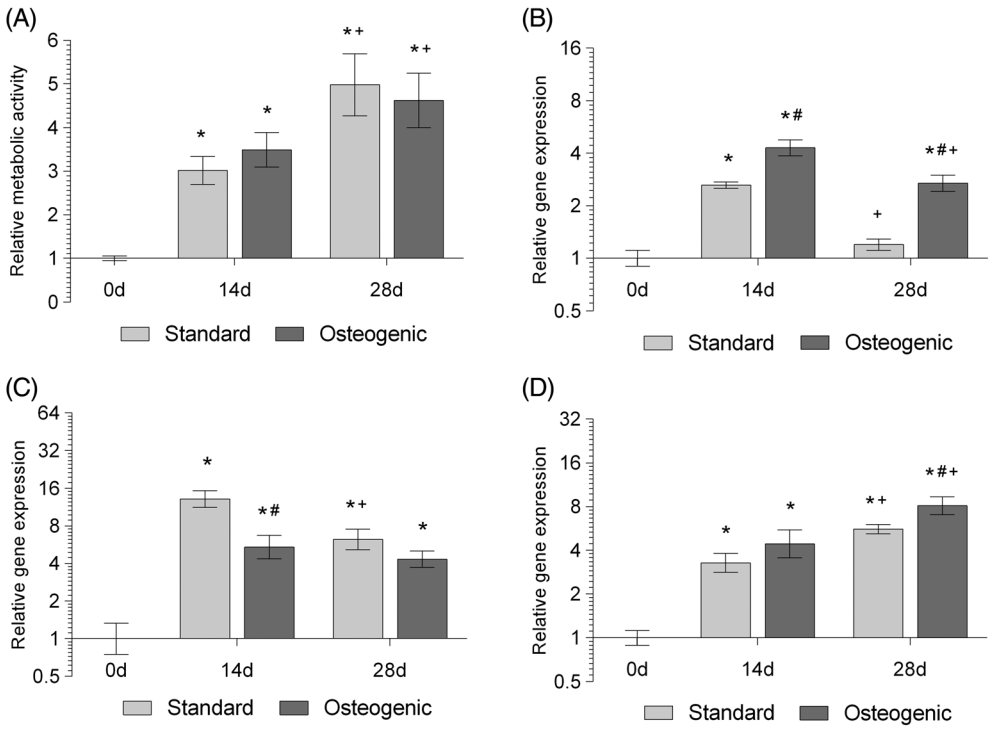

Figure 3. Alamar blue metabolic activity and quantitative real-time PCR for osteogenic marker gene expression of MSCs seeded on washed bone scaffolds and cultured for 14 or 28 days in either standard or osteogenic medium. Relative metabolic activity (A) was normalized to non-seeded bone controls and day 0 readings, whilst relative gene expression of (B) *RUNX2*, (C) *OPN* and (D) *OCN* was normalized to the housekeeping gene *MRPL19* and day 0 controls. Data represent mean ± SE. *, significant difference with respect to day 0 control ($p \leq 0.05$); #, significant difference between standard and osteogenic medium ($p \leq 0.05$); +, significant difference between days 14 and 28 in the same medium type ($p \leq 0.05$)

standard ($p < 0.001$) and osteogenic ($p < 0.001$) media, with significantly larger increases noted in osteogenic medium ($p = 0.005$). By day 28, *RUNX2* expression by MSCs in standard medium had returned to day 0 control levels, whereas expression in osteogenic medium remained significantly higher than both day 0 controls and standard medium at day 28 ($p < 0.001$).

Expression of the immature osteoblast marker gene *OPN* (Figure 3c) was also significantly increased by day 14 in both standard ($p < 0.001$) and osteogenic media ($p < 0.001$) compared to day 0 controls. However, levels were significantly lower in osteogenic medium compared to standard medium at day 14 ($p = 0.003$). By day 28, expression of *OPN* remained significantly higher than day 0 controls in both medium types ($p < 0.001$), with no significant difference noted between standard and osteogenic media.

Expression of the mature osteoblast marker gene *OCN* (Figure 3d) was upregulated to similar extents in both standard and osteogenic media compared to day 0 controls ($p < 0.001$ in both standard and osteogenic media). Expression was further increased in both media by day 28 ($p < 0.001$ in standard and osteogenic media relative to day 0; $p < 0.001$ and $p = 0.04$ in standard and osteogenic media, respectively, relative to the same medium type at day 14), with a small but significant increase noted in osteogenic medium compared to standard medium at day 28 ($p = 0.04$).

DOI: 10.1002/term

3.6. Washed bone is biomechanically stable

At the point of yield there were no significant differences to load at yield, stress or work at yield (Figure 4a, c, d). The washed material was compressed less at the point it lost its elasticity, with a significant decrease in the deflection at yield for washed bone compared to unwashed, from 1.49 ± 0.04 mm to 1.35 ± 0.04 mm ($p = 0.002$) (Figure 4c).

The parameters of elasticity indicated a significant increase in Young's modulus of washed bone over unwashed bone from 75.9 ± 3.4 MPa to 84.6 ± 3.6 MPa ($p = 0.02$) (Figure 5a), with a small but insignificant increase in stiffness. The results of parameters at failure indicated no significant differences between the washed and unwashed material in any parameter (Figure 6a–d).

4. Discussion

Allograft bone material is essential in surgical procedures aimed at replacing large areas of bone loss, sharing many of the characteristics of 'gold standard' autograft but with greater availability. However, whilst the use of allograft material has shown good long-term healing potential, its marrow material is comprised of dead cell matter containing no viable osteogenic cell source, diminishing its ability to osseointegrate (through immunogenicity and infection) and detrimentally affecting cell adherence and activity (Bonsignore *et al.*, 2013). Therefore, wash techniques are being developed to remove the marrow material. Importantly these wash methods aim not to detrimentally effect the latent abilities of the ECM in supporting the proliferation and regulation of cell activity (Dutra and French, 2010; Yates *et al.*, 2005; Declercq *et al.*, 2013; Choi *et al.*,

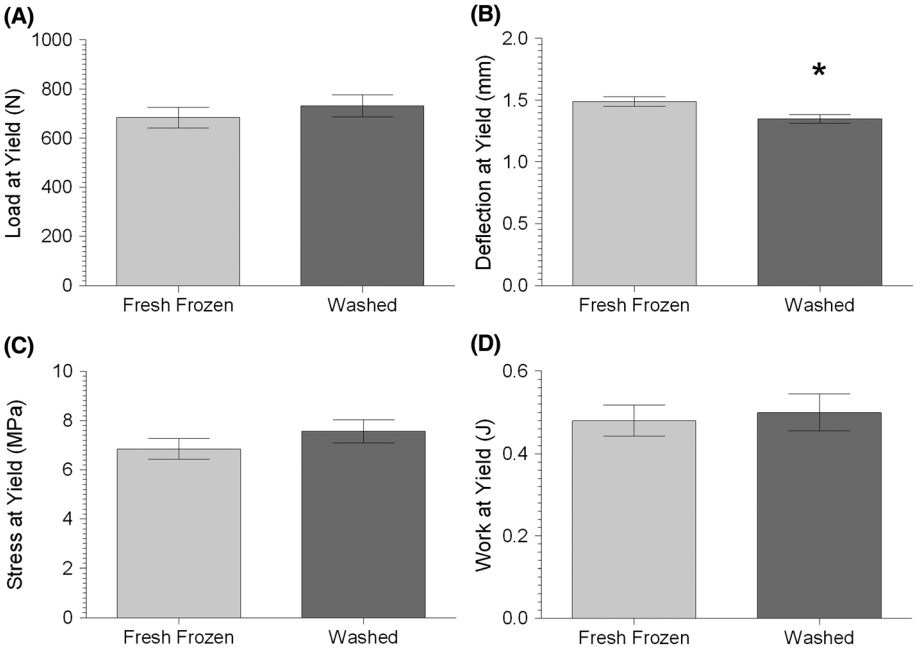

Figure 4. Compression testing results for parameters relating to yield of: (A) load to yield; (B) deflection of material at yield; (C) stress at yield; and (D) work at yield. Results of compression data were averaged for both fresh-frozen and washed bone ($n = 108$ for each) and displayed as mean ± SE; $^*p \leq 0.05$ between fresh-frozen and washed bone

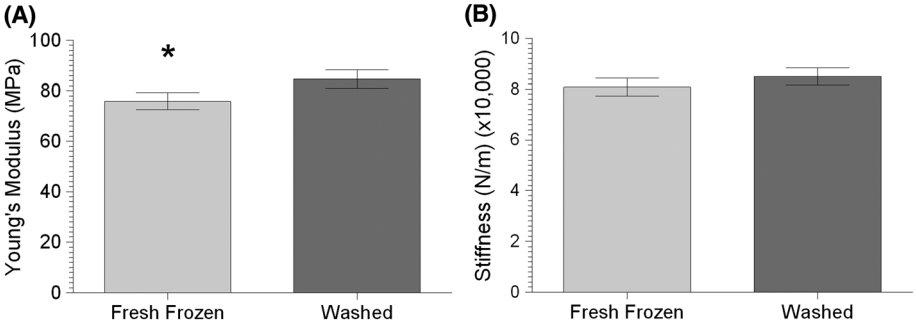

Figure 5. Compression testing results for parameters relating to elasticity of: (A) Young's modulus; (B) stiffness. Results of compression data were averaged for both fresh-frozen and washed bone ($n = 105$ for Young's modulus and $n = 108$ for stiffness in both cases) and displayed as mean ± SE; $^*p \leq 0.05$ between fresh-frozen and washed bone

DOI: 10.1002/term

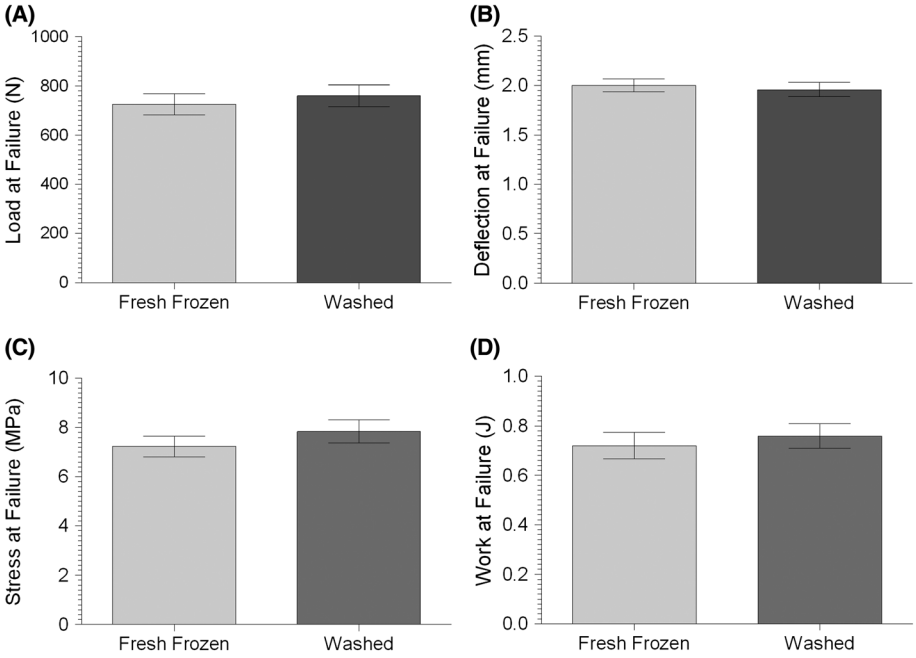

Figure 6. Compression testing results for parameters relating to failure of: (A) load to failure; (B) deflection at failure; (C) stress at failure; and (D) work at failure. Results of compression to failure were averaged for both fresh-frozen and washed bone ($n = 108$ for each) and displayed as mean ± SE. There is no significant difference between fresh-frozen and washed bone material in any parameter

2011; Polini *et al.*, 2011). In addition, the material and its properties may be exploited further as a scaffold in tissue engineering, with replication of the bone microenvironmental niche (Hammoudi *et al.*, 2012; Thebaud *et al.*, 2012), having been demonstrated to result in better osseointegration compared to standard allograft material (Coquelin *et al.*, 2012). Thus, this study used a novel rapid wash process to remove marrow material from fresh-frozen allograft femoral heads, assessing for marrow removal, biocompatibility, osteoinductive potential and biomechanical stability, and determining its potential as a scaffold for use in future bone tissue engineering.

The biochemical results provide evidence that the wash process removes a large proportion of soluble protein, DNA and haemoglobin trapped in the trabecular structure of the whole femoral head. This removal was equivalent to soluble protein removal reported by Yates *et al.* (2005) and superior in the removal of both soluble protein and DNA to Ibrahim *et al.* (2012); however, these processes did not include a chemical sterilant step. Our study resulted in a material with a low DNA value (16.9 ng DNA/mg dry material) and which, histologically, displayed a washed matrix devoid of a marrow component, which may otherwise affect osseointegration. These characteristics are in accordance with other studies producing decellularized bone (Hashimoto *et al.*, 2011) and other tissue structures (Dutra and French, 2010; Cornejo *et al.*, 2012) and the standards proposed by Crapo *et al.* (2011) for the evaluation of a decellularized soft tissue.

The cytotoxicity assays confirmed the biocompatibility of the washed bone material while, interestingly, highlighting the detrimental properties of the unwashed fresh-frozen bone in this *in vitro* study. The washed material caused no decrease in cell number or metabolic activity, with the alamarBlue® assays demonstrating the sustained viability of cells seeded into the materials' structure. Conversely fresh-frozen bone caused a significant reduction in both the total cell number and metabolic activity of the cultured cell population, suggesting a detrimental effect of non-washed, fresh-frozen bone. The cytotoxic effect of fresh-frozen material *in vitro* has previously been noted by Board *et al.* (2009), although there are no reports of trials comparing the clinical outcomes of fresh-frozen vs washed allograft. Despite the fact that fresh-frozen material displays good long-term healing, the leaching of cytotoxic factors from this material into the surrounding tissue could be detrimental to host-derived osseointegration, or affect the health of surrounding tissues *in vivo*, and thus requires investigation utilizing appropriate *in vivo* studies. It is of interest that through washing and the removal of the marrow, the material was able to maintain cell metabolic activity and viability, showing good biocompatibility and, importantly, not inducing any cytotoxic effects. This is in contrast to γ-irradiation, in which the technique itself is thought to affect cell viability through the production of cytotoxic peroxidized lipids (Moreau *et al.*, 2000).

Gene expression analysis demonstrated the osteoinductive capabilities of the washed bone and its ability to support differentiated cells. Interestingly, increased osteogenic gene expression was seen with standard medium alone, with increases in early marker *RUNX2*, as well as the osteoblast marker osteopontin and mature osteoblast gene osteocalcin, suggestive of differentiation and cell maturation. These results suggest that the induction and maturation of the MSCs is due to the bone ECM itself and may be due to the integrin–ECM binding (Frith *et al.*, 2012; Sun *et al.*, 2011) or encapsulated

DOI: 10.1002/term

bone-specific growth factors, such as bone morphogenetic proteins (BMPs), which elicit an osteogenic response upon release (Mauney *et al*., 2005). The induction of MSC osteogenesis by the washed bone without the addition of an osteogenic medium suggests that the ECM proteins and entrapped growth factors are relatively unaffected by the chemicals in the novel wash process, and still remain functional.

The material produced by this study demonstrates comparable biomechanical stability at both yield and failure to a fresh-frozen control. Whilst there were changes to Young's modulus and yield displacement, the small increase in rigidity did not negatively affect the overall structural stability. Additionally, the increase in Young's modulus seen after the removal of marrow is similar to that documented by Halgrin *et al*. (2011), who concluded that the marrow had caused increased transverse pressure and local stress on trabeculae, leading to its premature failure. Our results would also suggest that the material was not demineralized by the wash process, as this would have compromised the biomechanical stability of the bone (Chen and McKittrick, 2011). Utilization of halved femoral heads reduced interpatient variability, which may arise through changes in sex, age, weight or even disease state (Green *et al*., 2011; Homminga *et al*., 2002), and intrahead variability due to the differing compressive and tensile structures of the trabeculae (Martens *et al*., 1983).

Accurate determination of the biomechanical strength of the washed bone material is important in its eventual use, either directly as a surgical allograft, or as a scaffold for MSC-based tissue engineering. The three-dimensional (3D) structure itself is thought to influence the activity of osteogenic cells through mechanotransduction (Kilian *et al*., 2010; Shih *et al*., 2011) or simply through shear force (Yourek *et al*., 2010). Maintenance of rigidity and an appropriate porous 3D architecture is essential for osteoconductivity and new bone infiltration (Tagil *et al*., 2000), whilst preventing recoil of the impacted bone allograft that may negatively influence cementation (Kligman *et al*., 2003). The biomechanical compression results therefore suggest that washed bone is mechanically comparable to commonly used fresh-frozen allograft material and, together with improved biocompatibility and sustained osteoinductive potential, may thus offer an attractive alternative to existing unwashed bone allografts.

5. Conclusion

The results of this study depict a novel wash process for fresh-frozen allograft, able to remove ~99.5% of marrow components from whole femoral heads, leaving a biocompatible, mechanically stable, biological material, which, importantly, is still able to support cell proliferation and induce osteogenic differentiation. Additionally, the wash process removed the MHC class 1-positive marrow material present in fresh-frozen bone, which demonstrated detrimental cytotoxic effects on cultured cells *in vitro*. This large-scale removal of immunogenic marrow and the biocompatibility of the structure, together with the preservation of the materials' osteoinductive and mechanical properties, illustrate the potential of this washed bone material as a scaffold for bone tissue-engineering applications. Importantly, the novel wash process described in this study offers a number of potential benefits, including the rapid removal of marrow components from multiple whole femoral heads simultaneously, with minimal processing. The use of femoral heads in this process also allows for the production of large biological scaffolds for application in large-scale bone tissue engineering.

Conflict of interest

The authors have declared that there is no conflict of interest.

Acknowledgements

The authors wish to thank Joint Action, the NHSBT and Wrightington hospital for their funding of this research. Research Councils UK (RCUK) are acknowledged for funding a fellowship to SMR.

References

Aarvold A, Smith JO, Tayton ER *et al*. 2012; From bench to clinic and back: skeletal stem cells and impaction bone grafting for regeneration of bone defects. *J Tissue Eng Regen Med* doi: 10.1002/term.1577

American Association of Tissue Banks. 2006; Standards for Tissue Banking, 11th edn. American Association of Tissue Banks: Bethesda, MD.

Beswick A, Blom AW. 2011; Bone graft substitutes in hip revision surgery: a comprehensive overview. *Injury* **42**: S40–46.

Board TN, Rooney P, Kay PR. 2009; Biocompatibility of allograft for impaction grafting: effect of marrow removal. *J Bone Joint Surg (Br)* **91**: 169.

Bonsignore LA, Anderson JR, Lee Z. 2013; Adherent lipopolysaccharide inhibits the osseointegration of orthopaedic implants by impairing osteoblast differentiation. *Bone* **52**: 93–101.

Bormann N, Pruss A, Schmidmaier G, *et al*. 2010; *In vitro* testing of the osteoinductive potential of different bony allograft preparations. *Arch Orthop Trauma Surg* **130**: 143–149.

Bos GD, Goldberg VM, Zika JM *et al*. 1983; Immune response of rats to frozen bone allograft. *J Bone Joint Surg* **65**: 239–246.

Chen PY, McKittrick J. 2011; Compressive mechanical properties of demineralized and deproteinized cancellous bone. *J Mech Behav Biol Mater* **4**(7): 961–973.

Choi JS, Kim BS, Kim JY *et al*. 2011; Decellularized extracellular matrix derived from human adipose tissue as a potential scaffold for allograft tissue engineering. *J Biomed Mat Res* **97A**: 292–299.

Coquelin L, Fialaire A, Roux S *et al*. 2012; *In vivo* and *in vitro* comparison of three different allografts 'vitalized' with human mesenchymal stromal cell. *Tissue Eng A* **18**(17): 1921–1931.

Cornejo A, Sahar DE, Stephenson SM *et al*. 2012; Effect of adipose tissue-derived osteogenic and endothelial cells on bone allograft osteogenesis and vascularization in critical-sized calvarial defects. *Tissue Eng A* **18**(15–16): 1552–1561.

Cornu O, Boquet J, Nonclercq O *et al*. 2011; Synergetic effect of freeze-drying and γ-irradiation on the mechanical properties of human cancellous bone. *Cell Tissue Bank* **12**: 281–288.

Crapo PM, Gilbert TW, Badylak SF. 2011; An overview of tissue and whole organ decellularization processes. *Biomaterials* **32**: 3233–3243.

Czitrom AA, Axelrod T, Bernard F. 1985; Antigen presenting cells and bone allotransplantation. *Curr Orthop Pract* **197**: 27–31.

Declercq HA, De Caluwe T, Krysko O *et al*. 2013; Bone graft engineering from human adipose-derived stem cells in dynamic 3D environments. *Biomaterials* **34**: 1004–1017.

DePaula CA, Truncale KG, Gertzman AA *et al*. 2005; Effects of hydrogen peroxide cleaning procedures on bone graft osteoinductivity and mechanical properties. *Cell Tissue Bank* **6**: 287–298.

Djouad F, Guerit D, Marie M *et al*. 2012; Mesenchymal stem cells: new insights into bone regenerative applications. *J Biomater Tissue Eng* **2**: 14–28.

Dutra TF, French SW. 2010; Marrow stromal fibroblastic cell cultivation *in vitro* on decellularized bone marrow extracellular matrix. *Exp Mol Pathol* **88**: 58–66.

Dux SJ, Ramsey D, Chu EH *et al*. 2010; Alterations in damage processes in dense cancellous bone following γ-irradiation sterilization. *J Biomech* **43**: 1509–1513.

Frith JE, Mills R, Hudson JE *et al*. 2012; Tailored integrin–extracellular matrix interactions to direct human mesenchymal stem cell differentiation. *Stem Cells Dev* **21**(13): 2442–2456.

Green JO, Nagaraja S, Diab T *et al*. 2011; Age-related changes in human trabecular bone: relationship between microstructural stress and strain and damage morphology. *J Biomech* **44**: 2279–2285.

Haimi S, Vienonen A, Hirn M *et al*. 2009; The effect of chemical cleansing procedures combined with peracetic acid–ethanol sterilization on biomechanical properties of cortical bone. *Biologicals* **36**: 99–104.

Halgrin J, Chaari F, Makiewicz E. 2011; On the effects of marrow in the mechanical behaviour and crush response of trabecular bone. *J Mech Behav Biomed Mater* **5**: 231–223.

Hammoudi TM, Rivet CA, Kemp ML *et al*. 2012; 3D *in vitro* tri-culture platform to investigate effects of crosstalk between mesenchymal stem cells, osteoblasts and adipocytes. *Tissue Eng A* **18**: 1686–1697.

Hashimoto Y, Funamoto S, Kimura T *et al*. 2011; The effect of decellularised bone/bone marrow produced by high hydrostatic pressurization on the osteogenic differentiation of mesenchymal stem cells. *Biomaterials* **32**: 7060–7067.

Hassabella M, Mehendale S, Poniatowski S *et al*. 2009; Subsidence of the stem after impaction bone grafting for revision hip replacement using irradiated bone. *J Bone Joint Surg* **91**: 37–43.

Hernigou PH, Poignard A, Beaujean F *et al*. 2005; Percutaneous autologous bone-marrow grafting for nonunions. Influence of the number and concentration of progenitor cells. *J Bone Joint Surg Am* **87**(7): 1430–1437.

Homminga J, McCreadie BR, Ciarelli TE *et al*. 2002; Cancellous bone mechanical properties from normals and patients with hip fractures differ on the structural level, not on the bone hard tissue level. *Bone* **30**: 759–764.

Ibrahim T, Qureshi A, McQuillan TA *et al*. 2012; Intra-operative washing morcellised bone allograft with pulse lavage: how effective is it in reducing blood and marrow content? *Cell Tissue Bank* **13**: 157–165.

Kilian KA, Bugarija B, Lahn BT *et al*. 2010; Geometric cues for directing the differentiation of mesenchymal stem cells. *Proc Natl Acad Sci U S A* **107**(11): 4872–4877.

Kligman M, Rotem A, Roffman M. 2003; Cancellous and cortical morselized allograft in revision total hip replacement: a biomechanical study of implant stability. *J Biomech* **36**: 797–802.

Kolk A, Handschel J, Drescher W *et al*. 2012; Current trends and future perspectives of bone substitute materials – from space holders to innovative biomaterials. *J Craniomaxillofac Surg* **40**: 706–718.

Livak KJ, Schmittgen TD. 2001; Analysis of relative gene expression data using real-time quantitative PCR and the $2^{-\Delta\Delta C_T}$ method. *Methods* **25**: 402–408.

Ma R, Li M, Luo J *et al*. 2013; Structural integrity, ECM components and immunogenicity of decellularised laryngeal scaffold with preserved cartilage. *Biomaterials* **34**: 1790–1798.

Marcos-Campos I, Marolt D, Petridis P *et al*. 2012; Bone scaffold architecture modulates the development of mineralized bone matrix by human embryonic stem cells. *Biomaterials* **33**: 8329–8342.

Martens M, Van Audekercket R, Delport P *et al*. 1983; The mechanical characteristics of cancellous bone at the upper femoral region. *J Biomech* **16**(12): 971–983.

Mauney JR, Jaquiery C, Volloch V *et al*. 2005; *In vitro* and *in vivo* evaluation of differently demineralised cancellous bone scaffolds combined with human bone marrow stromal cells for tissue engineering. *Biomaterials* **26**: 3173–3185.

Miller LE, Block JE. 2011; Perspectives on the clinical utility of allografts bone regeneration within osseous defects: a narrative review. *Orthop Res Rev* **3**: 31–37.

Minogue BM, Richardson SM, Zeef LAH *et al*. 2010; Transcriptional profiling of bovine intervertebral disc cells: implications for identification of normal and degenerate human intervertebral disc cell phenotypes. *Arthritis Res Ther* **12**: R22.

Moreau MF, Gallois Y, Basle M *et al*. 2000; γ-Irradiation of human bone allograft alters medullary lipids and releases toxic compounds for osteoblast-like cells. *Biomaterials* **21**: 369–376.

National Joint Registry. 2012; 9th Annual Report: http: //www.njrcentre.org.uk

Polini A, Pisignano D, Parodi M *et al*. 2011; Osteoinduction of human mesenchymal stem cells by bioactive composite scaffolds without supplemental osteogenic growth factors. *PLoS One* **6**(10): e26211.

Pruss A, Gobel UB, Pauli G *et al*. 2003; Peracetic acid–ethanol treatment of allogenic avital bone tissue transplants – a reliable sterilization method. *Ann Transpl* **8**: 34–42.

Schubert T, Xhema D, Veriter S *et al*. 2011; The enhanced performance of bone allografts using osteogenic-differentiated adipose-derived mesenchymal stem cells. *Biomaterials* **32**: 8880–8891.

Seebach C, Schulthesis J, Wilhelm K *et al*. 2010; Comparison of six bone-graft substitutes regarding to cell seeding efficiency, metabolism and growth behaviour of human mesenchymal stem cells (MSC) *in vitro*. *Injury* **41**: 731–738.

Shih YRV, Tseng KF, Lai HY *et al*. 2011; Matrix stiffness regulation of integrin-mediated mechanotransduction during osteogenic differentiation of human mesenchymal stem cells. *J Bone Miner Res* **26** (4): 730–738.

Strassburg S, Richardson SM, Freemont AJ *et al*. 2010; Co-culture induces mesenchymal stem cell differentiation and modulation of the degenerate human nucleus pulposus cell phenotype. *Regen Med* **5**(5): 701–711.

Sun Y, Li W, Lu Z *et al*. 2011; Rescuing replication and osteogenesis of aged mesenchymal stem cells by exposure to a young extracellular matrix. *FASEB J* **25**: 1474–1485.

Tagil M, Jeppsson C, Aspenberg P. 2000; Bone graft incorporation: effects of osteogenic protein-1 and impaction. *Clin Orthop Rel Res* **371**: 240–245.

Thebaud NB, Siadous R, Bareille R *et al*. 2012; Whatever their differentiation status, human progenitor-derived or mature, endothelial cells induce osteoblastic differentiation of bone marrow stromal cells. *J Tissue Eng Regen Med* **6**(10): 51–60.

Varettas K, Taylor P. 2011; Bioburden assessment of banked bone used for allografts. *Cell Tissue Bank* **12**: 37–43.

Xie C, Reynolds D, Awad H *et al*. 2007; Structural bone allograft combined with genetically engineered mesenchymal stem cell as a novel platform for bone tissue engineering. *Tissue Eng* **13**: 435–447.

Yates P, Thomson J, Galea G. 2005; Processing of whole femoral head allografts: validation methodology for the reliable removal of nucleated cells, lipids and soluble proteins using a multi-step washing procedure. *Cell Tissue Bank* **6**: 277–285.

Yourek G, McCormick SM, Mao JJ *et al*. 2010; Shear stress induces osteogenic differentiation of human mesenchymal stem cells. *Regen Med* **5**(5): 713–724.

Zimmermann G, Moghaddam A. 2011; Allograft bone matrix versus synthetic bone graft substitutes. *Injury* **42**: S16–21.